Investigations into the Neuroprotective Effects of Osteopontin in In Vitro and In Vivo Models of Parkinsons Disease

Broom, Lauren

Awarding institution:
King's College London

Title: Investigations into the Neuroprotective Effects of Osteopontin in In Vitro and In Vivo Models of Parkinsons Disease

Author: Lauren Broom

Studies of the hindbrain roof plate organiser in the chick embryo

Emma Ruth Broom

MRC Centre for Developmental Neurobiology,

King's College, London

Thesis submitted for the degree of Doctor of Philosophy (PhD)

September 2011

Abstract

Organisers are specialised groups of cells that non-autonomously pattern adjacent cell populations. The dorsal midline, or roof plate, of the developing CNS is one such organiser and is required for the specification of specific subtypes of dorsal neurons. Organisers often comprise boundaries between molecularly distinguishable compartments, however the roof plate does not fit with this model; for the most part it constitutes a narrow strip of cells that separate two molecularly indistinguishable compartments (the two halves of the neural tube), but at certain anteroposterior locations, such as the hindbrain, it is expanded to form a thin epithelium that tents over a ventricle. Using chick embryos, I have investigated a hypothesis that reconciles the roof plate with this emergent model, in which the organiser properties of the roof plate are invested in its boundaries. Using *in vitro* co-culture, I show that the *gdf7*-positive roof plate boundary and its signalling properties can be regenerated in roof plate-derived tissue at the interface between hindbrain roof plate epithelium and neuroepithelium. Further, this *gdf7*-positive boundary is required for the expression of *cath1*, which marks the dorsal-most pool of neural progenitors in the hindbrain. Many organisers require Notch signalling and downstream Hairy/ Enhancer of split (Hes) transcription factors for their formation or maintenance. Using electroporation of the hindbrain roof plate epithelium – neuroepithelium boundary, I find that Delta-Notch signalling is sufficient to convert cells from a roof plate epithelial to a roof plate boundary fate. Further, correct levels of expression of *chairy2* (a *hes1* homologue) are required for the maintenance of the roof plate boundary. Finally, I show that the roof plate boundary is a bidirectional signalling centre that not only patterns adjacent neuroepithelium, but is also required for the differentiation of choroid plexus epithelium from roof plate epithelium.

Acknowledgements

Thanks must go to my supervisor, Richard for inspiring me with the idea of the project and for all the discussions and never-ending ideas along the way. Thank you to all other members of the Wingate-Bell conglomerate (Mary, Tracky Butts, Leigh, Laura, Tom and Esther) for all the bowling, rounders, cake and support (both scientific and in terms of keeping me sane!). Thank you to all other members of the Tea and Crossword Club; Megan, Kate, Peter, Liam, Oniz, Ellen and Bekah – you made the office such a fun place to be. Thanks must go to Alessio for his help and cloning guidance, to Jon Gilthorpe for the original *chairy2* construct, and to all the past and present attendees of the Lumsden group meetings, who gave me so many useful comments and advice. The MRC Centre has been such a great place to work for the past four years so I must thank everyone I've met here who have made it such a fun and collaborative environment. Thank you also to Sophie, Rachel and Sarah for experiencing the highs and lows with me from day one. Lastly, thank you so much Martin for putting up with me whilst in my thesis-writing mode and my parents for all their support and comfort cooking.

Table of Contents

Chapter 1 Introduction

A general principle of embryogenesis is that cells communicate in order for the process of regulative development to occur (reviewed in Gurdon, 1992). This is the process by which an embryo develops normally even if cells are removed or re-arranged at an early stage (reviewed in Wolpert et al., 2002). Specialised groups of cells, known as organisers, that direct the development of an adjacent field of cells via the process known as induction are central to this process. The first of these to be described is known as Spemann's organiser after its discovery by Hans Spemann and Hilde Mangold (1924) through transplantation experiments in salamander embryos. Their experiments showed that dorsal blastopore lip from a donor embryo is able to induce a secondary anteroposterior body axis when grafted into the ventral side of a host embryo. Most of the tissues in the secondary axis are derived from the host and so Spemann and Mangold termed the dorsal blastopore lip an 'organiser' as it was capable of patterning surrounding tissue in a non-autonomous fashion. Subsequently, equivalent organisers have been identified in mouse, chick and zebrafish and are referred to as the node in mouse, Hensen's node in chick and the shield in zebrafish (reviewed in Stern et al., 2006).

The initial 'organiser' region acts broadly before and during gastrulation to establish the anteroposterior and dorsoventral axes of the embryo (reviewed in De Robertis and Kuroda, 2004). It achieves this by secreting signalling molecules that generally act as morphogens (reviewed in Stern, 2001; De Robertis and Kuroda, 2004). Morphogens are proposed to signal to cells both adjacent to and at a distance from their source and induce different responses in cells in a concentration-dependent manner (Wolpert, 1969; reviewed in Wolpert, 1996).

After gastrulation secondary organisers act locally to direct growth and refine the broad patterning of the body axes that was laid down by the initial organiser. Examples of these secondary organisers include the apical ectodermal ridge and the zone of polarising activity that pattern growth of the vertebrate limb bud (Saunders, 1948; Honig, 1981; reviewed in Tickle, 1995), and a number of distinct organisers that reside within the neuroectoderm (reviewed in Kiecker and Lumsden, 2005) and pattern central nervous system (CNS) development that will be discussed in more detail below.

The signalling molecules secreted by organisers during development fall into a remarkably small number of classes that are used iteratively throughout development. The five main classes involved in patterning the vertebrate CNS are: the bone morphogenetic proteins (BMPs), which were originally identified for their ability to induce *de novo* cartilage

formation (Wozney et al., 1988), fibroblast growth factors (FGFs) that are so named for their ability to induce fibroblast proliferation (Gospodarowicz, 1974), Wnts, whose name originates as a hybrid of *wingless* (a *wnt* gene in Drosophila (Sharma and Chopra, 1976)) and *int* (*int1* being a mammalian homologue of *wingless*, originally identified in mouse as an oncogene whose expression is activated by the integration of mouse mammary tumour virus (Nusse et al., 1984; van Ooyen and Nusse, 1984)), Hedgehog proteins, of which Sonic Hedgehog is the main player during CNS development (Roelink et al., 1995; Chiang et al., 1996), and retinoic acid, which is not a protein but a small molecule derived from vitamin A (Durston et al., 1989; Duester, 2000; reviewed in Maden, 2002). The role of members of these signalling families in the organisation of the developing CNS will be described below.

1.1 Organisers in the developing central nervous system

For the most part the developing vertebrate CNS begins as a flat neural plate that bends to form a neural tube via the process of primary neurulation (reviewed in Lowery and Sive, 2004) (see Figure 1-2). From neural plate to neural tube stages the developing CNS is patterned in a Cartesian-coordinate manner, with cells being instructed on their anteroposterior and dorsoventral positions by signals deriving from the poles of both axes. An initially global anteroposterior pattern is established by signals emanating from 'the organiser', while the dorsoventral pattern is established by tissues deriving from the axial mesendoderm of the organiser (the notochord and prechordal plate) and the epidermal ectoderm (reviewed in Placzek, 1995; Lee and Jessell, 1999; Kiecker and Niehrs, 2001b; Stern, 2001). This initially global pattern is then re-fined by locally-acting secondary organisers located within the neuroepithelium, as will be described below (reviewed in Kiecker and Lumsden, 2005).

1.1.1 Anteroposterior patterning

During gastrulation the neural plate is globally patterned in a planar fashion, along the anteroposterior axis, by signals emanating from 'the organiser' (reviewed in Stern, 2001). These posteriorising signals include retinoic acid, Fgfs and Wnts, which act dose-dependently (Kiecker and Niehrs, 2001a; reviewed in Maden, 2002; Mason, 2007). At least in the case of Wnt signals, inhibitors are expressed by the anterior axial mesendoderm (derived from the organiser) that protect the anterior neural plate from posteriorising signals and thus induce anterior neural fates, such as forebrain (reviewed in Kiecker and Niehrs, 2001b; Stern, 2001). The posteriorising effects of the above morphogens can be demonstrated by their effects on expression of genes of the *hox* cluster, which are expressed in specific, overlapping domains along the anteroposterior axis in the hindbrain and spinal cord and encode transcription factors that endow neurons with their anteroposterior identity

(Carpenter et al., 1997; Bell et al., 1999; Liu et al., 2001; Bel-Vialar et al., 2002; Dasen et al., 2003; Nordstrom et al., 2006; In der Rieden et al., 2010).

This initially global anteroposterior patterning is later refined by local secondary organisers (Figure 1-1) (reviewed in Kiecker and Lumsden, 2005). The secondary organisers patterning the anteroposterior axis of the CNS that have so far been identified include: the anterior neural boundary, which lies at the anterior border of the neural plate and later forms the commissural plate, both of which pattern the forebrain via signals such as fibroblast growth factor 8 (Fgf8) (Shimamura and Rubenstein, 1997; Meyers et al., 1998; Fukuchi-Shimogori and Grove, 2001; Garel et al., 2003; Walshe and Mason, 2003; Toyoda et al., 2010), the zona limitans intrathalamica (ZLI), which patterns the adjacent thalamus and pre-thalamus via *sonic hedgehog* (*shh*) (Kiecker and Lumsden, 2004; Vieira et al., 2005; Scholpp et al., 2006; Vue et al., 2009) and the midbrain-hindbrain boundary, which patterns the adjacent midbrain and hindbrain primarily via Fgf8 (Crossley et al., 1996; Lee et al., 1997; Martinez et al., 1999; Irving and Mason, 2000).

In general, these organisers are highly conserved in vertebrates. However, for at least one set of boundaries, a role for signalling may be restricted to certain taxa of the vertebrate phylogeny. In the embryonic hindbrain, neuroectoderm is divided into a series of lineage restriction compartments known as rhombomeres (Fraser et al., 1990). Experiments in zebrafish have alluded to a role of rhombomere boundaries in patterning adjacent rhombomeres (Riley et al., 2004; Amoyel et al., 2005). Rhombomere boundaries express a number of *wnt* signalling molecules including *wnt1,* and upon morpholino knockdown of *wnt1* or a downstream component of the canonical Wnt signalling pathway, boundary markers expand while neurogenesis adjacent to the boundaries is inhibited (Riley et al., 2004; Amoyel et al., 2005). The neurogenesis that occurs in *wnt1/ wnt10b/wnt3a/wnt8b*-deficient embryos is extremely disorganised, but hindbrain segmentation is maintained, as assessed by the expression of segmentally expressed genes (Riley et al., 2004). However a recent study suggests that these effects may be mediated by non-specific toxicity of the *wnt1* morpholino and other morpholinos used in the above studies (Gerety and Wilkinson, 2011). However the loss of rhombomere boundaries in zebrafish mutants that disrupt boundary formation and maintenance coincides with disorganised neurogenesis, with a loss of neurons produced adjacent to boundaries but a compensatory increase in neurons produced at rhombomere centres (Riley et al., 2004). It is argued that this disruption of organised neurogenesis reflects a patterning role of the rhombomere boundaries, rather than excessive cell mixing between rhombomeres as expression of segmentally expressed genes are still

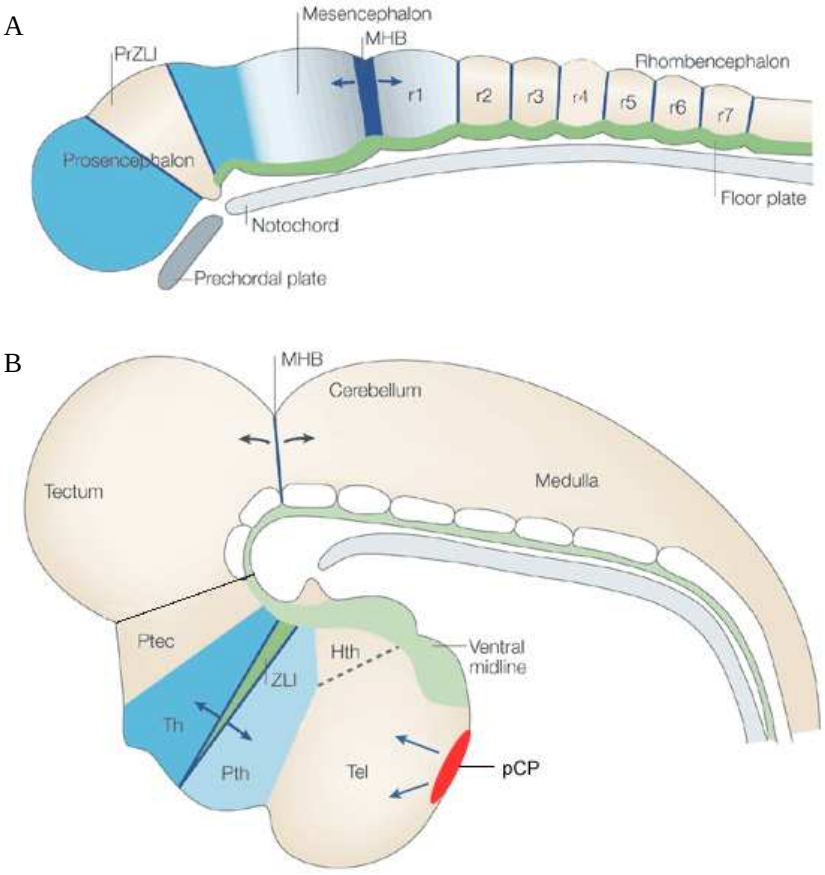

Figure 1-1 Schematic diagram showing secondary organisers in the developing CNS

Modified from (Kiecker and Lumsden, 2005). Diagrams illustrate lateral views of a Hamburger–Hamilton stage 13 (st13) (A) and a st24 chick embryos (B) with anterior to the left and dorsal oriented upwards. Anteroposterior secondary organisers include the pCP (prospective commissural plate), the ZLI (zona limitans intrathalamica), the MHB (midbrain-hindbrain boundary) and the rhombomere boundaries (solid blue lines between rhombomeres r1- r7). prZLI, prospective ZLI; Tel, telencephalon; Hth, hypothalamus; Pth, pre-thalamus; Th, thalamus; Ptec, pre-tectum.

maintained in their proper spatial domains (Riley et al., 2004). Overexpression of *wnt1* in these mutants could partially rescue the organisation of neurogenesis. Thus it is likely that rhombomere boundaries do have roles as organisers in zebrafish, but whether this is via Wnt signals is currently unclear. Whether rhombomere boundaries function as organisers in other vertebrates remains to be determined.

1.1.2 Dorsoventral patterning

After neural induction is complete, the mediolateral axis of the neural plate (which converts into the dorsoventral axis upon neurulation) is initially patterned by two non-neuronal tissues: the mesodermal notochord (or the prechordal plate at presumptive forebrain levels) and the epidermal ectoderm (reviewed in Lee and Jessell, 1999).

1.1.2.1 Ventralising signals

Elegant surgical grafting studies in chick showed that the notochord is necessary and sufficient to induce the formation of ventral cell types, such as the floor plate and motor neurons, but represses the formation of dorsal cell types in the spinal cord (Placzek et al., 1990; Placzek et al., 1991; Yamada et al., 1991; Ericson et al., 1992; Goulding et al., 1993; reviewed in Patten and Placzek, 2000) (Figure 1-2). The floor plate is itself an organiser of the ventral neuroepithelium as it can also ectopically induce ventral cell types in neuroepithelium (Yamada et al., 1991; Placzek et al., 1993; reviewed in Placzek, 1995).

The signalling molecule responsible for this inductive process was shown to be Sonic Hedgehog (Shh). Shh is expressed by both the notochord and the floor plate and can induce the ectopic formation of floor plate or motor neurons in mouse, zebrafish, chick and frog neuroepithelium (Echelard et al., 1993; Krauss et al., 1993; Roelink et al., 1994; Marti et al., 1995a; Marti et al., 1995b; Tanabe et al., 1995). Blocking of Shh activity inhibits the inductive effects of the notochord on chick neural plate explants and in mice carrying a mutant form of *shh*, the floor plate fails to form and ventral cell types are lacking, with a compensatory expansion of more dorsal markers (Marti et al., 1995a; Chiang et al., 1996; Ericson et al., 1996). Shh is known to act as a classic morphogen in the ventral neural tube, inducing different cell types at different exposure thresholds (Roelink et al., 1995; Ericson et al., 1996; Ericson et al., 1997; Briscoe et al., 2000; Dessaud et al., 2007).

Recently it has also been demonstrated by the expression of a fluorescently labelled Shh protein (Shh-GFP) in mouse that a dynamic ventral – dorsal gradient of Shh protein exists in the ventral neural tube, but that the profile of this gradient can be altered by the response of target-field cells (Chamberlain et al., 2008). Shh signalling has been shown to regulate the expression of various basic helix-loop-helix (bHLH) and homeodomain-containing transcription factors in the ventral neural tube that define different progenitor domains

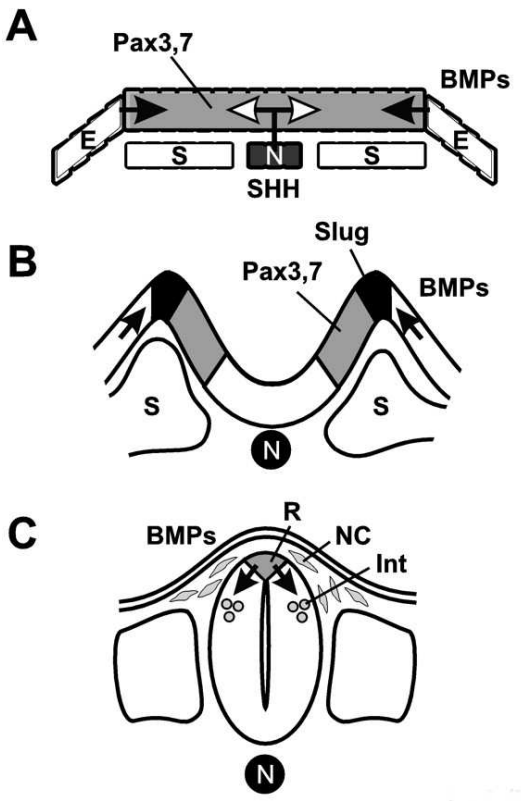

Figure 1-2 Initial patterning of the mediolateral/ dorsoventral axis of the neural primordium

Adapted from Lee and Jessell (1999). (A) The spinal cord is derived from the neural plate, an epithelial sheet overlying the notochord and somitic mesoderm and flanked by epidermal ectoderm. Initial mediolateral patterning of the neural plate is imposed by ventralising signals (SHH) (open arrows) from notochord cells and dorsalising signals (BMPs) (solid arrows) from epidermal ectoderm. Pax3 and Pax7 are initially expressed at all mediolateral positions in the neural plate, but are repressed medially (ventrally) by SHH signalling. (B) At the neural fold stage, BMP signalling promotes maintenance of Pax3/Pax7 expression and induces expression of Slug in premigratory NC cells. (C) During and after neural tube closure, neural crest cells (NC) emigrate from the dorsal neural tube and roof plate is generated at the dorsal midline. Roof plate cells are a source of molecules such as BMP that control the differentiation of dorsal interneurons (Int). N, notochord; S, somitic mesoderm; E, epidermal ectoderm; SHH, Sonic Hedgehog; BMP, bone morphogenetic protein; NC, neural crest; R, roof plate; Int, dorsal interneurons.

(Figure 1-3 A) (Briscoe et al., 2000; Dessaud et al., 2007). Shh acts to repress one set of transcription factors (those belonging to class 1, which includes *pax6, pax7, irx3, dbx1* and *dbx2*) while activating another set of transcription factors (those belonging to class 2, which includes *foxa2, nkx2.2, olig2* and *nkx6.1).* Additionally, different levels of Shh signalling are required for the repression or activation of the expression of individual class 1 and 2 genes, resulting in their nested expression patterns (Briscoe et al., 2000; Dessaud et al., 2007). Cross-repression of various combinations of these transcription factors acts to refine and maintain the progenitor domains (Briscoe et al., 1999; Briscoe et al., 2000). A combinatorial code of these transcription factors specifies specific neuronal cell types (Briscoe et al., 2000). Thus the notochord and the floor plate, via Shh signalling, work to pattern the ventral neural tube, partitioning it into distinct progenitor domains.

Although the induction of floor plate by notochord is a well-established phenomenon, it has been suggested that the floor plate and notochord arise from a node/ organiser-derived midline-precursor cell population and that the floor plate is inserted into the neural plate during the regression of the node/organiser (Catala et al., 1996; reviewed in Le Douarin and Halpern, 2000). It is suggested that the loss of floor plate seen in notochord-ablation experiments (Placzek et al., 1990; Yamada et al., 1991) may be due to accidental removal of the floor plate along with the notochord (Teillet et al., 1998). Therefore it may be that the notochord is not required for specification of the floor plate during neurulation as indicated by the notochord-ablation studies in chick, but whether the notochord is involved in the specification of floor plate cells at an earlier stage, during gastrulation, has not yet been determined (reviewed in Le Douarin and Halpern, 2000).

1.1.2.2 Dorsalising signals

In embryos where ventralising signals had been removed via the surgical removal of the notochord, dorsal neural cell types still formed (Yamada et al., 1991; Ericson et al., 1992). Indeed a ventral expansion of normally dorsally restricted genes such as *pax3* and *pax7* was seen in chick and mouse embryos lacking notochord or Shh signalling (Yamada et al., 1991; Goulding et al., 1993; Chiang et al., 1996; Ericson et al., 1996). Two explanations exist for this phenomenon. Either dorsal neuronal cell fates are the default but are normally repressed by ventralising signals, or dorsal cell types require induction by dorsalising signals that are normally opposed by Shh (reviewed in Lee and Jessell, 1999). Evidence supporting the latter of these two explanations first came from observations that definitively dorsal cell types, such as neural crest cells, are still restricted to their dorsal locations upon removal of ventralising signals from the notochord at neural plate stages (Liem et al., 1995).

A

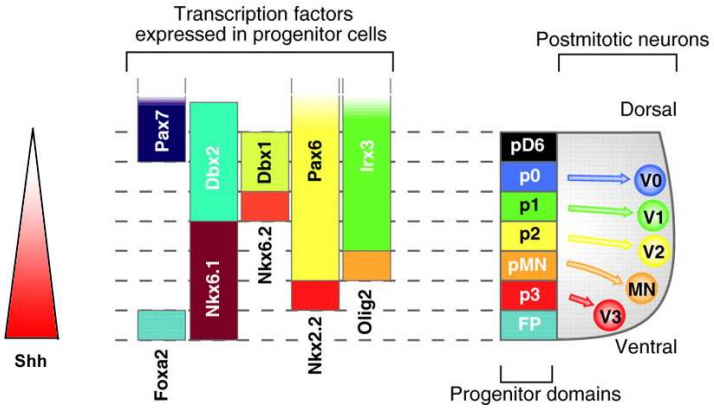
Transcription factors
expressed in progenitor cells
Postmitotic neurons
Dorsal
Ventral
Shh
Foxa2
Nkx6.1
Dbx2
Pax7
Dbx1
Nkx6.2
Pax6
Nkx2.2
Irx3
Olig2
pD6
p0
p1
p2
pMN
p3
FP
V0
V1
V2
MN
V3
Progenitor domains

B

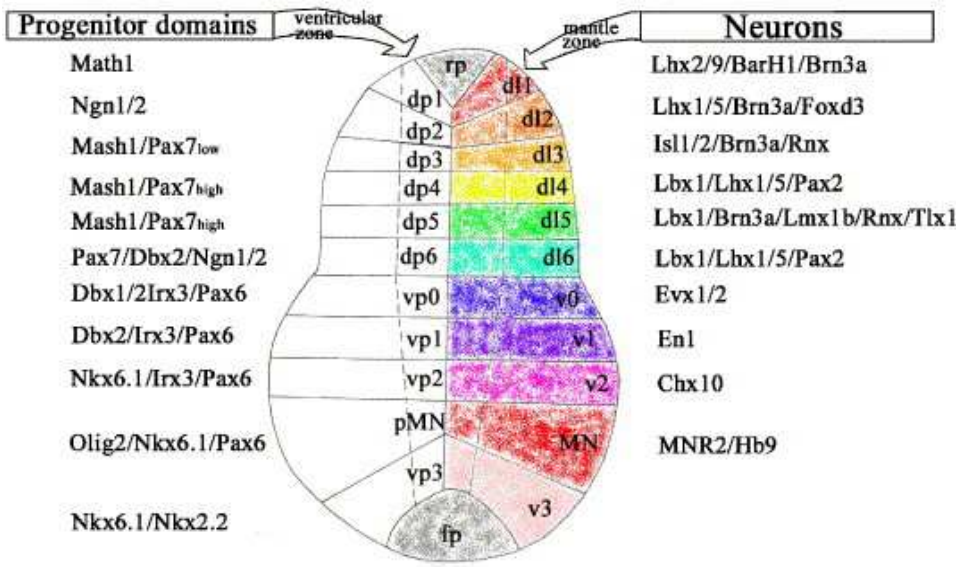
Progenitor domains
ventricular zone
mantle zone
Neurons
Math1
Ngn1/2
Mash1/Pax7low
Mash1/Pax7high
Mash1/Pax7high
Pax7/Dbx2/Ngn1/2
Dbx1/2Irx3/Pax6
Dbx2/Irx3/Pax6
Nkx6.1/Irx3/Pax6
Olig2/Nkx6.1/Pax6
Nkx6.1/Nkx2.2
rp
dp1
dp2
dp3
dp4
dp5
dp6
vp0
vp1
vp2
pMN
vp3
fp
dI1
dI2
dI3
dI4
dI5
dI6
v0
v1
v2
MN
v3
Lhx2/9/BarH1/Brn3a
Lhx1/5/Brn3a/Foxd3
Isl1/2/Brn3a/Rnx
Lbx1/Lhx1/5/Pax2
Lbx1/Brn3a/Lmx1b/Rnx/Tlx1
Lbx1/Lhx1/5/Pax2
Evx1/2
En1
Chx10
MNR2/Hb9

Figure 1-3 Dorsoventral subdivision of the spinal cord neural tube into distinct progenitor domains

(A) Modified from (Dessaud et al., 2008). Schematic of the ventral half of the neural tube, where the ventral gradient of Shh activity controls position identity by regulating the expression, in neural progenitors, of a set of transcription factors. These include Dbx1, Dbx2, Pax7, Pax6 and Irx3, which are repressed by Shh signalling, and Nkx6.1, Olig2, Nkx2.2 and Foxa2, which require Shh signalling for their expression. Thus progenitor domains are established that give rise to different postmitotic neurons. FP, floor plate; p0 – p3, progenitor domains 0 – 3 giving rise to v0 – v3 (ventral interneuron subtype 0 – 3) respectively; pMN, Motor neuron progenitor domain giving rise to MN (motor neurons); pD6, progenitor domain for dorsal interneuron subtype 6.

(B) Modified from (Wilson and Maden, 2005). Diagram of a transverse section through the spinal cord showing dorsoventral subdivision into progenitor domains at the ventricular zone giving rise to various postmitotic neurons situated in the mantle zone. Progenitor domains are marked by various combinations of transcription factors as are different neuronal cell types. dp1 – dp6, dorsal progenitor domains giving rise to dI1 – dI6 (dorsal interneuron subtypes 1 – 6) respectively; vp0 – vp3, ventral progenitor domains giving rise to v0 – v3 (ventral interneuron subtypes 0 – 3) respectively; pMN, motor neuron progenitor domain giving rise to MN (motor neurons); fp, floor plate; rp, roof plate.

The neural crest are a migratory, multipotent cell population that arise from the lateral edges (the dorsal-most regions) of the neural plate (Figure 1-2 B, C) and give rise to neurons and glia of the peripheral nervous system, as well as melanocytes and other non-neural cell types (LaBonne and Bronner-Fraser, 1998a). Early studies aiming to identify dorsalising signals focussed on signals inducing their formation. Grafting studies in chick and amphibian embryos showed that epidermal ectoderm, which flanks the lateral neural plate (Figure 1-2 A), can induce neural crest cell formation when grafted adjacent to the neural plate (Moury and Jacobson, 1989; Moury and Jacobson, 1990; Selleck and Bronner-Fraser, 1995). Neural crest cells arose from both prospective neural plate and prospective epidermal cells (Moury and Jacobson, 1990; Selleck and Bronner-Fraser, 1995). Similarly, *in vitro* studies using chick neural plate explants also show that interactions between epidermal ectoderm and neural plate can promote neural crest differentiation (Dickinson et al., 1995; Liem et al., 1995).

A number of studies in chick, amphibian and zebrafish embryos have identified multiple signalling families that can induce the formation of neural crest cells, such as BMPs, Wnts, FGFs and RA, although research has mainly focussed on the role of Bmps and Wnts (reviewed in Steventon et al., 2005). The Bmp signalling molecules, *bmp4* and *bmp7* are expressed by the epidermal ectoderm at neural fold stages and are sufficient to ectopically induce the formation of neural crest cells from caudal chick neural plate explants (Liem et al., 1995). The blockade of the Bmp signalling pathway using the secreted Bmp antagonists, Noggin and Follistatin, blocked the ability of epidermal ectoderm to induce neural crest cell formation in neural plate explants (Liem et al., 1997). Electroporation studies in chick have also shown that electroporation of the caudal neural tube with constitutively activated Bmp receptors (*bmpr1a* or *bmpr1b*) can ectopically induce neural crest marker expression and emigration of neural crest from the neural tube (Liu et al., 2004). In zebrafish, Bmp signalling has also been shown to be necessary for neural crest formation (Barth et al., 1999; Nguyen et al., 2000). Thus Bmps are important for neural crest formation in both chick and zebrafish.

A role for Wnt proteins in neural crest formation was first suggested by experiments in *Xenopus* in which co-expression of Wnt1 or Wnt3a, which are both specifically expressed at the dorsal midline of the neural tube, in neuralised ectodermal explants caused ectopic activation of neural crest markers (Wolda et al., 1993; Saint-Jeannet et al., 1997). Furthermore, in whole embryos, overexpression of Wnt1 or Wnt3a caused expansion of the neural crest population even when cell proliferation was inhibited. Wnt8/β-catenin signalling can also induce neural crest markers in neuralised *Xenopus* ectodermal explants or in whole embryos (LaBonne and Bronner-Fraser, 1998b). In chick, Wnt signals were shown to be

necessary and sufficient to induce neural crest cell formation, and Wnt6, expressed in the epidermal ectoderm, was suggested as a good candidate to mediate this process (Garcia-Castro et al., 2002). A requirement for canonical Wnt signalling for neural crest formation has also been demonstrated in Xenopus (LaBonne and Bronner-Fraser, 1998b; Tamai et al., 2000; Deardorff et al., 2001). Finally, in *wnt1*; *wnt3a* double mutant mice, neural crest and their derivatives are depleted (Ikeya et al., 1997). Although the evidence points towards Wnt signalling having an important role in neural crest formation, there has been some controversy about whether it is involved in the specification of neural crest or in the promotion of proliferation of an initially specified precursor pool (Wu et al., 2003). Ikeya et al. (1997) have argued that the loss of *wnt1* and *wnt3a* does not affect dorsoventral patterning in the hindbrain and spinal cord as dorsoventral markers were correctly localised. In the hindbrain, dorsal progenitor populations were reduced so Ikeya et al. (1997) suggested that this represents a specific requirement for Wnt signals in promoting the proliferation of dorsal progenitor pools. However, in Xenopus embryos where cell proliferation is blocked, neural crest are still induced in response to Wnt3a (Saint-Jeannet et al., 1997). Thus it is likely that differences may occur between species with regard to the role of Wnt in neural crest induction, but also that Wnts may be involved in multiple stages of the process of neural crest formation (reviewed in Wu et al., 2003).

Roof plate cells are another population of cells generated at the dorsal midline of the neural tube (Figure 1-2). Lineage-tracing studies in mouse and in chick have shown that roof plate cells and neural crest cells are derived from the same precursors (Bronner-Fraser and Fraser, 1988; Echelard et al., 1994) and definitive markers of roof plate and neural crest are co-expressed in the neural folds and neural tube (Chizhikov and Millen, 2004b; reviewed in Chizhikov and Millen, 2004c). Although the mechanisms that segregate this precursor population are not fully understood, it is understood that roof plate is induced in the lateral folds by epidermal ectoderm in a similar manner to neural crest. Epidermal ectoderm induces the formation of MafB-positive roof plate cells from intermediate chick neural plate explants, and this could be mimicked by application of Bmp4 and Bmp7 (Liem et al., 1997). Further, blockade of Bmp signalling using Noggin and Follistatin blocked the epidermal ectoderm-driven induction of roof plate cells. Further support for an instructive role of Bmp signalling in roof plate formation came from electroporation studies of the caudal chick neural plate and neural tube. Electroporation of *noggin* inhibited roof plate formation while overexpression of *bmp4*, *bmp7* or activated bmp receptors (*bmpr1a* or *bmpr1b*) greatly expanded the roof plate, as assessed by roof plate markers such as MafB and Lmx1a (Chizhikov and Millen, 2004b; Liu et al., 2004). Thus Bmp signalling is necessary and sufficient for roof plate formation.

Several members of the Wnt family are expressed in epidermal ectoderm and the dorsal midline region during roof plate development (Hollyday et al., 1995; Megason and McMahon, 2002). As described above, Wnt signals are required for the development of neural crest in chick, mouse and xenopus embryos (reviewed in Wu et al., 2003). Thus it seems likely that Wnt signals might be involved in the induction of roof plate formation, although no specific role for Wnt signals has yet been found. In disagreement with this, inhibition of the Wnt signalling pathway by electroporating a dominant negative *wnt1* or *tcf4* (a downstream effector of canonical Wnt signalling (Megason and McMahon, 2002)) construct into the caudal chick neural plate did not affect the formation of roof plate (Chizhikov and Millen, 2004b), although this does not preclude an earlier role for Wnt signalling in induction of roof plate specification.

1.1.2.3 The roof plate is an organiser

The roof plate itself expresses multiple Bmps and Wnts and its organiser activity has been shown to be required for the development of the three dorsal-most interneuron cell types of the developing spinal cord (Hollyday et al., 1995; Liem et al., 1997; Lee et al., 2000a; Megason and McMahon, 2002). Like the ventral half of the spinal cord, the dorsal half can also be subdivided into distinct progenitor domains marked by different sets of bHLH and homeodomain-containing transcription factors that give rise to different types of neurons (Figure 1-3 B). The dorsal half of the spinal cord gives rise to six groups of interneurons (dI1 – dI6), with the progenitor domain of dI1 being marked by *mouse atonal homolog 1* (*math1* or *cath1* in chick) (Helms and Johnson, 1998), the progenitor domain of dI2 being marked by *neurogenin 1* (*ngn1*)(Lee et al., 2000a) and the progenitor domain of dI3 being included in the *mouse achaete-scute homolog 1 (mash1* or *cash1* in chick)(Gowan et al., 2001) expression domain (reviewed in Wilson and Maden, 2005). In mice where the roof plate is ablated by the expression of diphtheria toxin A subunit driven by the *gdf7* locus, the progenitors and mature neurons of the dI1, dI2 and dI3 interneuron groups fail to form and there is a compensatory increase in the more ventral neuronal types (dI4-6) and the *mash1*-positive progenitor domain (Lee et al., 2000a; reviewed in Chizhikov and Millen, 2005).

The roof plate can induce the formation of dI1 – dI3 interneurons in chick intermediate neural plate explants (Liem et al., 1997). Just as Bmps are the main signalling family involved in the induction of the roof plate itself, Bmps have been shown to be the main signalling family involved in mediating the inductive properties of the roof plate. Application of the roof plate-expressed BMP family members, Bmp4, Bmp5, Bmp6, Bmp7 and Gdf7 (also known as Bmp12) to chick neural explants results in the induction of dorsal neural cell types *in vitro* (Liem et al., 1997; Lee et al., 1998), while blockade of Bmp signalling with Noggin and Follistatin inhibited the ability of the roof plate to induce dorsal

cell types in *in vitro* neural cultures (Liem et al., 1997; Lee et al., 1998). Electroporation studies in chick have further demonstrated that Bmp signalling is necessary and sufficient for dorsal interneuron formation (Timmer et al., 2002; Chesnutt et al., 2004; Chizhikov and Millen, 2004a; Liu et al., 2004). Chizhikov and Millen (2004a) also showed that the ability of an expanded roof plate (induced by the overexpression of *lmx1b*) to induce dI1 interneurons adjacent to it at the expense of dI2-6 neurons was mediated mostly by Bmp signalling. Timmer et al. (2002) have shown that induction of different dorsal cell types requires different thresholds of Bmp signalling, with the highest levels of Bmp signalling inducing the dI1 progenitors at the expense of dI2 progenitors, but low level signalling inducing the ventral expansion of the dI2 progenitor domain. Thus Bmp signals may act as classic morphogens in the induction of dorsal neuronal cell types.

Genetic deletion studies in mice have not provided much evidence for specific roles of individual Bmps in specification of dorsal neural cell types, presumably due to redundancy between Bmp family members (reviewed in Chizhikov and Millen, 2005). Gdf7 is the exception to this. Genetic loss of *gdf7* results in a loss of a specific subset of dI1 interneurons (formerly known as D1A) in mouse (Lee et al., 1998). This result raises the possibility that individual Bmp family members are responsible for promoting the formation of different dorsal neuronal cell types, rather than different thresholds of Bmp signalling, as proposed by Timmer et al. (2002). The reality is likely to be a combination of both of these scenarios. The above examples focus on the role of the roof plate in mouse and chick. However in zebrafish embryos, specific thresholds of Bmp signalling have been demonstrated to be necessary for the formation of dorsal and intermediate neuronal cell types in the spinal cord (Barth et al., 1999; Nguyen et al., 2000). Therefore graded Bmp signalling is likely to be a conserved mechanism required for the patterning of the dorsal neural tube.

Evidence that Wnt signals are important in the morphogenesis of the neural tube came from a study using antisense oligonucleotides to perturb the function of Wnt1 and Wnt3a. Mouse embryos treated with these oligonucleotides showed hypoplasia of the forebrain, midbrain and hindbrain, and lateral out-pocketings in the spinal cord (Augustine et al., 1993). Wnt1 and Wnt3a are expressed in the spinal cord roof plate and studies originally pointed towards a purely mitogenic role for these proteins in the development of the dorsal spinal cord (Dickinson et al., 1994; Megason and McMahon, 2002). In support of this Chesnutt et al. (2004) showed that expression of a dominant-negative *wnt*-receptor (*frizzled 8*) in the chick spinal cord caused a general reduction in cell number of dI1-6 cells, rather than having a specific effect on dI1-3. Additionally, overexpression of *wnt3a* did not have a significant effect on dI1-6 production and *wnt3a* overexpression could not rescue the loss of dI1 cells and the dorsal shift of dI2 – 6 cells caused by overexpression of *noggin*. However *wnt1-/-;*

wnt3a-/- double mutant mice show a specific reduction in dI1-3 neurons with a compensatory increase in more ventral interneurons (Muroyama et al., 2002). Furthermore, application of Wnt3a to the medial region of the chick neural plate could induce dI1 and dI2 neuronal production, without the involvement of BMP signalling. The discrepancies between the results of Chesnutt et al. (2004) and Muroyama et al. (2002) with regard to the overexpression of Wnt3a may be due to the differences in timing of the overexpression of Wnt3a. Indeed, recent work by Bonner et al. (2008) using zebrafish have shown that the effect of inhibition of the Wnt/β-catenin pathway is determined by its timing. Early inhibition shows that Wnt signalling is required for proliferation, whereas later inhibition shows that it is required for dorsoventral patterning of the spinal cord. A recent study re-addressing the role of Wnts in dorsoventral patterning of the chick spinal cord shows that co-electroporation of *wnt1* and *wnt3a* in the chick caused a ventral expansion of dorsal progenitor domains and dI2-4 interneuron populations at the expense of the more ventral dI6 interneurons, ventral V0 – 1 interneurons and motor neurons (Alvarez-Medina et al., 2008). Alvarez-Medina et al. (2008) also show that the activity of Wnt1/Wnt3a is independent of BMP signalling, but dependent on the Shh/Gli pathway. It was shown that Wnt1/Wnt3a antagonise Shh in order to orchestrate dorsoventral patterning of the chick spinal cord. Thus it is likely that Wnts and Bmps work in concert to specify dorsal neuronal cell types in the spinal cord in chick, mouse and zebrafish embryos.

1.1.2.4 The roof plate and dorsal patterning of the hindbrain

At the hindbrain, like in the spinal cord, the dorsal-most region of neuroepithelium adjacent to the roof plate is marked by Math1 (Cath1 in chick) (Wang et al., 2005; Wilson and Wingate, 2006). This Math1 expression domain is known as the rhombic lip, a germinative region that gives rise to excitatory neurons of the cerebellar and pre-cerebellar systems (Wingate and Hatten, 1999; Machold and Fishell, 2005; Wang et al., 2005; Wilson and Wingate, 2006; Rose et al., 2009a). The rhombic lip is subdivided into the upper rhombic lip (derived from rhombomere 1), which gives rise to cerebellar neurons and the lower rhombic lip (deriving from rhombomeres 2 – 8), which gives rise to pre-cerebellar neurons (Figure 1-4 B) (Machold and Fishell, 2005; Wang et al., 2005; Ray and Dymecki, 2009). Throughout this thesis I will refer to the upper roof plate as that dorsomedial to the upper rhombic lip and the lower roof plate as that located dorsomedially from the lower rhombic lip.

Research of the role of the roof plate in dorsoventral patterning of the hindbrain has focussed on its role in patterning the cerebellar anlage (upper rhombic lip level). In mouse, ablation of the roof plate results in a specific loss of the dorsal-most neural progenitor pool, which is marked by Math1, while the more ventrolaterally located progenitors are still specified but are present in smaller numbers (Chizhikov et al., 2006). Chizhikov et al. (2006) hence

A

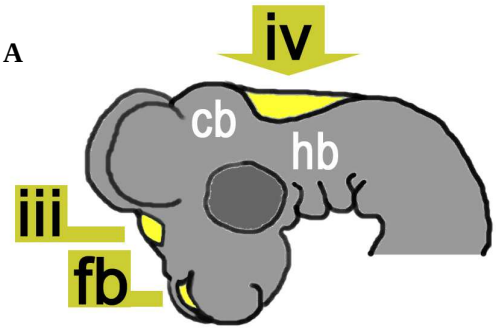

Lateral view of an E4 chick head

B

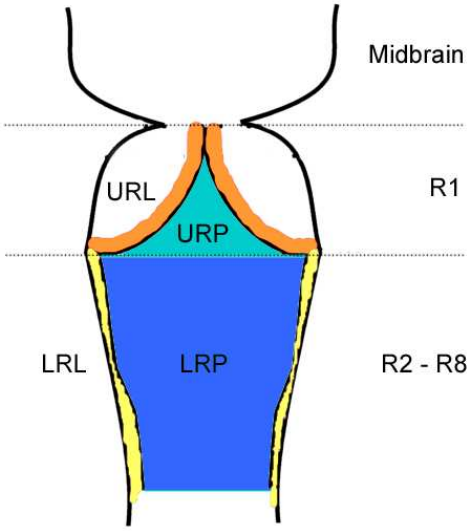

Dorsal view of E4 chick hindbrain

C

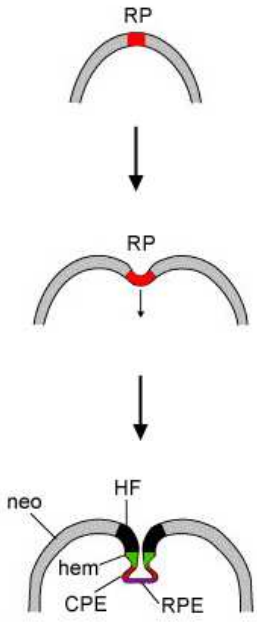

Development of the dorsal telencephalon of mouse in coronal section

Figure 1-4 Diagrams of brain ventricles

Figure 1-4 Diagrams of brain ventricles

(A) Schematic diagram of a lateral view of an E4 chick embryo head, showing the locations of the forebrain (fb), third (iii) and fourth (iv) ventricles. The head is oriented with anterior to the left.

(B) Diagram of dorsal view of E4 chick embryo hindbrain. The rhombic lip can be separated into the upper rhombic lip (URL), derived from rhombomere 1 (R1) of the hindbrain, and the lower rhombic lip (LRL), derived from rhombomeres 2 – 8 (R2 – R8) of the hindbrain. The roof plate immediately dorsomedial to the URL is referred to as the upper roof plate (URP), whereas the roof plate dorsomedial to the LRL is referred to as the lower roof plate (LRP). Anterior is oriented upwards.

(C) Diagram of (E9.5–E12.5) mouse dorsal telencephalon development in coronal section. Modified from (Chizhikov and Millen, 2005). Roof plate cells (RP, red) occupy the dorsal midline of the developing telencephalon at E9.5. As development proceeds, the roof plate invaginates relative to the lateral neuroepithelium forming the cortical hem (hem, green), the choroid plexus epithelium (CPE, red) and the roof plate epithelium (RPE, purple) by E12.5. These dorsal midline structures lie adjacent to the hippocampal field (HF, black), which itself is medial to the developing neocortex (neo, grey).

proposed that the hindbrain roof plate is required for specification of the rhombomere 1 Math1-domain, but only for proliferation of the more ventral cell types in the mouse. Ectopic roof plate was also sufficient to induce or expand the Math1 domain both *in vivo* and *in vitro*, and Chizhikov et al. (2006) showed that this induction was dependent on BMP signals. Previous studies have also demonstrated the importance of BMP family members in the induction of Math1-positive cells. Gdf7, Bmp6 and Bmp7 can induce Math1-positive cells *in vitro* and the BMP receptors, Bmpr1a and Bmpr1b, are required in a redundant fashion for the specification of the cerebellar granule cells (derived from Math1-positive progenitors), but not the Purkinje cells, which are derived from the slightly more ventrolateral Ptf1a -positive progenitor pool of the cerebellar anlage (Alder et al., 1999; Chizhikov et al., 2006; Qin et al., 2006; Pascual et al., 2007).

However, work in zebrafish, chick and mouse have indicated that Bmp signals (most probably deriving from the roof plate) are also involved in the specification of neurons generated in the intermediate hindbrain neural tube; neurons of the locus coeruleus. These neurons are generated at the dorsolateral aspect of rhombomere 1 and are *phox2a/b* positive (Guo et al., 1999; Vogel-Hopker and Rohrer, 2002). Vogel-Hopker and Rohrer (2002) showed in chick that the formation and position of these neurons rely on Bmp signals. Treatment of embryos with Noggin at Hamburger and Hamilton st10 – 11 (Hamburger and Hamilton, 1951) caused a loss of *phox2a*-positive locus coeruleus neurons in a small percentage of cases, but in the majority of cases caused the ectopic location of locus coeruleus neurons across the dorsal midline. This ectopic expansion correlated with a loss of the roof plate and a dorsal expansion of the intermediate neural tube marker, *pax6*. These results suggest a situation where graded Bmp signalling is required for dorsal development in rhombomere 1, with higher thresholds being required to restrict the dorsal extent of intermediate progenitors, but a low threshold of Bmp signalling being required for the development of intermediate progenitors. These findings are consistent with those in zebrafish where severe Bmp signalling mutants lack locus coeruleus cells, but ectopic locus coeruleus cells form in mild Bmp signalling mutants (Guo et al., 1999). The specific Bmp signals required for locus coeruleus development are likely to be Bmp5 and Bmp7 from the roof plate as locus coeruleus neurons are missing in *bmp5*-/-; *bmp7*-/- double knockout mice (Tilleman et al., 2010). Further work is required to reconcile the findings of Chizhikov et al. (2006), who find that only the specification of the dorsal-most Math1-positive progenitor pool requires signals from the roof plate for their specification, with those of Tilleman et al. (2010), who find that specification of the intermediate-domain produced locus coeruleus neurons depends on Bmp signals that most probably derive from the roof plate.

Little evidence currently exists to suggest a role for Wnt signals from the roof plate being involved in specification of the dorsal progenitor pools of the hindbrain. Indeed in *wnt1*; *wnt3a* double mutant mice, the hindbrain appeared to be correctly patterned along the dorsoventral axis, but there was a reduction in the dorsal-most progenitor pools, marked by *math1* and *pax3* (Ikeya et al., 1997). This was proposed to be due to a specific dependence of these pools on mitogenic Wnt signals. However, recent findings show that activation of the Wnt pathway causes tumours deriving from lower rhombic lip cells but that this was not due to increased proliferation in the lower rhombic lip (Gibson et al., 2010). Therefore, further work is required to determine the role of the Wnt signalling pathway in the specification and promotion of proliferation of dorsal neuronal cell types.

1.1.2.5 The roof plate and dorsal patterning of the diencephalon

Msx1 is a transcription factor that is a well described downstream effector of Bmp signalling (Timmer et al., 2002; Liu et al., 2004). *msx1* is expressed in the diencephalic roof plate and in *msx1*-/- mice the diencephalic roof plate is disrupted, particularly at the pretectum (Bach et al., 2003). This results in a downregulation of dorsolaterally expressed genes such as *pax6/7* and *lim1* in the diencephalon. Therefore the diencephalic roof plate is required for dorsolateral gene expression, however whether the reduction of dorsal gene expression is at the expense of more ventral gene expression is not known.

1.1.2.6 The roof plate and dorsal patterning of the telencephalon

The telencephalic roof plate sinks between the two cortical hemispheres and gives rise to three distinct subdomains (Shinozaki et al., 2004; reviewed in Chizhikov and Millen, 2005). From most lateral to most medial these are the cortical hem, the choroid plexus epithelium and the roof plate epithelium (Figure 1-4 C)(Shinozaki et al., 2004). A genetic ablation study in mouse showed that ablation of the roof plate and its derivatives by driving the expression of diphtheria toxin A subunit from the *gdf7*-locus resulted in a reduction in size of the cerebral cortices and a reduction of their dorsal – ventral graded *lhx2* expression (Monuki et al., 2001). Monuki et al. (2001) suggested that this effect was due to a loss of Bmp patterning signals from the roof plate as application of beads soaked in Bmp4 or Bmp2 to dorsal telencephalic explants could mimic the proposed action of the roof plate. Immediately adjacent to the beads, *lhx2* expression was downregulated (corresponding to the situation in the cortical hem and choroid plexus epithelium) whereas at a distance from the bead, *lhx2* expression was upregulated (corresponding to the dorsal – ventral graded expression of *lhx2* in the cortex).

The dorsal midline structures express multiple Bmps and the effects of Bmp2/4 *in vitro* on dorsal telencephalic explants prompted the further investigation of Bmp signalling in

dorsoventral patterning of the cerebral cortex (Furuta et al., 1997; Monuki et al., 2001; Shinozaki et al., 2004). However it was found that mice null for the Bmp receptor, *bmpr1a*, in the telencephalon display mostly normal dorsoventral patterning of the telencephalon (Hebert et al., 2002). The only phenotype observed in these mice was the specific loss of choroid plexus, as assessed by a reduction in the expression of the choroid plexus epithelial marker, *ttr*. In support of this, expression of a constitutively active form of *bmpr1a* throughout the ventricular zone of the brain results in the conversion of the telencephalic alar plate into choroid plexus, while the basal plate is unaffected (Panchision et al., 2001). These observations point towards a specific requirement for Bmp signals in the development of the choroid plexus, but do not support a dorsoventral gradient of Bmp signals that orchestrate global patterning of the telencephalon.

Multiple *wnt* genes are also expressed in the dorsal midline region, primarily in the cortical hem (Grove et al., 1998; Lee et al., 2000b; Shinozaki et al., 2004). Cortical hem expressed *wnt3a* has been shown to be essential for the development of the hippocampus, which develops from the domain immediately lateral from the cortical hem (Lee et al., 2000b). A loss of hippocampal neurons is also seen in mice mutant for the downstream Wnt pathway components, *lef1* and *β-catenin* (Galceran et al., 2000; Machon et al., 2003). Both studies support a role for Wnts in both the specification of cell types and the promotion of proliferation within the hippocampal fields.

The boundary between the pallium and the subpallium (PSB) expresses Wnt inhibitors, raising the possibility that a gradient of Wnt activity is established across the pallium between the hem and the PSB (which has also been called the ‘anti-hem’), which might serve to pattern the neocortex (Frowein et al., 2002; Assimacopoulos et al., 2003). However there is little evidence for a patterning role for Wnts in the pallium beyond the specification of the hippocampal fields (Chenn and Walsh, 2002; Hirabayashi et al., 2004; Muzio et al., 2005; Machon et al., 2007). The PSB also expresses several members of the epidermal growth factor family, transforming growth factor α, and FGF7 (Assimacopoulos et al., 2003), however the role of these signalling factors in dorsoventral patterning of the forebrain has yet to be determined.

1.1.3 Properties of secondary organisers

The secondary organisers described above that are resident within the neuroepithelium are mostly found at boundaries between molecularly distinguishable compartments of tissue, for example the anterior neural boundary (ANB), the zona limitans intrathalamica (ZLI) between the pre-thalamus and the thalamus, the midbrain-hindbrain boundary (MHB) and rhombomere boundaries (reviewed in Kiecker and Lumsden, 2005). The exceptions to this

are the roof plate and floor plate, which are located at boundaries between molecularly indistinguishable compartments (the two halves of the neural tube). Boundary-localised organisers display certain typical properties that reflect mechanisms required for their formation and maintenance. These properties are described below.

1.1.3.1 Lineage restriction

The identification of boundaries that compartmentalise tissues was first discovered in Drosophila. Clones of cells marked during Drosophila wing development were shown to respect certain lineage restriction boundaries that divide the wing primordium (the wing imaginal disc) into anterior-posterior and dorsal-ventral compartments (Garcia-Bellido et al., 1973; Morata and Lawrence, 1975; Garcia-Bellido et al., 1976). These boundaries were later demonstrated to be organisers that pattern the wing imaginal disc and direct its growth (reviewed in Irvine and Rauskolb, 2001). More recently, evidence for compartmentalisation within the developing vertebrate nervous system came from clonal analysis within the hindbrain, which demonstrated that rhombomere boundaries restrict cell mixing between rhombomeres (Fraser et al., 1990; Jimenez-Guri et al., 2010). The MHB has also been demonstrated to be a lineage restriction boundary in zebrafish and mouse embryos (Zervas et al., 2004; Langenberg and Brand, 2005), although evidence has been presented that it is not so in chick (Jungbluth et al., 2001). The ZLI is not composed of a single boundary but is a compartment in its own right, bounded anteriorly and posteriorly by lineage restriction boundaries (Larsen et al., 2001). Although its role as an organiser has not yet been formally demonstrated, the pallial – subpallial boundary (PSB) in the telencephalon has also been shown to be a boundary to cell movement (Fishell et al., 1993). It has been proposed that the function of lineage restriction at these boundary-localised organisers is to facilitate the maintenance of the organiser as a sharp, straight domain, thereby allowing consistent patterning to occur in the adjacent compartments by morphogen gradients emanating from the boundary (Irvine and Rauskolb, 2001).

1.1.3.2 Specialisations of cells, their organisation and rate of proliferation

Aside from the expression of signalling molecules, many boundaries in the developing CNS show certain specialised properties such as specialised extracellular matrix and a low rate of proliferation in comparison with cells within compartments (Baek et al., 2006). Studies have determined that the chick rhombomere boundaries and the ZLI share properties such as large extracellular spaces (Lumsden and Keynes, 1989; Heyman et al., 1993; Larsen et al., 2001), expression of the extracellular matrix component chondroitin sulphate proteoglycan (CSPG), the cell adhesion molecule NCAM or the radial glia marker Vimentin (Lumsden and Keynes, 1989; Heyman et al., 1995; Larsen et al., 2001), and a localisation of S-phase nuclei apically, rather than basally, within the ventricular zone (Guthrie et al., 1991; Larsen et al., 2001).

Another property associated with boundaries is a low level of proliferation. This has been demonstrated for the ZLI and the MHB in mouse (Trokovic et al., 2005; Baek et al., 2006) and the spinal cord roof plate and floor plate and the hindbrain rhombomere boundaries in mouse and chick embryos (Guthrie et al., 1991; Kahane and Kalcheim, 1998; Baek et al., 2006). Neuroepithelial organisers also display delayed or a lack of neurogenesis (Hirata et al., 2001; Bingham et al., 2003; Geling et al., 2003; le Roux et al., 2003; Geling et al., 2004; Ninkovic et al., 2005; Baek et al., 2006).

Therefore, boundaries in chick share a number of similar immunohistochemical markers such as CSPG, NCAM and Vimentin, although whether these also mark CNS boundaries in other organisms remains to be determined. A common feature of boundaries in many organisms is a low level of proliferation and a lack of neurogenesis. These are likely to reflect mechanisms that maintain boundaries as organisers.

1.1.3.3 Signalling across the boundary from adjacent compartments enables boundary formation and maintenance

The experimental recombination of tissues from adjacent compartments can induce the formation of organisers that are normally present at the boundaries between those compartments. Examples include the recombination of prospective pre-thalamus and thalamus inducing the formation of the ZLI *in vitro*, as assessed by the expression of *shh* (Guinazu et al., 2007), and the recombination of midbrain and hindbrain tissue *in vitro* and *in ovo*, inducing the formation of the MHB, as assessed by the expression of *fgf8* (Irving and Mason, 1999). Early experiments showed that the rhombomere boundaries of the chick could be regenerated upon juxtaposition of adjacent rhombomeres (Guthrie and Lumsden, 1991; Heyman et al., 1995), based on morphology and characteristic immunohistochemical markers. It should be noted, however, that the chick rhombomere boundaries have not yet been demonstrated as organisers of adjacent rhombomeres. Thus it is clear that signalling between juxtaposed compartment tissues can induce boundary cells at the interface between those juxtaposed compartments.

The mechanism that was originally investigated as mediating the processes of boundary formation and maintenance (and lineage restriction) between compartment tissues was differential cell affinity, which causes a sorting out of cells of different compartmental origin. Grafting and cell aggregation studies in avian embryos demonstrated the differential adhesive properties of alternating (odd and even-numbered) rhombomeres (Guthrie et al., 1993; Wizenmann and Lumsden, 1997). Subsequently it was demonstrated that repulsive interactions between Ephrins and Eph receptors could mediate cell sorting in zebrafish rhombomeres (Mellitzer et al., 1999; Xu et al., 1999; Cooke et al., 2001). The Eph receptor,

EphA4 has also been shown to be required for rhombomere boundary formation in zebrafish (Xu et al., 1995; Cooke et al., 2005). Although an instructive role of Eph–ephrin signalling for boundary formation has not yet been shown, the reconstitution of an ephrin-Eph interface resulted in a loss of gap junctions and cytoskeletal rearrangements, which are indicative of boundary formation (Xu et al., 1999; Cooke et al., 2001; Cooke and Moens, 2002).

A signalling pathway that has been shown to have an instructive role in the formation of boundary cells is the Notch signalling pathway. The Notch signalling pathway involves activation of transmembrane Notch receptors by transmembrane ligands of the Delta/ Serrate/ Lag2 [DSL] family, which results in the proteolytic cleavage of the Notch receptor and nuclear translocation of its intracellular domain (Notch ICD). The Notch ICD interacts with the DNA-binding protein CSL (named after CBF1, Su(H) and LAG-1) and activates transcription of Notch target genes such as the *hes* genes (reviewed in Bray, 2006). It has been implicated to act in numerous developmental situations, but usually in the context of regulating cell fate choices, such as in the process of lateral inhibition of neurogenesis (reviewed in Lewis, 1998) or in controlling the binary fate choice of neurogenic daughter cells in the ventral spinal cord, adopting either excitatory or inhibitory neuronal fates (Peng et al., 2007). However, as will be described, it is also involved in an inductive capacity in boundary formation and maintenance.

Although the Notch signalling pathway appears simple at first glance, there are in fact many different post-transcriptional mechanisms that regulate it (reviewed in Bray, 2006). Amongst these is c*is*-inhibition of Notch receptors by cell-autonomously expressed ligands (reviewed in del Alamo et al. 2011), which is proposed to amplify small differences between adjacent cells and thus facilitate the processes of lateral inhibition and the formation of sharp boundaries (Sprinzak et al., 2010). Ubiquitination of the ligands by the conserved E3-ubiquitin ligases, Neuralized and Mind bomb, which promotes ligand endocytosis, is required for ligand-driven Notch activation (Lai et al., 2001; Itoh et al., 2003). This highlights another layer of complexity of regulation via regulation of E3-ubiquitin ligase activity. Another important regulatory mechanism is glycosylation of the Notch receptor. The evolutionarily conserved Fringe family of proteins are glycosyl transferases that have been shown to extend carbohydrate chains on the EGF repeats of Notch receptors (Bruckner et al., 2000; Moloney et al., 2000). This modulates the ability of Notch to respond to its various ligands, for example in the developing Drosophila wing Fringe inhibits *trans*-activation of Notch by Serrate, but potentiates *trans*-activation by Delta (Fleming et al., 1997, Panin et al., 1997, Bruckner et al., 2000). Lunatic Fringe (Lfng), a vertebrate orthologue of Drosophila Fringe, has also been shown to inhibit *cis*-interactions of Notch

with Delta or Serrate (Sakamoto et al., 2002), which has been proposed to contribute to the mechanism of Lfng promotion of lateral inhibition (Nikolaou et al., 2009).

The importance of the Notch pathway in boundary formation and maintenance was first highlighted in the maintenance of lineage restriction at the dorsoventral compartment boundary of the Drosophila wing imaginal disc (Micchelli and Blair, 1999). Here an activated stripe of Notch signalling maintains the expression of the signalling molecule Wingless, which patterns and directs the growth of the wing (Diaz-Benjumea and Cohen, 1995; Rulifson and Blair, 1995). The stripe of activated Notch signalling is localised by the concurrent actions of the Notch ligands, Delta and Serrate. Serrate is expressed in dorsal compartment cells and specifically activates Notch signalling in cells immediately ventral to the boundary, while Delta is expressed in the ventral compartment and activates Notch signalling in cells immediately dorsal to the boundary (Diaz-Benjumea and Cohen, 1995; Kim et al., 1995; Doherty et al., 1996; de Celis and Bray, 1997). The action of Fringe serves to restrict Notch activation to the boundary. Fringe is expressed in the dorsal compartment and inhibits signalling through Notch by Serrate, but promotes Delta-Notch signalling, thereby restricting Notch activation by Serrate to the dorsoventral boundary (Fleming et al., 1997; Panin et al., 1997). Fringe has been implicated as a particularly important component of dorsoventral boundary formation as the ectopic juxtaposition of cells expressing and not expressing Fringe is sufficient to re-position the dorsoventral boundary (Irvine and Wieschaus, 1994; Kim et al., 1995; Panin et al., 1997; Rauskolb et al., 1999) (Figure 1-5).

Recently it has been shown that activation of Notch signalling by Serrate is necessary and sufficient to position the formation of the MHB in chick embryos, as assessed by the expression of the signalling molecules, *wnt1* and *fgf8* (Tossell et al., 2011). *lunatic fringe* (*lfng*) is a vertebrate homolog of Drosophila *fringe* (Moran et al., 1999). In striking similarity with the role of *fringe* at the dorsoventral boundary of the wing imaginal disc, Tossell et al. (2011) found that re-positioning the *lfng* expression border was also sufficient to re-position the MHB. The Notch signalling pathway has also been found to be essential for the maintenance of rhombomere boundaries in zebrafish (Cheng et al., 2004; Riley et al., 2004). The *delta* genes, *dlA, dlB* and *dlD*, are expressed in transverse stripes adjacent to rhombomere boundaries and are proposed to activate Notch within rhombomere boundaries to maintain them (Cheng et al., 2004; Riley et al., 2004). Interestingly, constitutive Notch pathway activation is not sufficient to induce rhombomere boundary formation (Cheng et al., 2004). Therefore in contrast with the dorsoventral boundary of the Drosophila wing imaginal disc and the chick MHB, Notch signalling is only involved in the maintenance of zebrafish rhombomere boundaries and not their formation.

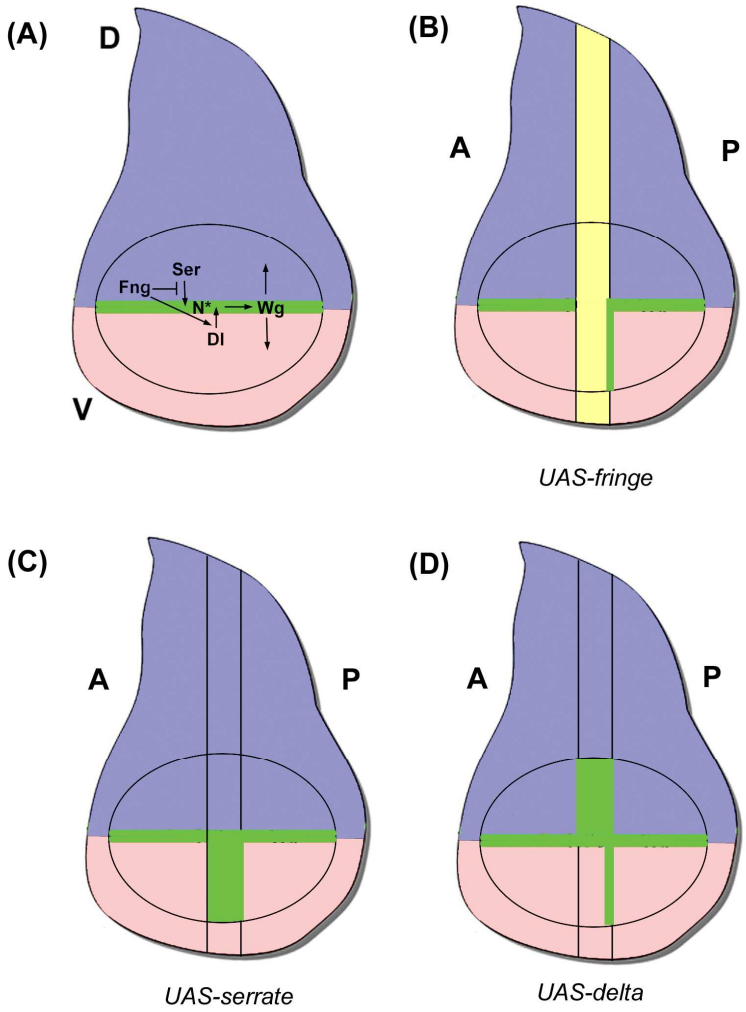
(A)
D
V
Ser
Fng
N*
Wg
Dl
(B)
A
P
UAS-fringe
(C)
A
P
UAS-serrate
(D)
A
P
UAS-delta

Figure 1-5 Schematic diagrams of signalling at the dorsoventral boundary of the Drosophila wing imaginal disc and experimental manipulations of Notch pathway genes

(A) Notch is activated (N*) at the dorsoventral boundary of the Drosophila wing imaginal disc by the concerted actions of Serrate (Ser) (expressed only in the dorsal [D] compartment) and Delta (Dl) (expressed in the ventral [V] compartment). Fringe (Fng) is only expressed in the dorsal compartment and restricts Notch activation to the boundary by inhibiting activation of Notch by Ser but potentiating the activation of Notch by Dl. Notch activation induces Wingless (Wg) expression. Wg patterns the wing primordium. Oval indicates the region that gives rise to the wing blade.

(B – D) summarise experiments carried out by Panin et al. (1997) and Doherty et al. (1996). *fringe* (B), *serrate* (C) or *delta* (D) are overexpressed in the *patched* expression domain (yellow) using the Gal4 – UAS overexpression system. The ectopic expression of *fringe* in the ventral compartment induces Wg expression at the border between *fringe*-negative and *fringe*-positive cells (B). Ectopic expression of *serrate* induces expression of Wg both within and adjacent to the overexpression domain in the ventral compartment (C). Overexpression of *delta* causes strong ectopic expression of Wg in the dorsal compartment and weaker ectopic expression in the ventral compartment (D). A, anterior; P, posterior.

Notch signalling has also been implicated in the formation or maintenance of the ZLI in chick embryos. The ZLI begins as an *lfng*-negative wedge between the *lfng*-positive prospective thalamus and pre-thalamus, which transforms into a narrow *shh*-expressing, *lfng*-negative domain (Zeltser et al., 2001). Ectopic expression of *lfng* within or across the ZLI abolishes *shh* expression and the lineage restriction normally seen at the borders of the ZLI (Zeltser et al., 2001). Thus, although the role of Notch signalling in the formation or maintenance of the ZLI has not been explicitly tested, it has been implied due to the essential role of an *lfng* expression border.

Thus Notch signalling across a boundary has been implicated in the formation or maintenance of the MHB, the ZLI and the rhombomere boundaries. This appears to be a conserved function of Notch signalling, conserved from chick to zebrafish embryos in the developing CNS, and involved in boundary-organiser maintenance and formation in Drosophila larvae.

1.1.3.4 Hes transcription factors

Hairy/ Enhancer of split (Hes) transcription factors are a family of repressor-type bHLH transcription factors (reviewed in Kageyama et al., 2008). They are well-known downstream effectors of Notch signalling, being essential in the maintenance of neural stem cells and inhibition of neurogenesis (Ohtsuka et al., 1999; Hatakeyama et al., 2004; reviewed in Kageyama et al., 2007). However, they have also been shown to play an essential role in the maintenance of boundary-localised organisers. While Hes1 expression is oscillatory in neural stem cells (Hirata et al., 2002; Shimojo et al., 2008), Baek et al. (2006) showed that in mice, boundaries in the CNS including the ZLI, MHB, rhombomere boundaries and the spinal cord roof plate and floor plate are characterised by the high and persistent expression of Hes1. In *hes1;hes3;hes5* triple-null mice, boundary-organisers such as the ZLI, the MHB and the spinal cord roof plate and floor plate are disrupted, as assessed by their nascent signalling molecules, *shh*, *fgf8* or *wnt1*, and ectopic neurogenesis occurs within the organiser domain (Baek et al., 2006). In this study it was not determined whether the disruption of boundary-localised organisers was due to disruption of its formation or its maintenance, however in *hes1*-/-; *hes3*-/- mice the MHB forms but fails to be maintained (Hirata et al., 2001). Therefore, it is likely that defects in boundary-localised organisers reported by Baek et al. (2006) in *hes1;hes3;hes5* triple-null mice was due to a lack of maintenance rather than formation.

In zebrafish, it has been shown that *hes* homologs, the *hairy-related* genes *her5* and *him*, are required for the maintenance of the MHB, to prevent ectopic neurogenesis there (Geling et al., 2003; Geling et al., 2004; Ninkovic et al., 2005). Thus the use of Hes transcription

factors in the maintenance of and prevention of ectopic neurogenesis within boundary-localised organisers is conserved from zebrafish to mice.

Although Hes genes are well known downstream effectors of Notch signalling, Geling et al. (2004) showed that the action of *her5* at the MHB was Notch-independent. Furthermore, *hes1* has been shown to function in Notch-independent pathways (Wall et al., 2009; Sanalkumar et al., 2010). Thus it has been suggested that the function of *hes* genes in the maintenance of boundary-organisers in the developing mouse CNS might also be Notch-independent (Kageyama et al., 2007), although this remains to be demonstrated.

1.2 Choroid plexus development

The role of the roof plate in the vertebrate CNS is not only as an organiser of the dorsal neuroepithelium. The roof plate is present along the entire anteroposterior axis of the CNS (Chizhikov and Millen, 2005). For the most part it constitutes a narrow strip of cells at the dorsal midline, but at certain regions it expands to form a thin epithelium that tents over a ventricle. This occurs at the lateral ventricles in the telencephalon, the third ventricle of the diencephalon, and the fourth ventricle situated in the hindbrain (Figure 1-4 A). The mechanisms that determine the anteroposterior locations of ventricle formation are not known, although studies in zebrafish have shown that the formation of ventricles requires apical junction- complex proteins and a sodium/potassium ion transporter (Lowery and Sive, 2005; Lowery et al., 2009). Cell division is also required for ventricle formation, and in *zic1* and *zic4* morphant embryos, a lack of fourth ventricle opening is correlated with a decrease in cell proliferation in the dorsal neuroepithelium (Lowery and Sive, 2005; Elsen et al., 2008).

At the ventricles the roof plate is not only expanded, but it also later transforms into the choroid plexus epithelium (reviewed in Dziegielewska et al., 2001). The choroid plexuses are a series of interfaces that form part of the blood-cerebrospinal fluid (CSF) barrier (reviewed in Johansson et al., 2008). CSF is the fluid that bathes the brain and the spinal cord and fills the ventricles. The choroid plexuses are responsible for the secretion of cerebrospinal fluid (CSF), regulating which molecules enter the CSF from the blood. The ventricle-CSF system functions during development and adulthood to provide physical protection for the brain and acts as a circulatory system, removing metabolites and distributing CSF-borne signalling molecules and nutrients (reviewed in Redzic et al., 2005). During development, the choroid plexuses secrete various growth factors and signalling molecules that stimulate the proliferation or differentiation of neural progenitors (Yamamoto et al., 1996; Redzic et al., 2005; Huang et al., 2010; Lehtinen et al., 2011). The telencephalic

choroid plexus has also been implicated in secreting chemorepulsive molecules, which function to orient neuronal migration (Hu, 1999; Nguyen-Ba-Charvet et al., 2004). Thus the choroid plexuses are important regulators of the internal environment of the brain and secrete molecules that are involved in patterning the development of the brain.

The choroid plexus is composed of two components: the choroid plexus epithelium and the heavily vascularised choroidal stroma. Early histological studies of mammals and other amniotes defined four stages of choroid plexus development on the basis of epithelial cell morphology and the glycogen content of cells (Dohrmann, 1970; Jacobsen et al., 1982; Dziegielewska et al., 2001). In summary, the pseudostratified epithelium of the roof plate invaginates and transforms into cuboidal epithelium known as choroid plexus epithelium, which undergoes complex morphological changes to form choroidal villi (reviewed in Dziegielewska et al., 2001). During this process of epithelial transformation both ingrowth of blood vessels and capillaries and angiogenesis within the choroidal stroma occurs (Strong, 1956; Dohrmann, 1970). In addition to changes in morphology the differentiation of choroid plexus epithelium can also be monitored by the expression of the *transthyretin* (*ttr*) gene, which encodes a thyroxine-binding protein (Thomas et al., 1988). In rat, *ttr* expression is first detected in the fourth ventricle, followed by the lateral and then the third ventricle choroid plexus epithelium (Thomas et al., 1988). In the fourth ventricle, *ttr* expression and patches of vascularisation appear in two lateral domains that later fuse to form a highly convoluted and vascularised structure at the midline of the roof plate that is symmetrical about the midline.

Recently genetic fate mapping studies in mice have shown that most, if not all of the fourth ventricle choroid plexus epithelium is derived from *gdf7*-positive, *wnt1*-positive progenitor pools at the lateral edges of the roof plate epithelium (the most dorsal neuroepithelium) (Awatramani et al., 2003; Currle et al., 2005; Landsberg et al., 2005; Hunter and Dymecki, 2007). These progenitor pools initially give rise to roof plate epithelium, which later transforms into choroid plexus epithelium. An elegant genetic fate-mapping study by Hunter and Dymecki (2007) described how the E11.5 roof plate epithelium can be subdivided into two domains, one medial and one lateral, with respect to whether they arose from *wnt1*-positive or *wnt1* and *gdf7*- positive progenitors, and whether they would contribute to the choroid plexus (Figure 1-6). Although initially the lateral progenitor domains contribute to roof plate epithelium that then transforms into choroid plexus epithelium, from E12.5 and throughout development, the lateral progenitor domains contribute directly to the choroid plexus epithelium (Hunter and Dymecki, 2007; Huang et al., 2009). At these stages the lateral progenitor pool is regulated by *shh* expressed by the choroid plexus epithelium itself

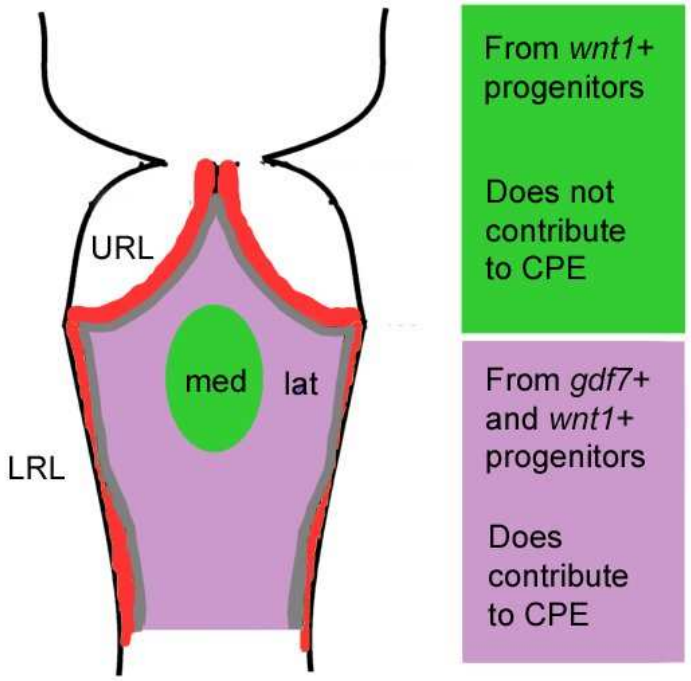

Figure 1-6 Subdivision of the roof plate epithelium into a medial and a lateral domain

Schematised diagram of a dorsal view of the mouse E11.5 roof plate epithelium showing subdivision into a medial (med) and a lateral (lat) domain. The medial domain (green) is derived from *wnt1*-positive progenitors and does not contribute to the choroid plexus epithelium (CPE), while the lateral domain (purple) is derived from *gdf7*-positive and *wnt1*-positive progenitors and does contribute to the CPE. Medial and lateral domains are non-mitotic so growth occurs via proliferation of progenitors at the lateral edges of the roof plate epithelium (grey lines). The rhombic lips (red) are subdivided into the upper rhombic lip (URL) and the lower rhombic lip (LRL).

(Huang et al., 2009). Thus the choroid plexus epithelium stimulates its own growth at later stages.

The diencephalic choroid plexus epithelium also arises from *gdf7*-positive progenitors, however only the anterior portion of the telencephalic choroid plexus epithelium receives contributions from *gdf7*-positive progenitors (Currle et al., 2005). Interestingly, the posterior portion of the telencephalic choroid plexus epithelium requires non-autonomous signals from the anterior portion for its development (Currle et al., 2005). These signals are likely to be BMPs as the BMP-responsive gene, *msx1* is downregulated in the posterior telencephalic choroid plexus epithelium after the ablation of the *gdf7*-positive progenitor-derived anterior domain (Currle et al., 2005).

Recent time-lapse studies of zebrafish choroid plexus development gave detailed insights into the process of choroid plexus epithelium differentiation and blood vessel ingrowth in zebrafish (Bill et al., 2008; Garcia-Lecea et al., 2008). Garcia-Lecea et al. (2008) described this process in three phases. In the first two phases the tela choroidea, a monolayered epithelial sheet, formed from the roof plate of the fourth ventricle and was contributed to by cells emerging from the rhombic lip. The third phase consisted of the tela choroidal cells converging on a distinct point forming a tight, rounded structure that obeyed anteroposterior and mediolateral boundaries. A choroidal vascular circuit dorsal to the choroid plexus epithelium also formed in this third stage via the branching of the dorsal longitudinal vein. Garcia-Lecea et al. 2008 did not observe any sprouting of capillaries from the choroidal vascular circuit into the choroid plexus epithelium, however Bill et al. 2008 have reported that this does occur. Whether these capillaries are orthologous to the fenestrated capillaries found in amniote choroid plexuses remains to be determined. *De novo* angiogenesis, as occurs in the developing amniote choroid plexus (Dohrmann, 1970), was not observed to contribute to the formation of the zebrafish choroid plexus capillary bed. Another difference between zebrafish and mammalian fourth ventricle choroid plexus development is that the mammalian choroid plexus differentiates from two lateral domains that later fuse, whereas the zebrafish choroid plexus epithelium differentiates at the midline of the roof of the fourth ventricle (Strong, 1956; Thomas et al., 1988; Bill et al., 2008; Garcia-Lecea et al., 2008).

1.2.1 Coordination of choroid plexus development

Despite its vital function, little is known about what mechanisms coordinate the development of the choroid plexus. It is known that the areas of the neural tube destined to give rise to choroid plexus epithelium are specified as early as E8.5 in mice, before the formation of ventricles, whereas the first choroid plexus epithelial cells differentiate at E9.5 (Thomas and Dziadek, 1993; Hunter and Dymecki, 2007). Experiments in avian embryos showed that

transplantation of E2/ E3 prospective choroid plexus epithelium to the body-wall resulted in the normal differentiation of the epithelium into choroid plexus epithelium, but also induced the body-wall mesenchyme to give rise to fenestrated capillaries, typical of the choroid plexus (Wilting and Christ, 1989). However the converse was not true. The transplantation of non-choroid plexus-forming neuroepithelium onto prospective choroid plexus-forming mesenchyme did not induce the differentiation of choroid plexus epithelium. These studies and the observation that *gdf7*-positive progenitors give rise to all of the diencephalic and hindbrain choroid plexus epithelium might lead one to conclude that all progeny of the *gdf7*-domain are pre-specified as choroid plexus epithelium and do not require inductive signals from external tissues. However, the timing of differentiation of the choroid plexus epithelium must still be regulated. Additionally the above is not sufficient to explain how the posterior portion of the telencephalic choroid plexus epithelium, which does not arise from *gdf7*-positive progenitors, develops (Currle et al., 2005). Indeed Currle et al. (2005) have shown that the posterior portion of the telencephalic choroid plexus epithelium requires non-autonomous signals (probably Bmps) from the anterior portion. It would be interesting to see if any non-autonomous signals are required for the early differentiation of the diencephalic and hindbrain choroid plexus epithelium.

As stated above, the prospective choroid plexus epithelium could induce the formation of organ-typical capillaries from body-wall mesenchyme in avian embryos (Wilting and Christ, 1989), however the signal responsible for this induction has yet to be determined. It has been shown that *shh* from the choroid plexus epithelium is required for vascular outgrowth in the mouse fourth ventricle choroid plexus (Nielsen and Dymecki, 2010). However organ-typical blood vessels are still present within the choroid plexus of *shh* mutant mice so this signal is not required for the original ingrowth of blood vessels and the specification of organ-typical capillaries. Thus the signals involved in the promotion of blood vessel ingrowth and the specification of choroid plexus capillaries have yet to be defined.

1.3 Re-examining the organiser properties of the roof plate

As detailed above most secondary organisers in the developing CNS are boundaries between two molecularly distinguishable compartments. The roof plate and the floor plate do not fit into this model; at spinal cord levels the roof plate and floor plate are boundaries between molecularly indistinguishable compartments (the two halves of the neural tube), and at the brain ventricles the roof plate is expanded to form an epithelial sheet that tents over the ventricle. This is most obvious at the fourth ventricle where the roof plate forms a large diamond shape (Figure 1-4 B). Furthermore, the roof plate of the ventricles gives rise to choroid plexus epithelium, however the consequence of this for its organiser function has not

been assessed. In this thesis I considered the hypothesis that the organiser properties of the roof plate are situated at its boundaries with the neuroepithelium. In order to study this I focussed on the chick fourth ventricle roof plate as the roof plate is greatly expanded at this location and therefore provides an easily accessible region for experimental manipulation of its boundaries. Through my consideration that the organiser properties of the hindbrain roof plate are located at its boundaries it was discovered that the roof plate boundaries contribute non-autonomous signals required for choroid plexus epithelium development.

Chapter 2 A study of gene expression patterns at the hindbrain roof plate boundary

2.1 Background

The roof plate is an organiser present at the dorsal midline of the neural tube along the entire antero-posterior axis of the CNS (reviewed in Chizhikov and Millen, 2005). The function of the roof plate as an organiser has been best studied in the spinal cord where genetic deletion experiments led to a loss of the three dorsal-most groups of neuronal cell types (dI1-3) and their progenitor domains (marked by *math1*and *ngn1*). This was accompanied by a compensatory increase in the more ventral neuronal types (dI4-6) and the *mash1* (mouse *achaete-scute homolog 1*) –positive progenitor domain (Lee et al., 2000a). The main candidates for the dorsalising signals emitted by the roof plate are BMP and Wnt proteins, which are strongly expressed along its entire extent.

In the chick, the ability of the roof plate to induce dorsal neuronal cell types has been shown to be mimicked by the application of roof plate-expressed BMP family members such as Bmp4, Bmp5, Bmp6, Bmp7 and Gdf7 (also known as Bmp12) (Liem et al., 1997; Lee et al., 1998; Chizhikov and Millen, 2004a). Further application of the Bmp inhibitors Noggin and Follistatin inhibited the ability of the roof plate to induce dorsal interneurons *in vitro* (Liem et al., 1997; Lee et al., 1998). Electroporation studies in chick have shown that expansion of the roof plate by overexpression of Lmx1b can induce dI1 neurons adjacent to the expanded roof plate, at the expense of dI2 – 6 interneurons, and that this signalling capacity was mediated by Bmp signalling (Chizhikov and Millen, 2004a). Conversely, knockdown of *smad4*, an essential downstream signal transduction component of BMP signalling, resulted in a reduction of dI1-3 interneurons and their progenitor domains, but an expansion of dI4-6 and their progenitor domains (Chesnutt et al., 2004). Genetic deletion studies in mice have not revealed much of a role for individual Bmps in specification of dorsal neural cell types, presumably due to the redundancy between Bmp family members (Chizhikov and Millen, 2005). However, genetic loss of *gdf7* results in a loss of a specific subset of dI1 interneurons (formerly known as D1A) in mouse (Lee et al., 1998). Thus Bmp signals, and particularly *gdf7* in mice, are necessary and sufficient for the specification of dorsal interneuron cell types in chick and mouse.

The Wnt signals, Wnt1 and Wnt3a are specifically expressed in the spinal cord roof plate and were previously thought to play a mostly mitogenic rather than a patterning role in the development of the dorsal spinal cord (Dickinson et al., 1994; Megason and McMahon,

2002; Chesnutt et al., 2004). However, in mouse it was shown that genetic knockdown of *wnt1* and *wnt3a* caused a specific reduction in dI1-3 neurons with a compensatory increase in more ventral interneurons (Muroyama et al., 2002). Further, application of Wnt3a to the medial region of the chick neural plate could induce dI1 and dI2 neuronal production, without the involvement of BMP signalling. More recently it has also been demonstrated in chick and zebrafish embryos that Wnt signalling is required for the dorsoventral patterning of the spinal cord (Alvarez-Medina et al., 2008; Bonner et al., 2008). Alvarez-Medina et al. (2008) showed that co-electroporation of *wnt1* and *wnt3a* in the chick caused a ventral expansion of dorsal progenitor domains and dI2-4 interneuron populations at the expense of the more ventral dI6 interneurons, ventral V0 – 1 interneurons and motor neurons. Wnt1/ Wnt3a were shown to antagonise Shh signalling to orchestrate the dorsoventral patterning of the spinal cord neural tube. Thus in chick and mouse embryos Wnt1 and Wnt3a play important roles in dorsoventral patterning of the spinal cord.

Previous work has shown that organisers in the developing vertebrate CNS are generally located at boundaries between compartments of tissue that are molecularly distinguishable from each other, for example the isthmus at the midbrain-hindbrain boundary, the zona limitans intrathalamica (ZLI) at the pre-thalamus – thalamus boundary and the rhombomere boundaries (Kiecker and Lumsden, 2005). For the most part, the roof plate is comprised of a narrow strip of cells at the dorsal midline that separates two molecularly indistinguishable halves of the neural tube, for example at spinal cord or midbrain level (Chizhikov and Millen, 2004c; Chizhikov and Millen, 2005). However at certain locations such as the hindbrain the roof plate is expanded to form a thin epithelium that tents over a ventricle. Thus the hindbrain provides a particularly amenable region to study whether roof plate organiser properties are localised to its boundaries and hence whether the roof plate also conforms to the model stated above.

At hindbrain level, the roof plate has been shown in the mouse to be required specifically for the specification of the dorsal-most neural progenitor pool of rhombomere 1, which is marked by Math1, while it is only required to regulate proliferation of more ventral cell-types (Chizhikov et al., 2006). Ectopic roof plate was also sufficient to induce or expand the Math1 domain, and Chizhikov et al. (2006) showed that this induction was dependent on BMP signals. Previous studies have also demonstrated the importance of BMP family members in the induction of Math1-positive cells as Gdf7, Bmp6 and Bmp7 can induce Math1-positive cells *in vitro* and the BMP receptors, Bmpr1a and Bmpr1b, are required in a redundant fashion for the specification of the cerebellar granule cells (derived from Math1-positive progenitors), but not the Purkinje cells, which are derived from the slightly more

ventrolateral Ptf1a -positive progenitor pool of the rhombomere 1-derived cerebellar anlage (Alder et al., 1999; Wingate and Hatten, 1999; Chizhikov et al., 2006; Qin et al., 2006).

The hindbrain roof plate is not only an organiser, but it also gives rise to the hindbrain choroid plexus epithelium later in development (reviewed in Dziegielewska et al., 2001). The choroid plexuses are a series of interfaces that contribute to the 'blood-cerebrospinal fluid barrier' and are essential for the secretion of cerebrospinal fluid (Dziegielewska et al., 2001; Redzic et al., 2005). Thus they are essential for the regulation of the internal environment of the developing brain. Despite their importance, the development of the chick choroid plexuses has not been well documented.

In this chapter, I describe in hindbrain the expression of mRNA of candidate roof plate signalling molecules, Notch signalling pathway components and markers of the developing choroid plexus. I find that the expression of *gdf7* in the chick definitively marks the hindbrain roof plate epithelium – neuroepithelium boundary from E3 until at least E6 (the latest age analysed) and that this expression pattern might be explained by the distribution of Notch signalling pathway components and chick *hes1*orthologues. The development of the chick hindbrain choroid plexus epithelium from the roof plate epithelium was assessed by the expression patterns of: *transthyretin* (*ttr*), a thyroxine-binding protein that represents a well-established marker of the differentiated choroid plexus epithelium (Thomas et al., 1988; Duan et al., 1991), *cytochrome P450 26C1* (*cyp26C1*), which encodes a retinoic acid metabolising enzyme that is strongly expressed in the hindbrain roof plate epithelium in chick (Reijntjes et al., 2004; Wilson et al., 2007) and *orthodenticle homeobox 2* (*otx2),* which encodes a homeodomain-containing transcription factor that has been shown to be expressed in the mouse and chick telencephalic choroid plexus epithelium (Shinozaki et al., 2004; von Frowein et al., 2006). These expression patterns showed that the chick choroid plexus epithelium differentiates at E4 in a specific pattern within the hindbrain roof plate, but also that *cyp26C1* expression marks sites of prospective choroid plexus epithelium differentiation.

2.2 Results

2.2.1 *gdf7* expression marks the boundaries between roof plate epithelium and hindbrain neuroepithelium in chick

In the chick, *gdf7* is specifically expressed by the roof plate at the dorsal midline of the neural tube from E3, and is still expressed at E6 (the latest stage examined). In the midbrain it can be seen as a double stripe at the dorsal midline (Figure 2-1 A, C arrowheads), whereas at the hindbrain it marks the boundary between the hindbrain neuroepithelium and the expanded roof plate epithelium persistently from E3 to E6 (the latest stage examined), at the level of both the upper and lower rhombic lip (Figure 2-1 A – H, arrows). This can be seen more clearly by taking transverse sections through embryos. At the level of both the upper and lower rhombic lip at E3 and E4, *gdf7* is expressed at the interface between the roof plate epithelium and the hindbrain neuroepithelium (Figure 2-2 A – D, G – J, arrows). More specifically, its domain of expression lies at the dorsal-most tip of the pseudostratified epithelium.

A transverse section through the spinal cord of an E3 embryo shows that *gdf7* expression is present as two stripes at the dorsal midline, like in the midbrain (Figure 2-1 A, arrowhead, Figure 2-2 E, F). Three *gdf7*-negative cells can be seen separating the two domains of *gdf7* expression (Figure 2-2 F open arrow). A section through the midbrain of an E4 embryo again shows *gdf7* expression at the dorsal midline, but in this section a *gdf7*-negative zone at the medial roof plate is not visible even though *gdf7* also appears as two stripes in the midbrain at E4 by whole-mount *in situ* hybridisation (Figure 2-1C arrowhead, Figure 2-2 K, L). This may be due to the thickness of the section (40µm) being too high to discern the small number of *gdf7*-negative cells.

gdf7 expression at the hindbrain roof plate-boundary is immediately adjacent to the dorsal-most neural progenitor domain, which is marked by the expression of *cath1* (Figure 2-2 M – P). Cells do not co-express these markers, which is consistent with the *gdf7* and *math1* (the mouse homolog of *cath1*) lineage-tracing mice, which show that *gdf7*-expressing progenitors only give rise to roof plate, whereas *math1*-expressing progenitors only give rise to neurons (Landsberg et al., 2005; Machold and Fishell, 2005; Wang et al., 2005; Hunter and Dymecki, 2007).

As *gdf7* marks an inducer of the *math1*-positive neural progenitor pool in mice (Alder et al., 1999; Lee et al., 2000a; Chizhikov et al., 2006) I hypothesised that its expression must precede that of *cath1*in chick embryos. To investigate this I examined the expression of *gdf7* in relation to *cath1* in the hindbrain of embryos from st10 (E2) (just after neural tube

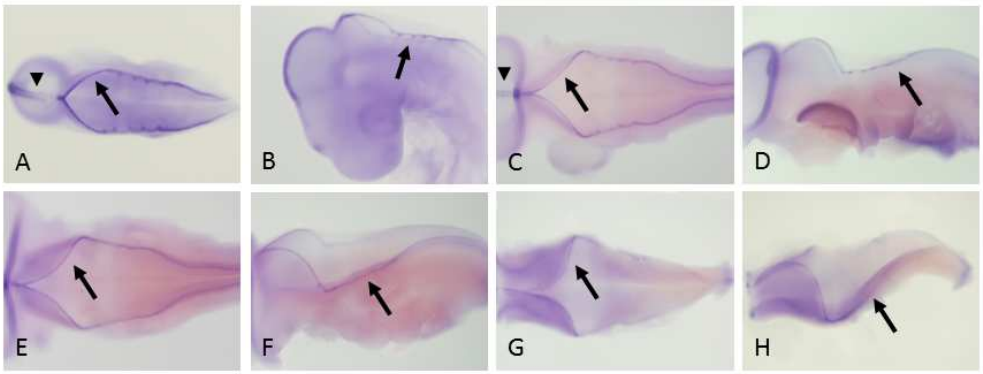

Figure 2-1 Whole-mount *gdf7* expression in E3 – E6 chick embryos

gdf7 expression as detected by whole-mount *in situ* hybridisation in E3 (A,B), E4 (C,D), E5 (E,F) and E6 (G,H) chicken embryos. A,C,E,G show dorsal views. B,D,F,H show lateral views. Anterior is to the left. Arrowheads indicate midbrain *gdf7* expression. Arrows in A, C, E, G indicate *gdf7* expression at upper rhombic lip level. Arrows in B, D, E, H indicate *gdf7* expression at lower rhombic lip level.

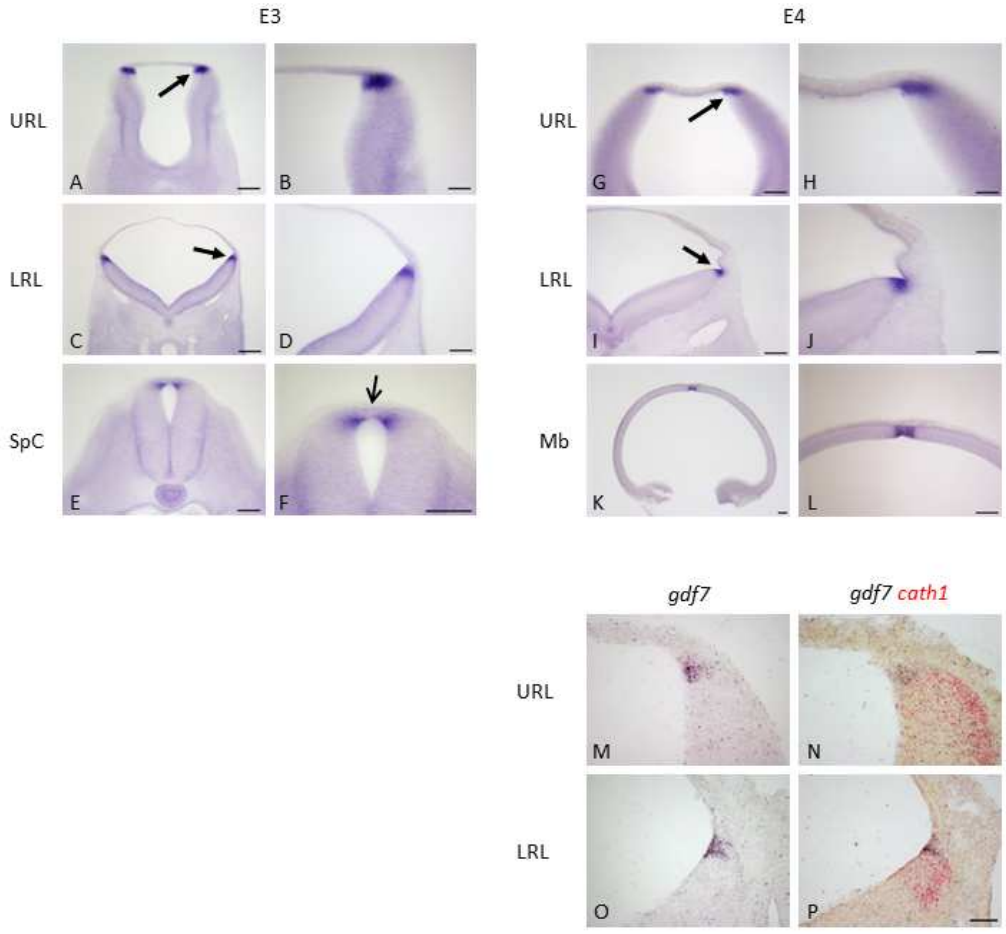

Figure 2-2 *gdf7* expression in chicken hindbrains sectioned in the transverse plane

A – F show sections through an E3 embryo. G – P show sections through E4 embryos. A – M and O show *gdf7* expression as detected by *in situ* hybridisation. N and P show *gdf7* and *cath1* expression as detected by double *in situ* hybridisation. A – L are vibrotome sections of embryos processed by whole-mount *in situ* hybridisation. M – P are serial cryostat sections that were processed for in situ hybridisation. Dorsal is oriented upwards. Arrows indicate *gdf7* expression at the hindbrain roof plate epithelium – neuroepithelium interface. Open arrow indicates *gdf7*-negative domain in spinal cord roof plate. URL: upper rhombic lip, LRL: lower rhombic lip, SpC: Spinal Cord, Mb: midbrain.

Scale bars: A, C, G, I, K: 100µm, B, D – F, H, J, L – P: 50µm.

closure) to st17 (E3). *gdf7* and *cath1* are not expressed at st10 (Figure 2-3 A). *gdf7* begins to be expressed in the midbrain by st13 (E2) (Figure B arrow), whereas it and *cath1* expression are still absent from the hindbrain at this stage (Figure 2-3 B). *gdf7* expression begins in the hindbrain at st14 (E3) at the level of the upper rhombic lip (Figure 2-3 C arrow) but *cath1* expression is still absent at this stage. By stage 16, *cath1* begins to be expressed in the hindbrain and *gdf7* expression is clearly visible in the hindbrain and midbrain (Figure 2-3 D arrow, hindbrain; arrowhead, midbrain). By stage 17 both *gdf7* and *cath1* are expressed strongly in the hindbrain and *gdf7* expression is also visible in the diencephalon (Figure 2-3 E arrow, diencephalon).

2.2.2 Expression of *bmp4, bmp7 and wnt1* at the hindbrain roof plate epithelium – neuroepithelium boundary

gdf7 expression was compared to that of *bmp4*, *bmp7* and *wnt1* in the chick hindbrain and midbrain roof plate first by whole-mount *in situ* hybridisation. *bmp4* is not expressed in the midbrain or hindbrain roof plate at E4 or E5 but expression is detectable in the pharyngeal arches (Figure 2-4 A – D, arrows, pharyngeal arches) (Kriebitz et al., 2009). *bmp7* is expressed by the midbrain roof plate at E4 and E5, but is not distinguishable by whole-mount *in situ* hybridisation in the hindbrain roof plate epithelium or roof plate boundary (Figure 2-4 E – G, arrowhead, midbrain roof plate). Like *bmp4*, *bmp7* expression is present in the pharyngeal arches (Figure 2-4 F arrow). *wnt1* is clearly expressed by both the midbrain roof plate and the hindbrain roof plate boundary at E4 and E5 (Figure 2-4 I – L, arrowheads: midbrain expression, arrows: hindbrain roof plate boundary expression), although there is an antero-posterior gradient of expression along the rhombomere 1 roof plate boundary at E4 (Figure 2-4 I, open arrow).

Since *wnt1* was expressed at the hindbrain roof plate boundary I compared its expression with that of *gdf7* by performing *in situ* hybridisation on serial transverse cryostat sections from an E4 embryo. *wnt1* is highly expressed in the *gdf7* expression domain at the level of both the upper and lower rhombic lip (Figure 2-5 B, E, arrows). However, it is also expressed at a lower level in the adjacent dorsal neuroepithelium at the level of the lower rhombic lip (Figure 2-5 E arrowhead), which is the same as in the mouse (Landsberg et al., 2005).

Since *bmp7* was clearly expressed in the midbrain roof plate at E4 and E5 but its expression could not be easily distinguished in the hindbrain roof plate I performed *in situ* hybridisation on serial transverse cryostat sections of an E4 embryo to compare the expression of *bmp7* in the hindbrain roof plate with that of *gdf7*. *bmp7* was expressed in the roof plate epithelium and *gdf7*-domain at both upper and lower rhombic lip levels (Figure 2-5 C, F, arrows). At the

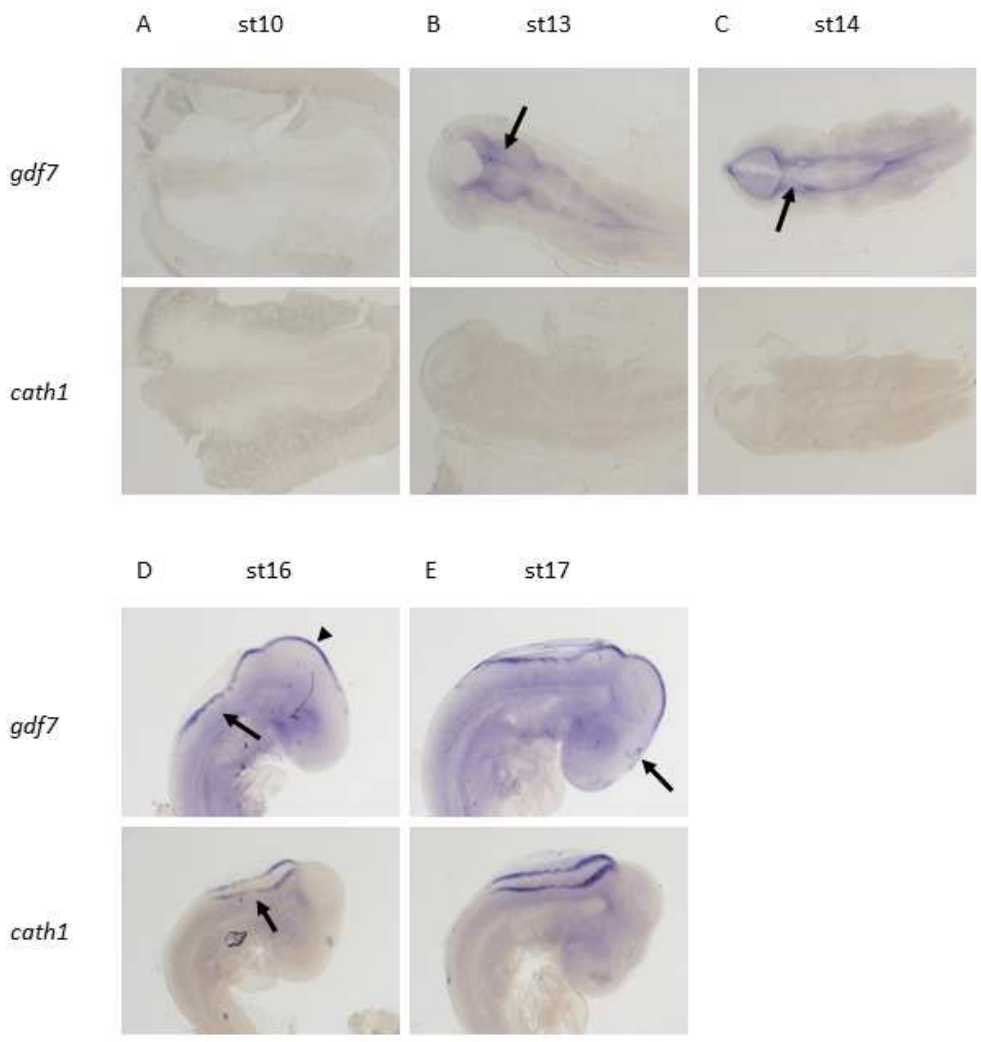

Figure 2-3 Early *gdf7* and *cath1* expression

gdf7 and *cath1* expression (as labelled) as detected by whole-mount *in situ* hybridisation at st10 (A), st13 (B), st14 (C), st16 (D), st17 (E). A – C show dorsal views with anterior to the left. D, E show lateral views with anterior to the right. B, arrow, midbrain *gdf7* expression. C, arrow, upper rhombic lip *gdf7* expression. D, arrows indicate hindbrain *gdf7* or *cath1* expression as indicated; arrowhead, midbrain *gdf7* expression. E, arrow, diencephalic *gdf7* expression.

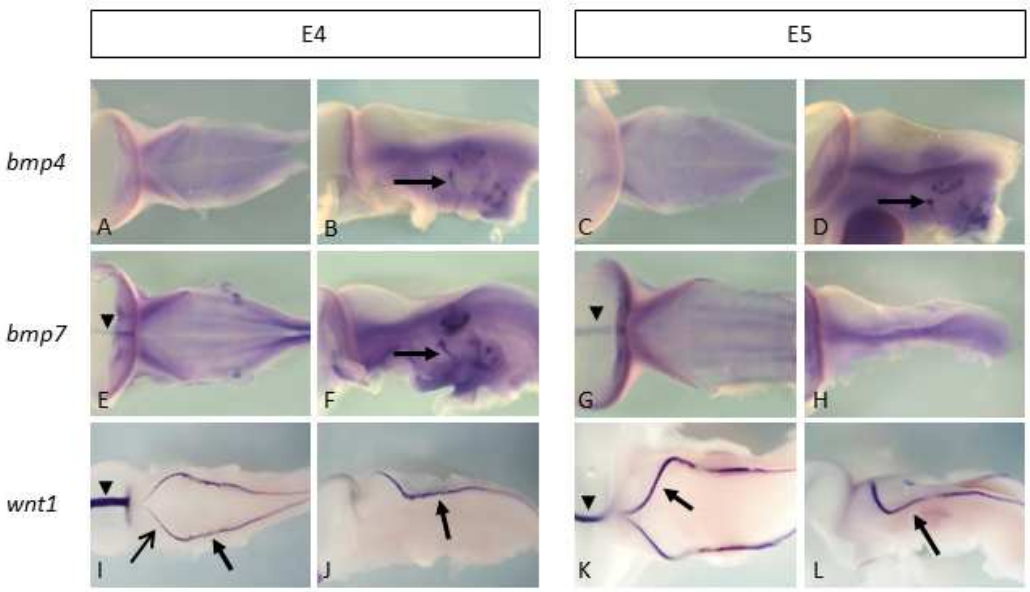

Figure 2-4 Whole-mount expression of *bmp4*, *bmp7* and *wnt1* in E4 and E5 embryos

A - D show *bmp4* expression, E – H show *bmp7* expression and I – L show *wnt1* expression as detected by whole-mount *in situ* hybridisation. A, C, E, G, I, K show dorsal views. B, D, F, H, J, L show lateral views. A, B, E, F, I, J show E4 embryos. C, D, G, H, K, L show E5 embryos. B, D, arrows, pharyngeal arch *bmp4* expression. F, arrow, pharyngeal arch *bmp7* expression. E, G, arrowheads, midbrain *bmp7* expression. I, K, arrowheads, midbrain *wnt1* expression; I – L, arrows, hindbrain roof plate boundary expression of *wnt1*. I, open arrow, anteroposterior gradient of *wnt1* expression along rhombomere 1.

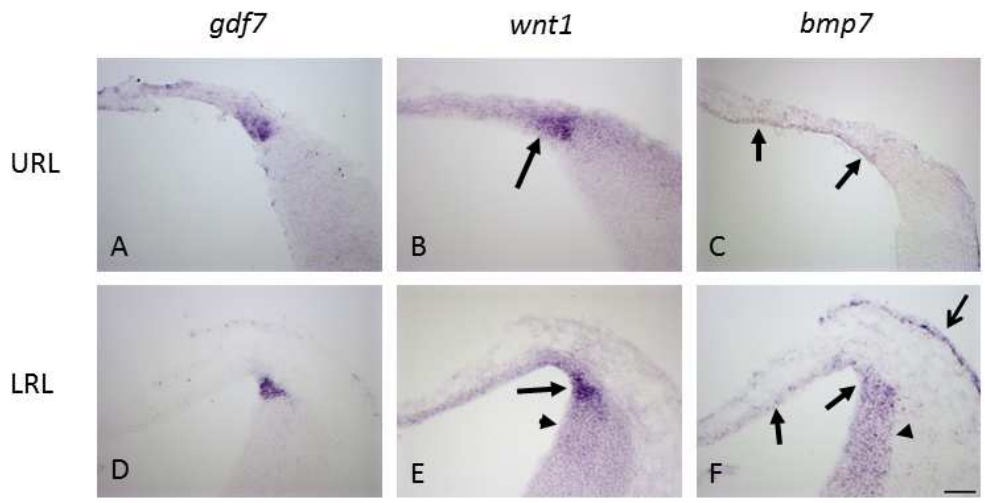

Figure 2-5 Expression domains of *wnt1* and *bmp7* in comparison with that of *gdf7*

Expression of *gdf7* (A, D), *wnt1* (B, E) and *bmp7* (C, F) as detected by *in situ* hybridisation performed on transverse, serial cryostat sections through the upper rhombic lip (A – C) or lower rhombic lip (D – F) of an E4 embryo. B, E, arrows, *wnt1* expression at the roof plate boundary. C, F, arrows, roof plate *bmp7* expression. E, arrowhead, dorsal neuroepithelium *wnt1* expression. F, arrowhead, dorsal neuroepithelium *bmp7* expression, open arrow, epidermis *bmp7* expression. URL: upper rhombic lip, LRL: lower rhombic lip.

lower rhombic lip it was also expressed in the neuroepithelium and was detected in the epidermis (Figure 2-5 F, arrowhead, neuroepithelium; open arrow, epidermis).

Thus of the morphogenetic proteins *bmp4*, *bmp7*, *wnt1* and *gdf7*, *gdf7* was the most specific marker of the hindbrain roof plate epithelium – neuroepithelium boundary in chick, although *wnt1* also exhibited a very similar expression pattern, with the exceptions of its antero-posterior graded expression at upper rhombic lip level and the low level expression domain in the adjacent neuroepithelium at lower rhombic lip level.

2.2.3 The chick *hes1* orthologues, *chairy1* and *chairy2* are persistently expressed at high levels at the roof plate epithelium – hindbrain neuroepithelium boundary

In mice Hairy/ Enhancer of split 1 (Hes1), which is a repressor-type bHLH transcription factor, is highly and persistently expressed at boundary-localised signalling centres in the developing central nervous system (Baek et al., 2006). *chairy1* and *chairy2* are the chick orthologues of *hes1*(Jouve et al., 2000) so their expression at the roof plate epithelium – hindbrain neuroepithelium boundary was examined to see if this boundary was also marked by characterised markers of boundary-localised signalling centres.

At stage 11 (E2), a diamond of high *chairy1* expression is visible in the prospective hindbrain (Figure 2-6 B arrow) as well as in the rest of the neuroepithelium, the presomitic mesoderm and Hensen's node (Figure 2-6 A, arrowheads: neuroepithelium, open arrowhead: presomitic mesoderm, open arrow: Hensen's node). At stage 11, *chairy2* is expressed fairly ubiquitously throughout the neural tube, but like *chairy1* it is also expressed in the presomitic mesoderm and Hensen's node (Figure 2-6 C, D, arrowheads: neural tube, open arrowhead: presomitic mesoderm, open arrow: Hensen's node).

By stage 18 (E3) *chairy1* expression clearly marks the roof plate epithelium – hindbrain neuroepithelium boundary as well as the floor plate (Figure 2-6 E, F, arrows: roof plate epithelium – hindbrain neuroepithelium boundary, arrowhead: floor plate). *chairy1* is also expressed in two uneven stripes along the antero-posterior axis in the hindbrain neuroepithelium (Figure 2-6 E, open arrowheads). At this stage, *chairy2* is expressed throughout the neuroepithelium and an elevated level of expression at the roof plate epithelium – hindbrain neuroepithelium boundary is not yet apparent (Figure 2-6 H). A lack of expression at the dorsal midline of the midbrain and in the floor plate is apparent, as are two stripes of elevated *chairy2* expression in the hindbrain neuroepithelium, similar to those of *chairy1* (Figure 2-6 G open arrow: midbrain roof plate, arrowhead: floor plate, open arrowheads: stripes of elevated *chairy2* expression).

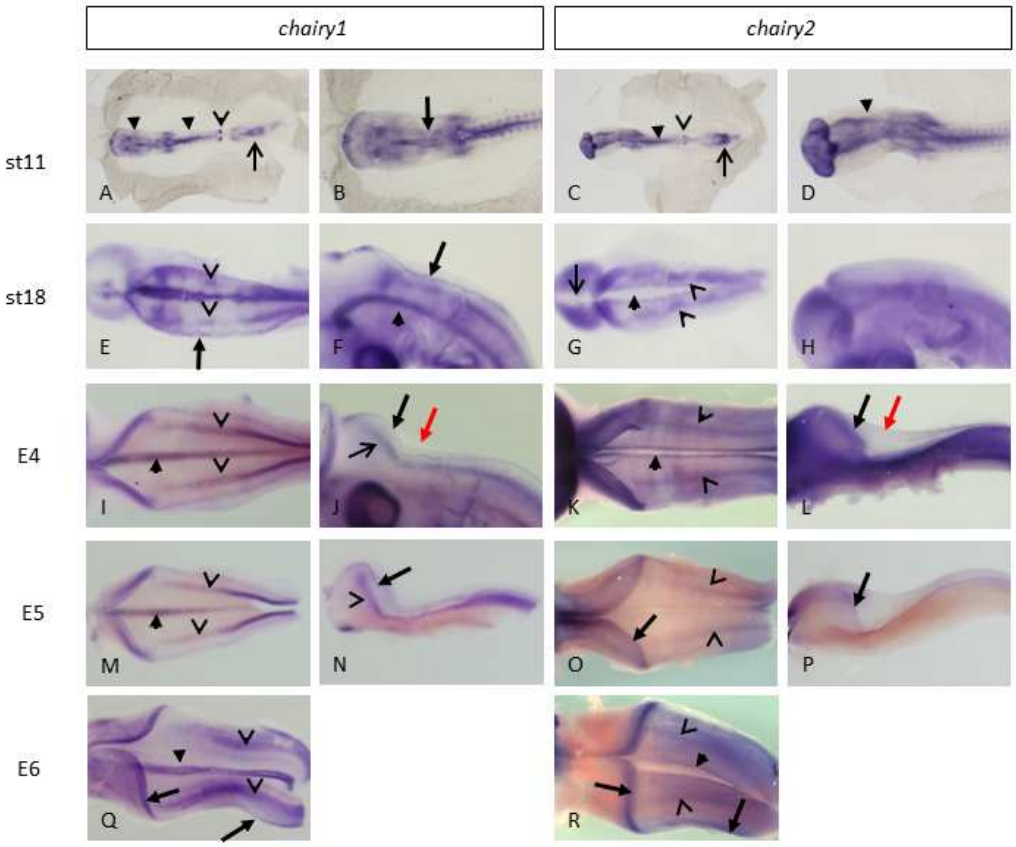

Figure 2-6 Whole-mount expression of *chairy1* and *chairy2* from st11 (E2) to E6

chairy1 (A, B, E, F, I, J, M, N, Q) and *chairy2* (C, D, G, H, K, L, O, P, R) expression as detected by whole-mount *in situ* hybridisation in st11 (E2)(A – D), st 18 (E3)(E – H), E4 (I – L), E5 (M – P) and E6 (Q, R) chick embryos. A-E, G, I, K, M, O, Q, R show dorsal views. F, H, J, L, N, P show lateral views. Anterior is oriented to the left in all images. A – D, arrowheads, neuroepithelium; open arrow, Hensen's node; open arrowhead, presomitic mesoderm. B, arrow, diamond of expression overlying the prospective hindbrain. E – R, arrows, hindbrain roof plate epithelium - neuroepithelium boundary; open arrowheads, longitudinal hindbrain stripes; arrowheads, floor plate. G, open arrow, midbrain roof plate. J, open arrow, rhombomere 1 longitudinal hindbrain stripe. J, L, red arrows, lack of expression in the roof plate epithelium.

At E4 *chairy1* expression still marks the roof plate epithelium – hindbrain neuroepithelium boundary and the floor plate (Figure 2-6 I, J arrow: roof plate epithelium – hindbrain neuroepithelium boundary, arrowhead: floor plate). Expression in the longitudinal hindbrain stripes has become more even along the antero-posterior axis and extends into rhombomere one by this stage (Figure 2-6 I, J, open arrowheads: longitudinal hindbrain stripes, open arrow: longitudinal hindbrain stripe in rhombomere 1). There is clearly no expression of *chairy1* in the roof plate epithelium (Figure 2-6 J red arrow).

By E4, *chairy2* is expressed throughout the hindbrain neuroepithelium but now shows elevated expression at the boundaries of the floor plate and at the roof plate epithelium – hindbrain neuroepithelium boundary (Figure 2-6 K, L, arrowhead: floor plate boundary, arrow: roof plate epithelium – hindbrain neuroepithelium boundary). The domain of elevated *chairy2* expression is broader than the expression domain of *chairy1* at the roof plate epithelium – hindbrain neuroepithelium boundary. Like *chairy1*, *chairy2* also shows two longitudinal stripes of elevated expression in the hindbrain neuroepithelium (Figure 2-6 K open arrowheads). *chairy2* is not expressed in the roof plate epithelium (Figure 2-6 L red arrow).

E5 *chairy1* expression is very similar to E4 expression. *chairy1* is expressed in the roof plate epithelium – hindbrain neuroepithelium boundary and in the floor plate, as well as the longitudinal hindbrain stripes (Figure 2-6 M, N, arrow: roof plate epithelium – hindbrain neuroepithelium boundary, arrowhead: floor plate, open arrowheads: longitudinal hindbrain stripes). E5 *chiary2* expression is also very similar to E4 expression. It too still shows upregulated expression at the roof plate epithelium – hindbrain neuroepithelium boundary and in the hindbrain longitudinal stripes (Figure 2-6 O, P, arrow: roof plate epithelium – hindbrain neuroepithelium boundary, open arrowheads: longitudinal hindbrain stripes), although the elevated expression at the floor plate boundaries is less apparent at this stage (Figure 2-6 O).

By E6, similar expression patterns for *chairy1* and *chairy2* still exist. *chairy1* is expressed highly at the roof plate epithelium – hindbrain neuroepithelium boundary, the floor plate and the two longitudinal hindbrain stripes (Figure 2-6 Q, arrows: roof plate epithelium – hindbrain neuroepithelium boundary, arrowhead: floor plate, open arrowheads: longitudinal hindbrain stripes). *chairy2* is expressed highly at the roof plate epithelium – hindbrain neuroepithelium boundary (Figure 2-6 R arrows). It is still expressed throughout the hindbrain neuroepithelium but slightly elevated levels of expression at the longitudinal hindbrain stripes and at the floor plate boundaries can be seen (Figure 2-6 R, arrowhead: floor plate boundaries, open arrows: longitudinal hindbrain stripes).

In order to determine more clearly the expression domains of *chairy1* and *chairy2*, I looked at their expression in transverse sections through E4 embryos. Elevated expression of *chairy1* and *chairy2* at the roof plate epithelium – hindbrain neuroepithelium boundary can be seen at both upper and lower rhombic lip levels in vibrotome sections (Figure 2-7 A – F, arrows). *chairy1* is also expressed in the floor plate and in a longitudinal hindbrain stripe (Figure 2-7 B, arrowhead: floor plate, open arrowhead: longitudinal hindbrain stripe). *chairy2* expression in the floor plate boundaries can be seen, and sections through the lower rhombic lip show that the longitudinal hindbrain stripe of *chairy2* expression is broader than that of *chairy1* (Figure 2-7 E, arrowhead: floor plate boundary, open arrowhead: longitudinal hindbrain stripe).

Despite *chairy1* and *chairy2* being clearly expressed at high levels at the roof plate epithelium – hindbrain neuroepithelium boundary, it was not clear how their expression patterns related to the *gdf7*-positive domain. In order to assess this, I took serial cryostat sections through the upper and lower rhombic lips of an E4 embryo and detected the expression of *chairy1*, *chairy2* and *gdf7* using *in situ* hybridisation on the serial sections. Sections through the upper rhombic lip clearly show upregulated expression of *chairy1* and *chairy2* within the *gdf7*-domain in comparison with expression in the adjacent neuroepithelium (Figure 2-7 G, arrows). At lower rhombic lip level, *chairy1* is clearly expressed in the *gdf7*-domain, however *chairy2* is expressed more ubiquitously in the hindbrain neuroepithelium with only a slight upregulation at the *gdf7*-domain in these sections (Figure 2-7 H, arrows).

In order to more closely assess the expression of *chairy2* in relation to *gdf7*, I carried out double *in situ* hybridisation for *chairy2* and *gdf7* on cryostat sections through the E4 upper and lower rhombic lips. This shows more clearly that *chairy2* is upregulated within the *gdf7*-positive domain at both upper and lower rhombic lip levels. (Figure 2-7 I – L, brackets: domain of upregulated *chairy2* expression within the *gdf7*-domain).

These results show that *chairy1* marks the *gdf7* – domain in the E4 hindbrain, as well as the floor plate. It is also expressed in two longitudinal stripes in the hindbrain neuroepithelium. *chairy2* is expressed at a low level throughout the hindbrain neuroepithelium at E4 but shows upregulated expression at the *gdf7*-domain, the floor plate boundaries and two longitudinal stripes in the hindbrain neuroepithelium.

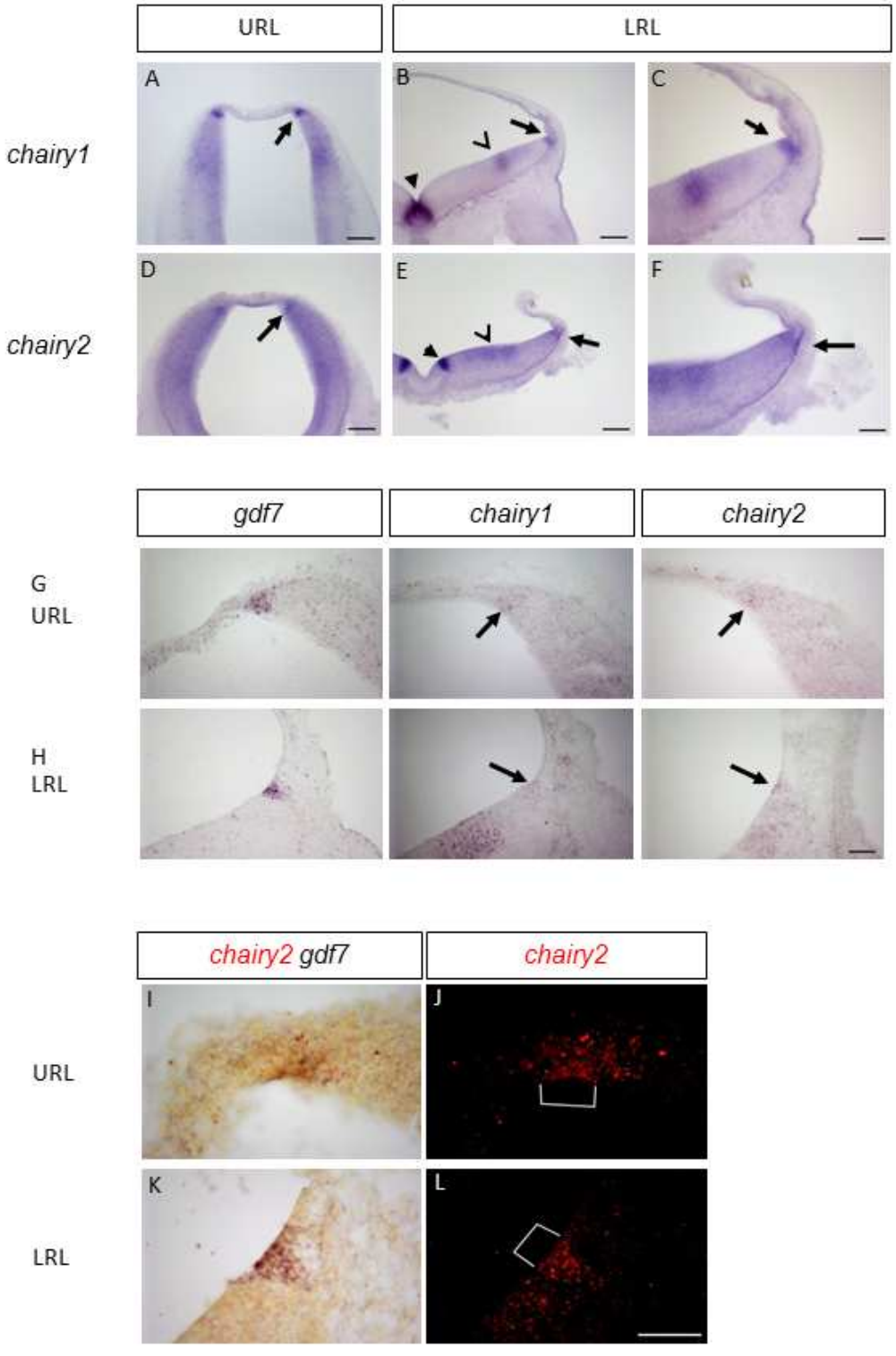
URL
LRL
A
B
C
chairy1
D
E
F
chairy2
gdf7
chairy1
chairy2
G
URL
H
LRL
chairy2 gdf7
chairy2
I
J
URL
K
L
LRL

Figure 2-7 Expression of *chairy1* and *chairy2* in sections through the E4 upper and lower rhombic lips

A – F show transverse vibrotome sections through E4 chick embryos where the expression of *chairy1* (A – C) or *chairy2* (D – F) had been detected by whole-mount *in situ* hybridisation. A and D show sections through the upper rhombic lip. B, C, E, F show sections through the lower rhombic lip. G and H show serial transverse cryostat sections through the upper (G) or lower rhombic lip (H) of an E4 chick embryo. The expression of *gdf7*, *chairy1* or *chairy2* (as labelled) was detected by *in situ* hybridisation on sections. I – L show transverse cryostat sections through the upper (I, J) and lower rhombic lips (K, L) of an E4 embryo. The expression of *chairy2* and *gdf7* are detected by double *in situ* hybridisation on sections. I and K show the expression of both genes, whereas J and L show the immune-fluorescence detection of *chairy2* expression alone. Dorsal is oriented upwards in all images. Arrows, hindbrain roof plate epithelium – neuroepithelium boundary. B, arrowhead, floor plate expression. E, arrowhead, floor plate boundary expression. B, E, open arrowheads, longitudinal hindbrain stripes.

Scale bars: A, B, D, E: 100µm, C, F – L: 50µm.

2.2.4 Expression of Notch receptors, ligands and downstream targets at the roof plate boundary

hes1 is a well-known downstream target of Notch signalling, although it has also been shown to be activated by Notch-independent pathways (Ohtsuka et al., 1999; Kageyama et al., 2007; Wall et al., 2009; Sanalkumar et al., 2010). Thus, upregulated expression of the chick *hes1* orthologues at the roof plate epithelium – hindbrain neuroepithelium boundary suggested that Notch signalling might be activated at the roof plate epithelium – hindbrain neuroepithelium boundary. To investigate this, the expression of various Notch ligands, receptors and modulators was examined at the roof plate epithelium – hindbrain neuroepithelium boundary.

Figure 2-8 A shows the expression of the Notch receptors, *notch1* and *notch2* in transverse, serial cryostat sections through the upper rhombic lip at E5. *notch1* is expressed in the ventricular zone of the hindbrain neuroepithelium but is downregulated in the *gdf7*-positive domain (Figure 2-8 A arrowhead). In contrast, *notch2* is highly expressed in the *gdf7*-positive domain (Figure 2-8 A arrow) and is also expressed in the more medial roof plate epithelium (Figure 2-8 A open arrow), whereas *notch1* is not expressed in the roof plate epithelium.

Figure 2-8 B shows the expression of the Notch ligands, *delta1* and *serrate1* in comparison with the expression of *gdf7*. *delta1* is expressed in a salt and pepper fashion in the ventricular zone of the hindbrain neuroepithelium in a domain abutting the *gdf7*-domain. There is an enrichment of expression in a border directly adjacent to the *gdf7*-domain (Figure 2-8 B arrow). *serrate1* is expressed highly within the *gdf7*-domain (Figure 2-8 B open arrow) but also in a domain adjacent to the *gdf7*-domain within the neuroepithelium (Figure 2-8 arrowhead).

Figure 2-8 C shows the expression of *lfng* in comparison with that of *gdf7*. *lfng* is expressed in a similar domain to *delta1*, although it is expressed in a continuous fashion in the ventricular zone, rather than a salt and pepper fashion. It is also expressed adjacent to the *gdf7*-domain and not within it.

The expression patterns of the Notch ligands, receptors and *lfng* at the level of the lower rhombic lip at E5 are very similar to those at upper rhombic lip level (Figure 2-8 D, E). *notch1* is again downregulated within the *gdf7*-domain (Figure 2-8 D arrowhead), but expressed throughout the ventricular zone of the hindbrain neuroepithelium. *notch2* is again expressed at a high level within the *gdf7*-domain (Figure 2-8 D arrow) and is expressed in the roof plate epithelium (Figure 2-8 D open arrow).

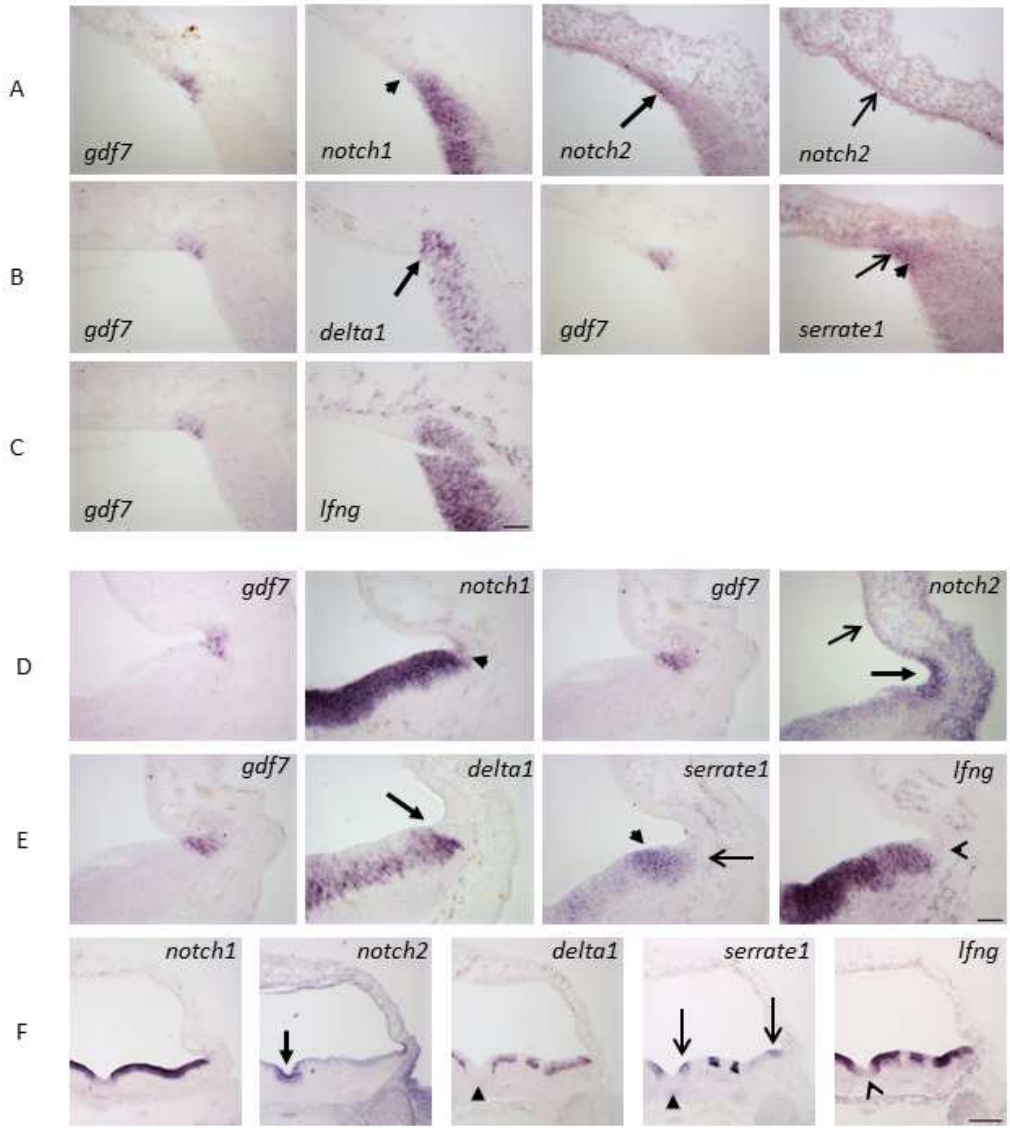
A
gdf7
notch1
notch2
notch2
B
gdf7
delta1
gdf7
serrate1
C
gdf7
lfng
D
gdf7
notch1
gdf7
notch2
E
gdf7
delta1
serrate1
lfng
F
notch1
notch2
delta1
serrate1
lfng

Figure 2-8 Expression of Notch pathway ligands, receptors and modulators at the roof plate boundary

In situ hybridisation on transverse serial cryostat sections from E5 embryos through the upper rhombic lip (A – C) and the lower rhombic lip (D - F) to compare the expression domain of *gdf7* with that of the Notch receptors ,*notch1* and *notch 2* (A, D and F as labelled), that of the Notch ligands, *delta1* and *serrate1* (B, E and F as labelled), or that of the *lfng* (C, E and F as labelled). Dorsal is oriented upwards. A, D, arrowheads, downregulated *notch1* expression in the *gdf7*-domain; arrows, upregulated *notch2* expression in the *gdf7*-domain; open arrows, roof plate epithelium *notch2* expression. B. E. arrows, border of *delta1* expression; open arrows, *serrate1* expression in the *gdf7*-domain; arrowheads, *serrate1* expression in the neuroepithelium. E, open arrowhead, lack of *lfng* expression in the *gdf7*-domain. F, arrow, floor plate *notch2* expression; arrowheads, lack of floor plate *delta1* and *serrate1* expression; open arrows, coincidental sites of *delta1* and *serrate1* expression; open arrowhead, floor plate *lfng* expression.

Scale bars: A – E, 50µm; F, 250µm.

delta1 is expressed in a salt and pepper pattern in the ventricular zone of the hindbrain neuroepithelium in a domain abutting the *gdf7*-expression domain. It shows a sharp boundary of expression adjacent to the *gdf7*-expression domain (Figure 2-8 E arrow). *serrate1* shows elevated expression in the ventricular zone of the hindbrain in a domain adjacent to the *gdf7*-expression domain (Figure 2-8 E arrowhead), and shows downregulated expression within the *gdf7*-domain itself (Figure 2-8 E open arrow). *lfng* is highly expressed throughout the ventricular zone of the hindbrain neuroepithelium up until the *gdf7*-domain. It is not expressed within the *gdf7*-domain (Figure 2-8 E open arrowhead).

Sections at lower rhombic lip level also show that *notch1* and *notch2* are expressed along the entire dorsoventral axis of the neuroepithelium, in the ventricular zone, but *notch1* expression is excluded from the floor plate, while *notch2* expression is upregulated within the floor plate (Figure 2-8 F, arrow). *delta1* and *serrate1* show mostly complementary expression within the ventricular zone of the neuroepithelium, except for expression adjacent to the floor plate and the roof plate (Figure 2-8 F, open arrows). Note that neither *delta1* nor *serrate1* are expressed within the floor plate (Figure 2-8, arrowheads). *lfng* is expressed in a very similar manner to *delta1* except that it is expressed slightly in the floor plate (Figure 2-8 F, open arrowhead).

2.2.5 The expression of hindbrain roof plate epithelium and choroid plexus epithelium markers from E3 – E7

The hindbrain roof plate epithelium is distinguishable from E3 in chick. *ttr* is expressed in the extraembryonic membranes and the liver at E3 (Figure 2-9 A arrow, liver). Expression in the hindbrain roof plate does not begin until E4 (st20), when patches of *ttr*-expressing cells appear in two lateral domains of the hindbrain roof plate, mostly in the lower roof plate (Figure 2-9 B, arrow). More *ttr*-expressing cells appear as development proceeds through E4, with more *ttr*-expressing cells appearing in the upper roof plate (Figure 2-9 B – E arrowhead). This suggests that the anterior hindbrain choroid plexus epithelium differentiates later than the posterior domain, which is in line with findings in mouse embryos (Hunter and Dymecki, 2007). *ttr* expression begins in a few scattered cells in the diencephalic choroid plexus epithelium at E4 (st23) (Figure 2-9 F, F', arrow). Two solid lateral domains of *ttr* expression are apparent by E5 in the hindbrain roof plate (st26) (Figure 2-9 G). By E5, the diencephalic *ttr* expression marks the choroid plexus epithelium and a domain around the developing pineal gland (Figure 2-9 H, arrow, choroid plexus epithelium; arrowhead, pineal gland). By E6 (st28) cells of the medial upper roof plate have differentiated and express *ttr*, leaving a medial circular *ttr*-negative domain (Figure 2-9 I, arrow, medial anterior *ttr* expression). The expression domain of *ttr* at E7 (st30) is very similar to that at E6, with the

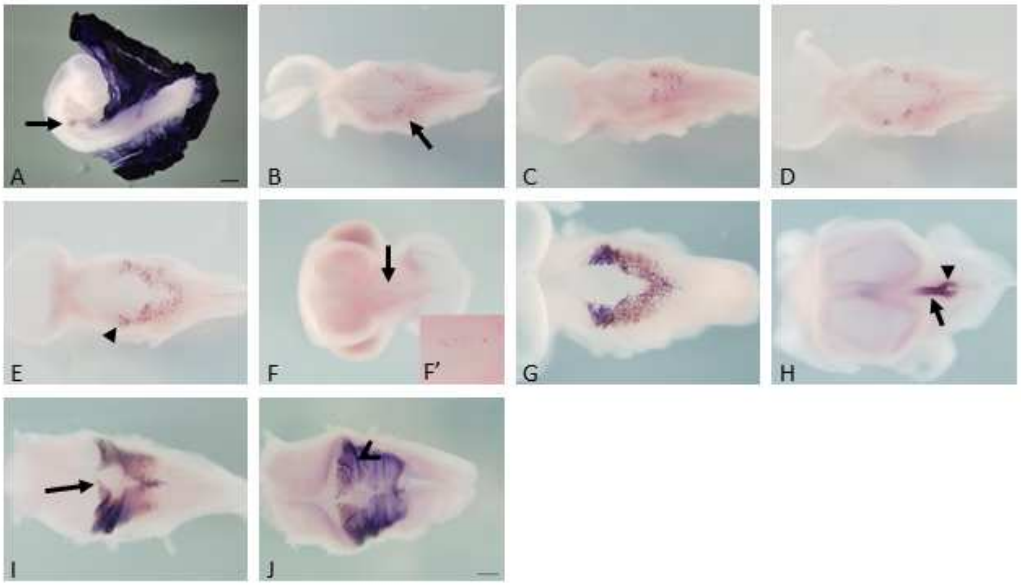

Figure 2-9 Expression of *transthyretin* (*ttr*) from st19 (E3) to st30 (E7) in whole-mount chick embryos

Ttr expression in st19 (E3) (A), st20 (E4) (B), st21 (E4) (C), st22 (E4) (D), st23 (E4) (E, F), st26 (E5) (G, H), st28 (E6) (I), st30 (E7) (J) chick embryos as detected by whole-mount *in situ* hybridisation. A is a lateral view. B – E, G, I, J are dorsal views of the hindbrain. F and H are frontal views of the diencephalon and telencephalic vesicles. F' is a x2.5 magnification of diencephalic *ttr* expression in F indicated by an arrow. Anterior is oriented to the left in all images. A, arrow, liver. B, arrow, lower roof plate *ttr* expression. E, upper roof plate *ttr* expression. F – H arrows, diencephalic *ttr* expression. H, arrowhead, *ttr* expression around the developing pineal gland. I, arrow, medial upper roof plate *ttr* expression. J, open arrowhead, folds in the roof plate epithelium along the mediolateral axis.

Scale bars represent 400μm.

distinct medial *ttr*-negative domain still present (Figure 2-9 J). Given that the images G, I and J in Figure 2-9 are all at the same magnification, the *ttr*-negative domain decreases in size over time between E5 and E7 while the *ttr*-positive domains increase in size. Three explanations for this exist. Either the cells originally residing in the medial *ttr*-negative domain at E5 later differentiate to add to the lateral *ttr*-expression domains, the roof plate epithelium folds within the *ttr*-negative domain giving the expression that it has decreased in size, or there is selective cell death within the medial *ttr*-negative domain. Although selective cell death cannot be excluded as an explanation for the decrease in size of the medial *ttr*-negative domain, the cause of its decrease in size is unlikely to be due to folding within this domain, as folding of the roof plate epithelium mainly seems to occur along the mediolateral axis at these stages (Figure 2-9 J, open arrowhead).

cyp26C1 expression begins earlier than that of *ttr* in the hindbrain roof plate. It begins to be expressed in an upper roof plate domain and a lower roof plate domain at E3 (st15) (Figure 2-10 A, arrows, upper roof plate domain; arrowhead, lower roof plate domain). By st18, hindbrain roof plate *cyp26C1* expression is still visible as separate anterior and posterior domains (Figure 2-10 B). By this stage there are also two small domains of expression visible at the dorsal midline of the diencephalon and the telencephalon, possibly demarcating future choroid plexus epithelium domains (Figure 2-10 C arrowhead, diencephalon; arrow, telencephalon). By E4 (st22), two separate upper and lower hindbrain roof plate domains of expression are no longer visible. *cyp26C1* expression marks most of the roof plate epithelium, including the lateral roof plate boundaries, but like *ttr* its expression is excluded from a medial domain (Figure 2-10 D, E, arrow, *cyp26C1*-negative domain; arrowhead, roof plate boundary). At E4, the expression of *cyp26C1* is also visible in the developing pineal gland, and in two domains of the telencephalic dorsal midline (Figure 2-10 F, arrowhead, pineal gland; arrow, telencephalic dorsal midline). By E5 (st26) the *cyp26C1*-negative domain has decreased in size as images G and D in Figure are at the same magnification, so *cyp26C1* expression has spread medially (Figure 2-10 G, H). At this stage *cyp26C1* expression is discernible in the developing pineal gland and in a domain posterior to the pineal gland (Figure 2-10 I, arrowhead, pineal gland). By E6 (st29) the hindbrain roof plate epithelium *cyp26C1*-negative domain has further decreased in size (Figure 2-10 J, K). By E7 (st30), *cyp26C1* expression marks the choroid plexus epithelium (Figure 2-10 L, M, by comparison with Figure J), but its expression is beginning to be downregulated there. Its expression no longer marks the roof plate boundaries (Figure 2-10 M, arrows).

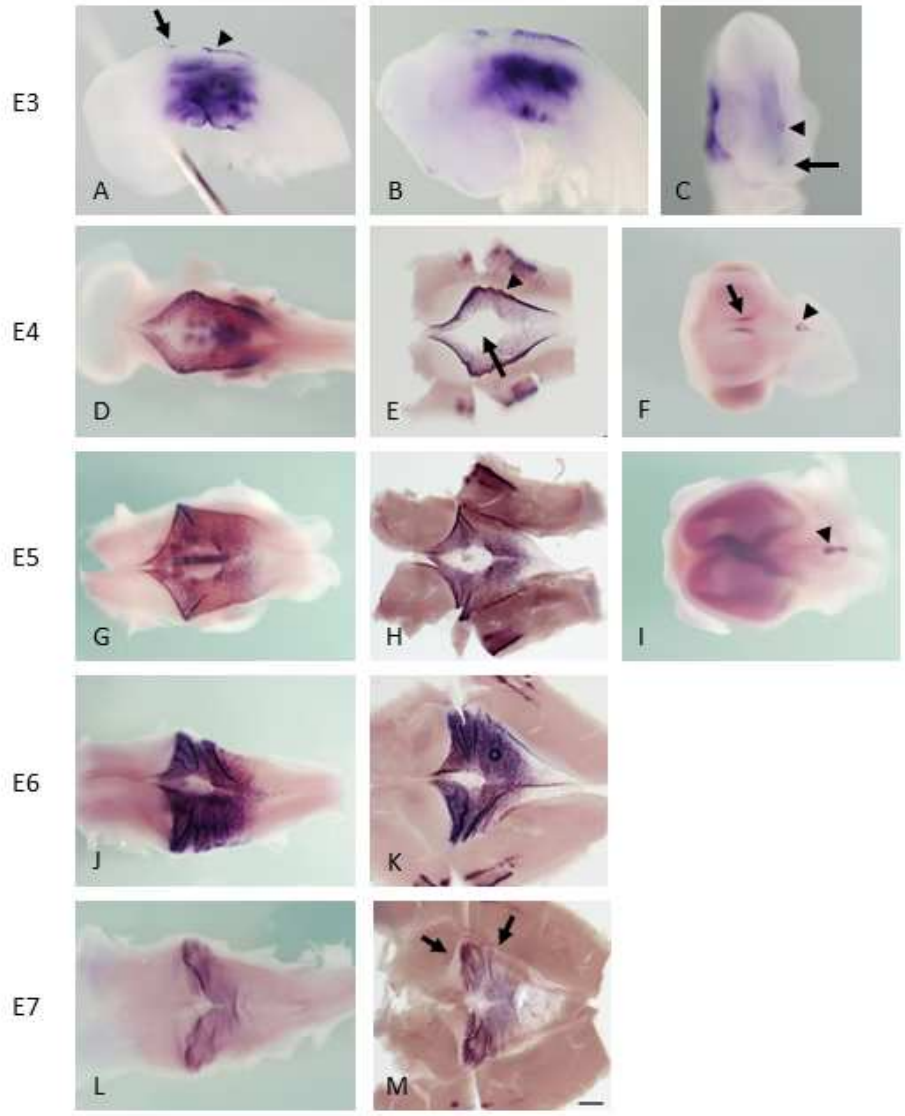

Figure 2-10 *cyp26C1* expression in whole-mount st15 (E3) – st30 (E7) chick embryos

Expression of *cyp26C1* as detected by whole-mount *in situ* hybridisation in st15 (E3) (A), st 18 (E3) (B, C), st22 (E4) (D – F), st26 (E5) (G – I), st29 (E6) (J, K) st30 (E7) (L, M) chick embryos. A, B show lateral views of the head. C, F, I show frontal views of the diencephalon and telencephalon. D, G, J, L show dorsal views of the hindbrain. E, H, K, M show views of the ventricular surface of flat-mounted hindbrain roof plates. All images are oriented with anterior to the left apart from C, which shows anterior oriented downwards. A, arrow, upper roof plate; arrowhead, lower roof plate. C, arrowhead, diencephalon; arrow, telencephalon. E, arrow, *cyp26C1*-negative domain; arrowhead, roof plate boundary. F, arrowhead, pineal gland; arrow, telencephalon. I, arrowhead, pineal gland. M, arrows, roof plate boundaries.

Scale bar represents 400μm.

In order to further analyse the onset of *ttr* expression in relation to *cyp26C1* expression, *in situ* hybridisation with riboprobes developed with contrasting colours were performed for these genes on E4 (st21 – 23) embryos. This double *in situ* hybridisation shows that *ttr* expression marks a subset of *cyp26C1* expressing cells, in medial regions of the two lateral *cyp26C1*domains of the hindbrain roof plate (Figure A – F, arrows), with expression of *ttr* first appearing in the lower roof plate epithelium, and then appearing in the upper roof plate epithelium by st23 (Figure E, F, arrowhead). The appearance of *cyp26C1* expression also proceeds in a posterior – anterior fashion with expression in the most upper roof plate epithelium being absent at st21 (Figure B, open arrowhead).

otx2 is highly expressed in the midbrain and diencephalon, and is expressed in the telencephalic vesicles at E4 (st22) (Figure A, B, arrowhead, midbrain; open arrow, diencephalon; open arrowhead, telencephalon), but it is also expressed highly at the lateral hindbrain roof plate boundaries and is faintly expressed in the roof plate epithelium, in a similar domain to *cyp26C1* (Figure A, arrow). At E5 (st26) *otx2* is still expressed at the hindbrain roof plate epithelium boundaries, but only shows very faint expression in the roof plate epithelium (Figure C, arrows, roof plate boundaries; arrowhead, roof plate epithelium). In the forebrain at E5 (st26), *otx2* has become downregulated in most of the telencephalon and diencephalon, but is still highly expressed in the developing pineal gland (Figure D, open arrow). At E6, *otx2* is expressed very highly at the hindbrain roof plate boundaries, but faint expression is also visible in the choroid plexus epithelium (Figure E, arrows, roof plate boundaries; arrowhead, roof plate epithelium; compare with Figure I). By E7 (st30), expression of *otx2* has become downregulated in the hindbrain choroid plexus epithelium but still persists in the anterior and anterior-lateral roof plate boundaries (Figure F, arrows).

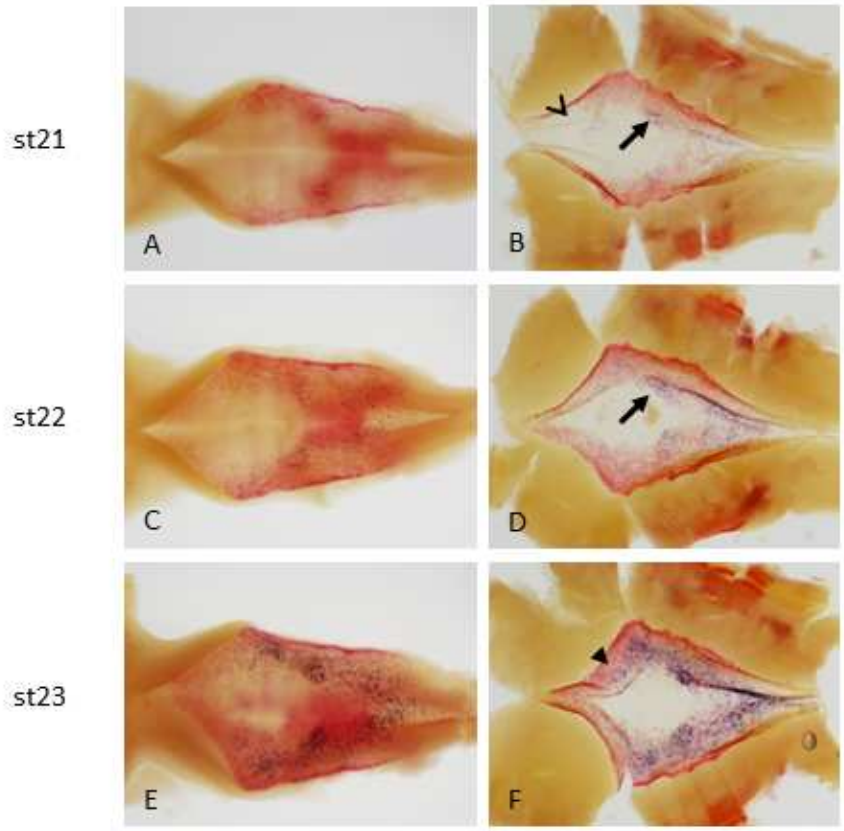

Figure 2-11 *ttr* expression marks a subset of *cyp26C1*-expressing cells

Whole-mount double *in situ* hybridisation to show expression of *cyp26C1* (red) and *ttr* (blue) in E4 chick embryos. A and B show st21 embryos, C and D show st22 embryos and E and F show st23 embryos. A, C, E show dorsal views of hindbrains. B, D, F show views of the ventricular surface of flat-mounted hindbrain roof plates. In all images, anterior is oriented to the left. B, D, arrows, *ttr*-expressing cells. B, open arrowhead, absence of *cyp26C1* expression in the upper roof plate epithelium. F, arrowhead, upper roof plate expression of *ttr*.

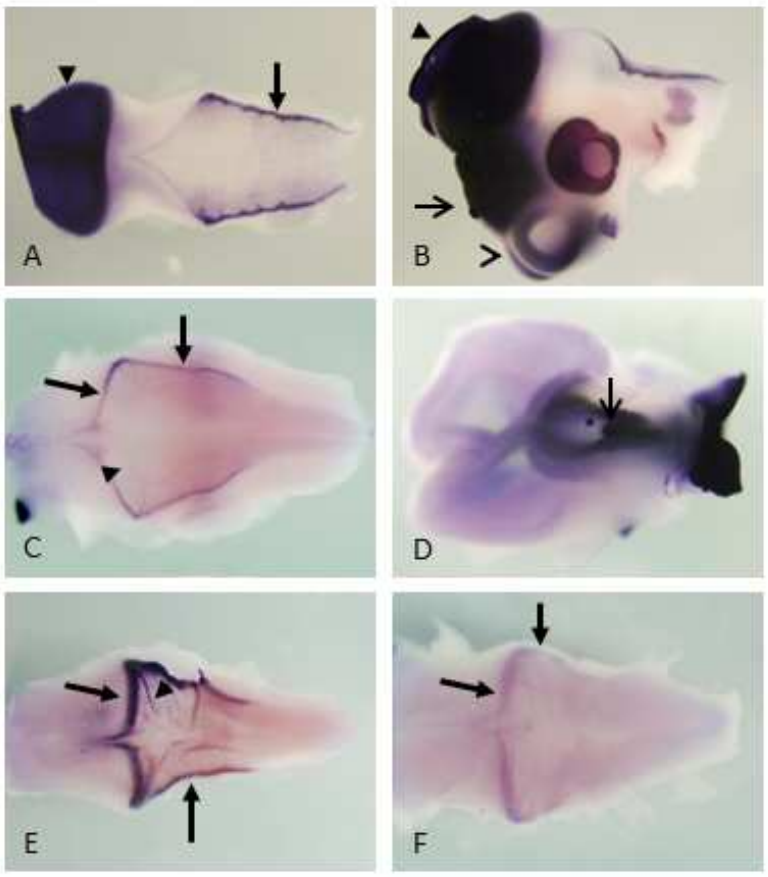

Figure 2-12 Expression of *otx2* in the hindbrain choroid plexus epithelium

Expression of *otx2* as detected by whole-mount *in situ* hybridisation in E4 (st22) (A, B), E5 (st26) (C, D), E6 (st28) (E) and E7 (st30) (F) chick embryos. A, C, E, F show dorsal views of the hindbrain. B shows a lateral view of the head. D shows a frontal view of the telencephalic vesicles and the diencephalon. Anterior is oriented to the left in all images. A – B, arrowheads, midbrain; open arrow, diencephalon; open arrowhead, telencephalon; arrow, roof plate boundary. C – F, arrows, roof plate boundaries; arrowheads, roof plate epithelium; open arrow, pineal gland.

2.3 Discussion

2.3.1 Choroid plexus epithelium development in chick

Other than being an organiser, the hindbrain roof plate also has another role in development. The roof plate epithelium differentiates into the choroid plexus epithelium, which constitutes part of the blood-brain barrier and produces cerebrospinal fluid (CSF) (Dziegielewska et al., 2001; Redzic et al., 2005). Despite its importance, its ontogenesis has not been well described in chick embryos. In this chapter the pattern of differentiation of the hindbrain choroid plexus epithelium was analysed by the appearance of *ttr* expression, the best described marker of differentiated choroid plexus epithelium (Thomas et al., 1988; Duan et al., 1991). *ttr* begins to be expressed in patches in two lateral domains in the lower roof plate epithelium at E4 (st20), but its expression proceeds anteriorly so that it is expressed in the upper roof plate epithelium by st23 (E4) (Figure 2-9, 2-11). This is homologous to the situation in the mouse where the expression of *ttr* in roof plate epithelium derived from rhombomeres 2 – 8 appears by E11.5, whereas expression of *ttr* only appears in rhombomere 1-derived roof plate epithelium by E13.5 (Hunter and Dymecki, 2007). The expression of *ttr* also seems to spread medially as the medial *ttr*-negative domain decreases in size between E5 (st26) and E7 (st30), although this could be due to selective cell death of the medial domain. The pattern of differentiation of the chick choroid plexus epithelium differs from the pattern of differentiation reported for the zebrafish. Using a GFP-tagged enhancer trap transgenic line (Gateways), Garcia-Lecea et al. (2008) showed that the choroid plexus primordium appears at the dorsal midline of the roof of the fourth ventricle at 36 hours post fertilisation (hpf) and that GFP-positive cells then coalesce between 72hpf and 144hpf to form a single circular domain that is the fourth ventricle choroid plexus. Thus, while the zebrafish choroid plexus epithelium differentiates at the dorsal midline, the chick choroid plexus epithelium differentiates in two lateral domains of the hindbrain roof plate epithelium that later fuse to form a highly convoluted and vascularised region at the midline of the roof plate (Thomas et al., 1988).

cyp26C1 was known to be expressed in the roof plate epithelium at E4 and E5 (Reijntjes et al., 2004; Wilson et al., 2007) so its expression was analysed in order to relate it to choroid plexus epithelium development. The expression domain of *cyp26C1* encompasses that of *ttr* in the hindbrain roof plate epithelium from E4 (st21) – E6 (st29) and double *in situ* hybridisation analysis of E4 embryos confirms that *ttr* expression appears in a medial subset of *cyp26C1* expressing cells, with the roof plate boundaries and an immediately adjacent roof plate epithelial domain being devoid of *ttr* expression (Figure 2-9, 2-10, 2-11). However, by E7, *cyp26C1* expression is only detected in the choroid plexus epithelium, but

is downregulated in comparison with expression at E6 (Figure 2-10). It would be interesting to see when *cyp26C1* expression stops being detected in the choroid plexus epithelium.

Thus the above analyses reveal that the chick choroid plexus differentiates in a very specific pattern within the roof plate epithelium, maturing in a posterior to anterior manner. Further, the above analyses revealed that the E4 chick roof plate epithelium can but subdivided into three distinct domains: a medial *cyp26C1*-negative and *ttr*-negative domain, a more lateral *cyp26C1*-positive and *ttr*-positive domain, and an even more lateral *cyp26C1*-positive, *ttr*-negative domain (illustrated in Figure 2-13). Thus signals, either endogenous or exogenous to the roof plate epithelium must operate to subdivide the roof plate epithelium and regulate the pattern of differentiation of the choroid plexus epithelium. Hunter and Dymecki (2007) have shown in mouse that the progeny of *gdf7*-expressing precursors populate the lateral domains of the roof plate epithelium but not the medial domain (see Figure 1-5) and that most, if not all, of the choroid plexus epithelium is derived from *gdf7*-expressing progenitors. This provides a potential autonomous mechanism for the differentiation of the lateral roof plate epithelial domains from the medial domain in the chick roof plate epithelium; however the mechanism behind the specification of the most lateral *cyp26C1*-positive, *ttr*-negative domain (margin), or the mechanism behind the posterior to anterior maturation of the choroid plexus epithelium has so far not been discovered.

cyp26C1 expression precedes that of *ttr* in the hindbrain roof plate epithelium, being expressed from E3 (st15) (Figure 2-10 A). Additionally, its expression precedes that of *ttr* at the diencephalic and telencephalic dorsal midlines, with detectable expression at st18 (Figure 2-10 C). However, diencephalic *cyp26C1* expression does not encompass *ttr* expression at E5 (st26) as its expression is restricted to the pineal gland and an area posterior to the pineal gland, whereas *ttr* is expressed around the pineal gland and anterior to the pineal gland. Thus *cyp26C1* may not be a marker of diencephalic choroid plexus epithelium. The choroid plexus epithelium in mouse has been shown to derive from the *wnt1*-positive, *gdf7*-positive roof plate boundary (Awatramani et al., 2003; Landsberg et al., 2005; Hunter and Dymecki, 2007). *cyp26C1* is expressed at the boundary in chick, and *cyp26C1* is expressed earlier than *ttr* in the hindbrain roof plate epithelium, diencephalic and telencephalic dorsal midlines, therefore *cyp26C1* may mark cells that are destined to become choroid plexus epithelial cells. A temporally regulated genetic fate-mapping approach is required to investigate whether this is the case.

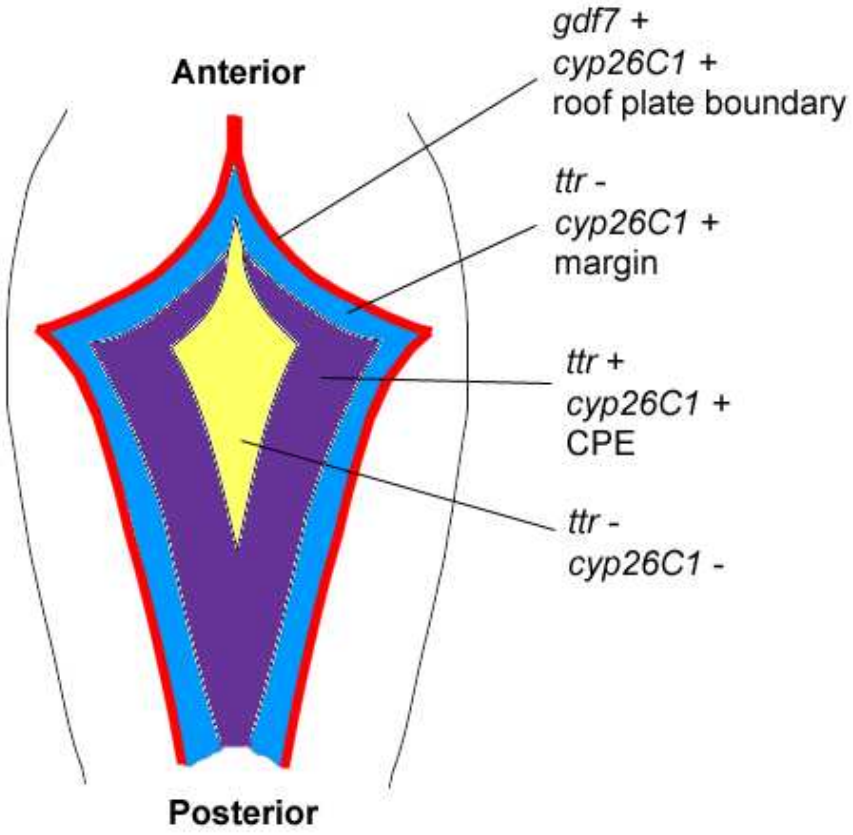

Figure 2-13 Schematic diagram of the subdivision of the E4 chick hindbrain roof plate epithelium into three domains

Diagram of the dorsal view of an E4 chick hindbrain. The roof plate epithelium can be subdivided into three domains: a lateral *ttr*-negative, *cyp26C1*-positive margin (blue), the differentiated choroid plexus epithelium (CPE; purple), which is *ttr*-positive, *cyp26C1*-positive, and a medial *ttr*-negative, *cyp26C1*-negative domain (yellow). The lateral roof plate boundaries (red) are *gdf7*-positive and *cyp26C1*-positive but *ttr*-negative.

otx2 is known to be expressed by the chick and mouse telencephalic choroid plexus epithelium (Shinozaki et al., 2004; von Frowein et al., 2006), however only faint expression in the chick hindbrain choroid plexus epithelium could be detected at E6 (st28), and no expression at E7 (st30) by whole-mount *in situ* hybridisation (Figure 2-12). *otx2* was, however, expressed highly at the roof plate epithelium – hindbrain neuroepithelium boundary from E4 (st22) to E7 (st30), so like *cyp26C1*, high *otx2* expression might mark hindbrain choroid plexus epithelium cell progenitors.

2.3.2 The presence of Notch ligands, receptors and downstream targets at the roof plate boundary suggests a role for Notch signalling across this boundary

Notch signalling has been shown to be responsible for the maintenance of boundary-localised organisers in developmental situations such as the dorsoventral boundary of the wing imaginal disc of Drosophila embryos or the zebrafish rhombomere boundaries (Rulifson and Blair, 1995; Rauskolb et al., 1999; Irvine and Rauskolb, 2001; Cheng et al., 2004; Riley et al., 2004). It is also well known that Hes transcription factors are downstream targets of Notch signalling (Ohtsuka et al., 1999; Kageyama et al., 2008), although Notch-independent pathways of activation of *hes1* have also been shown (Wall et al., 2009; Sanalkumar et al., 2010).

The chick *hes1*orthologues *chairy1* and *chairy2* both show high levels of mRNA expression at the roof plate epithelium – hindbrain neuroepithelium boundary from E4 – E6 (the latest stage examined) (Figure 2-6, 2-7), with *chairy1* and *chairy2* expression specifically upregulated within the *gdf7*-domain, at least at E4. *chairy1* also shows specific expression at the roof plate epithelium – hindbrain neuroepithelium boundary from E3 (st18), and may even mark the prospective roof plate epithelium – hindbrain neuroepithelium boundary from E2 (st11) (Figure 2-6, A, B, E, F). These results indicate that Notch signalling might be specifically activated at the roof plate epithelium – hindbrain neuroepithelium boundary.

Analysis of the expression patterns of Notch receptors and ligands at E5 show that Notch signalling is a good candidate to be upstream of the elevated expression of *chairy1* and *chairy2* at the roof plate epithelium – hindbrain neuroepithelium boundary at this stage (Figure 2-8). Although *notch1* is downregulated within the *gdf7*-domain and absent from the roof plate epithelium, *notch2* is expressed highly within the *gdf7* – domain so is a good candidate to mediate signalling there. The Notch ligands, *delta1* and *serrate1* are also well placed to mediate activation of Notch signalling at the roof plate boundary as they are expressed within the *gdf7* domain or adjacent to it in the hindbrain neuroepithelium. *delta1* shows a particularly striking boundary of expression adjacent to the *gdf7* domain.

Fringe (fng) encodes a glycosyltransferase that modulates Notch activation by Delta and Serrate and is required to maintain the dorsoventral boundary of the wing imaginal disc of Drosophila larvae (Irvine and Wieschaus, 1994; Panin et al., 1997; Rauskolb et al., 1999). This boundary is located at the interface between fringe-expressing and non-expressing cells and the ectopic expression of *fng* in the ventral compartment can re-position the boundary (Irvine and Wieschaus, 1994). *Lunatic fringe (lfng)* and *radical fringe (rfng)* are vertebrate homologues of Drosophila *fng*, and boundaries between *lfng*-expressing and non-expressing cells and between *rfng*-expressing and non-expressing cells have been shown to regulate the formation of the ZLI of the chick and the apical ectodermal ridge of the chick limb bud, respectively (Laufer et al., 1997; Rodriguez-Esteban et al., 1997; Zeltser et al., 2001). Additionally, *lfng*, along with *serrate1* has recently been shown to be important in regulating the formation of the midbrain-hindbrain boundary of chick embryos (Tossell et al., 2011). Thus in various developmental systems, *fng* and its homologues play an important role in establishing boundaries at the interface between *fng*-expressing and non-expressing cells. The chick roof plate epithelium – hindbrain neuroepithelium boundary also lies at the interface between *lfng*-expressing neuroepithelial cells and non-expressing roof plate epithelial cells (Figure 2-8), which hints towards an *lfng*-mediated mechanism of roof plate boundary maintenance. In the examples above *fng* expression is generally associated with *serrate* expression and in Drosophila, *fng* acts by decreasing the efficiency of Serrate-Notch signalling but potentiating Delta-Notch signalling (Fleming et al., 1997; Panin et al., 1997). At the chick roof plate epithelium – hindbrain neuroepithelium boundary, *lfng* is expressed in the neuroepithelium with both *delta1* and *serrate1* (Figure 2-8), so it will be interesting to establish how *lfng* is acting in this context. In a mouse cell co-culture system, Hicks et al. (2000) have shown that while Lfng inhibits Jagged1 (a mouse Serrate homologue) -mediated signalling and potentiates Delta1-mediated signalling through Notch1, it potentiates both Jagged1- and Delta1-mediated signalling via Notch2. Since *notch2* is expressed at the roof plate epithelium – hindbrain neuroepithelium boundary in chick, this could be the mechanism that mediates Notch activation at the roof plate epithelium – hindbrain neuroepithelium boundary.

Alternatively, the pattern of expression of *lfng* may simply reflect its role in the maintenance of neural stem cell pools within the neural tube. Nikolaou et al. (2009) have shown that *lfng* is required cell-autonomously to maintain neural progenitors and prevent ectopic neurogenesis in the zebrafish hindbrain. This function of *lfng* appears to be conserved from zebrafish to mouse as *lfng* is necessary and sufficient for the maintenance of neural stem cell pools in the developing mouse cerebral cortex (Kato et al., 2010), while the overexpression of *manic fringe* (*mfng*) causes a dorsoventral domain-specific inhibition of neurogenesis in

the chick spinal cord (only within the *delta1*-positive progenitor domains but not within the *serrate1*-positive progenitor domains) (Marklund et al., 2010). Thus *lfng* has an important role within the developing neural tube that is not related to boundary formation or maintenance.

Baek et al. (2006) showed that persistently high levels of expression of Hes1 marked organisers such as the MHB, ZLI, rhombomere boundaries, spinal cord roof plate and floor plate in the mouse. As stated above, the chick *hes1*orthologues *chairy1* and *chairy2* both show high levels of mRNA expression at the roof plate epithelium – hindbrain neuroepithelium boundary from E4 – E6 (the latest stage examined) (Figure 2-6, 2-7). Further, expression of *chairy1* is excluded from the roof plate epithelium from E3 and *chairy2* expression is excluded from E4 indicating that hindbrain roof plate organiser properties are localised to the roof plate epithelium – hindbrain neuroepithelium boundary from these stages.

Baek et al. (2006) and others have also shown that *hes* genes are required to maintain boundary-localised organisers in mice and in zebrafish, to prevent their ectopic neurogenesis (Geling et al., 2003; Geling et al., 2004; Ninkovic et al., 2005), so it is likely that *chairy1* and *chairy2* also play roles in maintaining the a roof plate boundary – localised organiser in chick.

2.3.3 *gdf7* is a specific marker of the roof plate epithelium – hindbrain neuroepithelium boundary in developing chick embryos

The expression patterns of Notch pathway genes and their downstream targets indicate that Notch signalling is activated at the boundary between roof plate epithelium and hindbrain neuroepithelium. Since activated Notch signalling is known to mark many boundary-localised organisers (reviewed in Irvine and Rauskolb, 2001; Cheng et al., 2004; Riley et al., 2004; Tossell et al., 2011), this indicates that the organiser properties of the hindbrain roof plate are localised to its boundaries. Indeed, in chick I found that *gdf7* (an organising molecule expressed by the roof plate) is specifically expressed at the boundaries between the hindbrain roof plate epithelium and neuroepithelium from E3 (st14) – E6 (st28) (the latest stage examined) (Figure 2-1, 2-2, 2-3). *chairy1* and *chairy2* are also both specifically upregulated within the *gdf7*-domain at E4 (Figure 1-8). The organiser properties of the spinal cord roof plate might also be localised to its boundaries as two *gdf7*-positive domains are separated by a medial *gdf7*-negative domain there (Figure 2-2 E, F). The same situation may also apply to the midbrain roof plate as *gdf7* expression there is visible as two stripes in whole-mount, although two separate domains of expression are not visible in vibrotome sections of whole-mount embryos (Figure 2-1, 2-2 K, L). This may be due to the thickness

of the section being too high to discern a small number of *gdf7*-negative cells there. Thus the hindbrain roof plate epithelium and the *gdf7*-negative domain in the spinal cord roof plate should be thought of as separate compartments of tissue from the neuroepithelium, and the organiser properties of the roof plate reside at the boundaries between the medial roof plate compartment and the neuroepithelium compartment.

The expression of *gdf7* in chick differs from that in mouse embryos at the hindbrain roof plate. In mice, *gdf7* is expressed highly at the roof plate epithelium – hindbrain neuroepithelium boundary but is also expressed at a lower mRNA level within the roof plate epithelium (Chizhikov et al., 2006; Mishima et al., 2009), whereas *gdf7* expression is absent from the chick hindbrain roof plate epithelium (Figure 2-1, 2-2). Nonetheless, the hindbrain roof plate of the mouse could still be divided into two domains; the roof plate epithelium and the roof plate boundaries, the latter equivalent to the *gdf7*-positive domain in chick. In mouse, the roof plate boundaries can be distinguished by their expression of high levels of *wnt1*, *gdf7* and *lmx1a* mRNA expression at both upper and lower rhombic lip levels (Landsberg et al., 2005; Chizhikov et al., 2006).

Of other genes known to play a role in dorsoventral patterning that were analysed (*bmp4*, *bmp7* and *wnt1)*, only *bmp7* and *wnt1* were expressed in the dorsal hindbrain at E4 and E5 (Figure 2-4). Although *bmp7* and *wnt1* are both expressed at the roof plate epithelium – hindbrain neuroepithelium boundary, within the *gdf7*-domain, they are also expressed in other neural tube domains such as in the dorsal neuroepithelium (*bmp7* and *wnt1*) and in the roof plate epithelium (*bmp7*) at E4 (Figure 2-5). Further, *wnt1* did not mark the most anterior roof plate boundary, adjacent to the isthmus, at E4 (Figure 2-4). Thus *gdf7* was the most specifically expressed at the hindbrain roof plate in chick, and was hence used as a marker of an intact roof plate epithelium – hindbrain neuroepithelium boundary for the rest of my analyses and experiments.

Chapter 3 Tissue interactions and the maintenance of the *gdf7* – positive organiser

3.1 Background

Organisers within the developing central nervous system (CNS) are often found at boundaries between molecularly distinguishable compartments (Kiecker and Lumsden, 2005). Experiments involving the recombination of compartment tissues have provided examples of boundary-localised organisers that can be regenerated at the interface between juxtaposed tissues. For example, the midbrain-hindbrain boundary can be regenerated by the juxtaposition of midbrain and rhombomere 1 tissues, as assessed by the expression of *fgf8,* in the chick (Irving and Mason, 1999). Likewise, Guinazu et al. (2007) showed that the zona limitans intrathalamica (ZLI) in chick can be regenerated at the interface between juxtaposed prospective pre-thalamus and the prospective thalamus, as assessed by the expression of *shh* (Guinazu et al., 2007). Further, although the hindbrain rhombomere boundaries have not yet been shown to be organisers in chick, their role as organisers has been alluded to by studies in zebrafish (Riley et al., 2004), and experiments have shown that rhombomere boundaries (as assessed by morphology and immunohistochemistry for molecular boundary markers such as Chondroitin Sulphate Proteoglycan (CSPG)) can be regenerated by the juxtaposition of adjacent rhombomeres, but generally not by the recombination of rhombomeres of the same type (even or odd numbered) (Guthrie and Lumsden, 1991; Heyman et al., 1995).

The studies detailed above indicated that signalling across boundaries served to either establish or maintain the boundary-localised organiser *in vivo.* Indeed repulsive Eph-ephrin signalling has been shown to drive cell sorting between adjacent rhombomeres, a mechanism that could underlie the initial formation of rhombomere boundaries (Mellitzer et al., 1999; Xu et al., 1999; Cooke et al., 2001; Cooke and Moens, 2002). For the midbrain-hindbrain boundary and the ZLI, Notch signalling and the Notch signalling modulator, *lunatic fringe* (*lfng*), have been shown to be important, with Notch signalling being necessary and sufficient for the positioning of midbrain-hindbrain boundary formation (Tossell et al., 2011), and *lfng* being important in the formation or maintenance of the ZLI (Zeltser et al., 2001).

The boundary between hindbrain roof plate epithelium and neuroepithelium shows high and persistent expression of the chick *hes1*-orthologues, *chairy1* and *chairy2* (Figure 2-6, 2-7) (Jouve et al., 2000). Such expression of Hes1 is characteristic of boundary-localised organisers (Baek et al., 2006). In Chapter 2 it was demonstrated that *gdf7* specifically marks

the roof plate epithelium – hindbrain neuroepithelium boundary in chick from E3 – E6 (Figure 2-1, 2-2). Therefore in this chapter I investigated whether the *gdf7*-positive boundary is also be maintained by signals across the boundary, another characteristic property of boundary-localised organisers. This was investigated in the same manner as detailed for the above studies; by the experimental juxtaposition of adjacent compartment tissues (in this case the hindbrain roof plate epithelium and the neuroepithelium).

3.1.1 Experimental approach

Previous studies using chick embryos have used both *in vitro* co-culture of adjacent compartment tissues and *in vivo* grafting of tissues to demonstrate regeneration of boundaries and boundary-localised organisers (Guthrie and Lumsden, 1991; Irving and Mason, 1999; Guinazu et al., 2007). The same approach can therefore be used to determine whether *gdf7* expression could be induced at the interface between roof plate epithelium and hindbrain neuroepithelium. Recent development of a green fluorescent protein (GFP)-transgenic chicken line (Helen Sang, Roslin Institute, Edinburgh) further allows the tissue origin of cells in co-cultures to be traced without any complications that might occur in cross-species experiments using chick-quail grafts (Irving and Mason, 1999; Guinazu et al., 2007), such as differences in cell affinities that might occur between tissues from different species.

gdf7 begins to be expressed at the chick roof plate epithelium – hindbrain neuroepithelium boundary at E2.5 (st14) and is strongly expressed there by E3 (st16) (Figure 2-3, C, D). Therefore E3 was initially chosen as a suitable age to investigate whether *gdf7* can be induced at an experimental roof plate epithelium – rhombic lip neuroepithelium boundary, by tissue grafting experiments. Heterochronic grafting experiment of E4-derived rhombic lip tissue into the E3 roof plate epithelium was carried out because of difficulty in the accurate dissection and isolation of rhombic lip tissue from E3 embryos. Subsequent *in vitro* experiments co-culturing roof plate epithelium and hindbrain neuroepithelium were orthochronic but focussed on E4 to E6 chick hindbrains as E3 hindbrains were too difficult to accurately dissect and isolate sufficient roof plate epithelium to be used in co-culture experiments.

While *gdf7* expression might give a read-out of the integrity of a recapitulated boundary, organiser activity can only be assessed by examining whether tissue adjacent to a “new” boundary can be patterned in a predictable manner. To asses this, *cath1* expression was also examined using *in situ* hybridisation. Previous studies in mouse have shown that the hindbrain roof plate is sufficient to ectopically induce Math1 expression in early neural

tissue (Chizhikov et al., 2006), therefore I assessed whether *cath1* was induced in the neuroepithelium adjacent to an induced *gdf7*-positive domain.

3.2 Results

3.2.1 *gdf7* is induced at a roof plate epithelium – rhombic lip neuroepithelium boundary *in vivo*

Heterotopic/ heterochronic grafts were carried out to determine whether *gdf7* is induced at an interface between roof plate epithelium and rhombic lip neuroepithelium. Pieces of rhombic lip were isolated from E4 (st22) GFP-transgenic chick embryos and transplanted into the roof plate epithelium of E3 (st16) wild-type chick host embryos, as illustrated in Figure 3-1-1. Hosts were then incubated for 24 hours prior to collection. *gdf7* was induced at the interface between grafted rhombic lip neuroepithelium and host roof plate epithelium, but was not induced when roof plate epithelium was grafted into roof plate epithelium (Figure 3-1-2 A, B, arrow; n=3/9 RLNe to RPE grafts; n=0/3 RPE to RPE grafts). However, *gdf7* induction was not seen in grafts of roof plate epithelium into upper rhombic lip, or in control rhombic lip neuroepithelium into upper rhombic lip (Figure 3-1-2 C, D, n=0/3 RPE to RLNe; n=0/3 RLNe to RLNe). Ectopic *cath1* expression in the hindbrain neuroepithelium was not induced by the roof plate epithelium graft (Figure 3-1-2 C, n=0/3). *cath1* expression was maintained in the rhombic lip neuroepithelium graft transplanted into the upper rhombic lip (Figure 3-1-2 D, arrows, n=3/3). In contrast, when rhombic lip neuroepithelium was transplanted into the midbrain the expression of *cath1* in the graft was downregulated or even absent after 24 hours (Figure 3-1-2 E, F, arrows n=2/2), implying that signals from the roof plate or surrounding upper rhombic lip tissue are required to maintain *cath1* expression in the transplanted rhombic lip neuroepithelium.

3.2.2 *gdf7* and *cath1* are induced at a roof plate epithelium – hindbrain neuroepithelium interface in co-culture

Although *gdf7* was induced at the interface between roof plate epithelium and rhombic lip neuroepithelium *in vivo*, the frequency of induction was rather low (Figure 3-1-2 A, n=3/9). Therefore a different experimental paradigm was used to investigate the induction of *gdf7* at the interface between roof plate epithelium and hindbrain neuroepithelium. Roof plate epithelium and hindbrain neuroepithelium were instead juxtaposed in an *in vitro* co-culture system, as illustrated in Figure 3-2. Hindbrains from E4, E5 and E6 chicken embryos were flat-mounted and the roof plate epithelium, *gdf7*- and *cath1*-domains were removed from both sides of the flat-mounted hindbrains. Removal of the roof plate epithelium generally completely removes the *gdf7*-domain, as verified by *in situ* hybridisation analysis of

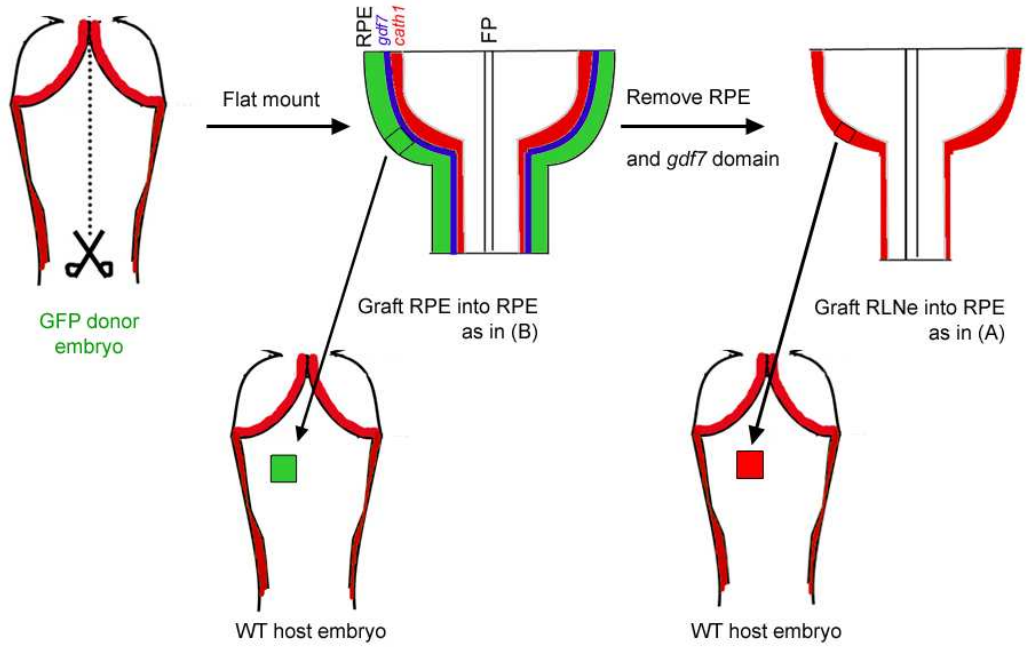

Figure 3-1-1 Diagram illustrating the procedure of grafting RPE or RLNe into host hindbrains

A hindbrain from an E4 GFP transgenic donor embryo is flat-mounted by cutting along the dorsal midline. RPE is dissected from flat-mounted hindbrains and grafted into the RPE of hindbrains of E3 WT host embryos, for RPE to RPE grafts (as in Figure 3-1-2 B). Host embryos are then re-incubated for 24 hours prior to collection.

For RLNe to RPE grafts (as in Figure 3-1-2 A), the RPE and *gdf7*-positive domain are removed from flat-mounted GFP transgenic hindbrains and pieces of *cath1*-positive rhombic lip are isolated. Pieces of GFP-positive rhombic lip are grafted into the RPE of E3 WT host embryos. Host embryos are then re-incubated for 24 hours prior to collection.

RPE, roof plate epithelium; FP, floor plate; RLNe, rhombic lip neuroepithelium; GFP, green fluorescent protein; WT, wild-type.

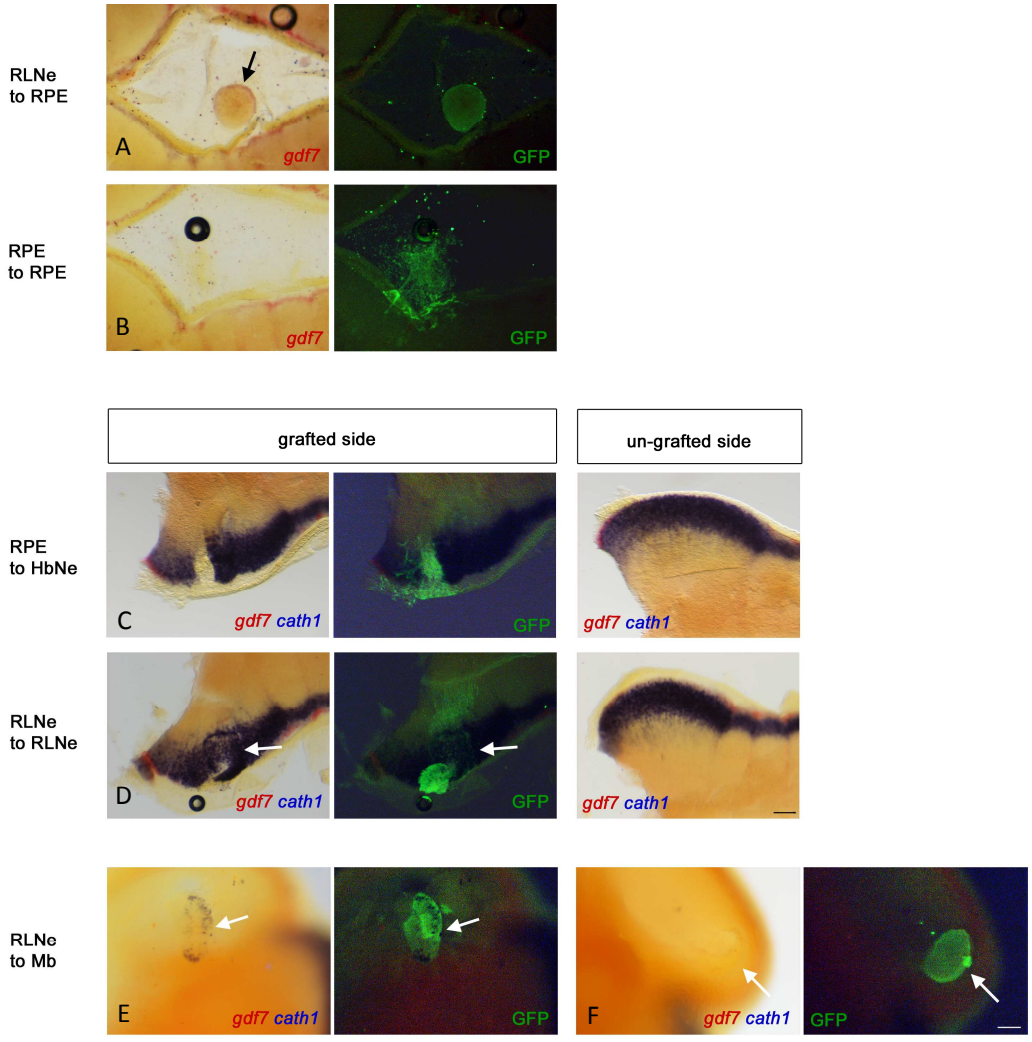
RLNe
to RPE
A
gdf7
GFP
RPE
to RPE
B
gdf7
GFP
grafted side
un-grafted side
RPE
to HbNe
C
gdf7 cath1
GFP
gdf7 cath1
RLNe
to RLNe
D
gdf7 cath1
GFP
gdf7 cath1
RLNc
to Mb
E
gdf7 cath1
GFP
F
gdf7 cath1
GFP

Figure 3-1-2 *in vivo* induction of *gdf7* occurs in RLNe to RPE grafts

Pieces of RLNe (A) or RPE (B) from st22 GFP-transgenic chick embryos were grafted into the RPE of st16 wild-type host chick embryos, which were then incubated for 24 hours and collected at st20 for processing for whole-mount *in situ* hybridisation. *gdf7* (red) was induced at the interface between RlNe and RPE (arrow) but not at the interface between RPE and RPE. Images show flat-mounted roof plates.

Pieces of RPE (C) or RLNe (D) from st22 GFP-transgenic chick embryos were grafted into the right-hand side upper rhombic lip of st16 wild-type host chick embryos. *gdf7* (red) was not induced at the boundaries of either of these grafts. Ectopic *cath1* was not induced by the RPE graft in (C), but was maintained in the RLNe graft in D (arrows). Images show flat-mounted hindbrains

Pieces of RLNe from st22 GFP-transgenic chick embryos were grafted into the Mb of st16 wild-type host embryos (E, F). *gdf7* (red) was not induced and *cath1* (blue) expression was downregulated or not present in the grafted RlNe. Images show whole-mount embryos.

Anterior is oriented to the left. RLNe, rhombic lip neuroepithelium; RPE, roof plate epithelium; Mb, midbrain.

Scale bars: 100µm

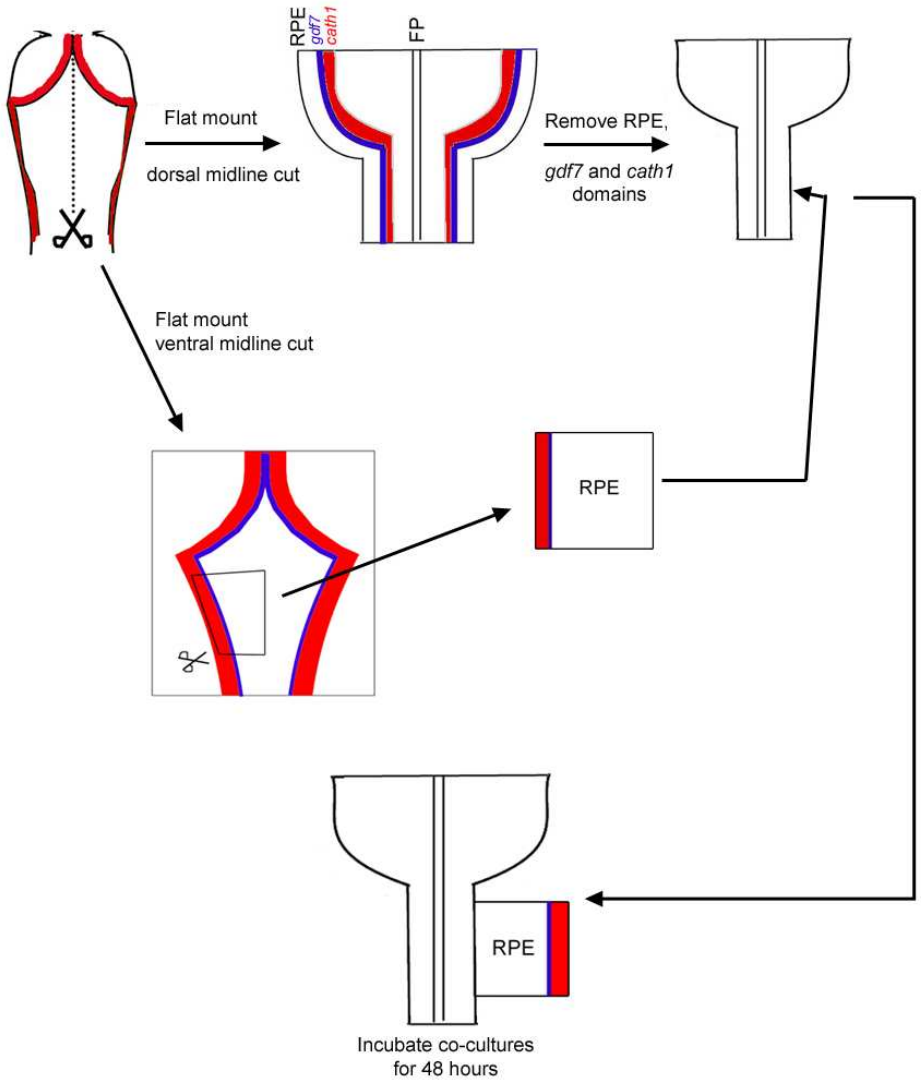

Figure 3-2 Diagram of the procedure used to co-culture roof plate epithelium and hindbrain neuroepithelium

Hindbrains from E4, E5 and E6 chicken embryos were flat-mounted by cutting along the dorsal midline. The RPE, *gdf7*- and *cath1*-domains were removed from both sides of the flat-mounted hindbrain. Other hindbrains were flat-mounted by cutting along the ventral midline. Large pieces of RPE, attached to *gdf7* domain and rhombic lip were then isolated. The pieces of RPE were cultured adjacent to flat-mounted hindbrain neuroepithelium as illustrated above. These co-cultures were then incubated for 48 hours at 37°C prior to fixation and processing for whole-mount *in situ* hybridisation. RPE, roof plate epithelium; FP, floor plate.

hindbrains immediately after roof plate epithelium removal (Figure 3-10, 3-11). Data from Chapter 1 provided an estimate of the size of the *cath1*-domain. To be certain of its complete removal, the dorsal third of the neuroepithelium was removed. Pieces of roof plate epithelium were dissected from other hindbrains in the manner illustrated in Figure 3-2 and cultured adjacent to one side of the flat-mounted hindbrain neuroepithelium. The side of the hindbrain that was not cultured adjacent to the roof plate epithelium served as the control for complete removal of the *gdf7* and *cath1* domains. Either the hindbrain neuroepithelium or the roof plate epithelium was derived from a GFP – transgenic chick embryo, while the other component of the co-culture was derived from a wild-type chick embryo. These co-cultures were then incubated for 48 hours at 37°C at an air-liquid interface with the pial surface of the hindbrain facing upwards, on 0.4μm culture plate inserts (Millicell – CM, Millipore) that had been placed in 3mls of sterile slice media, prior to fixation and processing for whole-mount *in situ* hybridisation.

In explants from E4, E5 and E6 brains, cultured for 48 hours, *gdf7* was induced at the interface between recombined hindbrain neuroepithelium and roof plate epithelium (Figure 3-3, 3-4, 3-5, arrows; Table 1). The expression of *cath1* was also induced adjacent to induced *gdf7* in explants derived from all ages (Figure 3-3, 3-4, 3-5 arrowheads), but at a lower frequency than *gdf7* induction (Table 1). In explants derived from E5 and E6 brains, *cath1* is also bilaterally expressed in post-mitotic neurons of the trigeminal and facial paramotor nuclei (Figure 3-4, D, E; 3-5, E – J, open arrows) (Rose et al., 2009b). In support of the findings of Thoby-Brisson et al. (2009), the expression of *cath1* in paramotor nuclei is autonomous of the removal of rhombic lip at these ages suggesting that these nuclei are not derivatives of E4-6 rhombic lip. The anterior domains of *cath1* expression in Figure 3-4 (E) and Figure 3-5 (H) indicated by open arrowheads have no equivalent in mice and it is so far unclear as to what cell types derive from these domains (Wingate, unpublished).

The percentage of explants that show *cath1* induction adjacent to induced *gdf7* decreases between E4 and E6, while the percentage showing *gdf7* induction alone increases (Figure 3-6). *cath1* induction was never seen without an adjacent domain of induced *gdf7*, therefore it is likely that the signals that induce *cath1* derive from the *gdf7*-domain and the competence of non-rhombic lip hindbrain tissue to respond to these signals decreases between E4 and E6.

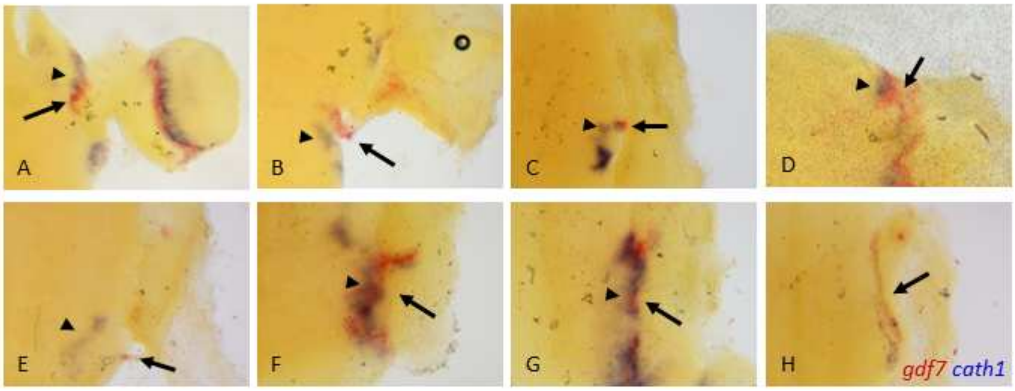

Figure 3-1 *gdf7* and *cath1* are induced at the interface between RPE and HbNe in co-cultures from E4 brains

Eight examples of co-cultures derived from E4 chick brains that were incubated for 48 hours where *gdf7* and *cath1* (A – G) or *gdf7* alone (H) are induced at the interface between RPE and HbNe. *gdf7* is in red, *cath1* is in blue. Arrows, induced *gdf7* expression; arrowheads, induced *cath1* expression. RPE, roof plate epithelium; HbNe, hindbrain neuroepithelium.

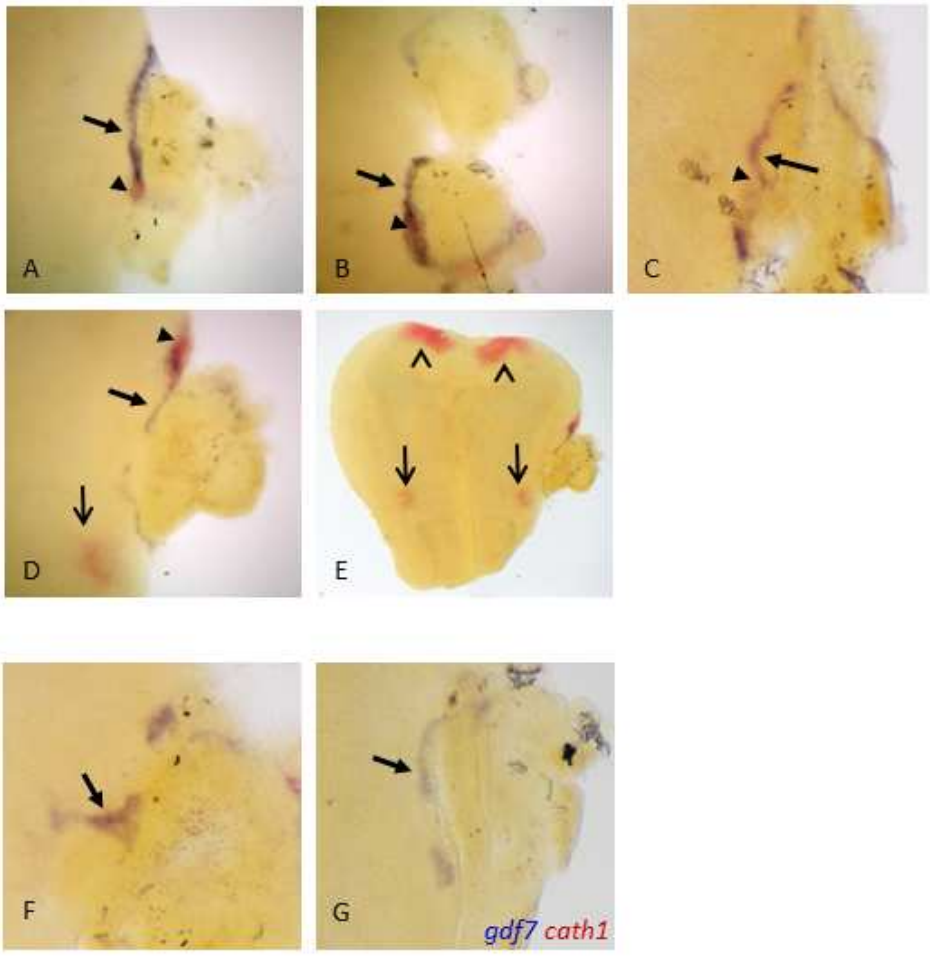

Figure 3-2 *gdf7* and *cath1* are induced at the interface between RPE and HbNe in co-cultures from E5 brains

Examples of co-cultures derived from E5 chick brains that were incubated for 48 hours where *gdf7* and *cath1* (A – E) or *gdf7* alone (F, G) are induced at the interface between RPE and HbNe. *gdf7* is in blue, *cath1* is in red. Arrows, induced *gdf7* expression; arrowheads, induced *cath1* expression; open arrows, paramotor nuclei; open arrowheads, anterior domains of *cath1* expression. RPE, roof plate epithelium; HbNe, hindbrain neuroepithelium.

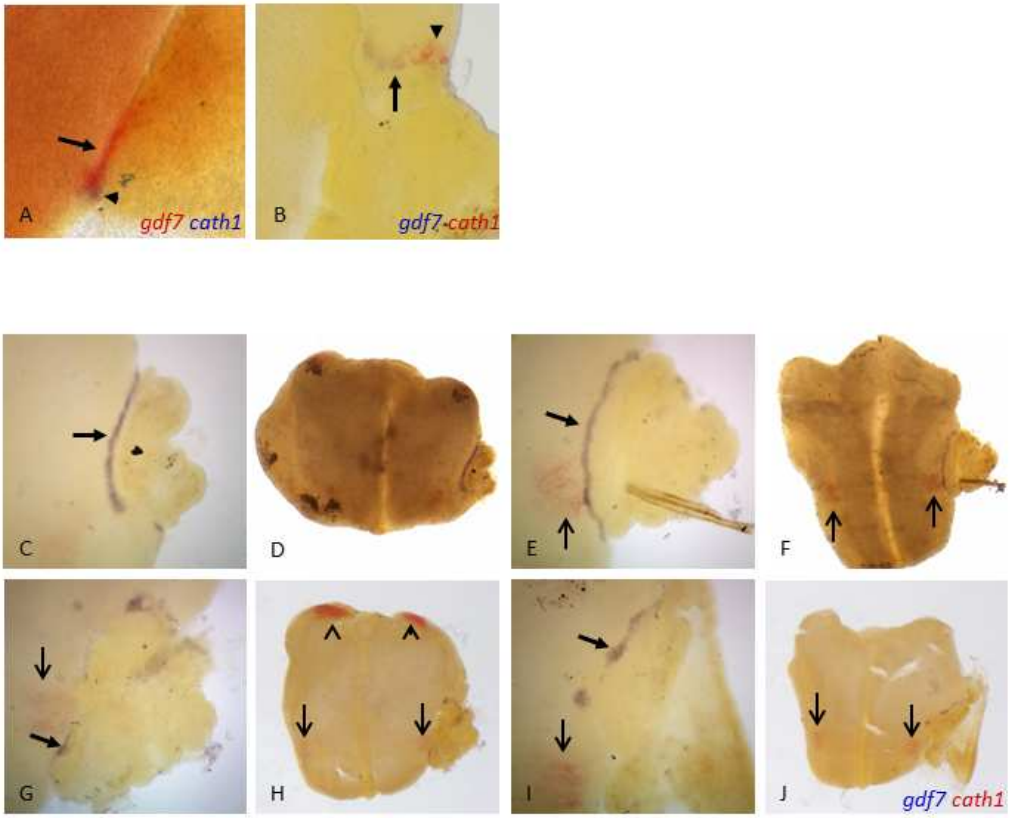

Figure 3-3 *gdf7* and *cath1* are induced at the interface between RPE and HbNe in co-cultures from E6 brains

Examples of co-cultures derived from E6 chick brains that were incubated for 48 hours where *gdf7* and *cath1* (A, B) or *gdf7* alone (C – J) are induced at the interface between RPE and HbNe. *gdf7* is in red and *cath1* is in blue in A. *gdf7* is in blue, *cath1* is in red in B - J. Arrows, induced *gdf7* expression; arrowheads, induced *cath1* expression; open arrows, paramotor nuclei; open arrowheads, anterior domain of *cath1* expression. RPE, roof plate epithelium; HbNe, hindbrain neuroepithelium.

Table 1 Frequency of *gdf7* and *cath1* induction in roof plate epithelium – hindbrain neuroepithelium co-cultures

	E4	E5	E6
gdf7 and *cath1* adjacent	7	6	2
gdf7 only	1	5	8
no induction	0	4	1
Total	8	15	11

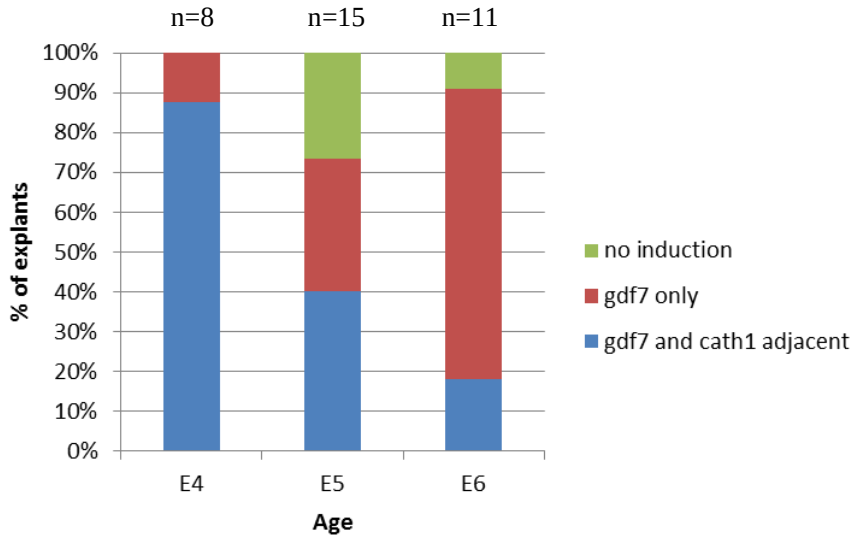

Figure 3-6 Percentage of explants showing either *gdf7* induction or the induction of *cath1* adjacent to *gdf7* expression

3.2.3 *gdf7* is induced in roof plate epithelium- derived cells and *cath1* is induced in hindbrain neuroepithelium- derived cells in co-cultures

Either the roof plate epithelium or the hindbrain neuroepithelium of a co-culture was labelled by GFP. Thus the source of the cells expressing *gdf7* could be determined by comparison of *in situ* hybridisation label with immunohistochemistry for GFP. A confocal micrograph of a flat-mounted E4 co-culture shows that *gdf7* expression co-localises with GFP, which in this case marks roof plate epithelium- derived cells (Figure 3-7 A – D). Sections through E6 co-cultures as indicated in Figure 3-4 E show that *gdf7* expression co-localises with GFP – positive roof plate epithelium-derived cells (Figure 3-7 F – I, arrows). Lastly, a section through an E4 co-culture also shows that *gdf7* is induced in roof plate epithelium-derived cells, which in this case are GFP – negative (Figure 3-7 J – M, arrows). In Figure 3-7 F – I, it is also possible to see that *gdf7* is not induced in all regions of roof plate epithelium that are adjacent to neuroepithelium (Figure 3-7, arrowhead). *gdf7* is only induced where the two tissues intermingle. This indicates a cell – cell contact-mediated mechanism of induction of *gdf7*, rather than a diffusion-based one. By contrast, non-overlapping *cath1* expression was induced in hindbrain neuroepithelium-derived cells adjacent to the domain of *gdf7* induction, as shown in Figure 3-4 K – M (arrowhead).

3.2.4 *gdf7* is not induced at the interface between roof plate epithelium and roof plate epithelium

In order to determine whether *gdf7* induction is specific to a particular tissue combination, roof plate epithelium derived from GFP- transgenic chick embryos was cultured adjacent to roof plate epithelium derived from wild-type chick embryos. Generally no *gdf7* is induced at the interface between the two tissues in such culture conditions (Figure 3-8 A, B, D – F; E5 n=2/3, E6 n=3/3). The approximate location of the interface in indicated with dotted lines on images in Figure 3-8. Due to high levels of auto-fluorescence it was difficult to discern the exact location of the interface between the two pieces of roof plate epithelium by whole-mount immunohistochemistry with anti-GFP antibodies. One co-culture derived from E5 brains showed a small region of *gdf7* expression at the indicated interface between the two pieces of roof plate epithelium. It is likely that this represents endogenous *gdf7* expression from contamination with roof plate-boundary tissue (Figure 3-8 C, arrow).

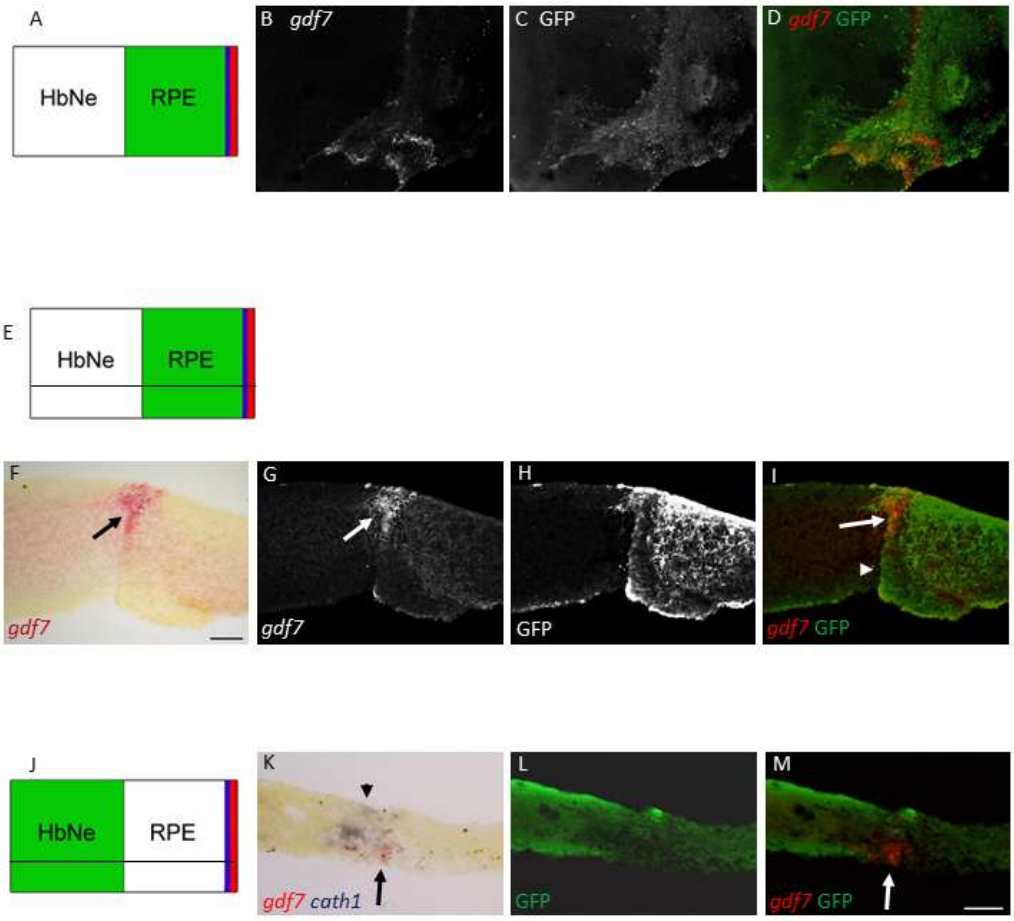

Figure 3-4 *gdf7* is induced in roof plate epithelium-derived cells and cath1 is induced in hindbrain neuroepithelial cells

B – D show a confocal microscope slice of a flat-mounted E4 co-culture. *gdf7* is expressed in GFP – positive cells, which are RPE derived as indicated in A.

F – I show images of a cryostat section through an E6 co-culture. *gdf7* is expressed in GFP-positive cells (arrows), which are RPE derived as indicated in E. Arrowhead indicates a lack of *gdf7* induction in roof plate epithelium that is not intermingled with neuroepithelium.

K – M show images of a cryostat section through an E4 co-culture. *gdf7* is expressed in GFP-negative cells (arrows), which are roof plate epithelial-derived as indicated in J. *cath1* is expressed in GFP-positive cells (arrowhead), which are hindbrain neuroepithelial-derived as indicated in J.

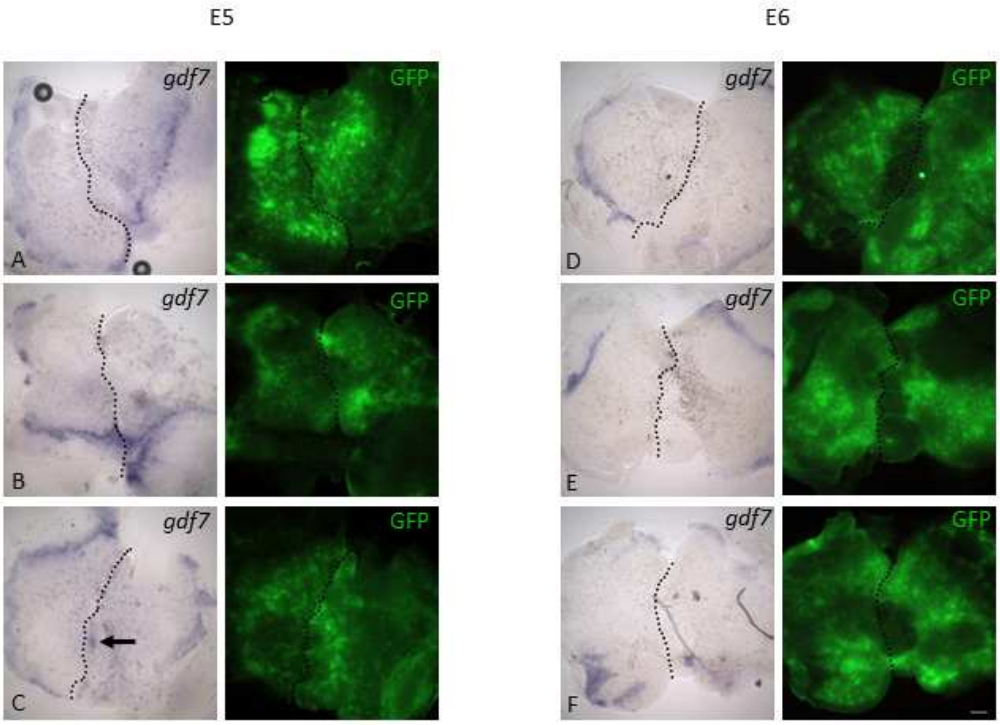

Figure 3-5 *gdf7* expression in RPE – RPE co-cultures

Three co-cultures derived from E5 (A – C) or E6 (D – F) chick brains where RPE is cultured adjacent to RPE, showing the expression of *gdf7*. In each co-culture, one rpe was derived from a GFP-transgenic chick and the other RPE was derived from a wild-type chick. However, due to auto-fluorescence of the RPE it is very difficult to tell the difference between GFP-positive and GFP-negative RPE by whole-mount immunohistochemistry. Dotted lines indicate the interface between pieces of RPE in a co-culture. Arrow indicates *gdf7* expression at the interface between roof plate tissues, but is likely to represent contamination by roof plate boundary tissue rather than induced expression. RPE, roof plate epithelium.

Scale bar: 100µm

3.2.5 *gdf7* is induced at the interface between hindbrain roof plate epithelium and spinal cord neuroepithelium

The juxtaposition of hindbrain roof plate epithelium and spinal cord neuroepithelium from E5 or E6 embryos shows that *gdf7* expression can be induced at the interface between roof plate epithelium and neuroepithelium of a different axial origin (Figure 3-9 B – D, arrows; E5 n= 1/2, E6 n=2/2). In these co-cultures, roof plate epithelium was always GFP-positive and was detected as such, after *in situ* hybridisation, by whole-mount immunohistochemistry.

3.2.6 The roof plate is required to maintain the expression of *cath1* in the adjacent rhombic lip

Roof plates (including the *gdf7*-domain) were dissected away from one side of flat-mounted hindbrains from E4, E5 and E6 embryos. Hindbrains were then assessed immediately for the expression of *cath1* and *gdf7* (0 hours incubation) or were cultured for 48hrs prior to fixation and assessment of *cath1* and *gdf7* expression. At 0 hours incubation, *cath1* expression is present in the rhombic lip on both the side of the hindbrain from which the roof plate was removed, and the side where it was not removed in explants deriving from all ages (Figure 3-10 A – C, G – I, M – O). These explants show that the *gdf7* domain and roof plate can be accurately removed from one side of the hindbrain, whilst leaving the rhombic lip *cath1* expression domain mostly intact (Figure 3-10 compare B to C, H to I, N to O). After 48 hours of incubation, *cath1* expression is lost in the rhombic lip on the side of the hindbrains from which the roof plate was removed, whilst being maintained on the side of the hindbrains where the roof plate was intact. (Figure 3-10 D – F, J – L, P – R, arrows, *cath1* expression maintained adjacent to roof plate). In contrast to rhombic lip *cath1* expression, the paramotor nucleus expression of *cath1* is present on both sides of hindbrain explants cultured for 48 hours so this domain of *cath1* expression is not dependent on acute signals from the roof plate for its maintenance (Figure 3-10 E, F, K, L, arrowheads).

In order to assess the time-course of the loss of *cath1* expression, the roof plate was removed from E6 hindbrains and the hindbrain explants were cultured for varying lengths of time between 0 and 48 hours. No change in the level of *cath1* expression in the rhombic lips of hindbrain explants was seen up to 8 hours after roof plate removal (Figure 3-11 A – E). By 16 hours, *cath1* expression begins to be down-regulated in the rhombic lips, with staining becoming much less intense, and is almost completely absent by 32 hours of incubation (Figure 3-11 F, G). At 32 hours of incubation *cath1* expression can be seen in the rhombic lips as small patches, but some of these patches of expression are associated with residual *gdf7* expression, which is due to incomplete removal of the *gdf7*-domain (Figure 3-11 I,

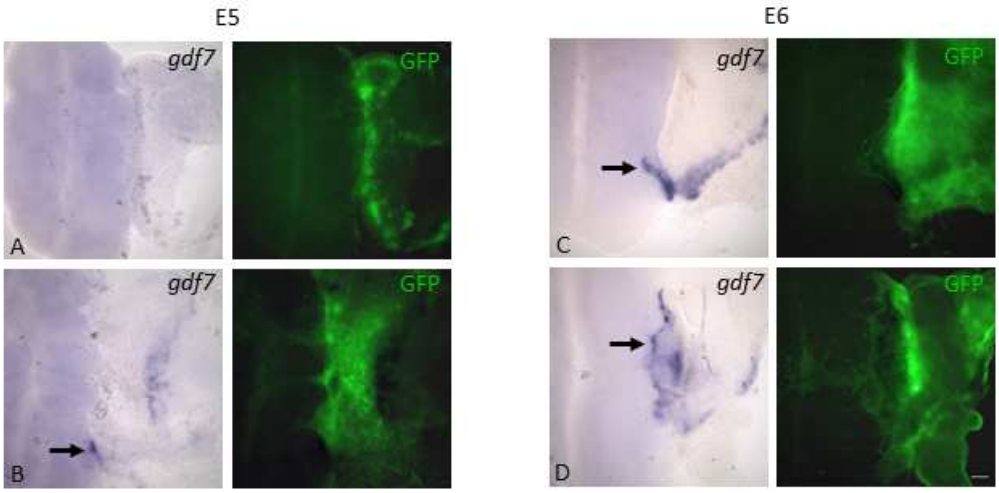

Figure 3-6 *gdf7* is induced at the interface between hindbrain RPE and spinal cord neuroepithelium

Two co-cultures derived from E5 (A, B) or E6 (C, D) chick embryos where RPE is cultured adjacent to flat-mounted spinal cord neuroepithelium. Images show *gdf7* expression as detected by whole-mount *in situ* hybridisation, and GFP expression as detected by whole-mount immunohistochemistry, labelling the RPE component of co-cultures. Arrows, indicate induced *gdf7* expression. RPE, roof plate epithelium.

Scale bar: 100µm

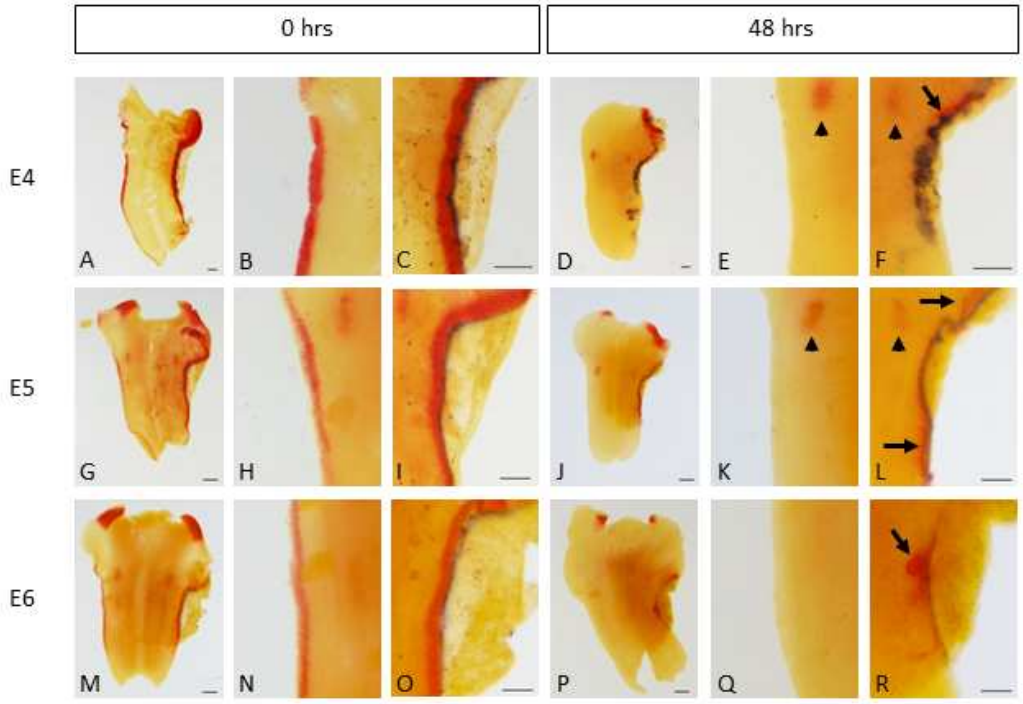

Figure 3-7 *cath1* expression is lost in hindbrain explants cultured for 48 hours when roof plate is removed

Roof plate (RPE and *gdf7* domain) is removed from one side of flat-mounted hindbrains from E4 (A – F), E5 (G – L) and E6 (M – R) chick embryos and either fixed immediately (0hrs; A – C, G – I, M – O) or cultured for 48 hours and then fixed (48 hrs; D – F, J – L, P – R). *cath1* (red) and *gdf7* (blue) are detected by whole-mount double *in situ* hybridisation. B, E, H, K, N, Q show the side of hindbrains where roof plate was removed. C, F, I, L, O, R show the side of hindbrains where the roof plate was not removed. Arrows indicate *cath1* expression maintained adjacent to intact roof plate; arrowheads, remaining paramotor nucleus *cath1* expression. Anterior is oriented upwards.

Scale bars: 200µm, A – F, H, I, L, O, R. 400µm, G,J, M, P

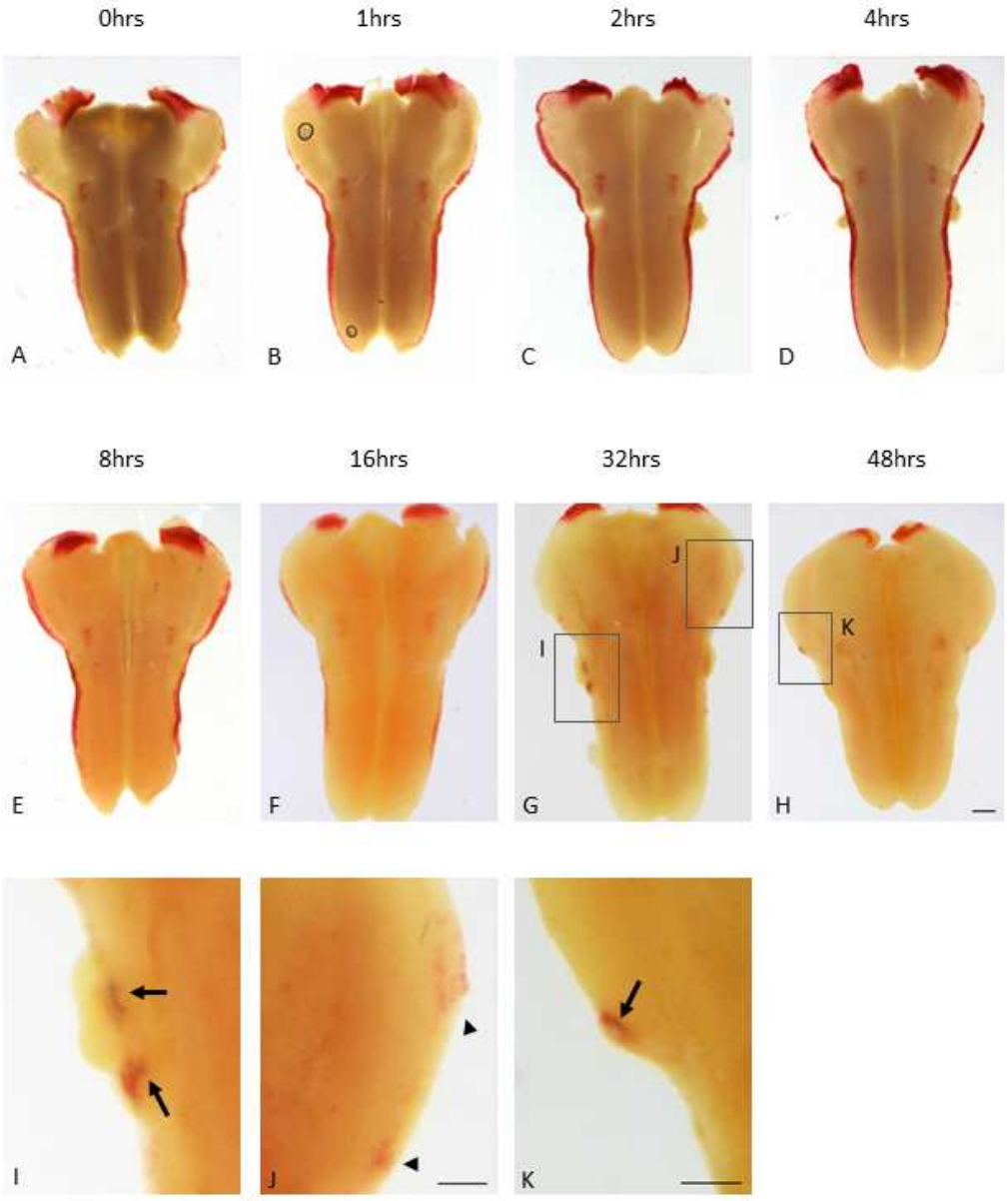

Figure 3-8 *cath1* expression is lost in the rhombic lips between 32 and 48 hours of culture

cath1 (red) and *gdf7* (blue) expression as detected by whole-mount in situ hybridisation in E6 chick hindbrain explants cultured for 0 hrs (A), 1 hrs (B), 2 hrs (C), 4hrs (D), 8 hrs (E), 16 hrs (F), 32 hrs (G) or 48 hrs (H). I and J show high magnification views of the areas indicated in G. K shows a high magnification view of the area indicated in H. hrs, hours. Arrows indicate sites of residual *gdf7* expression; arrowheads indicate *cath1* expression present in the rhombic lips not adjacent to any residual *gdf7* expression. Anterior is oriented upwards.

Scale bars: 400µm, H. 200µm, J, K.

arrows). Other patches of *cath1* expression present in the rhombic lips at 32 hours are not associated with any adjacent *gdf7* expression (Figure 3-11 J, arrowheads). By 48 hours all *cath1* expression in the rhombic lips has been lost apart from a small domain of expression that is associated with a patch of *gdf7* expression (Figure 3-11 H, K, arrow). Therefore *cath1* expression is completely lost in the E6 rhombic lip between 32 and 48 hours of culture after the removal of the roof plate.

In order to confirm that signals from the roof plate epithelium or *gdf7*-domain can maintain *cath1* expression in the rhombic lips of cultured hindbrains, roof plate epithelium was cultured adjacent to the rhombic lip (*cath1*-domain) of flat-mounted hindbrains from which the roof plate (including the *gdf7*-domain) had been removed. These types of co-cultures will be referred to henceforth as roof plate epithelium – rhombic lip neuroepithelium co-cultures. *gdf7* is induced at the interface between rhombic lip neuroepithelium and roof plate epithelium in E5 and E6 -derived explants in the same manner as described for when roof plate epithelium is cultured adjacent to non-rhombic lip hindbrain neuroepithelium (Figure 3-12, 3-13 A – G, arrows). *cath1* was maintained in the rhombic lip adjacent to the transplanted roof plate epithelium in explants deriving from E5 brains in 10/11 explants where *gdf7* was induced (Figure 3-12, arrowheads, Table 2). *cath1* expression was always maintained adjacent to induced *gdf7* expression. In explants deriving from E6 brains *cath1* was maintained in the rhombic lip adjacent to induced *gdf7*, but in a lower proportion of explants than for explants derived from E5 embryos (Figure 3-13 E – G, arrowheads, Figure 3-14). Correspondingly, the percentage of explants showing only *gdf7* induction was higher in E6 explants in comparison with explants from E5 embryos. In two explants derived from E6 embryos, *cath1* was expressed adjacent to the transplanted roof plate in the absence of apparent *gdf7* expression (Figure 3-13 H, I, arrowheads). One possible explanation for this could be that signals from the roof plate epithelium outside the *gdf7*-domain are sufficient to maintain *cath1* expression in the E6 rhombic lip. However another explanation is that induced *gdf7* levels were too low to detect in these cases by whole-mount double *in situ* hybridisation. Therefore it seems likely that signals that maintain *cath1* expression in the rhombic lip derive from the *gdf7*-positive domain rather than from the rest of the roof plate epithelium.

Figure 3-15 shows that the proportion of explants showing *gdf7* expression that also show adjacent *cath1* expression is higher in roof plate epithelium – rhombic lip neuroepithelium co-cultures than in roof plate epithelium – hindbrain neuroepithelium co-cultures of the corresponding age. Thus it is easier to maintain *cath1* expression in the rhombic lip than it is to induce it in non-rhombic lip tissue implying that there may be differences in competence of the hindbrain neuroepithelium to respond to roof plate-derived signals, along the

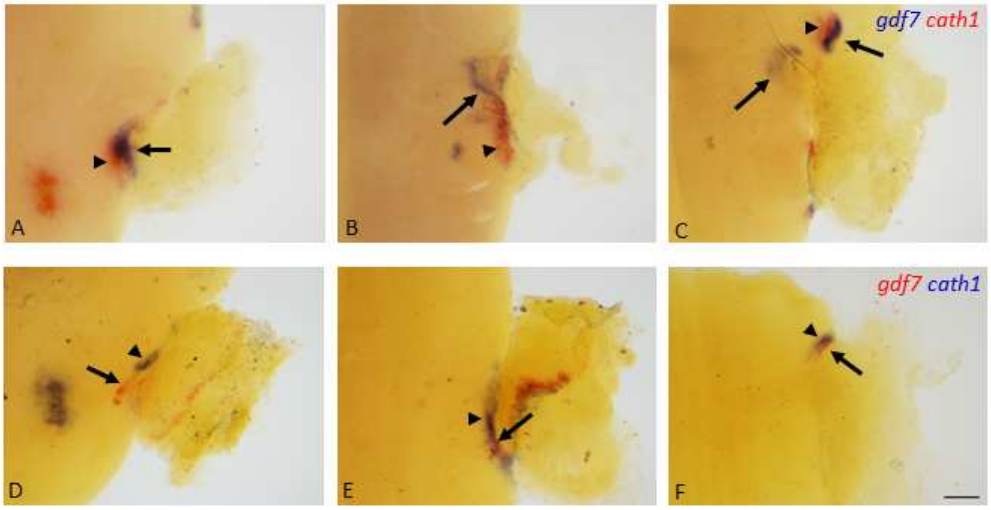

Figure 3-9 *cath1* is maintained adjacent to induced *gdf7* in E5 roof plate epithelium – rhombic lip neuroepithelium co-cultures

Six examples of explants where roof plate epithelium was cultured against flat-mounted hindbrains from E5 chick embryos where the rhombic lips had not been removed. Explants were cultured for 48hrs then assessed for the expression of *gdf7* and *cath1*. In A – C *gdf7* is in blue and *cath1* is in red. In D – F *gdf7* is in red and *cath1* is in blue. *gdf7* is induced at the interface between roof plate epithelium and rhombic lip neuroepithelium (arrows). *cath1* was maintained in the rhombic lips of cultured hindbrains adjacent to induced *gdf7* expression (arrowheads).

Scale bar: 200µm

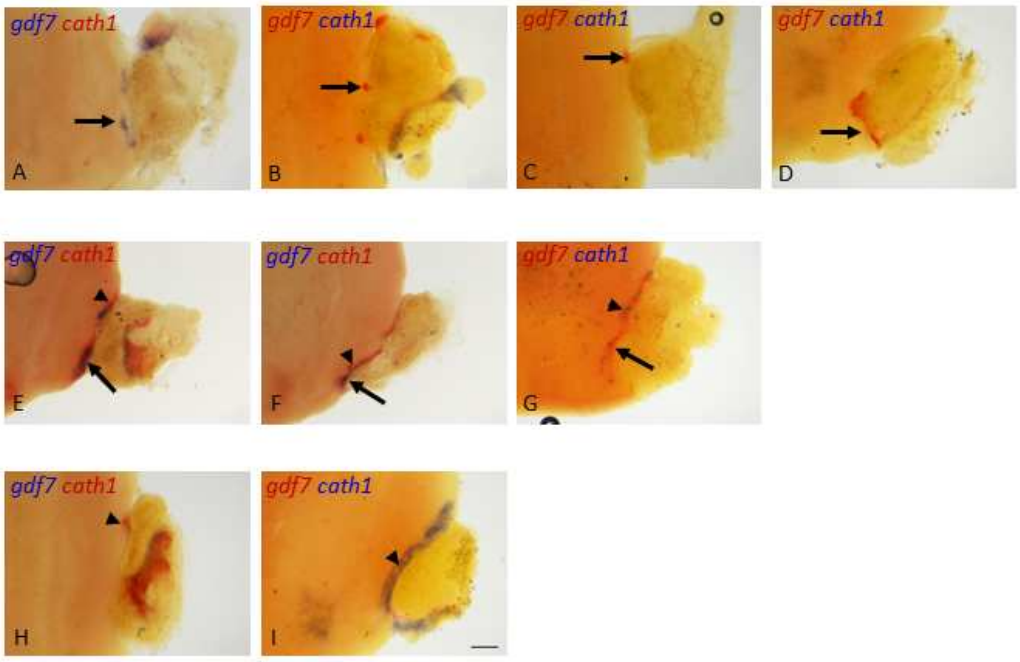

Figure 3-10 *cath1* is maintained adjacent to roof plate in E6 RPE– RlNe co-cultures

Examples of explants where roof plate epithelium was cultured adjacent to flat-mounted hindbrain neuroepithelium from E6 chick embryos where the rhombic lips had not been removed. Explants were cultured for 48 hours then assessed for the expression of *gdf7* and *cath1*. *gdf7* is in blue and *cath1* is in red in A, E, F, H. *gdf7* is in red and *cath1* is in blue in B – D, G, I. A – D show explants where only *gdf7* is induced at the interface between RPE and HbNE (arrows). E – G show explants where *cath1* is maintained adjacent to induced *gdf7* (arrowheads). Induced *gdf7* expression is indicated by arrows. H and I show explants where *cath1* is maintained adjacent to roof plate epithelium but no induced *gdf7* is visible (arrowheads). RPE, roof plate epithelium; RlNe, rhombic lip neuroepithelium.

Scale bar: 200µm.

Table 2 Frequency of *gdf7* induction and *cath1* maintenance in roof plate epithelium – rhombic lip neuroepithelium co-cultures

	E5	E6
gdf7 only	1	5
cath1 maintained adjacent to induced*gdf7*	10	3
cath1 maintained but not adjacent to *gdf7*	0	2
no induction	4	4
Total	15	14

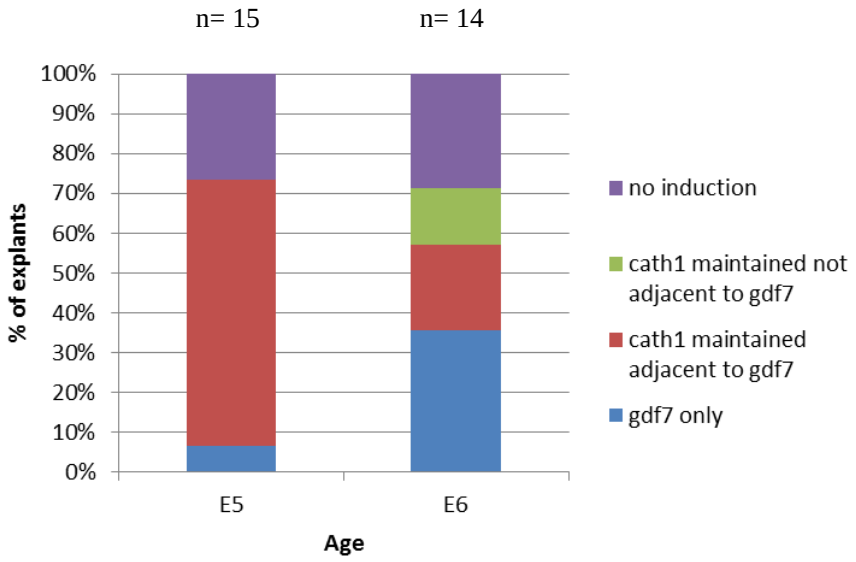

Figure 3-14 Percentage of roof plate epithelium – rhombic lip neuroepithelium co-cultures showing *gdf7* induction and *cath1* maintenance

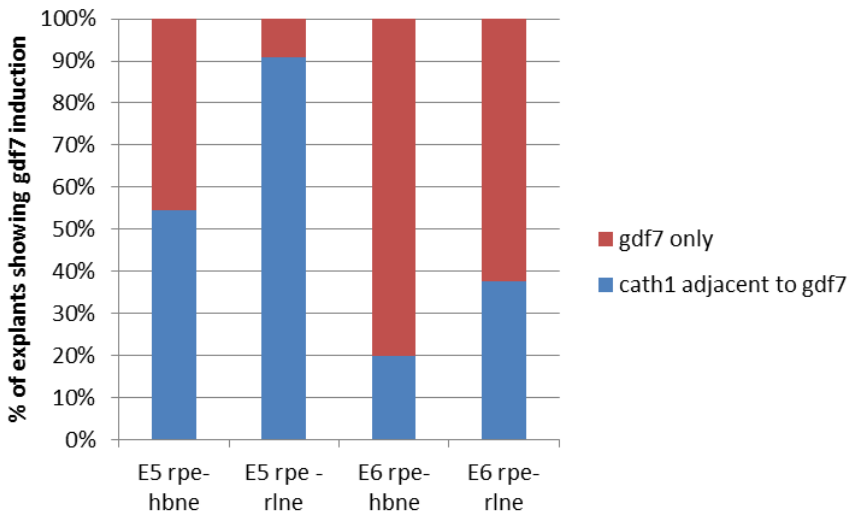

Figure 3-15 Percentage of explants showing *gdf7* expression that also show *cath1* expression adjacent to *gdf7* in E5 and E6 roof plate epithelium – hindbrain neuroepithelium (rpe – hbne) and roof plate epithelium – rhombic lip neuroepithelium (rpe – rlne) co-cultures.

dorsoventral axis.

3.2.7 *cath1* can be induced in ventral hindbrain neuroepithelium via an interaction with roof plate epithelium in co-cultures derived from E4 and E5 brains, but not from E6 brains

The competence of ventral hindbrain tissue to express *cath1* in response to signals from an induced *gdf7*-positive organiser in co-culture was examined at E4-E6 by juxtaposing roof plate epithelium along the dorsoventral axis of flat-mounted hindbrains as illustrated in Figure 3-16 A. In explants derived from E4 brains, 2/14 explants showed induction of *gdf7* and *cath1* at the interface between roof plate epithelium and hindbrain neuroepithelium (Table 3). *gdf7* was induced at the interface between the roof plate epithelium and the hindbrain neuroepithelium along most of the dorsoventral axis of the hindbrain, and even by an interaction between the roof plate epithelium and the floor plate (Figure 3-16 B, C, arrowheads, arrow marks interaction with floor plate). *cath1* was maintained adjacent to the induced *gdf7* in the rhombic lip (Figure 3-16 B open arrow), or was induced in the ventral hindbrain neuroepithelium (Figure 3-16 C, open arrow). *cath1* was only ever seen in the hindbrain neuroepithelium adjacent to induced *gdf7* expression (Table 3).

In explants derived from E5 brains, *gdf7* was induced at the interface between roof plate epithelium and hindbrain neuroepithelium in 8/18 explants (Figure 3-17 A – G, arrows,Table 3). As at E4, *gdf7* could be induced by an interaction between roof plate epithelium and the floor plate (Figure 3-17 D, open arrow). *cath1* was maintained adjacent to induced *gdf7* in the rhombic lip (Figure 3-17 B – D arrowheads, n=4/8), or was induced in the ventral hindbrain neuroepithelium (Figure 3-17 E – G, arrowheads n=3/8). In 1/18 explants *cath1* expression was seen at the interface between roof plate epithelium and hindbrain neuroepithelium, but was not adjacent to *gdf7* expression. As stated previously, this could have been due to undetectable levels of *gdf7* expression by double whole-mount *in situ* hybridisation (Figure 3-17 H, arrowhead, Table).

In explants derived from E6 brains, *gdf7* was again induced at the interface between roof plate epithelium and hindbrain neuroepithelium (Figure 3-18, arrows, n= 8/19). As in E4 and E5 explants, *gdf7* was induced by an interaction between the roof plate epithelium and ventral hindbrain neuroepithelium, including the floor plate (Figure 3-18 C, open arrow). *cath1* was also maintained adjacent to *gdf7* in 1/8 explants, but was never induced in ventral hindbrain neuroepithelium (Figure 3-18 E, arrowheads). This implies that there is a decrease

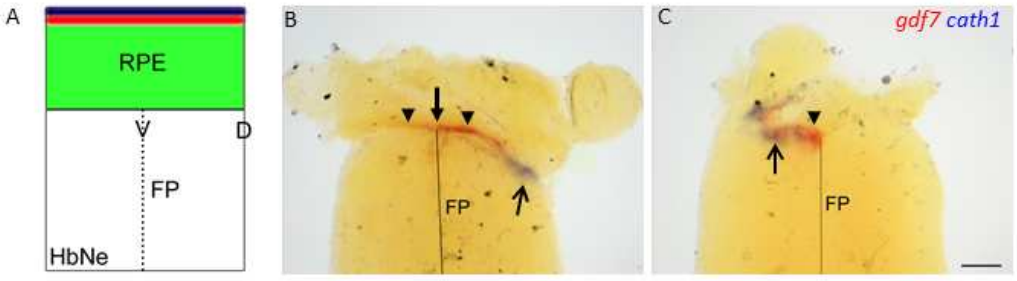

Figure 3-11 *gdf7* and *cath1* expression in RPE– HbNe co-cultures derived from E4 embryos where the RPE was cultured along the d-v axis of the hindbrain

(A) shows a diagram of the arrangement of RPE alongside the d-v axis of a flat-mounted hindbrain. The *gdf7*-domain is represented in red and the *cath1*-domain is represented in blue.

gdf7 (red) is induced at the interface between RPE and HbNe in E4-derived co-cultures (B, C, arrowheads). *gdf7* can be induced by an interaction between RPE and HbNe, including the FP (B, arrow). *cath1* (blue) is maintained in the rhombic lip (B, open arrow) or induced in ventral HbNe (C, open arrow). RPE, roof plate epithelium; FP, floor plate; HbNe, hindbrain neuroepithelium; D, dorsal; V, ventral.

Scale bar: 200µm

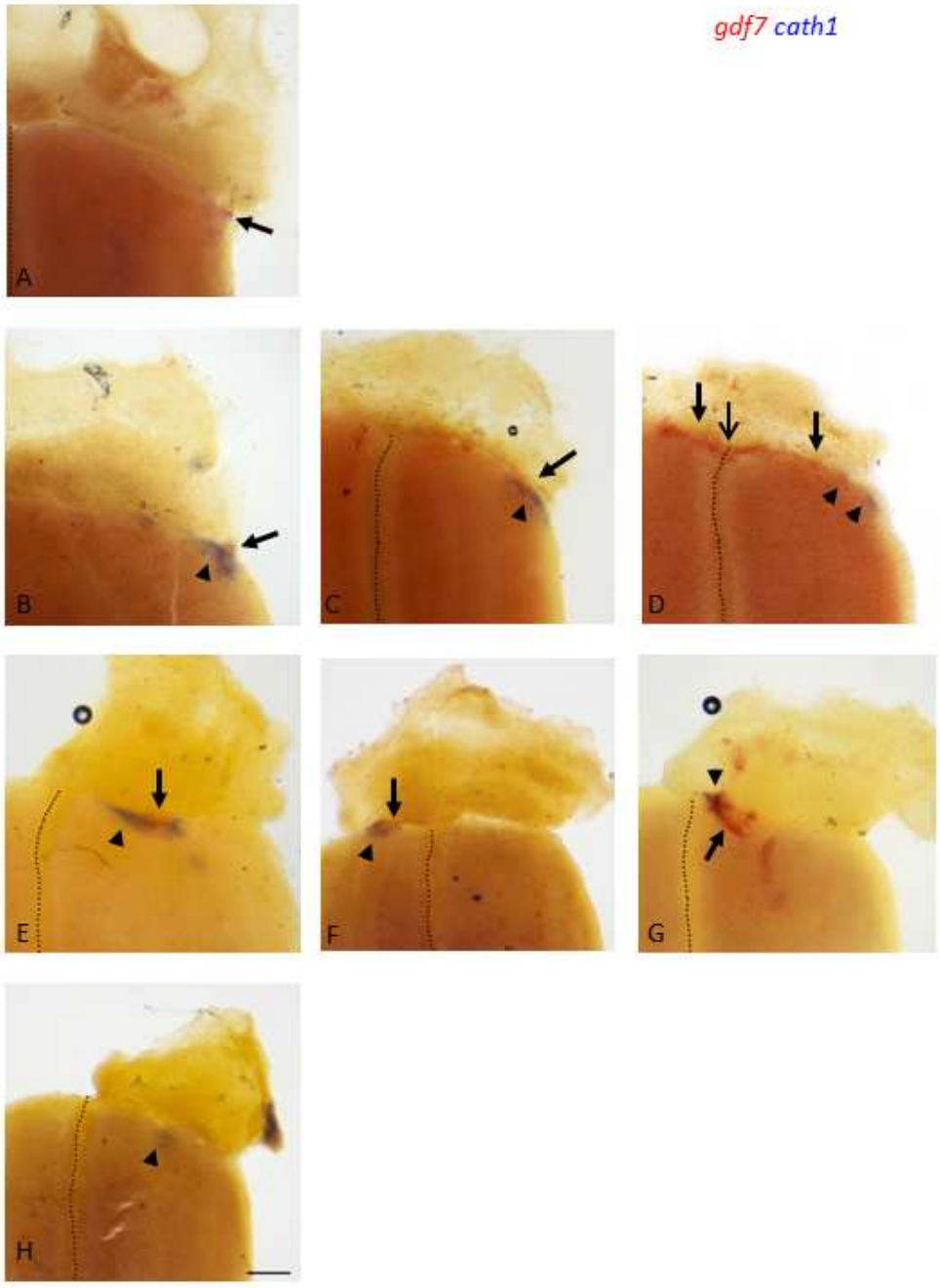
gdf7 cath1
A
B
C
D
E
F
G
H

Figure 3-12 *gdf7* and *cath1* expression in RPE– HbNe co-cultures derived from E5 embryos where the RPE was cultured along the d-v axis of the hindbrain

gdf7 (red) was induced at the interface between RPE and HbNe in E5-derived co-cultures where the RPE was cultured alongside the d-v axis of flat-mounted hindbrains (A – G, arrows). *cath1* was either maintained in the rhombic lip adjacent to induced *gdf7* (B – D, arrowheads) or induced in ventral HbNe adjacent to induced *gdf7* (E – G, arrowheads). In 1/18 explants *cath1* was induced in the ventral HbNe adjacent to the transplanted RPE but not adjacent to any visible *gdf7* expression (H, arrowhead). Dotted lines mark the ventral midline of flat-mounted hindbrains. RPE, roof plate epithelium; HbNe, hindbrain neuroepithelium; d-v, dorso-ventral.

Scale bar: 200µm

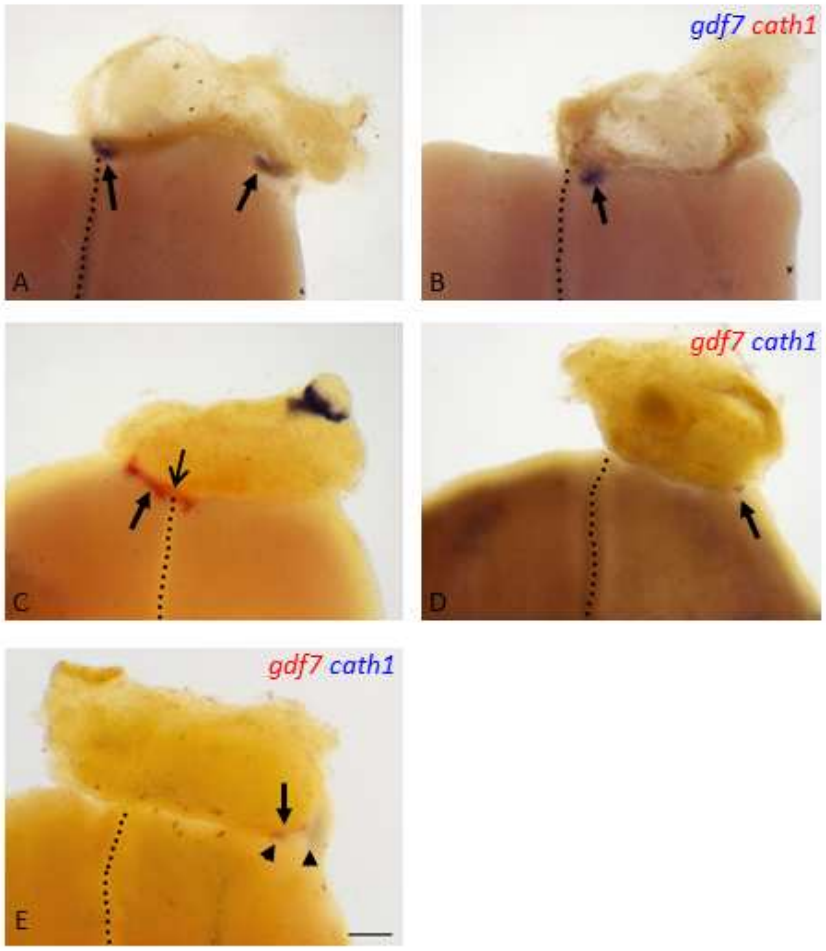

Figure 3-13 *gdf7* and *cath1* expression in RPE– HbNe co-cultures derived from E6 embryos where the RPE was cultured along the d-v axis of the hindbrain

gdf7 (A, B, in blue; C – E in red, arrows) was induced at the interface between RPE and HbNE in co-cultures where RPE was cultured adjacent to the d-v axis of flat-mounted hindbrains. *gdf7* was even induced by an interaction between RPE and the floor plate (C, open arrow). *cath1* (blue) was only induced adjacent to induced *gdf7* in the rhombic lip in 1/8 explants (E, arrowheads). Dotted lines indicate the ventral midline of flat-mounted hindbrains. RPE, roof plate epithelium; HbNe, hindbrain neuroepithelium.

Scale bar: 200µm

Table 3 Frequency of induction of *gdf7* and *cath1* in roof plate epithelium – hindbrain neuroepithelium co-cultures where roof plate epithelium was cultured along the dorsoventral axis of the hindbrain

	E4	E5	E6
gdf7 only	0	1	7
gdf7 and *cath1* dorsal	1	4	1
gdf7 and *cath1* ventral	1	3	0
cath1 not adjacent to *gdf7*	0	1	0
no induction	11	9	11
Total	13	18	19

in competence between E5 and E6 of the ventral hindbrain neuroepithelium to respond to inductive signals from the roof plate.

3.2.8 *chairy2* but not *chairy1* is induced in the roof plate epithelium at a roof plate epithelium – hindbrain neuroepithelium interface.

Elevated levels of *chairy1* and *chairy2* expression were shown to mark the roof plate epithelium – hindbrain neuroepithelium boundary *in vivo* from E4 – E6 (Figure 2-6, 2-7). I therefore investigated whether elevated expression of *chairy1* and *chairy2* was induced in roof plate epithelium – hindbrain neuroepithelium co-cultures.

Elevated *chairy1*expression was induced at the interface between roof plate tissue and hindbrain neuroepithelium in co-cultures derived from E5 brains (Figure 3-19 A, B, arrows n= 2/6). A gradient of expression of *chairy1* in the hindbrain neuroepithelium adjacent to the transplanted roof plate was induced in other explants deriving from E5 embryos (Figure 3-19 C – F, arrowheads, n=2/6). This graded expression was only seen on the side of the hindbrain adjacent to the transplanted roof plate (Figure 3-19 D, F).

Examination of explants derived from E6 embryos also showed that *chairy1* was induced at the interface between the roof plate tissue and the hindbrain neuroepithelium (Figure 3-19 G, H, I, K, M, arrows n=7/8). In a proportion of these explants, *chairy1* expression was also seen to be induced in a graded manner adjacent to the transplanted roof plate (Figure 3-19 I – N, arrowheads, n=5/7).This gradient of expression was only present on the side of the hindbrain adjacent to the transplanted roof plate epithelium.

In order to determine whether the induced expression of *chairy1* at the interface between roof plate and neuroepithelium was present in roof plate epithelial cells, I took transverse cryostat sections of explants and stained for GFP expression by immunohistochemistry, since either the roof plate epithelium component or the hindbrain neuroepithelium component of the co-culture was derived from a GFP – transgenic chick embryo (Figure 3-20 A, B, E, F). This revealed that elevated *chairy1* expression was present in the hindbrain neuroepithelium and in the mesenchyme overlying the roof plate epithelium in co-cultures derived from both E5 and E6 embryos, but was absent from the roof plate epithelium itself (Figure 3-20 C, D, G, H, arrows). Due to the auto-fluorescent nature of the roof plate epithelium and overlying mesenchyme, it is difficult to discern the GFP-positive hindbrain neuroepithelium by immunohistochemistry. However, it was easy to discern the outline of the roof plate epithelium in these co-cultures by morphology (Figure 3-20 C, D).

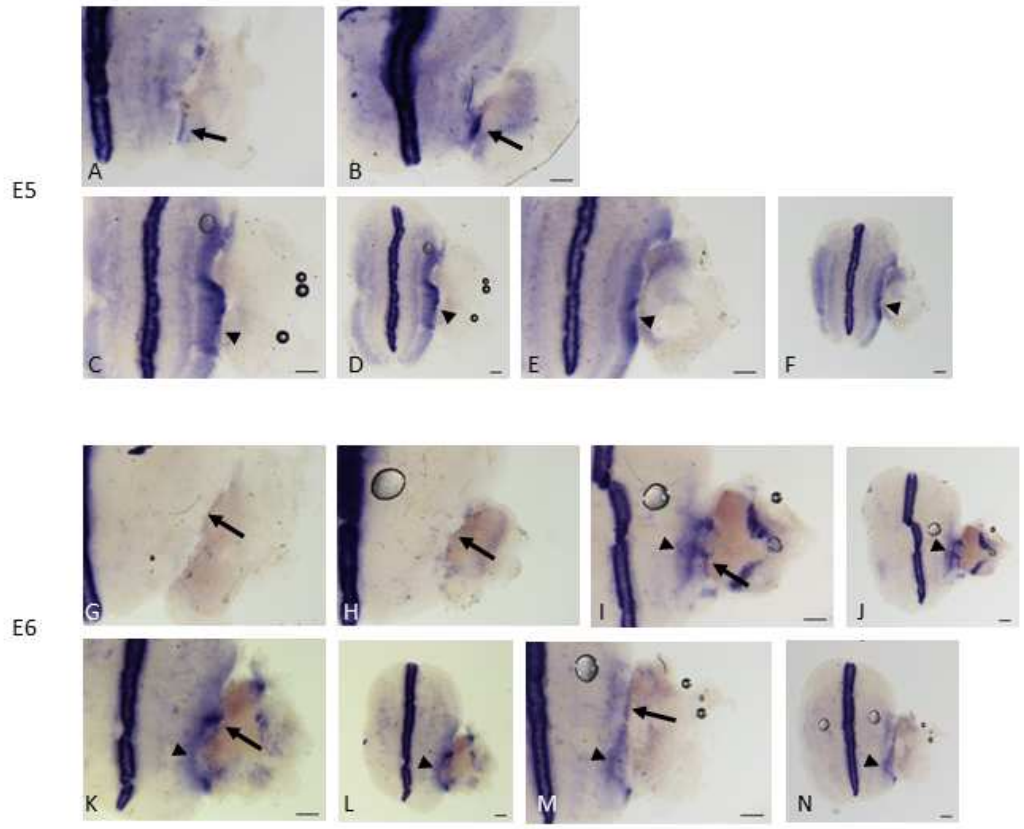

Figure 3-14 *chairy1* expression at an RPE - HbNe boundary

In RPE - HbNe co-cultures derived from E5 (A – F) or E6 (G – N) chick embryos, elevated *chairy1* is induced at the interface between the transplanted roof plate and the HbNe (A, B, G – N, arrows). A gradient of *chairy1* expression was induced in the HbNe adjacent to the transplanted roof plate (C – F, I – N, arrowheads). D, F, J, L, N are lower magnification views of C, E, I, K, M respectively. RPE, roof plate epithelium; HbNe, hindbrain neuroepithelium.

Scale bars: 200µm

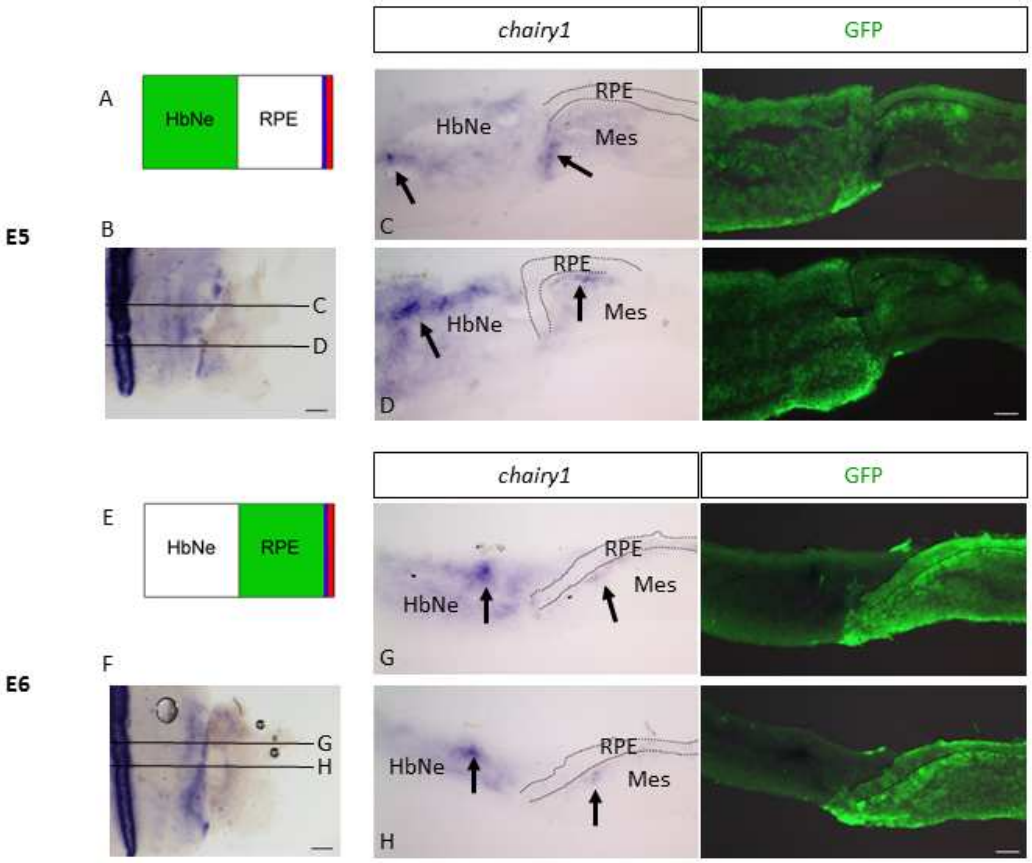

Figure 3-15 *chairy1* is not induced in the RPE at an RPE – HbNe interface

RPE – HbNe co-cultures derived from E5 (A – D) and E6 (E – H) were cryostat sectioned and immunostained for GFP expression. C and D are images of sections at approximately the levels indicated in B. G and H are images of the sections at approximately the levels indicated in F. Elevated levels of expression of *chairy1* is seen in the HbNe and the mesenchyme overlying the RPE (arrows), but not within the RPE itself. Dotted lines demarcate the RPE. RPE, roof plate epithelium; HbNe, hindbrain neuroepithelium; Mes, mesenchyme.

Scale bars: B, F, 200µm. D, H, 50µm.

chairy2 expression is induced at the interface between the roof plate epithelium and the hindbrain neuroepithelium in roof plate epithelium – hindbrain neuroepithelium co-cultures derived from E5 and E6 brains (Figure 3-21 A – G, arrows, E5 n=4/4, E6 n=3/4). Transverse cryostat sections through these explants show that *chairy2* expression is induced in the roof plate epithelium, at the interface between the hindbrain neuroepithelium and roof plate epithelium (Figure 3-22 A – H, arrows). As stated above, in co-cultures where the hindbrain neuroepithelium is the GFP – positive component of the co-culture it is difficult to discern the GFP fluorescent immunostaining due to auto-fluorescence from the roof plate epithelium and the overlying mesenchyme. However, due to the distinctive morphology of the roof plate epithelium it was easy to discern its outline (Figure 3-22 G, H).

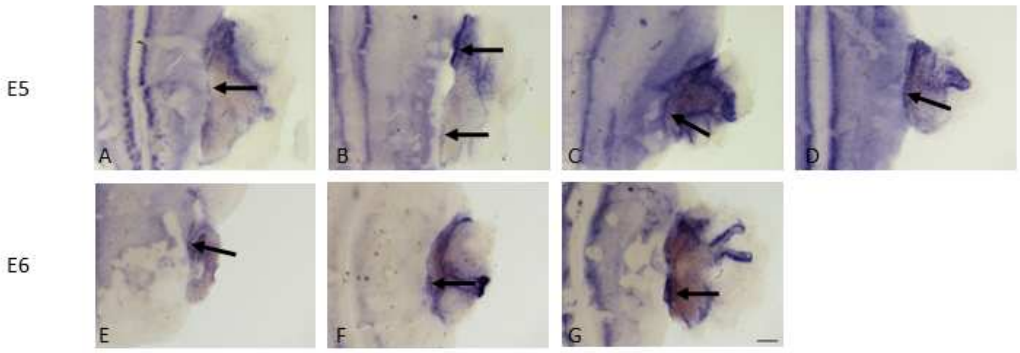

Figure 3-16 *chairy2* expression at an RPE - HbNe boundary

In RPE - HbNe co-cultures derived from E5 (A – D) or E6 (E – G) chick embryos, elevated *chairy2* was induced at the interface between RPE and HbNe (arrows). RPE, roof plate epithelium; HbNe, hindbrain neuroepithelium.

Scale bar: 200µm

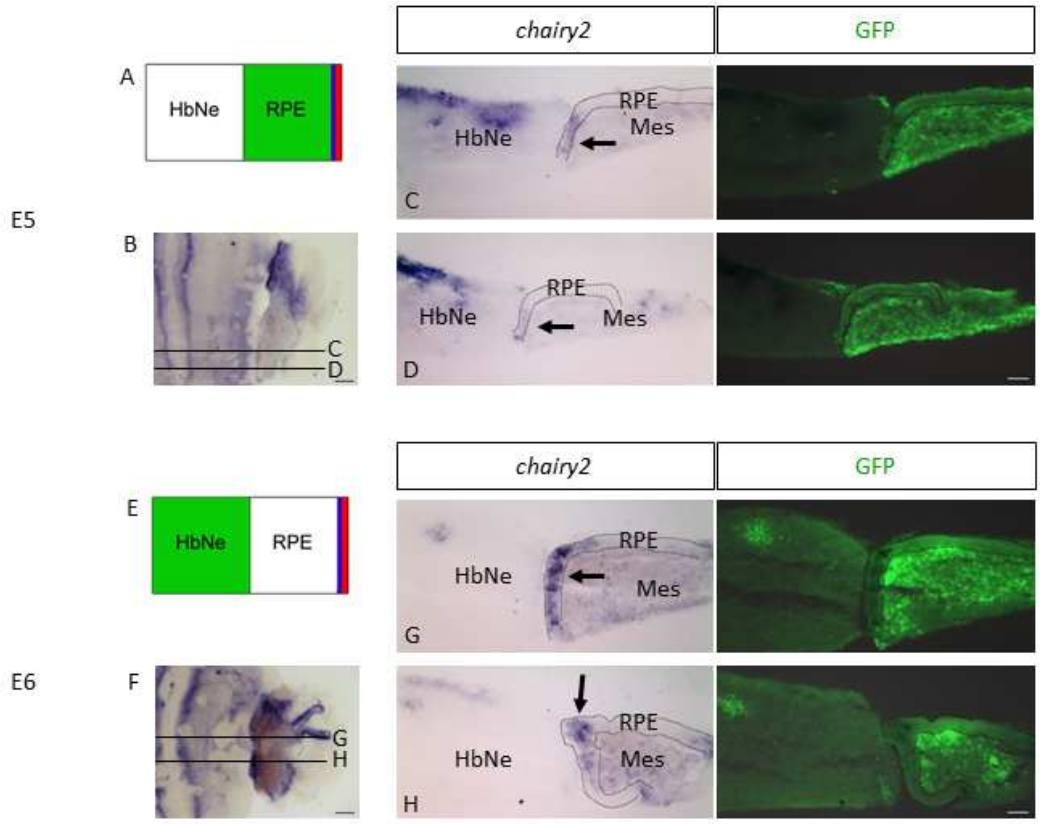

Figure 3-17 *chairy2* is induced in the RPE at an RPE – HbNe interface

RPE – HbNe co-cultures derived from E5 (A – D) and E6 (E – H) were cryostat sectioned and immunostained for GFP expression. C and D are images of sections through the levels indicated in B. G and H are images of the sections through levels indicated in F. Elevated *chairy2* expression is induced in the RPE at an RPE – HbNe interface (arrows). Dotted lines demarcate the RPE. RPE, roof plate epithelium; HbNe, hindbrain neuroepithelium; Mes, mesenchyme.

Scale bars: B, F, 200µm. D, H, 50µm.

3.3 Discussion

gdf7 marks the boundary between roof plate epithelium and hindbrain neuroepithelium from E3 to at least E6 in chick (the latest stage examined) (Figure 2-1, 2-2, 2-3) and upregulated expression of *chairy2* marks this boundary from E4 – E6 (Figure 2-6, 2-7). In this chapter I show that the experimental recombination of roof plate epithelium and hindbrain neuroepithelium derived from E4 – E6 embryos induces *gdf7* and *chairy2* in the roof plate epithelium at the interface between these two tissues, implying that signaling from the hindbrain neuroepithelium to the roof plate normally maintains *gdf7* expression at this interface at these stages. Induced *gdf7* marks an induced organiser as this domain can re-pattern the hindbrain neuroepithelium, inducing *cath1* expression in the ventral neuroepithelium, although the competence of the ventral neuroepithelium to respond to signals from the *gdf7*-domain decreases with age. The *gdf7*-domain is required, at least between E4 and E6, for the maintenance of *cath1* expression in the rhombic lip.

3.3.1 The pattern of *gdf7* induction in tissue recombinations suggests an interaction between a neural ligand and a roof plate receptor.

Previous studies have shown that the expression of other boundary-localised signalling molecules and indeed the regeneration of boundaries themselves can be induced via tissue interactions between neighbouring tissue compartments (Guthrie and Lumsden, 1991; Irving and Mason, 1999; Guinazu et al., 2007). Here I find that the expression of *gdf7* can be induced at an experimentally re-capitulated boundary between roof plate epithelium and hindbrain neuroepithelium both *in vitro*, (Figure 3-3, 3-4, 3-5) and *in ovo* (Figure 3-1-2 A). The efficiency of induction of *gdf7* via *in ovo* tissue grafting was lower than that achieved in the explants (rhombic lip into roof plate graft, 33%, n=9; E5 roof plate epithelium – rhombic lip neuroepithelium explants 73%, n=15; E6 roof plate epithelium – rhombic lip neuroepithelium 57%, n=14). This inefficient induction might have been due to differences in the ages of the embryos that were being manipulated, the heterochronic nature of the grafting experiments, a lower efficiency of inter-mingling of donor and host tissues in grafted embryos in comparison with explants, or the difference in the length of time that grafted embryos or explants were incubated for (grafted embryos were incubated for 24 hours whereas explants were incubated for 48 hours). Nevertheless, both experimental paradigms show that it is possible to recapitulate *gdf7* expression at an experimentally derived roof plate epithelium – rhombic lip interface.

gdf7 was induced in roof plate epithelium-derived tissue (Figure 3-7). Its induction was the result of a specific interaction between roof plate epithelium and hindbrain neuroepithelium rather than a spontaneous upregulation of *gdf7* at the cut edge of a piece of roof plate

epithelium as *gdf7* expression was not induced at a roof plate epithelium – roof plate epithelium interface (Figure 3-8, 3-1-2 B). *gdf7* seemed to be induced only where the roof plate epithelium and the hindbrain neuroepithelium intermingled (Figure 3-7). Therefore it is likely that the signal that induces *gdf7* in the roof plate epithelium is a cell-cell contact based signal and that the signal is directional – from neuroepithelium to roof plate, since *gdf7* is always induced in roof plate epithelium. Ligands for the signalling pathway must therefore be present in the hindbrain neuroepithelial tissue, while the receptor must be present in the roof plate epithelium. *gdf7* is induced by interactions between the roof plate epithelium and the entire dorsoventral axis of the hindbrain, including the floor plate (Figure 3-16, 3-17, 3-18), and spinal cord neuroepithelium (Figure 3-9 B, C, D), which suggests that the ligand or a family of ligands that activate the same signalling pathway are expressed broadly in both the hindbrain and spinal cord neuroepithelium.

As a corollary to this observation, it is possible that similar mechanisms of cell-cell interactions are responsible for the maintenance of *gdf7* expression in the spinal cord. In support of this, a *gdf7*-negative domain is present at the midline of the spinal cord roof plate that could represent a tissue compartment equivalent to the expanded hindbrain roof plate epithelium (Figure 2-2 E, F). While it would be virtually impossible to physically ablate this domain once it is formed, the original formation of this domain could be blocked to test the requirement for cell-cell interactions between this medial compartment and the spinal cord neuroepithelium for the maintenance of the spinal cord roof plate. The medial compartment is likely to be established upon neural tube closure, therefore neurulation could be blocked in some manner to test the requirement for interactions between the two sides of the neural tube for roof plate formation and maintenance. To achieve this physical blockade of neurulation using tantalum foil in chick could be carried out. Alternatively the mouse mutants *crash*, *loop-tail*, which carry mutations in genes that function in the planar-cell-polarity pathway and display extensive failure of neural tube closure (Murdoch et al., 2001; Curtin et al., 2003; Doudney and Stanier, 2005), could be analysed to examine the consequence on roof plate development.

3.3.2 *cath1* expression in the rhombic lip is maintained by roof plate signals likely to derive specifically from the *gdf7*-domain

Most previous studies of the role of the roof plate in patterning the dorsoventral axis of the neuroepithelium involved early genetic ablation of the roof plate and thereby focussed on the early establishment of progenitor domains within the neural tube (Lee et al., 2000a; Chizhikov et al., 2006). However, Krizhanovsky& Ben-Arie (2006) have shown that at E14.5 in mouse,, BMP-mediated signals from the choroid plexus are required to maintain

math1 expression in the rhombic lip. Here I find an acute requirement for the roof plate at E4, E5 and E6 in chick to maintain the expression of *cath1* in the rhombic lip, and that *cath1* expression is lost after 32 hours of *in vitro* culture of E6 hindbrains that have had their roof plates removed (Figure 3-10, 3-11). Although the removal of the hindbrain roof plate (the roof plate epithelium and the *gdf7*-domain combined) also removes part of the *cath1* domain, the expression of *cath1* in the rhombic lips can be rescued by the re-application of roof plate epithelium (Figure 3-12, 3-13). This argues for a specific requirement for the roof plate, rather than any part of the *cath1* domain removed when the roof plate was dissected from hindbrains, for the maintenance of the remaining *cath1* expression in the rhombic lips.

Existing *cath1* expression in the rhombic lip after roof plate removal and 48 hours of culture, was always coincident with a small domain of residual *gdf7* expression (Figure 3-11 H, K). Further, nearly all maintenance of *cath1* after the re-application of the roof plate epithelium coincided with induced *gdf7*-expression at the roof plate epithelium – neuroepithelium interface (Figure 3-12, 3-13). Therefore the requirement for the roof plate for the maintenance of *cath1* expression is likely to depend specifically on signals derived from the *gdf7*-positive roof plate boundary.

3.3.3 The induced *gdf7*-domain represents an induced organiser

cath1 expression was not only maintained adjacent to induced *gdf7*-expression, but it could also be ectopically induced in non-rhombic lip hindbrain neuroepithelium, adjacent to induced *gdf7* (Figure 3-3, 3-4 A – E, 3-5 A, B, 3-7 J – M). In such roof plate epithelium – hindbrain neuroepithelium co-cultures, *cath1* expression was never seen in the hindbrain neuroepithelium adjacent to the transplanted roof plate without induced *gdf7* expression. *cath1* expression could be induced in the ventral hindbrain neuroepithelium adjacent to induced *gdf7* expression in explants deriving from E4 and E5 embryos, but not from E6 embryos (Figure 3-16 C, 3-17 E – G, 3-18). In only 1/18 of E5 explants was *cath1* expression seen in the ventral hindbrain neuroepithelium adjacent to the transplanted roof plate, without adjacent induced *gdf7* expression (Figure 3-16 H). This may have been due to levels of induced *gdf7* expression that are below the threshold for staining by whole-mount double *in situ* hybridisation. Therefore it is likely that signals from the roof plate that induce *cath1* expression in the ventral hindbrain derive from the *gdf7*-positive domain and thus the induced *gdf7*-positive domain represents an induced organiser.

The competence of the rhombic lip to respond to signals from the *gdf7*-positive organiser is greater than the competence of the hindbrain neuroepithelium. This competence to respond decreases with age for both the rhombic lip and non-rhombic lip neuroepithelium (Figure 3-6, 3-15). Additionally, *cath1* induction in the ventral hindbrain neuroepithelium was never

seen in E6-derived explants, whereas it did occur in E4 and E5-derived explants (Table 3). Thus the competence of the hindbrain to respond to signals from the *gdf7*-positive organiser becomes increasingly dorsally restricted over time. The mechanism of this dorsal restriction could involve Shh signals from the floor plate as these are required for early dorsoventral patterning of the neural tube (Yamada et al., 1991; Yamada et al., 1993; Marti et al., 1995a), however the mechanism of temporal restriction of competence is unknown.

Studies in chick and mice have previously focussed on the ability of the roof plate to ectopically induce Math1 expression and ventrally shift the development of dorsal neurons, via early manipulations of the neural tube (E8.75-9.5 in mouse, E2 (st10-11) in chick) (Chizhikov and Millen, 2004a; Chizhikov et al., 2006). Here I show that *cath1* expression can be acutely induced in ventral hindbrain neuroepithelium until E5, showing that the dorsoventral axis of the hindbrain neuroepithelium is plastic and can be re-patterned even at this late stage. It would be interesting to determine the effect of this re-patterning on more ventral progenitor pool markers, such as *ptf1a*, *ngn1*, *ngn2* and *cash1* (Landsberg et al., 2005; Chizhikov et al., 2006; Liu et al., 2010), although detailed maps of these progenitor domains in the chick hindbrain would first have to be established.

chairy1 and *chairy2* are chick orthologues of mouse *hes1*, which is expressed highly and persistently in boundary-localised organisers and is known to be required, along with other *hes* genes, to maintain boundary-localised organisers in development (Hirata et al., 2001; Baek et al., 2006). Both *chairy1* and *chairy2* mark the roof plate epithelium – hindbrain neuroepithelium boundary in E4 – E6 chick embryos (Figure 2-6, 2-7), but only *chairy2* expression was induced in roof plate epithelial tissue at an experimentally derived roof plate epithelium – hindbrain neuroepithelium interface (Figure 3-20, 3-21, 3-22). Thus *chairy2* may play a specific role in maintaining the *gdf7*-positive roof plate epithelium – hindbrain neuroepithelium boundary during development. A specific role for cHairy2 rather than cHairy1 in the maintenance of the roof plate boundary may reflect its closer homology to mHes1 than cHairy1 to mHes1 (Jouve et al., 2000). The induction of *chairy2* at the hindbrain roof plate epithelium – neuroepithelium interface further supports the concept that an organiser is induced at this interface, which is marked by *gdf7* expression.

3.3.4 Conclusions

Tissue interactions between hindbrain roof plate epithelium and neuroepithelium induce a *gdf7*-positive, *chairy2*-positive organiser in the roof plate epithelium at the interface between the two tissues. The specific induction of *chairy2* may reflect a specific role for cHairy2 in maintaining the *gdf7*-positive organiser *in vivo*. A role of this *gdf7*-positive organiser is to maintain *cath1* expression in the rhombic lip, but I have also demonstrated that the hindbrain

neuroepithelium can be re-patterned by this organiser at stages much later than dorsoventral patterning is thought to occur (Yamada et al., 1993; Briscoe et al., 2000; reviewed in Briscoe and Ericson, 2001). Together these findings shed new light on the mechanisms that maintain the *gdf7*-positive roof plate boundary-organiser.

Chapter 4 Notch signalling and the maintenance of the roof plate boundary-organiser

4.1 Background

Notch signalling is important in many developmental situations to specify or maintain boundary-organisers. It involves the *trans*-activation of Notch receptors by transmembrane ligands of the Delta/ Serrate/ Lag2 [DSL] family. This *trans*-activation results in the proteolytic cleavage of the Notch receptor and nuclear translocation of its intracellular domain (Notch ICD). The Notch ICD interacts with the DNA-binding protein CSL (named after CBF1, Su(H) and LAG-1) and activates transcription of Notch target genes such as the *hes* genes (reviewed in Bray, 2006). The classic example of its role at boundaries is the dorsoventral boundary of the wing imaginal disc where a stripe of Notch activation is necessary and sufficient for the induction or maintenance of the expression of the organiser protein Wg (Diaz-Benjumea and Cohen, 1995; Rulifson and Blair, 1995; Doherty et al., 1996). This stripe of Notch activation is achieved via the concurrent actions of the Notch ligands, Serrate, expressed in the dorsal compartment, and Delta, expressed in the ventral compartment (Diaz-Benjumea and Cohen, 1995; Doherty et al., 1996). The expression of Notch itself is not restricted to the compartment boundary (Fehon et al., 1991), but the restriction of Notch activation is achieved through the action of Fringe, which is expressed in the dorsal compartment and increases the effectiveness of Delta-Notch signalling whilst inhibiting Serrate-Notch signalling (Panin et al., 1997).

In striking similarity with this, Notch signalling is required for the maintenance of rhombomere boundaries in zebrafish and for the expression of Wnt1 (a zebrafish orthologue of Wg) (Cheng et al., 2004; Riley et al., 2004). Similarly, Notch signalling and a boundary between *radical fringe* (a chick and mouse orthologue of Drosophila *fringe*) - expressing and non-expressing cells has been implicated in determining the formation of the apical ectodermal ridge, marked by *fgf8* expression, at the dorsoventral border of the limb bud ectoderm (Laufer et al., 1997; Rodriguez-Esteban et al., 1997; Sidow et al., 1997). Boundaries between *lunatic fringe* (another orthologue of Drosophila *fringe*) – expressing and non-expressing cells are also important for the formation or maintenance of the zona limitans intrathalamica in chick, a developmental compartment that patterns the adjacent thalamus and pre-thalamus via the signalling molecule Shh (Zeltser et al., 2001; Kiecker and Lumsden, 2004). Recently, Notch activation mediated by *serrate1* and modulated by *lfng* has been shown to be necessary and sufficient for the formation of the midbrain-hindbrain boundary and localisation of expression of its nascent signalling molecules, *wnt1* and *fgf8*

*(*Tossell et al., 2011). Together these studies indicate that Notch activation at a boundary within an epithelium, which is modulated by the action of Fringe or its orthologues, is an evolutionarily conserved mechanism that is deployed in multiple instances of boundary organiser formation and maintenance in development.

The restricted expression of *gdf7* at the roof plate epithelium – hindbrain neuroepithelium boundary and the upregulated expression of the Notch downstream target genes (*chairy1* and *chairy2*) at this boundary (Chapter 2) indicated that Notch signalling might play a role in the maintenance of this boundary. The pattern of induction of *gdf7* in the roof plate epithelium in *in vitro* co-culture experiments where roof plate epithelium was cultured adjacent to hindbrain neuroepithelium indicated that a cell-cell contact based signal is involved in the induction of *gdf7* (Chapter 3). This supports a role for Notch signalling in maintaining *gdf7* expression at a hindbrain roof plate epithelium – neuroepithelium interface. Furthermore, since *gdf7* expression is only induced in the roof plate, the receptor of the inducing signal must be present in this epithelium. *In situ* hybridisation analysis showed that *notch2* is a good candidate to mediate this signal as it is expressed in the roof plate epithelium of E5 chick embryos (Figure 2-8). Further, *delta1* was a good candidate as being the ligand present in the hindbrain neuroepithelium as it was expressed in the ventricular zone throughout most of the hindbrain neuroepithelium, along the dorsoventral axis, and showed a sharp boundary of expression adjacent to the *gdf7*-domain (Figure 2-8). Therefore, in this chapter, I investigated the role of Notch signalling in maintaining the *gdf7*-positive roof plate boundary (specifically, the role of *delta1*) by overexpressing *delta1* in the roof plate epithelium to see if it was sufficient to induce an ectopic roof plate boundary, as assessed by *gdf7* expression.

hairy/ enhancer of split (hes) genes are repressor-type basic helix-loop-helix (bHLH) transcription factors that are well-known downstream effectors of Notch signalling (reviewed in Kageyama et al., 2007). They function in the maintenance of neural stem cells, preventing ectopic neurogenesis, but have also been shown to be essential for the maintenance of boundary-localised organisers, preventing ectopic neurogenesis within these organisers (Ohtsuka et al., 1999; Hirata et al., 2001; Geling et al., 2003; Geling et al., 2004; Hatakeyama et al., 2004; Ninkovic et al., 2005; Baek et al., 2006). Although Hes transcription factors are well known to be targets of Notch signalling, whether they function downstream of Notch to maintain boundary-localised organisers is debateable. The zebrafish *hes*-related gene *her5* has been shown to be involved in a Notch-independent fashion in the maintenance of the midbrain-hindbrain boundary (Geling et al., 2003; Geling et al., 2004). Furthermore it has been shown that *hes1* can be regulated through Notch-independent pathways, such as through the *shh* pathway (Yoon and Gaiano, 2005; Wall et al., 2009; Sanalkumar et al., 2010). Thus it was proposed that *hes1* expression at boundaries of the

developing mouse CNS might also be Notch-independent (Kageyama et al., 2007). Experiments carried out in this chapter indicate that the *hes1* orthologue, *chairy2*, functions downstream of Notch signalling at the roof plate epithelium – hindbrain neuroepithelium boundary as its expression is induced downstream of Notch activation in the roof plate epithelium.

Both chick orthologues of mouse *hes1, chairy1* and *chairy2* were seen to be upregulated at the roof plate epithelium – hindbrain neuroepithelium boundary *in vivo* in E4 – E6 chick embryos (Chapter 2). However, only *chairy2* expression was induced in the roof plate epithelium at an experimental roof plate epithelium – hindbrain neuroepithelium interface in co-culture experiments (Chapter 3). Therefore, in this chapter, the specific role of cHairy2 in the maintenance of the roof plate boundary organiser was investigated. The function of cHairy2 was disrupted in two ways: through construction of electroporation constructs encoding a putative dominant negative and an overexpression construct. Dominant negative cHairy2 was created by deleting the c-terminal WRPW domain that is required for the recruitment of Groucho/TLE co-repressors (Paroush et al., 1994; Fisher et al., 1996; Grbavec et al., 1998). Hes genes homodimerise and bind to DNA and recruit Groucho/TLE co-repressors to actively repress the expression of target genes (reviewed in Kageyama et al., 2007). Therefore a cHairy2ΔWRPW protein should act in a dominant negative manner by sequestering functional cHariy2 proteins and preventing the recruitment of Groucho/TLE co-repressors to DNA. In support of this, the deletion of the WRPW domain from E(Spl) proteins in Drosophila renders them dominant negative (Giebel and Campos-Ortega, 1997).

Given the localisation of organiser properties at the roof plate boundaries (Chapter 3) and the fact that the hindbrain choroid plexus epithelium differentiates in a specific pattern within the roof plate epithelium (Figure 2-9, 2-11), it was hypothesised that signals from the roof plate epithelium – hindbrain neuroepithelium boundary might be involved in the patterning or specification of choroid plexus epithelium differentiation. Investigation of the role of cHairy2 in the maintenance of the *gdf7*-positive roof plate boundary led to the development of the *chairy2ΔWRPWv2-IRESeGFPm5* and *chairy2-IRESeGFPm5* expression constructs and an electroporation technique to target the upper roof plate epithelium – hindbrain neuroepithelium boundary that could be used to investigate the effects of disruption of the roof plate epithelium – hindbrain neuroepithelium boundary on roof plate epithelial (*cyp26C1*) and choroid plexus epithelial (*ttr*) markers. In addition, the ectopic expression of *delta1* in the roof plate epithelium essentially expanded the roof plate epithelium – hindbrain neuroepithelium boundary, and could therefore be used to assess whether this had any effect on the patterning of choroid plexus differentiation. These experiments demonstrated that signals from the roof plate epithelium – hindbrain neuroepithelium boundary are required for

the formation or maintenance of roof plate epithelium and choroid plexus epithelium identity, and that an expanded roof plate epithelium – hindbrain neuroepithelium boundary affects the pattern of choroid plexus epithelium differentiation.

4.2 Results

4.2.1 Co-electroporation of 1:1 RCAS-*delta1*: CAβ-*GFP* constructs

Details of the electroporation constructs used in the experiments described in this chapter and explanations of the abbreviations used can be found in Appendix C. The RCAS-*delta1* expression construct did not encode GFP either as a fusion protein with Delta1 or as *IRES-GFP*. Therefore in order to test whether a technique of co-electroporation with a CAβ-*GFP* construct could be used to trace effective electroporations, I tested whether RFP and GFP are co-expressed when the RCAS-*RFP* and CAβ-*GFP* are co-electroporated into the lower roof plate epithelium and adjacent rhombic lip of E3 chick embryos and embryos are incubated for 48 hours prior to collection. The co-electroporation of embryos with RCAS-*RFP* and CAβ-*GFP* at a 1:1 concentration ratio gave almost complete co-expression of RFP and GFP, with 97.3 ± 2.0% of electroporated cells co-expressing RFP and GFP, as determined by confocal microscopy to detect the fluorescent RFP and GFP proteins (Figure 4-1 A, B). 1.6 ± 1.6% cells showed only GFP expression and 1.1 ± 0.4% cells showed only RFP expression so it was deemed that this concentration ratio for co-electroporation would give efficient co-expression of an RCAS expression construct and the CAβ-*GFP* expression construct at the protein level.

When the RCAS-*delta1* and the CAβ-*GFP* DNA constructs are co-electroporated into the lower roof plate epithelium and rhombic lip of E3 chick embryos at a concentration ratio of 1:1, *delta1* is effectively ectopically expressed in the roof plate epithelium after 48hrs (Figure 4-2 A – C, black arrows, n=3/5). However, unlike the coincident expression of RFP and GFP as detected by confocal microscopy when RCAS-*RFP* and CAβ-*GFP* constructs were co-electroporated at a 1:1 concentration ratio, *delta1* expression was not completely coincident with GFP expression. *delta1* expression, as detected by single whole-mount *in situ* hybridisation, was mostly confined within the electroporation site, however some *delta1*-positive, GFP-negative cells were present outside the electroporation site (Figure 4-2 A, white arrows). Further, some GFP-positive cells appear to be *delta1*-negative (Figure 4-2 A – C, white arrowheads). Therefore co-electroporation of the RCAS-*delta1* and CAβ-*GFP* constructs at a 1:1 concentration ratio appears not to give as effective a level of co-expression as observed for the co-electroporation of RCAS-*RFP* and CAβ-*GFP* expression constructs.

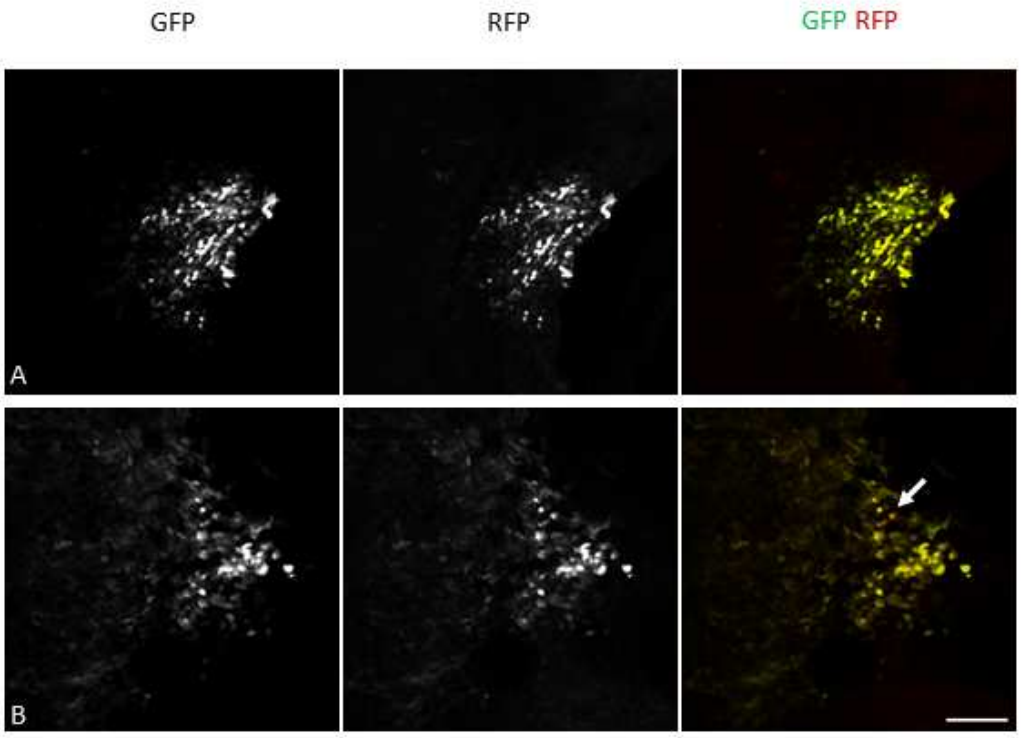

Figure 4-1 Co-expression of GFP and RFP when RCAS-*RFP* and CAβ-*GFP* are co-electroporated at a 1:1 concentration ratio

RCAS-*RFP* and CAβ-*GFP* were electroporated at a 1:1 concentration ratio into the lower rhombic lip and adjacent roof plate epithelium of an E3 chick embryo. Embryos were incubated for 48hrs prior to collection. A and B show a confocal optical section of flat-mounted roof plates. 97.3 ± 2.0% cells showed co-expression of RFP and GFP. 1.6 ± 1.6% cells showed only GFP expression and 1.1 ± 0.4% cells showed only RFP expression. Arrow indicates a cell co-expressing RFP and GFP but with a higher level of RFP expression so it appears more red. Scale bar: 100μm.

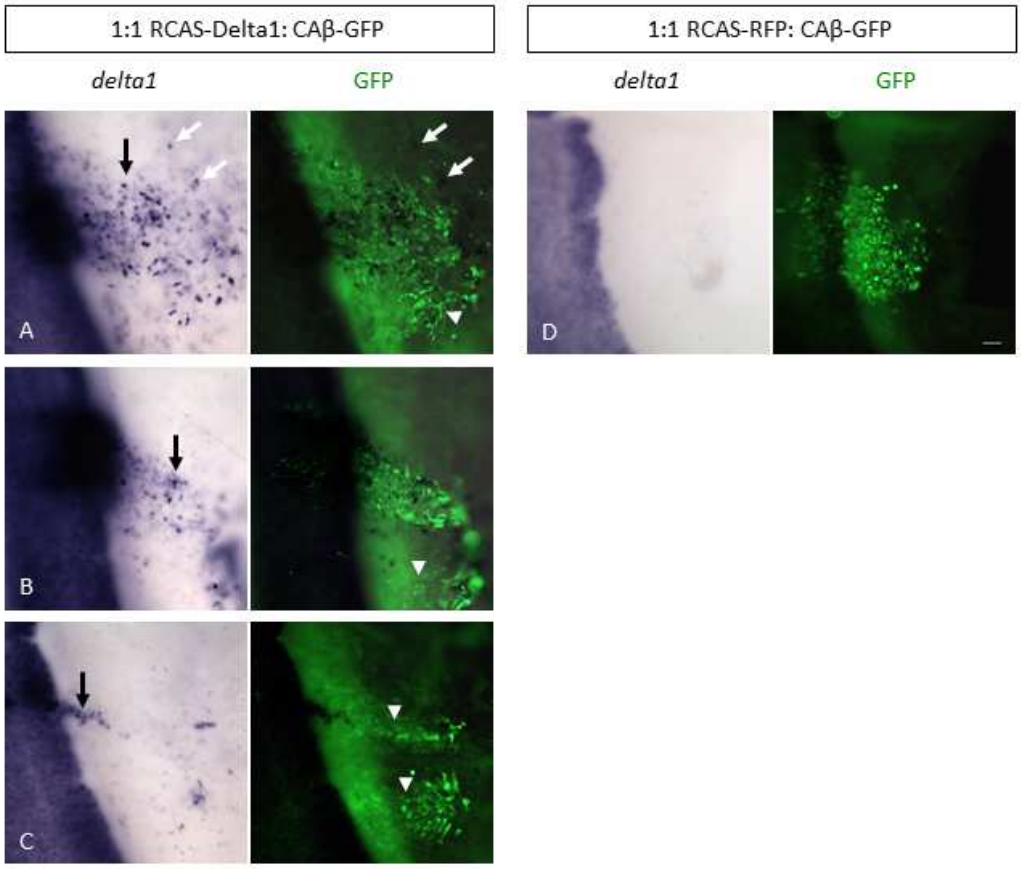

Figure 4-2 Overexpression of *delta1* in the RPE by co-electroporation of RCAS-*Delta1* with CAβ-*GFP*

A DNA mix of 1:1 RCAS-*Delta1*: CAβ-*GFP* (A, B, C) or 1:1 RCAS-*RFP*: CAβ-*GFP* (D) was electroporated into the lower rhombic lip and adjacent RPE of an E3 chick embryo. Embryos were incubated for 48hrs prior to collection. *delta1* expression was detected by whole-mount *in situ* hybridisation and the electroporation site was detected by whole-mount immunohistochemistry for GFP. *delta1* expression is not present in all GFP-labelled electroporated cells (white arrowheads) but ectopic *delta1* expression is generally contained in the electroporated domain (black arrows). However, some *delta1*-positive cells are not present within the electroporated domain (white arrows). Anterior is oriented upwards. RPE, roof plate epithelium.

Scale bar: 50μm.

An explanation for this could be that the whole-mount *in situ* hybridisation process does not detect low-level *delta1* mRNA expression, whereas low-level RFP and GFP expression could be detected by confocal microscopy, creating the impression that cells are GFP-positive but *delta1*-negative. In support of this, although 97.3 ± 2.0% of cells co-expressed RFP and GFP, the ratio of expression of RFP and GFP varied from cell to cell so some cells appeared more red or green than others (Figure 4-1 B, arrow). Another explanation is that the blue precipitate that forms from the whole-mount *in situ* hybridisation process quenches the fluorescence of the fluorophore-conjugated secondary antibody used in the immunohistochemical detection of the GFP protein, giving the impression that cells are *delta1*-positive but GFP-negative. Despite some cells apparently not co-expressing *delta1* and GFP, most *delta1* expression was confined to the GFP-positive electroporation domain so this co-electroporation technique was subsequently used to study the effect of overexpression of *delta1* in the roof plate epithelium.

Co-electroporation of the lower roof plate epithelium and adjacent rhombic lip with the RCAS-*RFP* and CAβ-*GFP* DNA constructs mixed at a 1:1 concentration ratio had no effect on *delta1* expression in either the rhombic lip or the roof plate epithelium (Figure 4-2 D, n=0/2).

4.2.2 Ectopic expression of *delta1* in the roof plate epithelium induces *gdf7* expression

Co-electroporation of RCAS-*RFP* and CAβ-*GFP* constructs mixed at a 1:1 concentration ratio into the lower rhombic lip and roof plate epithelium of E3 embryos that were then incubated for 48hrs prior to collection, had no effect on *gdf7* expression (Figure 4-3 A, n=0/3). In contrast, co-electroporation of RCAS-*delta1* and CAβ-*GFP* into the roof plate epithelium of E3 chick embryos induced ectopic expression of *gdf7* in the roof plate epithelium after 48hrs incubation (Figure 4-3 B – I, arrows, n=4/4). *delta1* was also overexpressed in the rhombic lip by this method but *gdf7* was not induced there (Figure 4-3 F, H, arrowheads). This shows that induction of *gdf7* by *delta1* overexpression was specific to the roof plate epithelium.

The induction of *gdf7* expression seemed to be cell non-autonomous as *gdf7*-expressing cells were generally GFP-negative and adjacent to GFP-positive cells (Figure 4-3 C, E, G, I, arrows). However, this could have been due to quenching of the fluorescent signal detecting GFP expression by the blue whole-mount *in situ* precipitate as mentioned above. Additionally, induction of *gdf7* by *delta1* may be cell-autonomous as some *delta1*-positive cells are found outside the GFP-positive electroporation domain (Figure 4-2 A, white arrows), although for the most part *delta1*-expressing cells are found within the GFP-positive

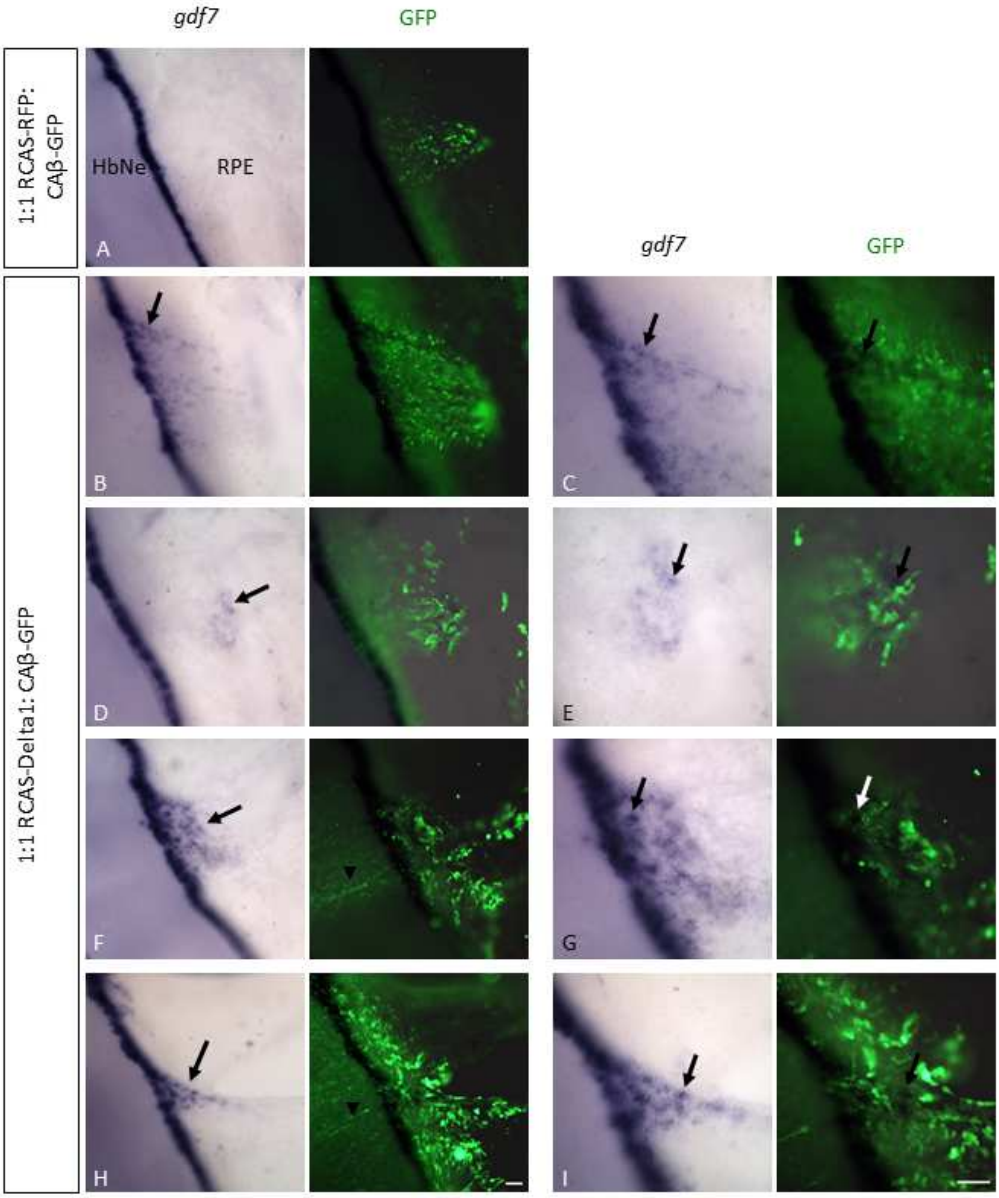

Figure 4-3 Overexpression of *delta1* in the RPE induces *gdf7* expression

A DNA mix of 1:1 RCAS-*RFP*: CAβ-*GFP* (A) or 1:1 RCAS-*Delta1*: CAβ-*GFP* (B - I) was electroporated into the lower rhombic lip and adjacent RPE of an E3 chick embryo. Embryos were incubated for 48hrs prior to collection. *gdf7* expression was detected by whole-mount *in situ* hybridisation and the electroporation site was detected by whole-mount immunohistochemistry for GFP. C, E, G and I show magnifications of electroporated regions shown in B, D, F and H. Anterior is oriented upwards. *gdf7* expression is ectopically induced in the roof plate epithelium (arrows), but not in the rhombic lip (arrowhead). C, E, G, I arrows indicate that *gdf7* expression is located adjacent to GFP-positive cells. RPE, roof plate epithelium; HbNe, hindbrain neuroepithelium.

Scale bars: 50μm.

domain. Therefore due to the potential for quenching of GFP detection and the fact that co-electroporation of roof plate epithelium with RCAS-*delta1* and CAβ-*GFP* at a 1:1 ratio does not give complete co-expression of the two constructs, further work was required to determine whether *gdf7* induction by *delta1* in the roof plate epithelium was cell autonomous or non-autonomous.

To further investigate this the RCAS-*delta1* and CAβ-*GFP* constructs were electroporated at a 1:1 ratio into the lower roof plate epithelium and rhombic lip and double *in situ* hybridisation to detect *gdf7* and *delta1* expression was carried out. Co-electroporation of RCAS-RFP and CAβ-GFP at a 1:1 ratio had no effect on either *delta1* or *gdf7* expression (Figure 4-4 A, B, n=0/3). When RCAS-*delta1* and CAβ-*GFP* were co-electroporated into the roof plate epithelium it could be seen that only a subset of GFP-positive cells co-expressed *delta1* (Figure 4-4 D, F, H, white arrows). 2 of 3 embryos that showed *delta1* overexpression in the roof plate epithelium also showed *gdf7* induction in the roof plate epithelium (Figure 4-4 E, G, arrows). This induction appeared to be non-autonomous in relation to *delta1* expressing cells, however the red precipitate detecting *delta1* expression may obscure *gdf7* expression (detected by blue precipitate), and so mask cell autonomous induction of *gdf7*. These results show that *delta1* expression in the roof plate epithelium induces *gdf7* expression there, but whether *gdf7* induction is cell autonomous, non-autonomous or both requires further analysis. This could be achieved if *delta1* was cloned into an expression construct containing *IRES-GFP*, or if fluorescent *in situ* hybridisation to detect *gdf7* expression was used in combination with immunohistochemistry to detect Delta1 expression.

4.2.3 Ectopic *delta1* expression in the roof plate epithelium induces *chairy2* expression

Co-electroporation of RCAS-*RFP* and CAβ-*GFP* at a 1:1 concentration ratio in the rhombic lip and roof plate epithelium had no effect on *chairy2* expression (Figure 4-5 C, D, n=0/11). In contrast, co-electroporation of RCAS-*delta1* and CAβ-*GFP* did induce *chairy2* expression in the roof plate epithelium (Figure 4-5 A, B, arrows, n=6/13).

4.2.4 Ectopic *delta1* expression in the roof plate epithelium causes upregulation of *cyp26C1* expression within the electroporation domain

In order to study the effect of an expanded *gdf7* domain within the roof plate epithelium on roof plate epithelial-expressed genes, I examined the expression of the roof plate epithelium-expressed *cyp26C1* in embryos where RCAS-*delta1* and CAβ-*GFP* constructs were co-electroporated into the lower rhombic lip and adjacent roof plate epithelium. Co-electroporation of RCAS-*RFP* and CAβ-*GFP* into the lower rhombic lip and adjacent roof

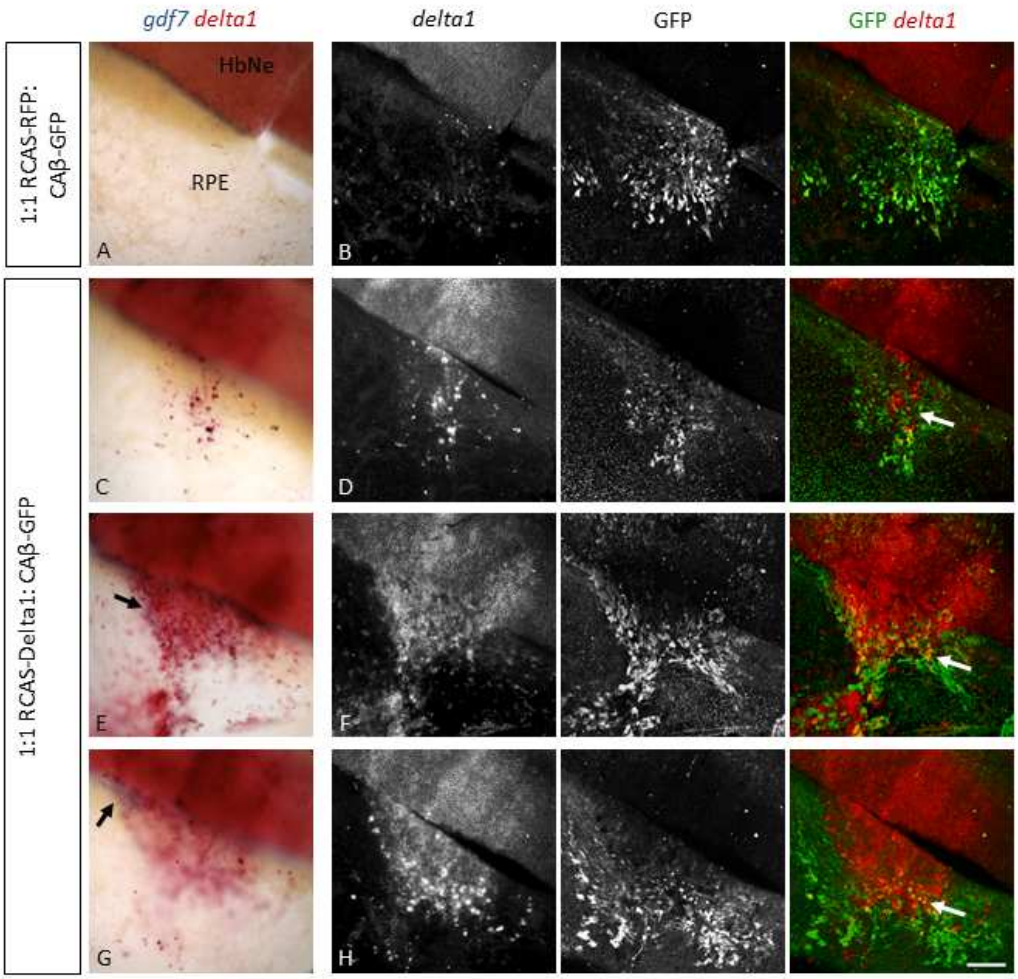

Figure 4-4 Overexpression of *delta1* in the RPE and detection of *delta1* and *gdf7* expression

A DNA mix of 1:1 RCAS-*RFP*: CAβ-*GFP* (A, B) or 1:1 RCAS-*Delta1*: CAβ-*GFP* (C - H) was electroporated into the lower rhombic lip and adjacent RPE of an E3 chick embryo. Embryos were incubated for 48hrs prior to collection. *delta1* (red) and *gdf7* (blue) expression was detected by whole-mount double *in situ* hybridisation and the electroporation site was detected by whole-mount immunohistochemistry for GFP. A, C, E, G show bright-field images taken using a compound microscope. B, D, F, H show confocal micrographs of the regions shown in A, C, E, G respectively. Anterior is oriented to the left. Black arrows, *gdf7* induced in the roof plate epithelium. White arrows, the subset of GFP-positive cells that co-express *delta1*. RPE, roof plate epithelium; HbNe, hindbrain neuroepithelium.

Scale bars: 100μm.

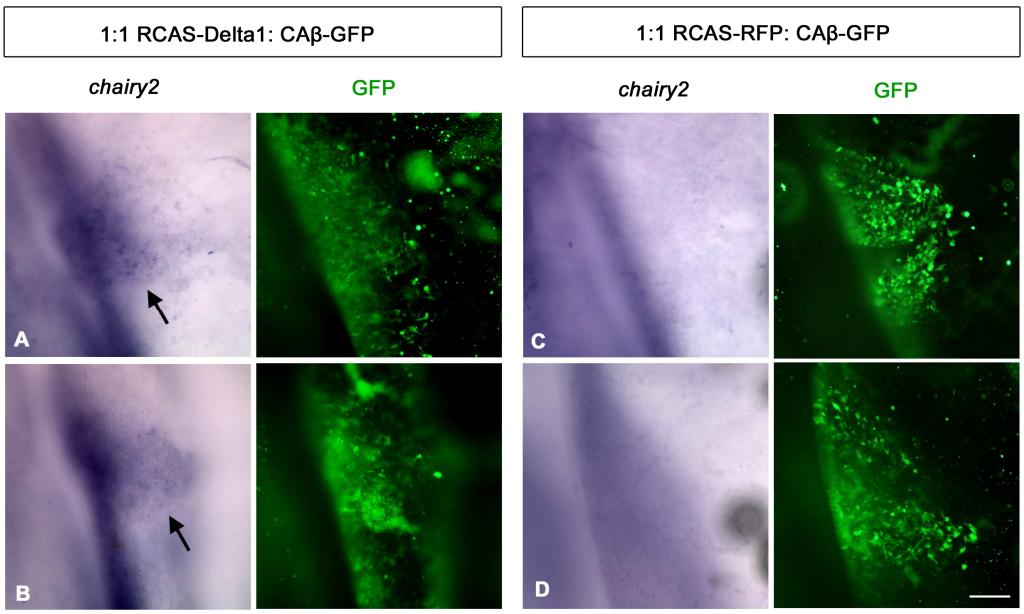

Figure 4-5 Overexpression of *delta1* in the RPE induces *chairy2* expression

A DNA mix of 1:1 RCAS-Delta1: CAβ-GFP (A, B) or 1:1 RCAS-RFP: CAβ-GFP (C, D) was electroporated into the lower rhombic lip and adjacent RPE of E3 chick embryos. Embryos were incubated for 48hrs prior to collection. *chairy2* expression was detected by whole-mount *in situ* hybridisation and the electroporation site was detected by whole-mount immunohistochemistry for GFP. Anterior is oriented upwards. Arrows indicate induced *chairy2* expression in the RPE after electroporation with 1:1 RCAS-Delta1: CAβ-GFP. No *chairy2* was induced in the RPE after electroporation with 1:1 RCAS-RFP: CAβ-GFP. RPE, roof plate epithelium; HbNe, hindbrain neuroepithelium.

Scale bars: 100μm.

plate epithelium had no effect on *gdf7* or *cyp26C1* expression, when compared with expression on the un-electroporated side (Figure 4-6 A – C, arrows indicate electroporated region, n=0/3). However, co-electroporation of RCAS-*delta1* and CAβ-*GFP* constructs caused an upregulation of *cyp26C1* expression within the electroporated domain (Figure 4-6 D, E, G, H arrows, n=2/5). No induction of *gdf7* expression in the roof plate epithelium was observed in these electroporated embryos, however this could have been due to detection of *cyp26C1* expression obscuring detection of *gdf7* expression (Figure 4-6 F, open arrow). On one occasion, *cyp26C1* expression was downregulated non-autonomously, adjacent to the region of upregulated *cyp26C1* expression (Figure 4-6 D, E arrowheads). However whether this downregulation was due to non-autonomous signals from the electroporated domain, or whether it reflects sorting of electroporated from non-electroporated cells is not clear.

4.2.5 Ectopic expression of *delta1* in the roof plate epithelium induces *gdf7* expression but causes a downregulation of *ttr* expression

Co-electroporation of RCAS-*RFP* and CAβ-*GFP* into the right hand-side lower rhombic lip and adjacent roof plate epithelium had no effect on *gdf7* or *ttr* expression, as compared with the un-electroporated side (Figure 4-7 A – C, arrows indicate electroporated region, n=0/3). Co-electroporation of RCAS-*delta1* and CAβ-*GFP* constructs induced *gdf7* expression in the roof plate epithelium, in agreement with findings stated above (Figure 4-7 D – F, arrows, n=1/5). This showed that induction of *gdf7* was non-autonomous to the electroporated domain, although due to the nature of the co-electroporation described above, it cannot be ruled out that some GFP-negative cells are *delta1*-positive. Expression of *delta1* in the roof plate epithelium caused downregulation of *ttr* expression autonomously, within the electroporated domain (Figure 4-7 E, G, H, J, K arrowheads n=3/5).

4.2.6 Expression of truncated cHairy2 at the roof plate epithelium – hindbrain neuroepithelium boundary results in a loss of *gdf7* and *cath1* expression

hairy/ enhancer of split (*hes*) genes are known downstream effectors of Notch signalling and are well known in their own right to be required for the maintenance of boundary-localised organisers (Geling et al., 2003; Geling et al., 2004; Ninkovic et al., 2005; Baek et al., 2006; reviewed in Kageyama et al., 2008). *chairy1* and *chairy2* are two chick orthologues of mouse *hes1* (Jouve et al., 2000). Both are upregulated within the *gdf7*-domain in chick at E4 (Figure 2-7, 2-8), but only *chairy2*, like *gdf7*, is induced in the roof plate epithelium at an experimental interface between hindbrain roof plate epithelium and neuroepithelium (Figure 3-22). Consequently the requirement for cHairy2 function for the maintenance of the *gdf7*-domain and adjacent *cath1* expression was investigated. To achieve this the roof plate epithelium – hindbrain neuroepithelium boundary was electroporated with a construct

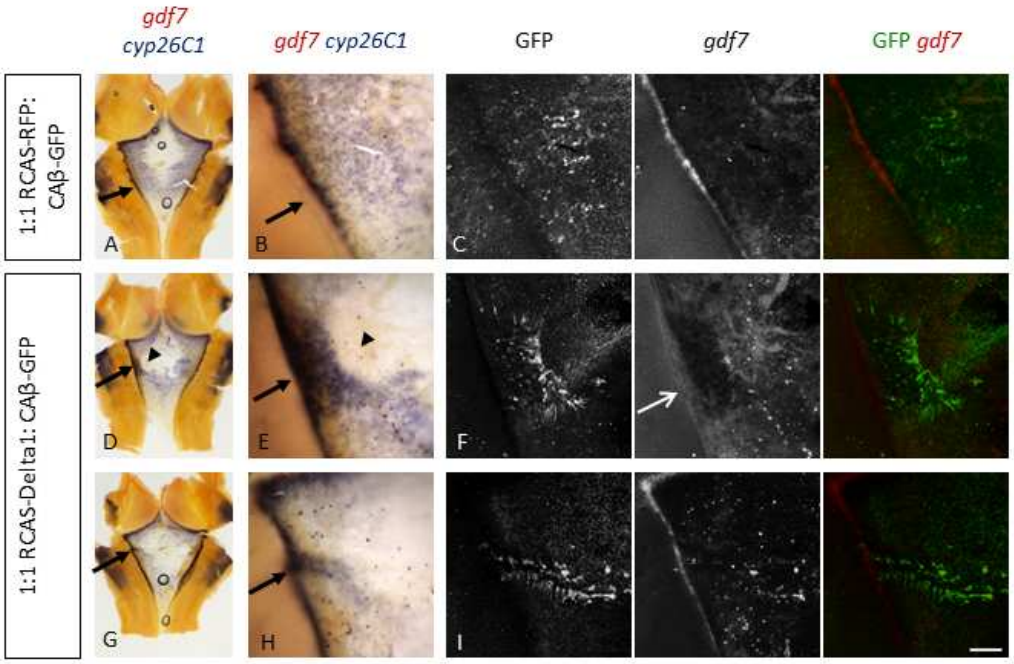

Figure 4-6 Expression of *delta1* in the RPE upregulates *cyp26C1* expression

A DNA mix of 1:1 RCAS-*RFP*: CAβ-*GFP* (A – C) or 1:1 RCAS-*Delta1*: CAβ-*GFP* (D - I) was electroporated into the lower rhombic lip and adjacent RPE of an E3 chick embryo. Embryos were incubated for 48hrs prior to collection. *gdf7* (red) and *cyp26C1* (blue) expression was detected by whole-mount double *in situ* hybridisation and the electroporation site was detected by whole-mount immunohistochemistry for GFP. B, C, E, F, H, I show high magnification views of electroporated regions in A, D, G. C, F, I show confocal micrographs of the region shown in B, E and H respectively. Anterior is oriented upwards and hindbrains are mounted with the ventricular surface upwards. A, B, arrows indicate electroporated region. D, E, G, H, arrows indicate upregulated *cyp26C1* expression after ectopic *delta1* expression in the RPE. E, arrowhead, non-autonomous downregulation of *cyp26C1* expression. F, open arrow, detection of *gdf7* expression is obscured by detection of *cyp26C1* expression.

Scale bar: 100µm

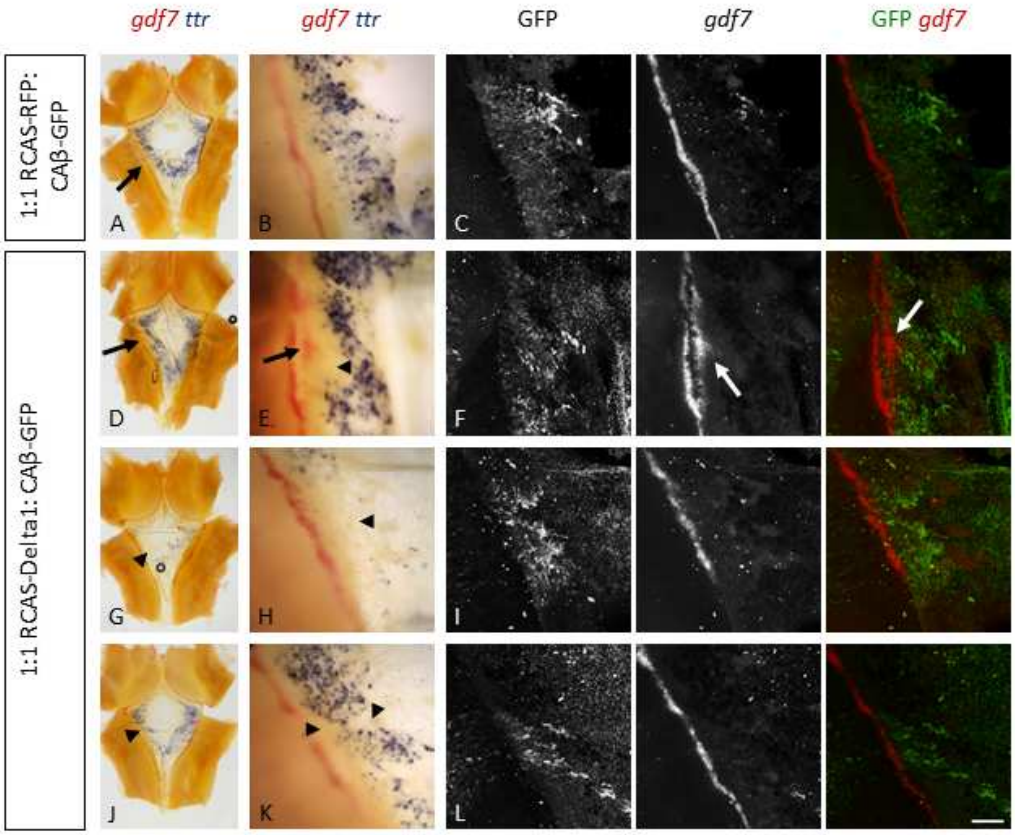

Figure 4-7 Expression of *delta1* in the RPE induces *gdf7* but causes downregulaiton of *ttr*

A DNA mix of 1:1 RCAS-*RFP*: CAβ-*GFP* (A – C) or 1:1 RCAS-*Delta1*: CAβ-*GFP* (D - L) was electroporated into the lower rhombic lip and adjacent RPE of an E3 chick embryo. Embryos were incubated for 48hrs prior to collection. *gdf7* (red) and *ttr* (blue) expression was detected by whole-mount double *in situ* hybridisation and the electroporation site was detected by whole-mount immunohistochemistry for GFP. B, C, E, F, H, I, K, L show high magnification views of electroporated regions in A, D, G, J. C, F, I, L show confocal micrographs of the region shown in B, E, H and K respectively. Anterior is oriented to the upwards and hindbrains are mounted with the ventricular surface upwards. A, arrow, electroporated region. D – F, arrows, *gdf7* expression induced in the RPE. E, G, H, J, K, downregulation of ttr expression within the electroporated domain.

Scale bar: 100µm.

encoding a truncated version of cHairy2 (*chairy2ΔWRPWv1-IRESeGFPm5,* gift from J. Gilthorpe, Umeå University), where the conserved c-terminal WRPW domain that is required for the recruitment of Groucho/TLE co-repressors was deleted (Paroush et al., 1994; Fisher et al., 1996; Grbavec et al., 1998). This truncated version of cHairy2 has been proposed to act in a dominant negative fashion, similar to the effect of such a truncation on the E(Spl) proteins of Drosophila (Giebel and Campos-Ortega, 1997).

Electroporation of this construct at the upper roof plate epithelium – hindbrain neuroepithelium boundary of E4 embryos resulted in a downregulation of *gdf7* and adjacent *cath1* expression in an autonomous manner, after 24 hours incubation (Figure 4-8 A – I, arrows, n=4/25), as compared with the control (un-electroporated) side of the brains.

As a control experiment a GFP expression construct (CAβ-*GFP*) was electroporated at the roof plate epithelium – hindbrain neuroepithelium boundary of E4 embryos, and the hindbrains were assessed for *gdf7* and *cath1* expression after 24 hours incubation. For the most part, *gdf7* and *cath1* expression were unaffected by electroporation with the GFP expression construct (Figure 4-9 A – D, n=9/11), however on one occasion electroporation resulted in a slight downregulation of *gdf7* and adjacent *cath1* expression (Figure 4-9 E, F arrow, n=1/11), and on another occasion electroporation resulted in a slight downregulation of *cath1* expression within the electroporated domain in comparison with the un-electroporated side of brains (Figure 4-9 G, H arrow, n=1/11). These effects were milder than those achieved by electroporation with the *chairy2ΔWRPW* expression construct leading to the conclusion that expression of *chairy2ΔWRPW* causes a loss of *gdf7* and *cath1* expression above and beyond a baseline effect that is the result of electroporation of any construct at the roof plate epithelium – hindbrain neuroepithelium boundary.

4.2.7 Electroporation with the *chairy2ΔWRPW* expression construct causes cell death within the electroporated domain

In order to investigate the mechanism behind the loss of *gdf7* and *cath1* expression after electroporation at the roof plate epithelium – hindbrain neuroepithelium boundary with the *chairy2ΔWRPW* or the *GFP* expression construct, a stain to detect cell death was carried out. LysoTracker Red staining to detect cell death shows that electroporation of the rhombic lip with either the CAβ-*GFP* or the *chairy2ΔWRPWv1-IRESeGFPm5* construct results in a significant increase in cell death in the electroporated domain compared with a similar region of the rhombic lip on the control (un-electroporated) side of the hindbrain (Figure 4-10 A – E, arrows, n=3, $p<0.05$, Wilcoxon paired comparison test). However, after subtraction of the number of dead cells on the control side from the number of dead cells within the electroporated domain on the electroporated side of the hindbrain, the domain electroporated

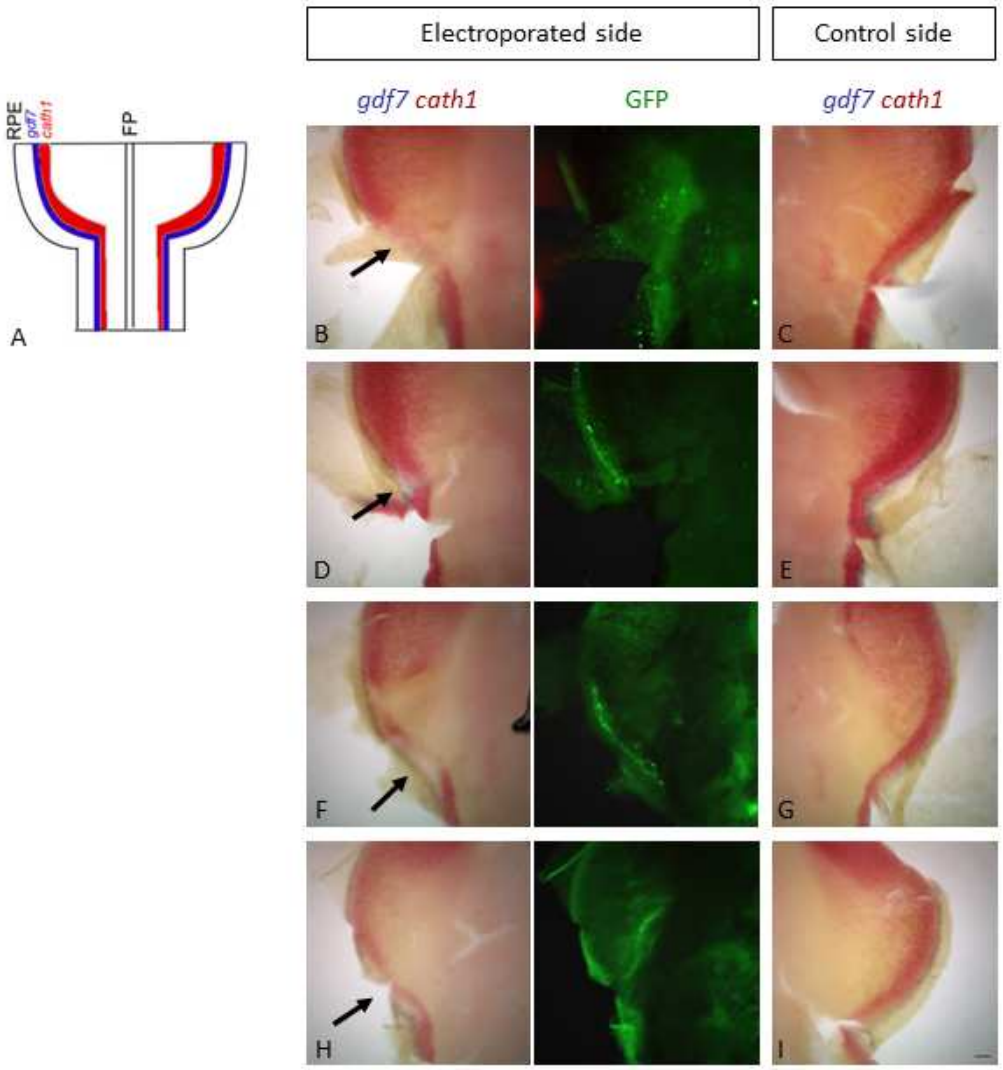

Figure 4-8 Electroporation of the *gdf7*-domain and rhombic lip with a *cHairy2ΔWRPW* expression construct causes downregulation of *gdf7* and adjacent *cath1* expression

E4 embryos were electroporated with a *cHairy2ΔWRPW* expression construct into the right-hand side upper rhombic lip and *gdf7* domain. Embryos were incubated for 24 hours prior to collection. The expression of *gdf7* (blue) and *cath1* (red) was assessed by whole-mount *in situ* hybridisation and the electroporation site was detected by whole-mount immunohistochemistry for GFP. Hindbrains were flat-mounted as illustrated in A for imaging. B, D, F, H show the electroporated side and C, E, G, I show the un-electroporated (control) side of flat-mounted hindbrains. Arrows indicate autonomous downregulation of *gdf7* and *cath1* expression within the electroporated domain. RPE, roof plate epithelium; FP, floor plate.

Scale bar: 100µm

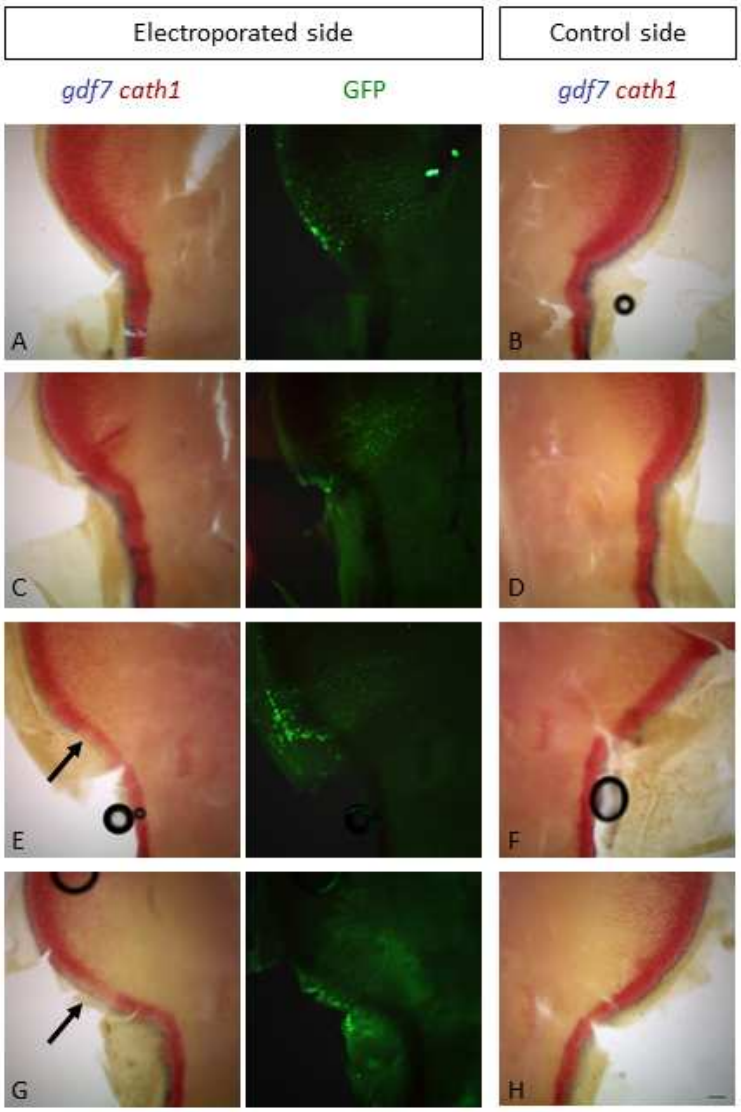

Figure 4-9 Electroporation of the *gdf7*-domain and rhombic lip with a *GFP* expression construct

E4 embryos were electroporated with a GFP expression construct into the right-hand side upper rhombic lip and *gdf7* domain. Embryos were incubated for 24 hours prior to collection. The expression of *gdf7* (blue) and *cath1* (red) was assessed by whole-mount *in situ* hybridisation and the electroporation site was detected by whole-mount immunohistochemistry for GFP.A, C, E, G show the electroporated side and B, D, F, H show the un-electroporated (control) side of flat-mounted hindbrains. E, arrow, slight downregulation of expression of *gdf7* and *cath1*. G, arrow, slight downregulation of *cath1* expression.

Scale bar: 100µm

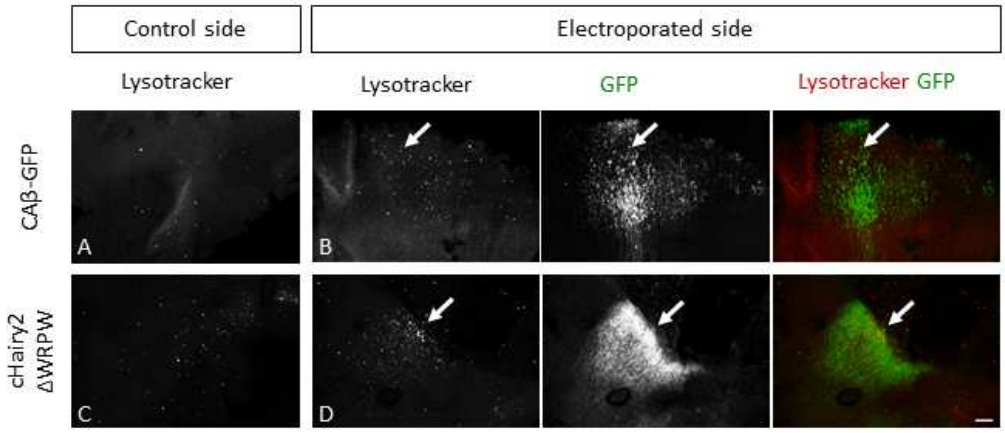
Control side
Electroporated side
Lysotracker
Lysotracker
GFP
Lysotracker GFP
CAβ-GFP
cHairy2 ΔWRPW
A
B
C
D

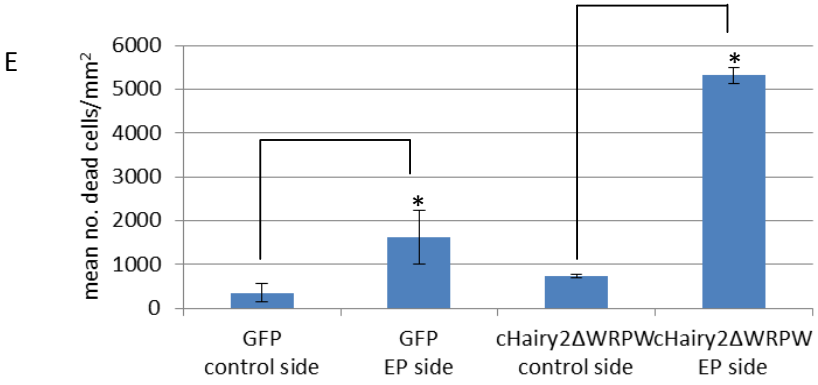
E
mean no. dead cells/mm2
6000
5000
4000
3000
2000
1000
0
*
*
GFP control side
GFP EP side
cHairy2ΔWRPW control side
cHairy2ΔWRPW EP side

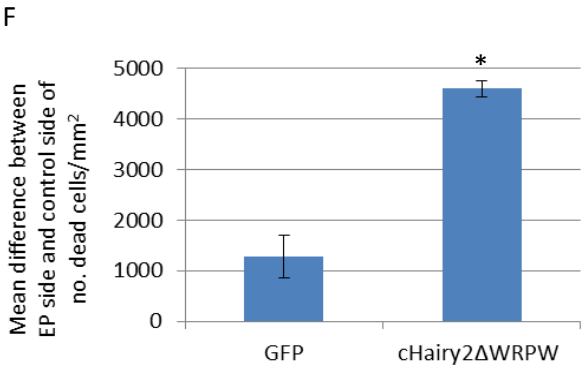
F
Mean difference between EP side and control side of no. dead cells/mm2
5000
4000
3000
2000
1000
0
*
GFP
cHairy2ΔWRPW

Figure 4-10 Cell death after electroporation with a *GFP* or a *cHairy2ΔWRPW* expression construct

E4 embryos were electroporated with a *GFP* (CAβ-*GFP*) (A, B) or a *cHairy2ΔWRPW* (*cHairy2ΔWRPWv1-IRESeGFPm5*) (C, D) expression construct into the right-hand side upper rhombic lip and *gdf7* domain. Embryos were incubated for 24 hours then collected and stained for cell death using LysoTracker Red then fixed in PFA. A – D show confocal micrographs of the upper rhombic lip of flat-mounted hindbrains, with A and C showing the control (un-electroporated) side, and B and D showing the electroporated side of the hindbrain . Anterior is oriented to the left. Arrows indicate cell death within the electroporated domain. Scale bar: 100µm

E, graph showing numbers of dead cells/ mm^2. * indicates $p<0.05$, n=3, determined using the Wilcoxon paired comparison test. Bars indicate the standard error of the mean.

F, graph showing the mean difference between the electroporated (EP) side and control side of the number of dead cells/ mm^2. * indicates $p<0.05$, n=3, determined using the Mann-Whitney test.

with the *chairy2ΔWRPWv1-IRESeGFPm5* construct shows a significantly higher level of cell death than the domain electroporated with CAβ-*GFP* (Figure 4-10 F, n=3, $p<0.05$, Mann-Whitney test). Therefore the downregulation of *gdf7* or *cath1* expression after electroporation with CAβ-*GFP* or *chairy2ΔWRPWv1-IRESeGFPm5* can be attributed, at least in part, to cell death. Further, however, electroporation with the *chairy2ΔWRPWv1-IRESeGFPm5* construct causes significantly more cell death than electroporation with the CAβ-*GFP* construct, and this is reflected in the higher severity of effects on *gdf7* and *cath1* expression observed after electroporation with the *chairy2ΔWRPWv1-IRESeGFPm5* construct.

4.2.8 Cloning and electroporation of a new *chairy2ΔWRPW* and a full length *chairy2* expression construct

Sequencing of the *chairy2ΔWRPWv1-IRESeGFPm5* construct revealed an ATG translation start codon upstream and out of frame of the correct translation start site for the cHairy2 coding sequence (Figure 4-11). This may have resulted in inefficient translation of the protein, which could explain the low penetrance of the observed downregulation of *gdf7* and *cath1* expression upon electroporation of the construct (Figure 4-8, n=4/25). To investigate whether a more penetrant effect could be achieved, the cHairy2ΔWRPW coding sequence was re-cloned from E3 chick cDNA into the pCAβ-*IRESeGFPm5* vector (Andreae et al., 2009) as described in the Methods. This new construct will be termed *chairy2ΔWRPWv2-IRESeGFPm5*. A full length coding sequence for cHairy2 was also cloned into the pCAβ-*IRESeGFPm5* vector as described in the Methods. This construct will be termed *chairy2-IRESeGFPm5*.

As noted previously, for the most part, electroporation of CAβ-*GFP* into the roof plate epithelium – hindbrain neuroepithelium boundary had no effect on *gdf7* and *cath1* expression, in comparison with the control (un-electroporated) side of the brain (Figure 4-12 A, B, n=7/8). However, on one occasion *cath1* expression was downregulated in the electroporated domain in comparison with the same region on the control side of the brain (Figure 4-12 C, D, arrows, electroporated region; arrowhead, similar region on the un-electroporated side n=1/8). Electroporation of the *chairy2ΔWRPWv2-IRESeGFPm5* construct caused downregulation of both *gdf7* and *cath1* expression in the electroporated domain, in comparison with the same region on the control side of the brain, although at a similar level of penetrance as achieved with the original *chairy2ΔWRPWv1-IRESeGFPm5* construct (Figure 4-12 E – H, arrows, electroporated region; arrowheads, similar region on the un-electroporated side n=2/9). This indicates that the presence of the additional ATG translation start site upstream of the correct translation start site in the *chairy2ΔWRPWv1-*

```
3     GGC CGC CCA TGG AAT AAC ACC ACC ATG CCT GCC GAC CTG ATG GAG   47
                                      Met Pro Ala Asp Leu Met Glu   6

48    AAG AGC AGC GCC TCG CCG GTG GCC GCC ACC CCC GCC AGC ATC AAC   92
7     Lys Ser Ser Ala Ser Pro Val Ala Ala Thr Pro Ala Ser Ile Asn   21

93    GCG ACG CCC GAT AAG CCC AAA ACG GCG GCG GAG CAC CGG AAG TCC   137
22    Ala Thr Pro Asp Lys Pro Lys Thr Ala Ala Glu His Arg Lys Ser   36

138   TCC AAA CCC ATC ATG GAG AAG CGG CGG CGG GCG CGC ATC AAC GAG   182
37    Ser Lys Pro Ile Met Glu Lys Arg Arg Arg Ala Arg Ile Asn Glu   51

183   AGC CTG GGG CAG CTG AAG ACG CTG ATC CTG GAC GCG CTG AAG AAG   227
52    Ser Leu Gly Gln Leu Lys Thr Leu Ile Leu Asp Ala Leu Lys Lys   66

228   GAT AGT TCG CGG CAC TCC AAG CTG GAG AAG GCC GAC ATC CTG GAG   272
67    Asp Ser Ser Arg His Ser Lys Leu Glu Lys Ala Asp Ile Leu Glu   81

273   ATG ACC GTC AAG CAC CTG CGG AGC CTG CAG CGG GCG CAG ATG ACC   317
82    Met Thr Val Lys His Leu Arg Ser Leu Gln Arg Ala Gln Met Thr   96

318   GCT GCG CTG AGC ACA GAC CCT ACG GTG CTG GGC AAG TAC CGC GCC   362
97    Ala Ala Leu Ser Thr Asp Pro Thr Val Leu Gly Lys Tyr Arg Ala   111

363   GGC TTC AGC GAG TGC ATG AAC GAA GTG ACG CGG TTC CTC TCC ACC   407
112   Gly Phe Ser Glu Cys Met Asn Glu Val Thr Arg Phe Leu Ser Thr   126
```

```
408   TGC GAA GGC GTC AAC GCT GAG GTG CGC ACC CGG CTC CTG GGC CAC   452
127   Cys Glu Gly Val Asn Ala Glu Val Arg Thr Arg Leu Leu Gly His   141

453   CTG GCC AGC TGC ATG ACC CAG ATC AAC GCC ATC AAC TAC CCC GTG   497
142   Leu Ala Ser Cys Met Thr Gln Ile Asn Ala Ile Asn Tyr Pro Val   156

498   CCG CCC CCG CCG CTG CCA CCC CCA CCC GCA GCC TTC GGG CCG CCC   542
157   Pro Pro Pro Pro Leu Pro Pro Pro Pro Ala Ala Phe Gly Pro Pro   171

543   CTG GTG CCG CCG GGC GGA GGC GCG GGG CCG CTC CCA GCC GTA CCC   587
172   Leu Val Pro Pro Gly Gly Gly Ala Gly Pro Leu Pro Ala Val Pro   186

588   TGC AAG CCA GGT GCC GAT GCG GCC AAG GTG TAC GGT GGT TTC CAG   632
187   Cys Lys Pro Gly Ala Asp Ala Ala Lys Val Tyr Gly Gly Phe Gln   201

633   CTG CTG CCT GCC TCT GAT GGG CAG TTC GCC TTC CTC ATC CCC AGC   677
202   Leu Leu Pro Ala Ser Asp Gly Gln Phe Ala Phe Leu Ile Pro Ser   216

678   GCT GCC TTT GCT CCC GGC GGG GCT GTG CTG CCC CTC TAT GGC GGT   722
217   Ala Ala Phe Ala Pro Gly Gly Ala Val Leu Pro Leu Tyr Gly Gly   231

723   CCC CCC ACA GCT GCC ACC ACC GCC TCG CCT CCC GGC CCC TCA CCC   767
232   Pro Pro Thr Ala Ala Thr Thr Ala Ser Pro Pro Gly Pro Ser Pro   246

768   GGC ACC GCT GAC TCA GTC TGA   788
247   Gly Thr Ala Asp Ser Val End   253
```

Figure 4-11 Sequence of *chairy2ΔWRPWv1-IRESeGFPm5*

Arrow indicates an ATG start codon upstream and out of frame of the correct translation start codon.

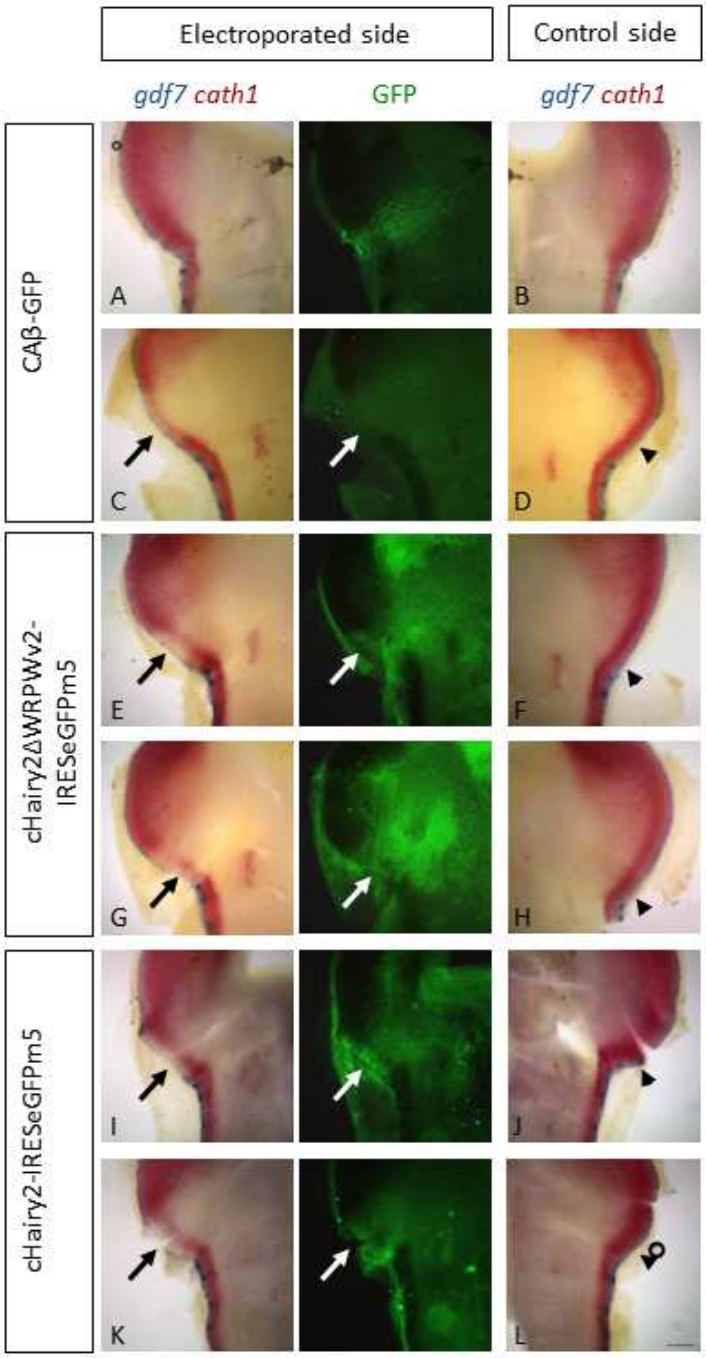
Electroporated side
Control side
gdf7 cath1
GFP
gdf7 cath1
CAβ-GFP
cHairy2ΔWRPWv2-IRESeGFPm5
cHairy2-IRESeGFPm5
A
B
C
D
E
F
G
H
I
J
K
L

Figure 4-12 Electroporation of the *gdf7*-domain and rhombic lip with the *cHairy2ΔWRPWv2-IRESeGFPm5* or *cHairy2-IRESeGFPm5* constructs

E4 embryos were electroporated with CAβ-*GFP* (A – D), *cHairy2ΔWRPWv2-IRESeGFPm5* (E – H) or *cHairy2-IRESeGFPm5* (I – L) constructs into the right-hand side upper rhombic lip and *gdf7* domain. Embryos were incubated for 24 hours prior to collection. The expression of *gdf7* (blue) and *cath1* (red) was assessed by whole-mount in situ hybridisation and the electroporation site was detected by whole-mount immunohistochemistry for GFP. A, C, E, G, I, K show the electroporated side and B, D, F, H, J, L show the un-electroporated (control) side of flat-mounted hindbrains. Anterior is oriented upwards. C, black arrow *cath1* expression is slightly downregulated within the electroporated domain. E, G, I, K, black arrows, downregulated *gdf7* and *cath1* expression. C, E, G, I, K, white arrows, the electroporated domain. D, F, H, J, L, arrowheads, an equivalent domain to the electroporated domain on the un-electroporated side.

Scale bar: 200µm

IRESeGFPm5 construct did not have a significant effect on the efficacy of translation of cHairy2ΔWRPW.

Electroporation of the *chairy2-IRESeGFPm5* construct had the same effect as electroporation of the *chairy2ΔWRPWv2-IRESeGFPm5* construct. Overexpression of full length *chairy2* at the roof plate epithelium – hindbrain neuroepithelium boundary also caused a downregulation of *gdf7* and *cath1* expression in the electroporated domain in comparison with the same region of the un-electroporated side of the brain (Figure 4-12 I – L, arrows, electroporated domain; arrowheads, similar region on the un-electroporated side n= 5/11).

4.2.9 Overexpression of *chairy2ΔWRPW* or full length *chairy2* at the roof plate epithelium – hindbrain neuroepithelium boundary causes a non-autonomous loss of roof plate epithelium- expressed *cyp26C1*

The localisation of organiser properties at the hindbrain neuroepithelium – roof plate epithelium boundary, marked by *gdf7* expression (Chapter 3), leads to the hypothesis that this domain could signal not only to the adjacent neuroepithelium, but also to the adjacent roof plate epithelium to direct development of the choroid plexus. Since the overexpression of *chairy2ΔWRPW* or *chairy2* at the roof plate epithelium – hindbrain neuroepithelium boundary disrupts *gdf7* and adjacent *cath1* expression, I investigated whether the electroporation of these constructs into the roof plate epithelium – hindbrain neuroepithelium boundary had any effect on the expression of the roof plate epithelium- expressed *cyp26C1*.

For the most part electroporation of the CAβ-*GFP* construct into roof plate epithelium – hindbrain neuroepithelium boundary had no effect on roof plate epithelial *cyp26C1* expression (Figure 4-13 A – D, n=3/4). However, on one occasion there was a slight downregulation of roof plate epithelial *cyp26C1* expression within the electroporated domain (Figure 4-13 E, F, arrows, n=1/4). The other GFP-positive cells in Figure 4-13 F are electroporated overlying skin cells (arrowhead).

In contrast, electroporation of *chairy2ΔWRPWv2-IRESeGFPm5* or *chairy2-IRESeGFPm5* into the roof plate epithelium – hindbrain neuroepithelium boundary caused both an autonomous and a non-autonomous loss of roof plate epithelial *cyp26C1* expression (Figure 4-14 A – H, arrows indicate non-autonomous loss of *cyp26C1* expression, *chairy2ΔWRPWv2-IRESeGFPm5* n=3/8, *chairy2-IRESeGFPm5* n=4/6). Therefore not only does overexpression of *chairy2ΔWRPW* or *chairy2* into the hindbrain neuroepithelium – roof plate epithelium boundary cause a downregulation of *gdf7* expression, but it also disrupts a

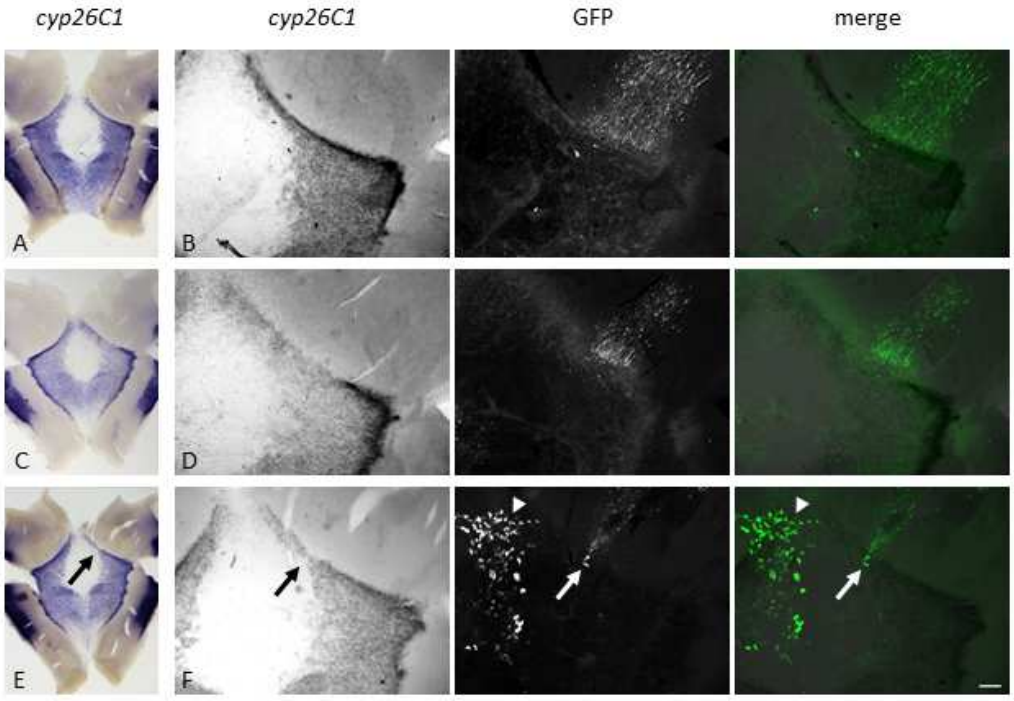

Figure 4-13 Effect of electroporation of the *gdf7*-domain and rhombic lip with CAβ-*GFP* on *cyp26C1* expression

E4 embryos were electroporated with CAβ-*GFP* into the right-hand side upper rhombic lip and *gdf7* domain (A – F). Embryos were incubated for 24 hours prior to collection. The expression of *cyp26C1* was assessed by whole-mount in situ hybridisation and the electroporation site was detected by whole-mount immunohistochemistry for GFP. B, D, F are confocal micrographs of the electroporated region indicated in A, C, E. Roof plates are mounted with the pial surface upwards and anterior oriented upwards. Arrows, slight downregulation of *cyp26C1* expression within the electroporated domain. Arrowheads indicate electroporated epithelial cells.

Scale bar: 100µm

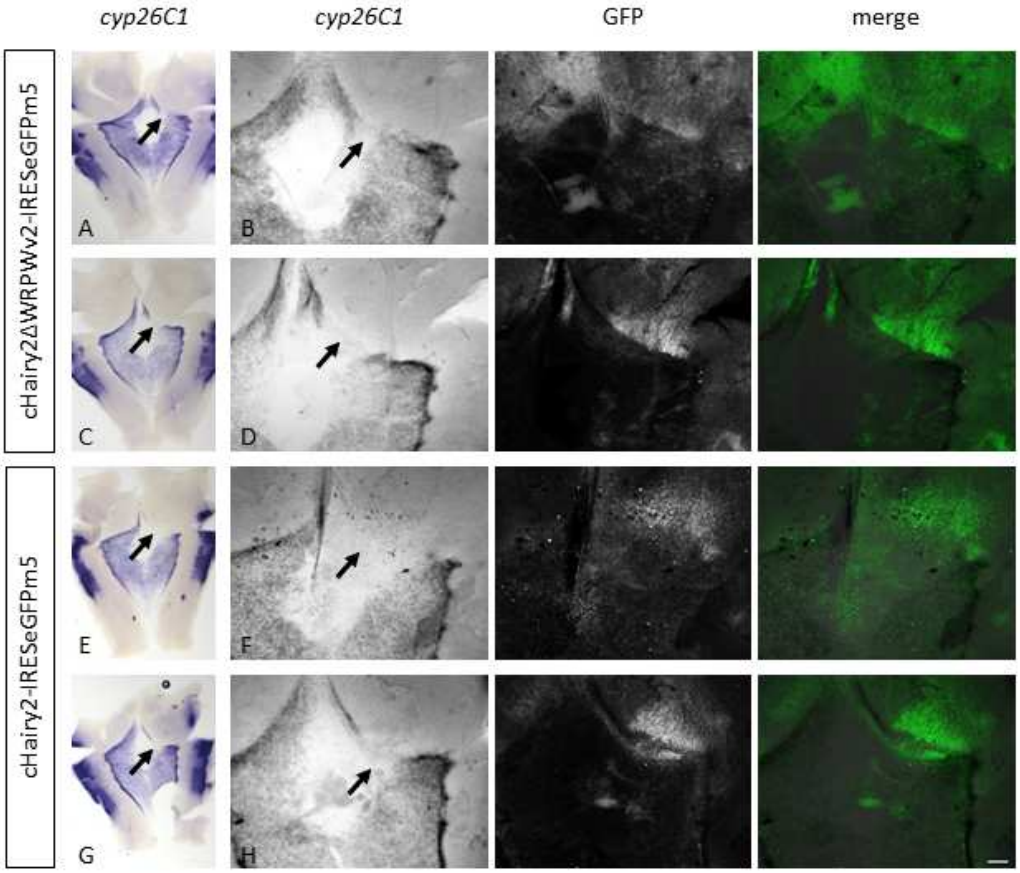

Figure 4-14 Electroporation of *cHairy2ΔWRPWv2-IRESeGFPm5* or *cHairy2-IRESeGFPm5* into the *gdf7*-domain and rhombic lip causes non-autonomous loss of *cyp26C1* expression

E4 embryos were electroporated with *cHairy2ΔWRPWv2-IRESeGFPm5* (A – D) or *cHairy2-IRESeGFPm5* (E – H) into the right-hand side upper rhombic lip and *gdf7* domain. Embryos were incubated for 24 hours prior to collection. The expression of *cyp26C1* was assessed by whole-mount *in situ* hybridisation and the electroporation site was detected by whole-mount immunohistochemistry for GFP. B, D, F, H are confocal micrographs of the electroporated region indicated in A, C, E, G. Roof plates are mounted with the pial surface upwards and anterior oriented upwards. Arrows indicate non-autonomous loss of roof plate epithelial *cyp26C1* expression.

Scale bar: 100µm

signalling centre there that is required to maintain the expression of *cyp26C1* in the roof plate epithelium.

4.2.10 The effects on *gdf7* and adjacent *ttr* expression of electroporation of the roof plate epithelium – hindbrain neuroepithelium boundary with *chairy2ΔWRPWv2-IRESeGFPm5* or *chairy2-IRESeGFPm5*

Since autonomous signals from the roof plate epithelium – hindbrain neuroepithelium boundary were required to maintain the expression of *cyp26C1* in the roof plate epithelium, I investigated whether these signals were also required for the expression of the choroid plexus epithelial marker, *ttr*, which begins to be expressed at the fourth ventricle roof plate at E4 in chick (Figure 2-9).

Electroporation of the upper roof plate epithelium – hindbrain neuroepithelium boundary at E4 with CAβ-*GFP*, for the most part, did not have any effect on *gdf7* and *ttr* expression (Figure 4-15 A – F, n=3/4). However, in one instance, *gdf7* expression was downregulated within the electroporated domain (Figure 4-15 G – I, arrows, n=1/4), confirming that there is a non-specific effect on gene expression that occurs occasionally with the electroporation of constructs at the roof plate epithelium – hindbrain neuroepithelium boundary in E4 chick embryos.

Electroporation of the upper roof plate epithelium – hindbrain neuroepithelium boundary at E4 with *chairy2ΔWRPWv2-IRESeGFPm5* caused a downregulation of *gdf7* expression in the electroporated domain and a non-autonomous loss of *ttr* expression in the adjacent roof plate epithelium after 24 hours (Figure 4-16 A – F, arrowheads indicate downregulation of *gdf7*, arrows indicate non-autonomous loss of *ttr* expression, n=3/4). On one occasion, *ttr* expression was lost non-autonomously, but *gdf7* expression was intact within the electroporated domain (Figure 4-16 G – I, arrow indicates non-autonomous loss of *ttr* expression, n=1/4). This is likely to reflect a disruption of the signalling centre present at the roof plate epithelium – hindbrain neuroepithelium boundary that is required to induce or maintain *ttr* expression, but the disruption may not have been sufficient to result in a downregulation of *gdf7* expression.

Electroporation of the upper roof plate epithelium – hindbrain neuroepithelium boundary at E4 with *chairy2-IRESeGFPm5* had similar effects to those observed when *chairy2ΔWRPWv2-IRESeGFPm5* was electroporated. *gdf7* expression was downregulated within the electroporated domain and *ttr* expression was lost non-autonomously in the adjacent roof plate epithelium (Figure 4-17 A – F, arrowheads indicate downregulation of *gdf7* expression, arrows indicate non-autonomous loss of *ttr* expression, n=3/5). As with

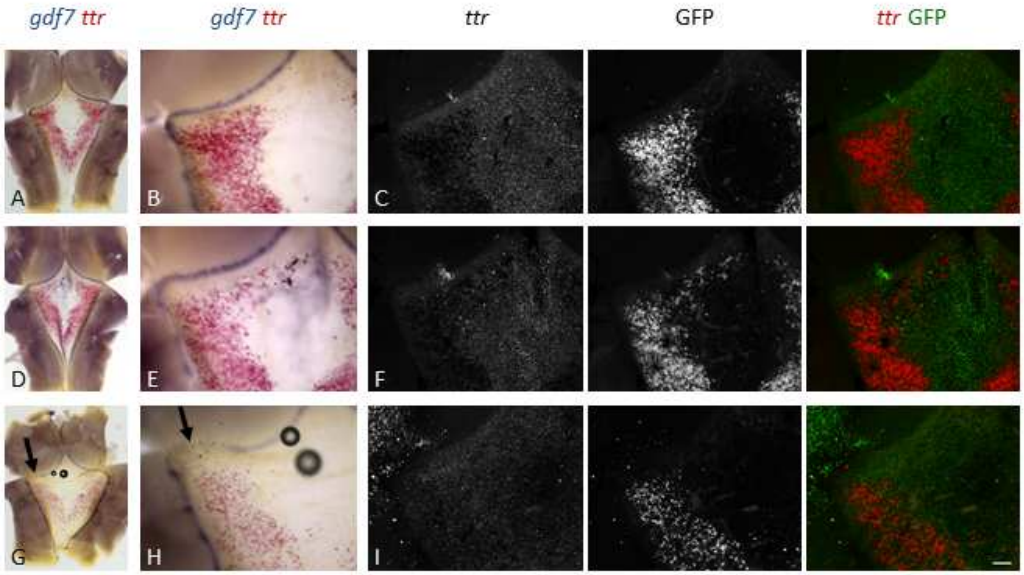

Figure 4-15 Effect of electroporation of the roof plate epithelium – hindbrain neuroepithelium boundary with CAβ-*GFP* on *gdf7* and *ttr* expression

E4 embryos were electroporated with CAβ-*GFP* into the right-hand side upper roof plate epithelium – hindbrain neuroepithelium boundary (A – I). Embryos were incubated for 24 hours prior to collection. The expression of *gdf7* and *ttr* was assessed by whole-mount *in situ* hybridisation and the electroporation site was detected by whole-mount immunohistochemistry for GFP. B, E, H are higher magnification images of the electroporated region shown in A, D, G. C, F, I are confocal micrographs of the regions shown in B, E, H. Roof plates are mounted with the ventricular surface upwards and anterior oriented upwards. Arrows indicate loss of *gdf7* expression in the electroporated domain.

Scale bar: 100µm.

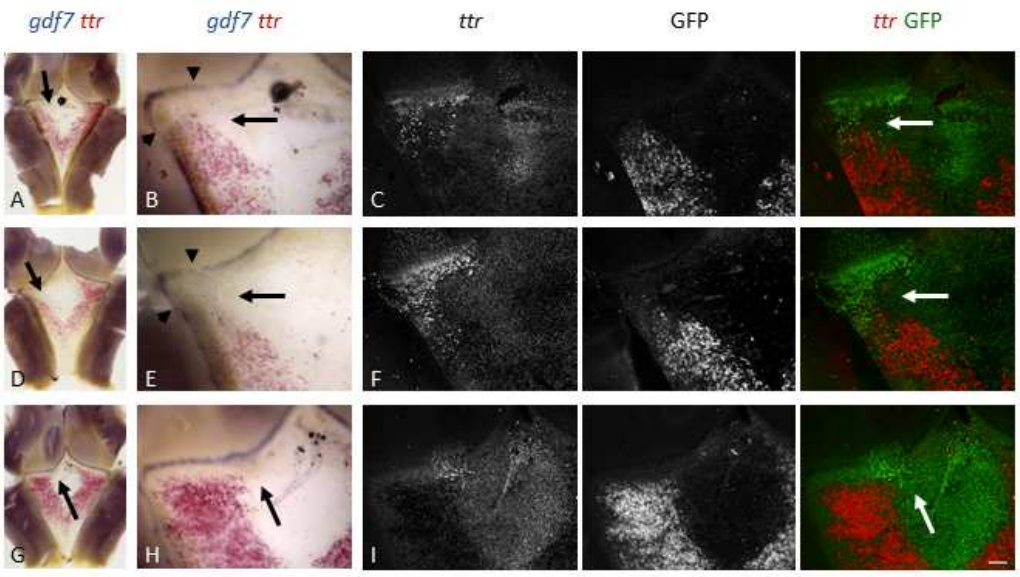

Figure 4-16 Effect of electroporation of the roof plate epithelium – hindbrain neuroepithelium boundary with *cHairy2ΔWRPWv2-IRESeGFPm5* on *gdf7* and *ttr* expression

E4 embryos were electroporated with *cHairy2ΔWRPWv2-IRESeGFPm5* into the right-hand side upper roof plate epithelium – hindbrain neuroepithelium boundary (A – I). Embryos were incubated for 24 hours prior to collection. The expression of *gdf7* and *ttr* was assessed by whole-mount *in situ* hybridisation and the electroporation site was detected by whole-mount immunohistochemistry for GFP. B, E, H are higher magnification images of the electroporated region shown in A, D, G. C, F, I are confocal micrographs of the regions shown in B, E, H. Roof plates are mounted with the ventricular surface upwards and anterior oriented upwards. Arrowheads, downregulation of *gdf7* expression within the electroporated domain. Arrows, non-autonomous downregulation of *ttr* expression in the roof plate epithelium adjacent to the electroporated domain.

Scale bar: 100µm.

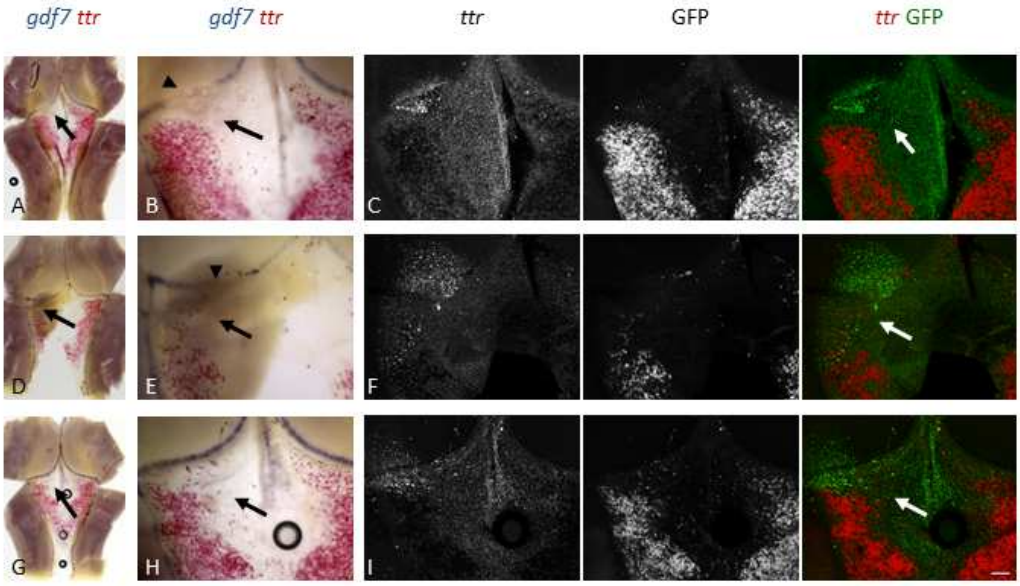

Figure 4-17 Effect of electroporation of the roof plate epithelium – hindbrain neuroepithelium boundary with *cHairy2-IRESeGFPm5* on *gdf7* and *ttr* expression

E4 embryos were electroporated with *cHairy2-IRESeGFPm5* into the right-hand side upper roof plate epithelium – hindbrain neuroepithelium boundary (A – I). Embryos were incubated for 24 hours prior to collection. The expression of *gdf7* and *ttr* was assessed by whole-mount *in situ* hybridisation and the electroporation site was detected by whole-mount immunohistochemistry for GFP. B, E, H are higher magnification images of the electroporated region shown in A, D, G. C, F, I are confocal micrographs of the regions shown in B, E, H. Roof plates are mounted with the ventricular surface upwards and anterior oriented upwards. Arrowheads, loss of *gdf7* expression within the electroporated domain. Arrows, non-autonomous loss of *ttr* expression.

Scale bar: 100µm

electroporation of the *chairy2ΔWRPWv2-IRESeGFPm5* construct, on one occasion, electroporation of the roof plate epithelium – hindbrain neuroepithelium boundary with *chairy2-IRESeGFPm5* caused a non-autonomous loss of *ttr* expression but had no effect on *gdf7* expression (Figure 4-17 G – I, arrows indicate a non-autonomous loss of *ttr* expression, n=1/5). Therefore electroporation of the upper roof plate epithelium – hindbrain neuroepithelium boundary with *chairy2ΔWRPWv2-IRESeGFPm5* or *chairy2-IRESeGFPm5* disrupts a signalling centre there, resulting in a non-autonomous loss of *ttr* expression in the roof plate epithelium and, for the most part, an autonomous downregulation of *gdf7* expression.

4.3 Discussion

The results described in this chapter show that ectopic expression of *delta1* in the roof plate epithelium induces the conversion of roof plate epithelial cells into roof plate boundary cells, marked by the expression of *gdf7* and upregulated *cyp26C1* expression (Figure 4-3, 4-6). *delta1* expression also induced *chairy2* expression in the roof plate epithelium and *chairy2* expression is required at the correct level at the roof plate epithelium – hindbrain neuroepithelium boundary for roof plate boundary *gdf7* expression to be maintained (Figure 4-5, 4-8, 4-10, 4-12, 4-16, 4-17). In this chapter it was also shown that the roof plate boundary not only signals to the adjacent neuroepithelium but it is also required to signal to the adjacent roof plate epithelium to maintain the expression of *cyp26C1* and permit the induction or maintenance of *ttr* expression and hence choroid plexus epithelium differentiation (Figure 4-16, 4-17, 4-14). However, it was also noted that immediately adjacent to an expanded roof plate boundary domain, *ttr* expression was repressed (Figure 4-7). This leads to a model of roof plate boundary function presented below in Figure 4-18 where the roof plate boundary both promotes choroid plexus differentiation at a distance from it, but inhibits its differentiation immediately adjacent to it. The possible function of this *ttr*-negative margin is discussed below.

4.3.1 Problems associated with the use of electroporation of the E4 chick roof plate epithelium – hindbrain neuroepithelium boundary to assess gene function

The E4 chick roof plate epithelium – hindbrain neuroepithelium boundary is a very thin region of tissue so it is unsurprising that electroporation of a control CAβ-*GFP* construct can cause a basal level of damage to the tissue that is observed as a small increase in cell death (Figure 4-10) and a downregulation of gene expression (Figure 4-9, 4-12, 4-13, 4-15). However, cell death associated with electroporation of the *chairy2ΔWRPWv1-IRESeGFPm5* construct was significantly higher than that associated with electroporation of the CAβ-*GFP* construct (Figure 4-10). Additionally, the effect of electroporation of the CAβ-*GFP* construct on *gdf7*, *cath1* and *cyp26C1* expression was qualitatively milder than the effect of electroporation of the *chairy2ΔWRPWv1-IRESeGFPm5*, the *chairy2ΔWRPWv2-IRESeGFPm5* or the *chairy2-IRESeGFPm5* constructs (Figure 4-12, 4-14, 4-16, 4-17). Lastly, electroporation of the CAβ-*GFP* construct never resulted in a non-autonomous loss of *cyp26C1* or *ttr* expression. Therefore although electroporation of CAβ-*GFP* may result in autonomous effects on gene expression, only the overexpression of *chairy2ΔWRPW* or *chairy2* resulted in a reduction in signalling capacity of the roof plate epithelium – hindbrain neuroepithelium boundary. Thus if electroporation of the roof plate epithelium – hindbrain neuroepithelium boundary with control constructs such as CAβ-*GFP* is carried out alongside

electroporation with experimental constructs, valid conclusions can be drawn about gene function by comparing the effects of electroporation of experimental constructs with the effects of electroporation of control constructs.

4.3.2 Ligand driven Notch signalling in the roof plate epithelium is sufficient to convert roof plate epithelial cells to roof plate boundary cells

Tissue interactions between roof plate epithelium and hindbrain neuroepithelium are sufficient to convert roof plate epithelial cells to a roof plate boundary-organiser fate, marked by *gdf7*-expression (Chapter 3). Activation of Notch signalling by overexpression of *delta1* in the roof plate epithelium is also sufficient to induce the expression of *gdf7* and *chairy2* there (Figure 4-3, 4-4, 4-5), indicating that Delta-Notch interactions mediate the hindbrain neuroepithelial – roof plate epithelial induction of *gdf7* and *hairy2* expression observed in co-culture experiments. Analysis of the expression patterns of Notch ligands and receptors at the roof plate epithelium – hindbrain neuroepithelium boundary of the E5 chick embryo shows that *delta1* expression has a sharp boundary adjacent to the *gdf7*-domain, and that *notch2* is expressed in the roof plate epithelium (Figure 2-6). Therefore it is likely that the induction of *gdf7* observed when *delta1* is expressed in the roof plate epithelium, is mediated by *notch2*, and that *in vivo*, a Delta1 – Notch2 interaction serves to maintain the *gdf7*-positive roof plate boundary-organiser.

Induction of *gdf7* in the roof plate epithelium appeared to be cell-non autonomous (Figure 4-3, 4-4, 4-7). This fits with the known mechanism of action of the DSL family of ligands, which are present at the plasma membranes of cells but *trans*-activate Notch receptors on adjacent cells (reviewed in Bray, 2006). The DSL family of ligands are also known to cell-autonomously inhibit the activation of Notch receptors (known as *cis*-inhibition) (de Celis and Bray, 1997; Micchelli et al., 1997; Sakamoto et al., 2002; reviewed in del Alamo et al., 2011) thereby limiting the effects of overexpression of *delta1* to cells adjacent to those ectopically expressing *delta1*.

The electroporation technique utilised in theses experiments resulted in overexpression of *delta1* in the roof plate epithelium but also in the neighbouring rhombic lip (Figure 4-2), however, *gdf7* expression was only induced in the roof plate epithelium (Figure 4-3, 4-7). One explanation for this is that *cis*-inhibition by *serrate1* and *delta1* expressed in the rhombic lip (Chapter 2) prevent induction of *gdf7* in this tissue. However an alternative explanation is that hindbrain neuroepithelium is not competent to express *gdf7* and only hindbrain roof plate-derived tissue is competent. It would be interesting to investigate if the overexpression of *lmx1a* (a transcription factor that is necessary and sufficient for roof plate

specification (Millonig et al., 2000; Chizhikov and Millen, 2004b; Chizhikov et al., 2006)) along with *delta1*is sufficient to induce *gdf7* expression in the hindbrain neuroepithelium.

Overexpression of *delta1* in the roof plate epithelium not only induced *gdf7* expression, but also upregulated *cyp26C1* within the electroporated domain. This indicates that high-level expression of *cyp26C1* is also a marker of the roof plate boundary-organiser. Interestingly, the induction of *cyp26C1* and *chairy2* expression in the roof plate epithelium by ectopic expression of *delta1* appears to be cell-autonomous (Figure 4-5, 4-6), unlike the induction of *gdf7* expression. A possible explanation for this is that a lower threshold of Notch activation within cells is required for the expression of *cyp26C1* and *chairy2* in comparison with *gdf7*. By this hypothesis, the level of *cis*-inhibition of Notch activation by Delta1 would not be sufficient to completely abolish *trans*-activation by Delta1 from neighbouring cells and hence the low level of Notch activation within *delta1*-expressing cells would be sufficient to induce *cyp26C1* and *chairy2* expression, but not *gdf7* expression.

Activated Notch signalling has been shown in numerous developmental situations to be important for the specification or maintenance of boundary-cell fates, such as the dorsoventral boundary of the Drosophila wing imaginal disc, hindbrain rhombomere boundaries in zebrafish, the apical ectodermal ridge of the chick limb bud, the zona limitans intrathalamica and, more recently, the midbrain-hindbrain boundary in the chick (Rulifson and Blair, 1995; Laufer et al., 1997; Rodriguez-Esteban et al., 1997; Zeltser et al., 2001; Cheng et al., 2004; Tossell et al., 2011). Thus the E3 – E5 chick hindbrain roof plate boundary represents another case where a boundary cell-fate is induced or maintained by the action of activated Notch signalling, and therefore provides support for the idea that Notch signalling operating to specify or maintain boundary-organiser cell fate within an epithelium is an ancient, evolutionarily conserved mechanism.

Aside from the studies carried out on zebrafish rhombomere boundaries, previous studies have largely involved experimental manipulations carried out prior to the formation of boundaries so can either not distinguish between an involvement of Notch activation for the specification or maintenance of boundary cells, or focus mainly on the specification of boundary cells. In studies described here, manipulations were carried out at E3 (st16 – 17) when the roof plate boundary (as assessed by *gdf7* expression) had already formed (Figure 2-3). Any conclusions can hence only address the involvement of Notch signalling in the maintenance of the roof plate boundary. Whether Notch signalling is also involved in the establishment of the roof plate boundary requires further investigation.

The hindbrain roof plate boundary is known to be a proliferative source of choroid plexus epithelial cells from E12.5 onwards in the mouse embryo (Huang et al., 2009). My findings

therefore shed new light on the findings of Hunter & Dymecki (2007) who showed that constitutive activation of Notch in all derivatives of *gdf7*-expressing cells in mouse results in greatly expanded choroid plexus epithelium that is ectopically proliferative at P0. My findings suggest that rather than the expression of Notch-intracellular domain promoting proliferation in all *gdf7*-positive cell derivatives, the expression of activated Notch may specify cells as boundary-organiser cells that divide asymmetrically to maintain their own population as well as give rise to differentiated choroid plexus epithelial cells.

4.3.3 The role of cHairy2 in the maintenance of the roof plate boundary-organiser

Hes genes are well known downstream effectors of Notch signalling, but in addition to this, are also well characterised as being essential for the maintenance of boundary-localised organisers in the mouse and in the zebrafish, but not necessarily in a Notch-dependant fashion (Hirata et al., 2001; Geling et al., 2003; Geling et al., 2004; Ninkovic et al., 2005; Baek et al., 2006; Kageyama et al., 2007). *chairy2*, a chick orthologue of mouse *hes1* (Jouve et al., 2000), shows upregulated expression within the wild-type *gdf7*-positive roof plate boundary (Figure 2-7). In the same manner as I have demonstrated for *gdf7*, *chairy2* is induced in the roof plate epithelium at both an experimentally derived interface between hindbrain roof plate epithelium and neuroepithelium (Figure 3-21, 3-22) and after ectopic expression of *delta1* in the roof plate epithelium (Figure 4-5). Conversely, electroporation of the roof plate epithelium – hindbrain neuroepithelium boundary of E4 chick embryos with either *chairy2ΔWRPWv1-IRESeGFPm5* or *chairy2ΔWRPWv2-IRESeGFPm5* results in a downregulation of expression of *gdf7* at E5 (Figure 4-8, 4-12, 4-16). Together, these results support a role for cHairy2 in maintaining the *gdf7*-positive boundary downstream of Notch signalling.

In these experiments the expression of *cath1* is also downregulated adjacent to downregulated *gdf7* expression. Given the dependence of *cath1* on an intact roof plate boundary in culture experiments (Chapter 3), a parsimonious explanation is that its expression is regulated non-autonomously by the *gdf7*-positive roof plate boundary. Due to the breadth of the electroporated territory, a cell autonomous effect of *chairy2* disruption on *cath1* cannot be discounted. If the signals responsible for the induction or maintenance of *cath1* by an ectopic *gdf7*-positive organiser (demonstrated in Chapter 3) could be determined (likely to be Gdf7 itself or other Bmps expressed there), then these signals could be co-expressed with *chairy2ΔWRPW* to determine whether *cath1* could be rescued independent of endogenous *chairy2* levels.

Studies of the role of *hes* genes in the formation and maintenance of boundaries have indicated that the experimentally induced loss of *Hes* expression at these boundaries results in increased neurogenesis and the spread of neighbouring neurogenic genes into boundary regions (Geling et al., 2003; Geling et al., 2004; Ninkovic et al., 2005; Baek et al., 2006). In contrast, in my experiments, the ectopic expression of the proneural gene *cath1* was never observed in the *gdf7*-domain following electroporation with the *chairy2ΔWRPWv1-IRESeGFPm5* construct. Instead, the downregulation of *gdf7* is, at least in part, due to increased cell death in the electroporated domain caused by expression of *chairy2ΔWRPW,* in comparison with electroporation with the control CAβ-*GFP* construct (Figure 4-10). An explanation for the disparity between previous studies and this study may be that in the previous studies, Hes activity was removed from the outset, whereas here the loss of Hes function was induced acutely, after boundary formation. Early Hes activity may thus, during boundary formation or immediately afterwards, be required to prevent ectopic neurogenesis within the boundary, whereas later Hes activity may be required to maintain cells in an organiser-like state and prevent their ectopic cell death.

Overexpression of full length *chairy2* at the E4 roof plate epithelium – hindbrain neuroepithelium boundary had the same effect as expression of *chairy2ΔWRPW*. Both caused autonomous downregulation of *gdf7* and adjacent *cath1* expression (Figure 4-12), but also autonomous downregulation of *cyp26C1* at the roof plate boundary, and a non-autonomous loss of roof plate epithelial *cyp26C1* and *ttr* expression (Figure 4-14, 4-16, 4-17). One explanation for this is that the cHairy2ΔWRPW protein does not act in a dominant negative fashion and instead both cHairy2ΔWRPW and full length cHairy2 directly repress the expression of *gdf7*, *cath1* and *cyp26C1*. Hes proteins are repressor-type basic helix-loop-helix (bHLH) transcription factors and are known to actively mediate repression of gene expression through homodimerisation and the recruitment of Groucho/TLE co-repressors through their WRPW domain (Paroush et al., 1994; Fisher et al., 1996; Grbavec et al., 1998; Kageyama et al., 2008). However, Hes transcription factors can also passively repress transcription via heterodimerisation with activator-type bHLH transcription factors, a mechanism which does not require the WRPW domain (Dawson et al., 1995; Kageyama et al., 2007). Therefore cHairy2 ΔWRPW could still be a functional repressor even though it is missing the WRPW domain. However this explanation cannot explain the non-autonomous loss of *cyp26C1* and *ttr* expression in the roof plate epithelium adjacent to the electroporated roof plate epithelium – hindbrain neuroepithelium boundary. Instead an alternative explanation is favoured whereby the precise level of *chairy2* expression is important for the correct maintenance of the *gdf7*-positive boundary-organiser. In support of this, particular modes of expression of Hes1 correlate with the specification of cells, and the mode of Hes1

expression is regulated by an autoregulatory negative feedback loop (Takebayashi et al., 1994; Hirata et al., 2002; Baek et al., 2006; Shimojo et al., 2008). Therefore overexpression of full length *chairy2* could disrupt its own mode of expression and therefore its function in the maintenance of boundary cells, thereby also acting in a dominant negative manner.

Although *chairy2* expression is induced in the roof plate epithelium both at an experimentally derived interface between hindbrain roof plate epithelium and neuroepithelium (Figure 3-21, 3-22) and after ectopic expression of *delta1* in the roof plate epithelium (Figure 4-5), its ectopic expression in the roof plate epithelium is not sufficient to induce *gdf7* or upregulate *cyp26C1* expression there, as ectopic activation of Notch signalling by *delta1* is capable of doing. This implies that Notch activation by *delta1* in the roof plate epithelium induces other pathways in parallel to *chairy2* activation that are responsible for the induction *gdf7* expression. However, the lack of expansion of the roof plate boundary by *chairy2* overexpression in the roof plate epithelium could have been due to embryos being electroporated at E4 and assessed for effects at E5, rather than being electroporated at E3 and assessed for effects at E5.The lack of expansion of the roof plate boundary into the hindbrain neuroepithelium or the roof plate epithelium is also in contradiction with the findings of Baek et al. (2006), who find that misexpression of Hes1 in telencephalic compartments via retrovirus is sufficient to decrease cell proliferation rates and neurogenesis, both characteristics of boundary cells. However, they did not demonstrate the complete conversion of cells to boundary cells by the expression of boundary cell markers.

4.3.4 The roof plate epithelium – hindbrain neuroepithelium boundary signals to both the hindbrain neuroepithelium and the roof plate epithelium

In Chapter 3 I showed that the roof plate epithelium – hindbrain neuroepithelium boundary marked by *gdf7* expression signals to the hindbrain neuroepithelium to induce *cath1* expression in the adjacent neuroepithelium. In this chapter I have demonstrated that signals from the roof plate epithelium – hindbrain neuroepithelium boundary are also required to maintain *cyp26C1* expression (Figure 4-14) and maintain or induce *ttr* expression in the roof plate epithelium (Figure 4-16, 4-17), as the expression of these genes are lost non-autonomously when the roof plate epithelium – hindbrain neuroepithelium boundary is perturbed by the expression of *chairy2ΔWRPW* or the overexpression of full length *chairy2*. Therefore the roof plate boundary signals to both the hindbrain neuroepithelium and the roof plate epithelium to regulate gene expression.

Since *cyp26C1* expression is present in the roof plate epithelium at E4 (Figure 2-10) and electroporations were carried out at E4, it can be concluded that signals from the roof plate epithelium – hindbrain neuroepithelium boundary are required for the maintenance of

cyp26C1.As *ttr* expression starts at E4 in the chick fourth ventricle roof plate epithelium (Figure 2-9) it cannot be concluded whether induction or maintenance of *ttr* expression was perturbed by electroporations of the roof plate epithelium – hindbrain neuroepithelium boundary. To determine this, the roof plate epithelium – hindbrain neuroepithelium boundary of E5 chicken embryos could be electroporated with the *cHairy2ΔWRPWv2-IRESeGFPm5* or the *cHairy2-IRESeGFPm5* construct to determine if maintenance of *ttr* expression is specifically affected.

Interestingly, expansion of the roof plate epithelium – hindbrain neuroepithelium boundary, marked by expanded *gdf7* and high-level *cyp26C1* expression after ectopic *delta1* expression in the roof plate epithelium, did not induce ectopic *ttr* expression adjacent to it (Figure 4-7). This shows that although signals from the roof plate epithelium – hindbrain neuroepithelium boundary are necessary for the induction or maintenance of *ttr* expression in the E5 chick hindbrain roof plate epithelium, these signals are not sufficient to ectopically induce *ttr* expression in the E5 roof plate epithelium. This may represent a lack of competence of the E5 roof plate epithelium to respond to signals from an expanded roof plate boundary. Earlier manipulations, prior to E3, may therefore demonstrate an ability of the roof plate boundary to induce ectopic choroid plexus differentiation, although targeted electroporation of a small domain of the hindbrain roof plate at earlier stages represents a significant technical challenge.

ttr expression was downregulated within the roof plate epithelium domain of *delta1* overexpression. Thus activation of Notch signalling by *delta1* within the roof plate epithelium cell-autonomously downregulates choroid plexus epithelium differentiation. This may represent conversion of the roof plate epithelium to a roof plate boundary-cell fate, although this conversion could only have been partial as *gdf7* expression was not cell-autonomously induced in all electroporated roof plate epithelial cells (Figure 4-7 D – L). Alternatively, the loss of *ttr* expression could have been due to non-autonomous signals from an expanded roof plate epithelium – hindbrain neuroepithelium boundary. In Figure 4-7 D – F, this expanded boundary was marked by induced *gdf7* expression, however in Figure 4-7 G – L it is possible that a functional, expanded roof plate epithelium – hindbrain neuroepithelium boundary was induced by *delta1* expression in the roof plate epithelium, but a complete conversion of roof plate epithelial cells to a roof plate boundary cell fate was not achieved so *gdf7* was not ectopically expressed. By this hypothesis, the *gdf7*-positive boundary-organiser is required to induce or maintain *ttr* expression at a distance from it, but might repress its expression immediately adjacent to it, as illustrated in Figure 4-18. To test this, more refined electroporations of *delta1* into the roof plate epithelium – hindbrain

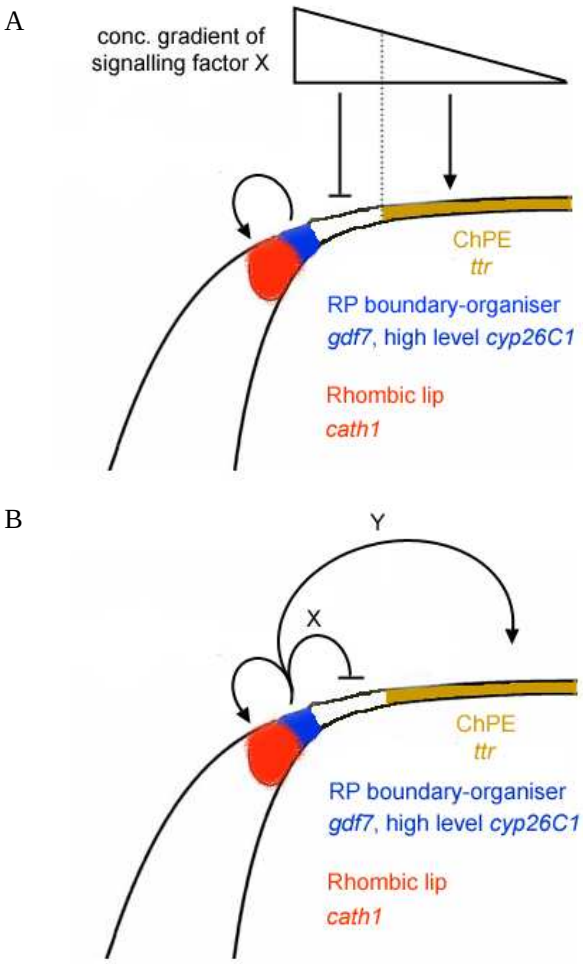

Figure 4-18 Models of how the roof plate boundary-organiser signals to both neuroepithelium and roof plate epithelium

Schematic of the roof plate (RP) epithelium – neuroepithelium boundary in a transverse section through the chick hindbrain. The RP boundary-organiser is marked by *gdf7* expression and high *cyp26C1* expression. The RP boundary-organiser signals to the adjacent neuroepithelium to maintain *cath1* expression in the rhombic lip (Chapter 3). One proposed model for how the RP boundary-organiser patterns the adjacent RP epithelium is that it expresses a signal (X), which exhibits a concentration gradient in the RP epithelium. At high concentrations this inhibits choroid plexus epithelium (ChPE) differentiation, but below a certain threshold it is required to promote or permit ChPE differentiation (A).

An alternative model (B) is that short range signals (X) from the RP boundary-organiser inhibit ChPE differentiation, but long range signals (Y) that can diffuse further than short range signals promote or permit ChPE differentiation.

neuroepithelium boundary could be carried out to test if a non-autonomous loss of *ttr* expression is ever observed adjacent to the electroporated domain.

Two models of how signals from the roof plate boundary could both inhibit *ttr* expression adjacent to it and promote *ttr* expression at a distance from it are presented in Figure 4-18. One signal from the roof plate boundary-organiser could be responsible for both inhibition and be required for *ttr* expression, if it is present in the roof plate epithelium in a concentration gradient away from the roof plate boundary. At high concentrations it would inhibit expression of *ttr*, but at low concentrations it would promote it. Alternatively the signals that inhibit and promote *ttr* expression could be different. Short range signals might mediate inhibition of *ttr* expression, but long range signals might be responsible for promotion of *ttr* expression.

Despite its importance, relatively little was known about the specification of the fourth ventricle choroid plexus epithelium. In mice it is known that most, if not all, of the hindbrain choroid plexus epithelium derives solely from *gdf7*-positive progenitor cells (Hunter and Dymecki, 2007), but whether mechanisms are required to specify and pattern the differentiation of the hindbrain roof plate epithelium into choroid plexus epithelium was not known. Here I demonstrate that non-autonomous signals from the roof plate epithelium – hindbrain neuroepithelium boundary are required for the development of the chick hindbrain choroid plexus epithelium and propose a model whereby signals from the roof plate epithelium – hindbrain neuroepithelium boundary are not only required to specify the choroid plexus epithelium, but also pattern the roof plate epithelium, inhibiting ectopic choroid plexus differentiation in the domain immediately adjacent to the roof plate epithelium – hindbrain neuroepithelium boundary. The function of this inhibition would likely be to reserve a domain of progenitors that would go on to contribute to choroid plexus epithelium growth throughout development. Such a domain has recently been demonstrated to exist in mouse embryos (Huang et al., 2009).

Chapter 5 Discussion

Studies that make up this thesis have shown that the chicken embryonic hindbrain roof plate can be divided into at least two domains, the roof plate epithelium and the roof plate boundaries. The organiser properties of the hindbrain roof plate are localised at the roof plate boundaries, which are marked by the expression of *gdf7* and high levels of expression of the chick *hes1* orthologues, *chairy1* and *chairy2*. A *gdf7*-positive domain can induce or maintain the expression of *cath1* in the adjacent hindbrain neuroepithelium of E4 – E6 chicken embryos. This *gdf7*-positive roof plate boundary is also required to non-autonomously maintain the roof plate epithelium-expressed *cyp26C1,* and permit the differentiation of the choroid plexus epithelium from roof plate epithelium, as assessed by *ttr* expression, in E5 brains. I have presented a model whereby signals from the roof plate boundary repress *ttr* expression immediately adjacent to it but promote *ttr* expression at a distance from it (Figure 4-18).

As part of this thesis I have also shown that tissue interactions between hindbrain roof plate epithelium and neuroepithelium can regenerate the *gdf7*-positive organiser in roof plate epithelium-derived tissue at the interface between the two tissues, shedding light on the mechanism that maintains the *gdf7*-positive organiser *in vivo*. The molecular basis of this interaction is likely to be largely mediated by Notch signalling as ectopic expression of *delta1* in the roof plate epithelium can induce a boundary-cell fate. This induction is likely to be via the *notch2* receptor. As further support for the role of activated Notch signalling at the roof plate boundary, *chairy1* and *chairy2,* which are upregulated in the roof plate boundary, are well-known downstream targets of Notch signalling (Jouve et al., 2000). *chairy2* was also induced by *delta1* expression in the roof plate epithelium and was induced in the roof plate epithelium at an experimental interface between roof plate epithelium and hindbrain neuroepithelium. The role of cHairy2 at the roof plate boundary was further investigated and it was found that overexpression of both a truncated version of cHairy2 (cHairy2ΔWRPW) and a full length version had dominant negative effects on the *gdf7*-positive roof plate boundary organiser, in line with observations in *hes1;hes3;hes5* triple-null mice that show that *hes* genes are required for the formation or maintenance of all boundary-localised organisers in the developing CNS (Baek et al., 2006).

Together my findings redefine the hindbrain roof plate organiser, confirm and extend an emergent consensus model for organiser characteristics and shed new light on how choroid plexus development is coordinated. Specifically, the roof plate appears to be another example of an organiser that is maintained by a well-conserved mechanism involving tissue

interactions that activate Notch signalling and downstream Hes transcription factors at boundaries.

5.1 Re-definition of the hindbrain roof plate organiser

For the most part the roof plate comprises a narrow strip of cells present at the dorsal midline of the developing vertebrate central nervous system (CNS), however at hindbrain level it is expanded to form a diamond-shaped epithelium that tents over the fourth ventricle (Chizhikov and Millen, 2005). The results of this thesis demonstrate that the E4 – E5 diamond-shaped roof plate should not be thought of as a single domain. In chick it can be separated into at least two different regions; a roof plate boundary, which is characterised by the expression of *gdf7* and high level *wnt1, cyp26C1, chairy1* and *chairy2* expression, and the roof plate epithelium that comprises the domain that lies between the two roof plate boundaries. The roof plate epithelium can be further subdivided into a lateral *cyp26C1*-positive, *ttr*-negative domain, a more medial *cyp26C1*-positive, *ttr*-positive domain, and an even more medial *cyp26C1*-negative, *ttr*-negative domain, at the ages when the choroid plexus epithelium is beginning to differentiate (E4 – E5). The subdivision of this domain indicates that the roof plate epithelium is patterned at these stages by various mechanisms that will be discussed later in this chapter.

I have presented several lines of evidence that suggest that the organiser properties of the chick hindbrain roof plate localise to the *gdf7*-positive boundaries. Signals from the *gdf7*-positive roof plate boundary are required for the maintenance of *cath1* expression in the adjacent neuroepithelium from E4 – E6. Furthermore, an induced *gdf7*-positive domain could rescue the loss of *cath1* expression in the rhombic lip, thus demonstrating that the *gdf7*-positive roof plate boundary is necessary and sufficient for the maintenance of *cath1* expression in the rhombic lip at these ages. An induced *gdf7*-domain could also induce *cath1* expression at an ectopic dorsoventral position within the hindbrain neuroepithelium from E4 to E5, raising the possibility that organiser properties resident at the roof plate boundary serve to pattern the dorsoventral axis of the hindbrain from the outset, inducing the expression of *cath1* in the rhombic lips. Indeed *gdf7* expression in the hindbrain begins at st14 (E2.5), preceding that of *cath1*, suggesting that the roof plate boundary differentiates prior to the specification of the *cath1*-positive progenitor pool.

chairy1 and *chairy2* are the chick orthologues of *hes1* (Jouve et al., 2000). High and persistent Hes1 expression has been shown to mark organisers such as the zona limitans intrathalamica (ZLI), the midbrain-hindbrain boundary and the spinal cord roof plate and floor plate in mouse (Baek et al., 2006). Therefore the persistent, elevated *chairy1* and

chairy2 expression at the chick hindbrain roof plate boundary and the lack of expression in the roof plate epithelium itself, from E4 to E6, supports the model that the roof plate organiser properties are localised to its boundaries.

Previous studies have presented a model of hindbrain roof plate as a homogenous signalling domain, required for the specification of the dorsal-most neural progenitor pool, which is marked by the expression of the bHLH transcription factor *math1* in mouse, or *cath1* in chick (Chizhikov et al., 2006). This is a reasonable assumption as, in the mouse, *gdf7* and another roof plate marker, the LIM-homeodomain transcription factor, *lmx1a*, are expressed both at the roof plate boundary and in the lateral roof plate epithelium at upper and lower rhombic lip levels at E10.5/ 11.5 (equivalent to E4/ E5 in chick) (Landsberg et al., 2005; Chizhikov et al., 2006; Mishima et al., 2009). However *gdf7* and *lmx1a* are both expressed in the roof plate boundary at a higher mRNA level than in the roof plate epithelium. Further, the roof plate boundary is also characterised by high level mRNA expression of *wnt1* at both upper and lower rhombic lip levels (Landsberg et al., 2005; Chizhikov et al., 2006; Mishima et al., 2009). Therefore although no specific marker of the hindbrain roof plate boundary has yet been identified in mouse, the roof plate boundary displays characteristic high-level mRNA expression of *gdf7*, *lmx1a* and *wnt1*. It is therefore likely that the boundary-localised organiser model proposed for the chick hindbrain roof plate may also apply to the mouse hindbrain roof plate at these stages.

The situation in zebrafish embryos also supports a distinction between the roof plate boundaries and the rest of the roof plate epithelium as *gdf6a/7* is expressed at the roof plate boundaries not by the entire hindbrain roof plate (Elsen et al., 2008; Chaplin et al., 2010).

5.2 Towards a general model for CNS organisers

A number of organisers in the developing CNS are found at boundaries between molecularly distinguishable compartments of tissue that they are responsible for patterning (Kiecker and Lumsden, 2005). Examples include the ZLI, which patterns the adjacent thalamus and pre-thalamus (Kiecker and Lumsden, 2004), the midbrain-hindbrain boundary, which patterns the adjacent midbrain and rhombomere 1 of the hindbrain (Wassef and Joyner, 1997), and rhombomere boundaries, which have been shown to pattern neurogenesis in adjacent rhombomeres in zebrafish (Riley et al., 2004). The chick hindbrain roof plate is now another example of an organiser that fits into this model, with its organiser properties being located at its boundaries with the neuroepithelium. The spinal cord roof plate might also fit into this model as it is composed of two *gdf7*-positive domains separated by a medial *gdf7*-negative domain, therefore its organiser properties might be localised to these *gdf7*-positive

'boundaries'. These discoveries raise the possibility that the roof plate at other anteroposterior locations must also be defined as a boundary-localised organiser located between molecularly distinguishable compartments. The ablation of the telencephalic roof plate via the expression of diphtheria toxin A subunit under the control of the *gdf7*-locus in mouse caused the reduction of *lhx2* expression and a decrease in cortical size, showing that the roof plate is required to signal to the lateral telencephalon for its proper development (Monuki et al., 2001). The telencephalic midline begins as a narrow medial roof plate domain located at the dorsal midline, but later invaginates forming three distinct regions (Monuki et al., 2001; Shinozaki et al., 2004). From most lateral to most medial these are the cortical hem, the choroid plexus epithelium and the roof plate epithelium (Shinozaki et al., 2004). These three domains express a range of signalling molecules belonging to the Wnt and Bmp family (Furuta et al., 1997; Lee et al., 2000b; Shinozaki et al., 2004), however a boundary-localised organiser domain equivalent to the *gdf7*-positive roof plate boundary of the chick hindbrain might be resident at the interface between the cortical hem and the choroid plexus domain. Whether such a boundary-localised signalling centre exists within the telencephalic roof plate has not been considered, although more recently focus has been placed on how the hem and the choroid plexus epithelium become established as separate domains that arise from the same primordium, and how the position of the border between these two domains is established (Currle et al., 2005; Yoshida et al., 2006; Louvi et al., 2007; Subramanian and Tole, 2009).

Boundary-localised organisers employ certain key mechanisms for their maintenance. Many have been demonstrated to show lineage restriction, which may be important in maintaining the organiser domain as a sharp, straight line (Fraser et al., 1990; Irvine and Rauskolb, 2001; Larsen et al., 2001; Zervas et al., 2004; Langenberg and Brand, 2005; Jimenez-Guri et al., 2010). Other mechanisms that are also widely employed to maintain neural boundary-localised organisers include Notch signalling across the boundary and the use of Hes transcription factors, which will be discussed below.

5.2.1 Activated Notch signalling

Activation of Notch signalling has been shown to be important for the formation and maintenance of a number of developmental boundary-localised organisers, not just within the developing vertebrate CNS. The classic example of this is the Drosophila wing where a stripe of Notch activation is required for the formation or maintenance of the dorsoventral boundary of the wing imaginal disc (Rulifson and Blair, 1995). The *notch* receptor itself shows widespread expression within the wing imaginal disc (Fehon et al., 1991), but a stripe of Notch activation at the border is brought about by the localised expression of the Notch ligands, *delta* and *serrate*, and the modulator of Notch signalling, *fringe*. *delta*, expressed

mainly in the ventral compartment, activates Notch signalling in dorsal boundary cells while *serrate*, which is only expressed in the dorsal compartment, activates Notch signalling in ventral boundary cells (Diaz-Benjumea and Cohen, 1995; Doherty et al., 1996). This activation of Notch signalling is restricted to the dorsoventral boundary by the action of *fringe*, which is also expressed in the dorsal compartment and modulates the signalling efficiency of the Notch receptor causing the cell-autonomous inhibition of Serrate – Notch signalling, but potentiation of Delta-Notch signalling (Figure 5-1 A) (Fleming et al., 1997; Panin et al., 1997).

Strikingly similar situations have also been described for the midbrain-hindbrain boundary (MHB) in the chick and the zebrafish rhombomere boundaries. At the chick MHB *serrate1* and activated Notch signalling are necessary and sufficient to determine the positioning of formation of the midbrain – hindbrain boundary, as assessed by its nascent signalling molecules (*wnt1* and *fgf8*) (Tossell et al., 2011). *serrate1* is expressed both anterior and posterior to the MHB, although it is excluded from the isthmic constriction itself and rhombomere 1. *lfng* (a homologue of Drosophila *fringe*) is expressed in the same domain as *serrate1* and is also sufficient to re-define the position of MHB formation (Tossell et al., 2011). The expression of *delta1* differs from that of *serrate1* in that it is upregulated posterior to the MHB in rhombomere 1, although its specific role in MHB formation has not yet been investigated (Figure 5-1 B) (Tossell et al., 2011).

Delta- Notch signalling is required for the maintenance of the zebrafish rhombomere boundaries, as assessed by the expression of various boundary-marker genes, including the signalling molecule *wnt1* (Cheng et al., 2004; Riley et al., 2004). *rfng* (another homolog of Drosophila *fringe*) is expressed by rhombomere boundary cells and is required for *wnt1* expression in the boundary cells (Cheng et al., 2004). The zebrafish *delta* homologs, *deltaA*, *deltaB* and *deltaD* are expressed in transverse stripes flanking rhombomere boundaries and thus mediate the activation of Notch signalling at the rhombomere boundaries (Cheng et al., 2004; Riley et al., 2004). Thus the action of *rfng* in zebrafish may differ from the action of *fringe* and *lfng* in Drosophila and chick respectively, as it shows complementary rather than coincident expression with the expression of Notch ligands. Therefore *rfng* may act to potentiate Delta-mediated Notch signalling, rather than act to restrict the domain of Notch activation to boundaries (Figure 5-1 C).

The floor plate is an organiser present at the ventral midline of the developing CNS. Although it does not strictly fit into the boundary-localised organiser model as it is a boundary between molecularly indistinguishable compartments, it is another example of an organiser that requires Notch signalling for its maintenance (Bingham et al., 2003; le Roux et

al., 2003). Loss of Notch signalling resulted in ectopic neurogenesis of the floor plate in both zebrafish and chick (Bingham et al., 2003; le Roux et al., 2003).

In this thesis I determined that *delta1* expression in the roof plate epithelium can convert roof plate epithelium cells to a roof plate boundary cell fate, as determined by the expression of *gdf7*, *chairy2* and elevated *cyp26C1* expression. This is likely to reflect an *in vivo* mechanism of maintenance of the roof plate boundary whereby *delta1*, expressed in the hindbrain neuroepithelium, signals via *notch2*, expressed in the roof plate, to activate notch signalling and maintain the identity of the roof plate boundary-organiser (Figure 5-1 D). In similarity with the dorsoventral boundary of the Drosophila wing imaginal disc and the midbrain-hindbrain boundary of the chick, Notch activation is sufficient to re-specify compartment cells as boundary cells (Kim et al., 1995; Doherty et al., 1996; Fleming et al., 1997; Tossell et al., 2011). Interestingly, this is not the case for zebrafish rhombomere boundaries. Notch activation was not sufficient to re-specify rhombomere compartment cells as rhombomere boundary cells implying that other mechanisms might be involved in their formation (Cheng et al., 2004). One difference between the above examples and the chick roof plate boundary is that, for the above examples, the Notch ligands are expressed on both sides of the boundary, activating Notch signalling in boundary cells immediately adjacent to the boundary (Doherty et al., 1996; Cheng et al., 2004; Tossell et al., 2011). In contrast, signalling to induce *gdf7*-expression appears to be unidirectional as the recombination of roof plate epithelium and hindbrain neuroepithelium only induces *gdf7* expression in roof plate epithelium-derived cells. Further, the Notch ligands, *delta1* and *serrate1* were only expressed on the neuroepithelial side of the roof plate boundary, although the expression of other Notch ligands such as *serrate2* has not yet been assessed (Figure 5-1).

In Drosophila a boundary between *fringe*-expressing and non-expressing cells positions the dorsoventral boundary of the wing imaginal disc (Irvine and Wieschaus, 1994). In chick, boundaries between *lfng*-expressing and non-expressing cells regulate the formation of the ZLI and the MHB, and boundaries between *rfng*-expressing and non-expressing cells regulate the formation of the apical ectodermal ridge of the limb bud (Laufer et al., 1997; Rodriguez-Esteban et al., 1997; Zeltser et al., 2001). Studies in this thesis show that the roof plate boundary is also located at the boundary between *lfng*-expressing and non-expressing cells. Whether *lfng* plays a role in the restriction of Notch activation to the *gdf7*-domain, as *fringe* does in Drosophila (Panin et al., 1997), remains to be determined. In Drosophila, *fringe* has been shown to potentiate Delta – Notch signalling, while inhibiting Serrate – Notch signalling, however in chick somitogenesis, Lfng inhibits Delta – Notch signalling (Dale et al., 2003). Thus the role of *fringe* and its homologues is species dependent. Its action in vertebrates is also context-dependent, as it has been shown that Lfng has different

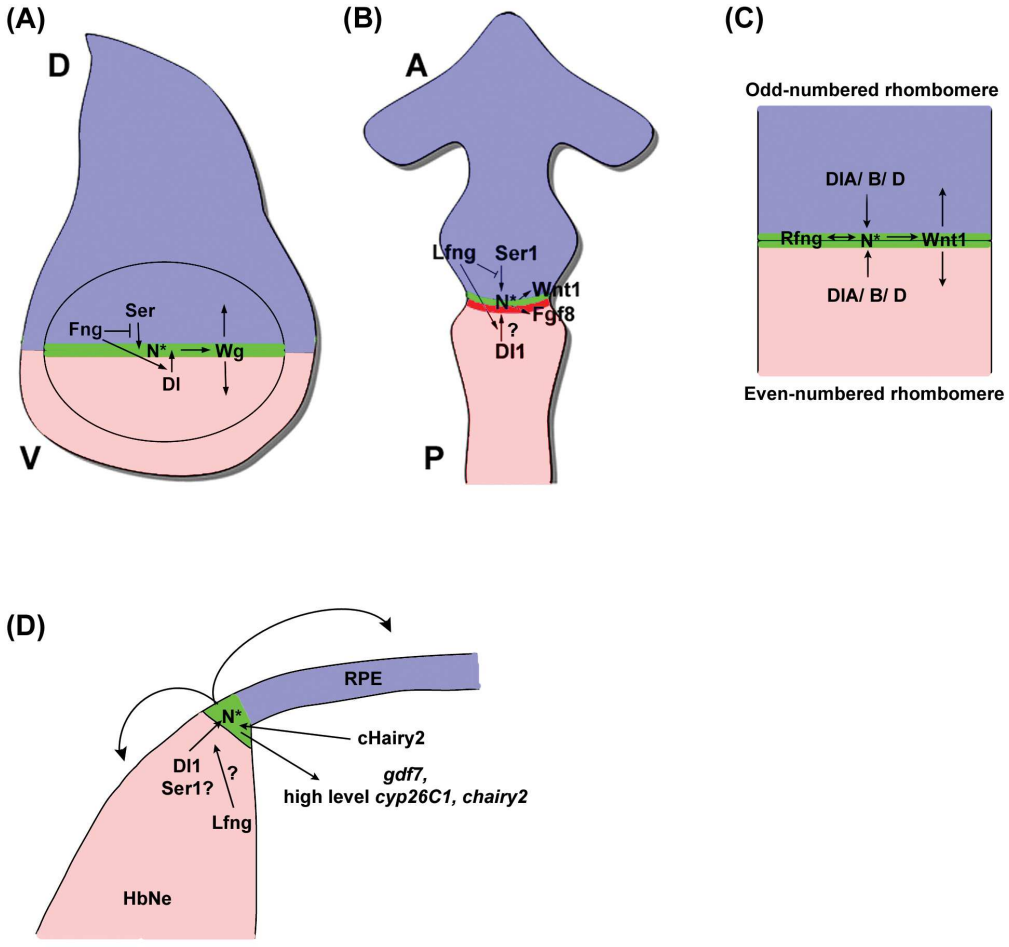
(A)
D
V
Ser
Fng
N*
Wg
Dl
(B)
A
P
Lfng
Ser1
N*
Wnt1
Fgf8
?
Dl1
(C)
Odd-numbered rhombomere
DlA/ B/ D
Rfng
N*
Wnt1
DlA/ B/ D
Even-numbered rhombomere
(D)
RPE
N*
cHairy2
Dl1
Ser1?
?
Lfng
gdf7,
high level cyp26C1, chairy2
HbNe

Figure 5-1 Schematic diagrams of Notch activation at boundary-localised organisers

(A) and (B) modified from (Tossell et al., 2011).

(A) Notch is activated (N*) at the dorsoventral boundary of the Drosophila wing imaginal disc by the concerted actions of Serrate (Ser) and Delta (Dl). Ser activates Notch in ventral boundary cells and Dl activates Notch in dorsal boundary cells. Fringe (Fng) is only expressed in the dorsal compartment and restricts Notch activation to the boundary by inhibiting activation of Notch by Ser but potentiating the activation of Notch by Dl. Notch activation induces Wingless (Wg) expression. Wg patterns the wing primordium. D, dorsal; V, ventral.

(B) Model of signalling at the chick midbrain-hindbrain boundary (MHB). Serrate1 (Ser1) and Lfng are expressed abutting the anterior (A) border of the MHB. Ser1 is proposed to activate Notch signalling (N*) at the MHB, which is sufficient to induce Wnt1 expression and re-position Fgf8 expression. Delta1 (Dl1) is expressed posterior (P) to the MHB so may contribute to the positioning of the stripe of Notch activation.

(C) At zebrafish rhombomere boundaries, DeltaA, DeltaB and DeltaD (DlA/ B/ D) are expressed adjacent to the boundaries. Delta-Notch signalling is required to activate Notch (N*) at boundaries and maintain expression of Rfng and Wnt1. Rfng is also required for boundary maintenance. Wnt signals are required to organise neurogenesis within rhombomeres.

(D) Model of chick hindbrain roof plate boundary maintenance. Delta1 (Dl1) is expressed in the hindbrain neuroepithelium (HbNe) and signals to the roof plate to activate Notch (N*) at the roof plate boundary and maintain *gdf7* and high-level *cyp26C1* and *chairy2* expression. Serrate1 and Lfng are also expressed in the HbNe but their roles have not yet been determined. cHairy2 function is required to maintain the roof plate boundary. The roof plate boundary signals to the HbNe and the RPE.

effects depending on which Notch receptor Delta1 and Jagged1 (the mouse homolog of Serrate1) are signalling through in mouse (Hicks et al., 2000). Therefore the specific role of Lfng at the chick roof plate boundary must be investigated in terms of its effects on Delta and Serrate signalling through the Notch2 receptor.

Studies of the chick hindbrain roof plate boundary therefore provide further evidence that activated Notch signalling is a highly conserved mechanism involved in the formation or maintenance of boundary-localised organisers within epithelia. It will be interesting to see if it is also involved in the formation or maintenance of other potential boundary-localised organisers, such as the telencephalic cortical hem – choroid plexus epithelium boundary.

5.2.2 Hes transcription factors

The Hes family of transcription factors has been shown to be important for the formation or maintenance of neural organisers in mouse and in zebrafish. Baek et al. (2006) showed that in *hes1;hes3;hes5* triple-null mice the midbrain-hindbrain boundary, ZLI, spinal cord roof plate and floor plate are not formed properly, as assessed by the expression of their nascent signalling molecules (*wnt1, fgf8* and *shh*). The loss of these organisers is coincident with ectopic neurogenesis within the organiser domains, although Baek et al. (2006) do not establish whether the *hes* transcription factors are required for the formation or maintenance of the organisers. However, Hirata et al. (2001) show that *hes1* and *hes3* are specifically required for the maintenance of the midbrain-hindbrain boundary in mice, and that the loss of this organiser also coincides with ectopic neurogenesis.

In zebrafish the *hairy/ enhancer of split* related genes *her5* and *him* have been shown to be required for the maintenance of the MHB, preventing the expression of proneural genes and ectopic neurogenesis there (Geling et al., 2003; Geling et al., 2004; Ninkovic et al., 2005). In similarity with the functions of *hes1* and *hes3* at the mouse MHB, *him* and *her5* are not required for the initial specification of the MHB, as determined by the expression of MHB markers such as *wnt1* and *fgf8* (Geling et al., 2003; Ninkovic et al., 2005).

In this thesis I have established that the chick *hes1* orthologues, *chairy1* and *chairy2* are upregulated at the hindbrain roof plate boundary from E4 – E6 and that the correct level of *chairy2* expression is required for the maintenance of the *gdf7*-positive roof plate boundary-organiser (as assessed by the loss of expression of *cath1* in the adjacent neuroepithelium and *cyp26C1* and *ttr* in the adjacent roof plate epithelium) (Figure 5-1 D). *chairy1* may also play a role in the maintenance of this boundary, although its expression was not induced in the roof plate epithelium at an experimental hindbrain roof plate epithelium – neuroepithelium boundary, so its role was not investigated. In zebrafish, the overexpression of *her5* is not sufficient to expand the MHB domain (Geling et al., 2003). Similarly, the overexpression of

chairy2 across the roof plate epithelium – hindbrain neuroepithelium boundary did not expand the *gdf7*-positive domain, implying that it is not sufficient to induce ectopic *gdf7*-positive roof plate boundary cells. This is in contrast with the result of overexpression of *hes1* in the mouse telencephalon, which results in reduced neurogenesis and cell proliferation, characteristic properties of boundary-localised organisers (Baek et al., 2006). However Baek et al. (2006) did not demonstrate the complete conversion of compartment cells to boundary cells by the expression of boundary cell markers. Therefore it is likely that *hes* genes do not drive the initial formation of boundary-localised organisers but instead are only required for their maintenance.

The above studies show that the loss of *hes* genes at boundaries coincides with ectopic expression of neighbouring neurogenic genes within boundary regions (Geling et al., 2003; Geling et al., 2004; Ninkovic et al., 2005; Baek et al., 2006). The ectopic expression of the proneural gene *cath1* was never observed in the *gdf7*-domain following perturbation of cHairy2 function, therefore ectopic neurogenesis is not the cause of the loss of this organiser. Instead, the downregulation of *gdf7* is likely to be due, at least in part, to cell death. An explanation for the disparity between previous studies and this study may be that in previous studies, Hes activity was removed from the outset, whereas here Hes function was perturbed after boundary formation. Early Hes activity during boundary formation or immediately afterwards may thus be required to prevent ectopic neurogenesis within the boundary, whereas later Hes activity may be required to maintain cells in an organiser-like state and prevent their ectopic cell death.

Hes genes are well known downstream effectors of Notch signalling (Ohtsuka et al., 1999; Kageyama et al., 2007), however the inhibition of proneural gene expression at the MHB by *her5* in zebrafish has been shown to be Notch-independent (Geling et al., 2004). Here I demonstrate that *chairy2* is induced by activated Notch signalling in the roof plate epithelium, and is therefore likely to be required downstream of Notch signalling for the maintenance of the *gdf7*-positive roof plate boundary. This suggests that the requirement for *hes* genes for the formation or maintenance of the ZLI, MHB and spinal cord roof plate and floor plate in the mouse, described by Baek et al. (2006), might also be downstream of Notch signalling. It will be interesting to see if other boundary-localised organisers such as the zebrafish rhombomere boundaries that have been shown to require Notch signalling for their maintenance (Cheng et al., 2004; Riley et al., 2004) also require downstream *hes* transcription factors.

In this thesis I also documented how *chairy2* shows upregulated expression at the floor plate boundaries from E4 – E6 in chick. This raises the possibility that the organiser properties of

the floor plate are also localised to its boundaries and therefore the floor plate might fit with the boundary-localisation model for organisers where organisers are localised at boundaries between molecularly-distinguishable compartments. Indeed Notch signalling has already been shown to be required for the maintenance of the floor plate in chick and in zebrafish (Bingham et al., 2003; le Roux et al., 2003), however whether this represents an interaction between a medial floor plate domain and the neuroepithelium adjacent to the floor plate, or whether it represents signalling from the ventral neuroepithelial to the entire floor plate remains to be determined.

5.2.3 Tissue interactions – other signalling pathways?

Tissue interactions between compartment tissues have been shown to induce the formation of boundaries at their interface, such as the rhombomere boundaries, the ZLI and the MHB (Guthrie and Lumsden, 1991; Heyman et al., 1995; Irving and Mason, 1999; Guinazu et al., 2007). Activated Notch signalling has been shown to be upstream of the positioning of the MHB *in ovo* in chick and it has been suggested that Notch signalling might also mediate the formation of the ZLI at the interface between the pre-thalamus and the thalamus, due to the requirement for the Notch signalling modulator *lfng* (Zeltser et al., 2001; Tossell et al., 2011). Indeed the Notch ligands, *delta1* and *serrate1* are expressed abutting the prospective ZLI territory, however a role for Delta- Notch or Serrate-Notch interactions in the formation of the ZLI has not been formally tested (Zeltser et al., 2001). However, in the Drosophila wing imaginal disc it has been shown that *fringe* can influence dorsoventral compartmentalisation of cells in an environment of constitutively active Notch signalling (Rauskolb et al., 1999). Therefore *fringe* and its homologues may also be involved in Notch-independent pathways to influence boundary formation.

Notch signalling is required for the maintenance of rhombomere boundaries in zebrafish but is not sufficient to induce their formation (Cheng et al., 2004; Riley et al., 2004). Instead, interactions between Eph receptors and ephrin ligands, which are expressed in a complementary pattern in odd and even-numbered rhombomeres (Xu and Wilkinson, 1997), have been shown to mediate the cell sorting that occurs between odd and even-numbered rhombomeres (Guthrie et al., 1993; Wizenmann and Lumsden, 1997; Mellitzer et al., 1999; Xu et al., 1999), and the loss or disruption of EphA4 function results in a disruption of rhombomere boundaries (Xu et al., 1995; Cooke et al., 2005). These studies indicate that a signalling pathway other than the Notch signalling pathway is involved in the formation of this boundary-organiser, although Eph-ephrin signalling has not yet been shown to be sufficient to induce boundary formation.

In my studies of the regeneration of the roof plate boundary-organiser at the interface between hindbrain roof plate epithelium and neuroepithelium, it was seen that *gdf7* expression could be induced by an interaction between the roof plate epithelium and any part of the hindbrain neuroepithelium, along the dorsoventral axis, including the floor plate. Ligand-driven Notch signalling robustly induces *gdf7* in the roof plate epithelium, however neither *delta1* nor *serrate1* are expressed by the floor plate at these stages (this study and Myat et al. (1996)). This implies that either other Notch ligands such as *serrate2* are expressed in the floor plate, or a signalling pathway other than the Notch signalling pathway, such as the Eph-ephrin pathway, is also involved in the induction and maintenance of the *gdf7*-positive organiser. It will be interesting to see if this is indeed the case.

5.2.4 Lineage restriction

As mentioned above, the ZLI, MHB and rhombomere boundaries have all been shown to demonstrate lineage restriction (Fraser et al., 1990; Irvine and Rauskolb, 2001; Larsen et al., 2001; Zervas et al., 2004; Langenberg and Brand, 2005; Jimenez-Guri et al., 2010). At the roof plate – rhombic lip interface, genetic fate maps in mouse demonstrate that *math1*-positive progenitors only ever give rise to neurons, while *gdf7*-positive progenitors only contribute to the roof plate and choroid plexus epithelium (Landsberg et al., 2005; Machold and Fishell, 2005; Wang et al., 2005; Hunter and Dymecki, 2007). Therefore a molecular lineage restriction boundary exists at this interface. However, whether a *math1*-negative, *gdf7*-negative progenitor cell with the potential to give rise to either neurons or roof plate exists at this interface has not yet been tested. Evidence for this idea comes from evidence of fate switches between the two lineages when *lmx1a* or *math1* is lost. Lmx1a is expressed predominantly in the hindbrain roof plate epithelium and roof plate boundary, but is also expressed in the rhombic lip in both Math1-positive and -negative cells (Chizhikov et al., 2010). In *lmx1a* -/- mice there is a loss of choroid plexus epithelial cells and a compensatory ectopic contribution of roof plate cells (cells derived from *gdf7*-positive progenitors) to the deep cerebellar nuclei, which normally derive from the Math1-positive rhombic lip (Machold and Fishell, 2005; Wang et al., 2005; Chizhikov et al., 2010). Conversely, in *math1* null mice, cells that have lost functional Math1 ectopically contribute to the choroid plexus epithelium (Rose et al., 2009a). These results show that cells exist at the roof plate – rhombic lip interface that have the potential to become both choroid plexus epithelium or rhombic lip- derived neurons, implying that there is no physical lineage restriction at the roof plate – rhombic lip interface. Single-cell labelling experiments will enable the investigation of whether a single progenitor gives rise to neurons and non-neuronal roof plate/ choroid plexus epithelium in the wild-type situation.

In parallel with the above, a fate switch between neural and non-neuronal cells at the dorsal telencephalic midline has been shown to be regulated by *hes* genes. At the telencephalic dorsal midline the cortical hem, which gives rise to Cajal-Retzius neurons, is situated adjacent to the non-neuronal choroid plexus epithelium (Takiguchi-Hayashi et al., 2004; Yoshida et al., 2006; Imayoshi et al., 2008) In mice where *hes1*, *hes3* and *hes5* are inactivated in the dorsal telencephalon there is a loss of choroid plexus epithelium and a compensatory increase in Cajal-Retzius cell formation (Imayoshi et al., 2008). This implies that the telencephalic choroid plexus epithelium – cortical hem boundary is also not a strict lineage restriction boundary. Therefore both the hindbrain and telencephalic roof plate – neuroepithelium boundaries are likely to be maintained by genetic mechanisms rather than physical boundaries to cells mixing.

5.2.5 Roof plate organiser formation

My studies show that tissue interactions, Notch signalling and Hes transcription factors are involved in the maintenance of an established *gdf7*-positive organiser in the hindbrain. This leads to a number of questions about how the *gdf7*-positive boundary is established in the first place.

Notch signalling has been shown to be upstream of the formation of the MHB in chick, marked by the expression of *fgf8*, *wnt1* and *fgf3* (Tossell et al., 2011). The expression of *delta1* in the roof plate epithelium is sufficient to induce roof plate boundary marker expression at E5 *in ovo*. Therefore it would be interesting to see if Notch signalling is required for the initial formation of the *gdf7*-positive roof plate boundary that is established at E3. As mentioned above, the overexpression of *chairy2* at the roof plate epithelium – hindbrain neuroepithelium boundary was not sufficient to induce an expansion of the roof plate boundary domain at E5, therefore it is likely that *chairy2* is not involved in the initial formation of the boundary but is involved in the maintenance of the roof plate boundary after its formation.

The hindbrain roof plate epithelium could represent an expanded version of the *gdf7*-negative domain present at the midline of the spinal cord roof plate, but this raises the question of how this *gdf7*-negative domain is specified. One could hypothesise that this *gdf7*-negative domain represents a piece of non-neural ectoderm inserted at the dorsal midline of the neural tube upon neurulation (similar to the proposed insertion of organiser/ node-derived mesendoderm into the neural plate to form the floor plate (Le Douarin and Halpern, 2000)). Perhaps markers of epidermal ectoderm could be used to assess any contribution of this tissue to the neural tube upon neurulation. It is important to note that in zebrafish and regions of the posterior spinal cord, neural tube formation occurs via cavitation of a solid rod

of tissue (Lowery and Sive, 2004). Therefore mechanisms other than the one proposed above must come into play to specify a midline roof plate domain in these regions.

5.2.6 Beyond the CNS – a generalised model for organisers?

The striking conservation of the use of tissue interactions, Notch signalling and Hes transcription factors for the maintenance of not only neural organisers, but other epithelial organisers such as the apical ectodermal ridge of the vertebrate limb bud or the dorsoventral boundary of the Drosophila wing imaginal disc raises the possibility that this set of mechanisms represents a conserved cassette that might be employed by other localised organisers in embryonic development. Perhaps all secondary organisers are localised to boundaries between molecularly distinguishable compartments of tissue as this reflects their requirement for tissue interactions between adjacent compartments for their maintenance.

In striking homology with the hindbrain roof plate boundary, *gdf5/6/7* are expressed at sites of joint formation in the developing mammalian skeleton (Storm and Kingsley, 1996; Francis-West et al., 1999; Settle et al., 2003) and *math1* expression marks epiphyseal chondrocytes that are located adjacent to joint interzones and are destined to become articular chondrocytes (Ben-Arie et al., 2000; Pacifici et al., 2000). *gdf5* is the most extensively expressed member of the *gdf5/6/7* group, being expressed in every developing joint of the limbs of mouse embryos, and is therefore the best studied (Storm and Kingsley, 1996). The overexpression of Gdf5 causes cartilaginous overgrowth and inhibits joint formation in the developing chick and mouse limbs (Francis-West et al., 1999; Merino et al., 1999; Storm and Kingsley, 1999). The effect of Gdf5 on cartilaginous growth is thought to occur via both recruitment of mesenchymal cells to the chondrocyte lineage at early stages and stimulation of epiphyseal chondrocyte proliferation and accelerated differentiation at later stages (Francis-West et al., 1999; Tsumaki et al., 1999). Conversely, loss of *gdf5* caused a reduction in cartilage markers, but a spreading of joint markers in the digit region of mice, reminiscent of the reported role of *wnt1* in the restriction of boundary-marker expression at the zebrafish rhombomere boundaries (Storm and Kingsley, 1999; Amoyel et al., 2005).

In Drosophila, as in the dorsoventral boundary of the wing imaginal disc, activated Notch signalling demarcates boundaries between future leg segments (de Celis et al., 1998). Activated Notch signalling is further necessary and sufficient for the formation of joints between leg segments (de Celis et al., 1998). The loss of joints by the clonal inhibition of Notch signalling was autonomous, however there was also a non-autonomous effect on the growth of leg segments. Therefore, analogous to the situation in the Drosophila wing, the formation of leg segment boundaries was required to direct the growth of the adjacent leg segments (Diaz-Benjumea and Cohen, 1995; Kim et al., 1995; de Celis and Bray, 1997). In

contrast however, Delta and Serrate do not activate Notch signalling from either side of the boundary. Rather Notch signalling activation is asymmetric with Delta and Serrate expressed in a stripes of cells adjacent and proximal to the ring of cells showing activated Notch signalling (Diaz-Benjumea and Cohen, 1995; Doherty et al., 1996; de Celis et al., 1998; Bishop et al., 1999). These ligands are required in composite for correct leg segmentation (Parody and Muskavitch, 1993; de Celis et al., 1998; Bishop et al., 1999).

Notch receptors and ligands show restricted domains of expression in developing joint regions of the avian limb (Williams et al., 2009). However, despite its conserved role in specifying boundary cells and its role in segmentation of Drosophila legs, the role of activated Notch signalling in the segmentation of vertebrate skeletal elements has not yet been investigated. Given my findings that Delta-mediated activation of Notch signalling lies upstream of *gdf7* expression at the hindbrain roof plate boundary of chick embryos, it would be interesting to see if Notch signalling is involved in the localisation of expression of *gdf5/6/7* at future skeletal joint locations in chick and mice. Analogous to the situation in the hindbrain, these domains of *gdf5/6/7* expression might then signal to adjacent *math1*-expressing epiphyseal chondrocytes to direct their proliferation or differentiation.

5.3 Choroid plexus development

The choroid plexuses are a series of interfaces that form at the roof of the lateral, third and fourth ventricles of the vertebrate brain, forming part of the blood-brain barrier (Dziegielewska et al., 2001). They are responsible for the secretion of cerebrospinal fluid (CSF) and thus the regulation of the internal environment of the brain during embryogenesis and in the adult (Redzic et al., 2005). Despite their vital function little is currently known about how the development of the choroid plexuses is coordinated.

5.3.1 Choroid plexus epithelium development

The choroid plexus is comprised of two components; the choroid plexus epithelium and the heavily vascularised choroidal stroma. The choroid plexus epithelium of the fourth ventricle mouse choroid plexus has been shown to derive mostly, if not completely from *gdf7*-positive progenitors (Currle et al., 2005; Landsberg et al., 2005; Hunter and Dymecki, 2007). Mitotic events in the choroid plexus epithelium are rare (Knudsen, 1964; Sturrock, 1979; Hunter and Dymecki, 2007), therefore choroid plexus epithelium cells are likely to differentiate directly from roof plate epithelium cells, which in turn are derived from progenitors situated at the *wnt1*-positive, *gdf7*-positive roof plate boundary (Awatramani et al., 2003; Currle et al., 2005; Landsberg et al., 2005; Hunter and Dymecki, 2007). However, from E12.5 throughout the rest of development in mice, a lateral roof plate progenitor domain, which includes the

roof plate boundary, can give rise to choroid plexus epithelium directly (Hunter and Dymecki, 2007; Huang et al., 2009). Whether this proliferative domain also includes an equivalent of the lateral *ttr*-negative, *cyp26C1*-positive domain of E4 chick embryos, remains to be determined. In the telencephalon, *gdf7*-positive progenitors only give rise to the anterior portion of the choroid plexus epithelium, however the posterior portion requires non-autonomous signals from the anterior portion for its formation (Currle et al., 2005). This highlights a non-autonomous patterning mechanism required for the formation of choroid plexus epithelium.

Other than the above lineage studies, little work has been done to identify the mechanisms that induce choroid plexus differentiation from roof plate epithelium. It has been suggested that insulin-like growth factor II, which is expressed in the overlying mesenchyme prior to and during choroid plexus morphogenesis, might play a role (Cavallaro et al., 1993). However, Wilting and Christ (1989) showed that the prospective telencephalic choroidal stroma of chick embryos could not induce the differentiation of choroid plexus epithelium from grafted non-choroid plexus-forming dorsal neuroepithelium of quail embryos. In contrast, prospective choroid plexus epithelium from quail embryos both differentiated into choroid plexus epithelium and induced the differentiation of choroid plexus-typical capillaries from non-choroid plexus-forming mesenchyme. These experiments highlighted the early specification of choroid plexus epithelial cells (at E2 – 3) and the inability of choroidal stroma to induce the differentiation of choroid plexus epithelium. Studies in mice have also shown that the choroid plexus epithelium is specified this early (at E8.5, equivalent to E2 in chick) (Thomas and Dziadek, 1993). These studies, together with the results of the lineage studies in mice that show that most, if not all, of the hindbrain choroid plexus epithelium is derived from *gdf7*-positive progenitors, might lead one to conclude that all progeny of *gdf7*-expressing cells are fated to give rise to choroid plexus epithelium and do not require inductive signals. However, in the mouse telencephalon this is not the case (Currle et al., 2005), and in this thesis I have demonstrated that inductive signals from the roof plate boundary are required for hindbrain choroid plexus epithelium development.

In my studies I found that signals from the roof plate boundaries of the fourth ventricle are required for the non-autonomous induction or maintenance of choroid plexus epithelium differentiation (Figure 4-18). The expansion of the roof plate boundary via activation of Notch signalling in the roof plate epithelium did not non-autonomously alter the pattern of choroid plexus epithelium differentiation, therefore I have not demonstrated that the roof plate boundary is sufficient to induce differentiation of the choroid plexus epithelium. Embryos were manipulated at E3 and incubated until E5. Choroid plexus epithelium differentiation begins at E4, however the above manipulations first required the induction of

roof plate boundary by *delta1*-mediated Notch activation in the roof plate epithelium, and a subsequent effect of this induced boundary on adjacent roof plate epithelial cells. Therefore manipulations at E3 may have been too late to have any inductive effects on choroid plexus epithelium differentiation. Perhaps earlier manipulations or assessment of embryos at a later time point would show that choroid plexus epithelial cells are induced by an expanded roof plate boundary.

Although no induction of choroid plexus epithelial cells by an ectopic roof plate boundary was seen, a loss of choroid plexus epithelial cells adjacent to an expanded roof plate boundary domain was seen, within the domain of Notch activation. This could be a result of Notch activation in the roof plate epithelium directly causing downregulation of *ttr* expression, although this is unlikely as the expression of the constitutively active Notch1-intracellular domain (ICD) under the control of the *gdf7* locus in mouse causes a massive expansion of *ttr*-positive choroid plexus epithelium (Hunter and Dymecki, 2007). Instead a different model is favoured whereby signals from the expanded roof plate boundary signal to the immediately adjacent roof plate epithelium to inhibit *ttr* expression (Figure 4-18). A *ttr*-negative but *cyp26C1*-positive domain adjacent to the roof plate boundary exists in the E4 wild-type chick embryo. What might be the function of this lateral *ttr*-negative domain? In mouse embryos, a proliferative, *shh*-responsive domain at the lateral edges of the choroid plexus epithelium is required to contribute to the growth of the choroid plexus epithelium from E12.5 throughout development (Huang et al., 2009). Therefore the lateral *ttr*-negative domain in chick might represent a reserved, undifferentiated pool that will be required later to proliferate and contribute directly to choroid plexus epithelium growth. Further work is required to determine if a *shh*-responsive, lateral, proliferative domain does indeed exist in chick embryos and if it is derived from the *cyp26C1*-positive, *ttr*-negative domain present at E4.

My finding that ligand-driven Notch signalling in the roof plate epithelium induces roof plate boundary fate offers new insights into the phenotype of *gdf7::cre; R26::stop-notch1-ICD* mice (Hunter and Dymecki, 2007). In these mice an expanded choroid plexus epithelium was largely *ttr*-positive at postnatal day 7 (P7) and at P0 only 20% of choroid plexus epithelium cells were proliferative. Therefore the forced expression of *notch1-ICD* in *gdf7*-positive progenitors did not simply result in symmetric proliferative cell divisions. In light of my findings one might hypothesise that expression of *notch1-ICD* induced a roof plate boundary fate, which is part of the *shh*-responsive proliferative domain that gives rise to differentiated choroid plexus epithelial cells through development (Huang et al., 2009). It would be interesting to see if the phenotype of *gdf7::cre; R26::stop-notch1-ICD* mice is augmented by

activated *shh* signalling, such as by the expression of constitutively active Smoothened, an essential component of Hedgehog signalling (Huang et al., 2009).

Whether Notch signalling is involved in the maintenance of a hindbrain roof plate boundary that is required for the induction or maintenance of choroid plexus epithelium in other vertebrates remains to be determined. However, clues come from studies of zebrafish choroid plexus development that show that global inhibition of Delta – Notch signalling results in malformations of the fourth ventricle choroid plexus epithelium, as it exceeds its anteroposterior and mediolateral bounds (Bill et al., 2008; Garcia-Lecea et al., 2008). Whether this was an autonomous or non-autonomous role of Notch signalling, however, remains to be determined.

The presence of an organiser at the boundary between roof plate epithelium and neuroepithelium at the hindbrain that is required for choroid plexus epithelium development raises the possibility that an equivalent boundary-organiser also exists at other axial regions where choroid plexus develops; at the telencephalic and diencephalic roof plates. Support for an organiser in the cortical hem that directs the development of the choroid plexus came from the genetic loss of function of *gli3* in the *extra-toes* mouse mutant. *gli3* encodes a transcriptional regulator of *wnt* gene expression and is expressed in the cortical neuroepithelium including the cortical hem, but not the developing choroid plexus epithelium (Grove et al., 1998). In *extra-toes* mice the cortical hem expression of *wnt2b*, *wnt3a*, and *wnt5a* was lost and the choroid plexus epithelium, as assessed by *ttr* expression did not form. This suggested a non-autonomous role of cortical-hem derived *wnts* for the specification of the choroid plexus epithelium. However cortical hem progenitors contribute to the choroid plexus epithelium, implying that loss of *gli3* function could have had an autonomous effect on choroid plexus epithelial cell differentiation (Yoshida et al., 2006; Louvi et al., 2007). Focal electroporation, as utilised in my studies of the hindbrain roof plate boundary-organiser, would help to determine if signalling molecules from the cortical hem are required non-autonomously to direct the differentiation of telencephalic choroid plexus epithelial cells.

5.3.2 Candidates for the signals derived from the roof plate boundary

What are the molecular signals derived from the roof plate boundary that signal to the roof plate epithelium to induce or maintain choroid plexus epithelium differentiation? One candidate group of signalling molecules are the BMP signals, including Gdf7 itself, as BMP signalling is known to be specifically required for the development of the telencephalic choroid plexus epithelium (Hebert et al., 2002). However, in some embryos where *chairy2ΔWRPW* or full length *chairy2* was overexpressed at the rhombic lip – roof plate

boundary, *ttr* expression was lost non-autonomously but there was no autonomous downregulation of *gdf7* expression. This suggests that the expression of signals other than Gdf7 were perturbed by the overexpression of full length or truncated *chairy2*, and that these signals are required for *ttr* expression in the roof plate epithelium.

Another good candidate molecule is Wnt1 as it is not expressed in the roof plate epithelium but is expressed highly in the roof plate boundary of both mouse and chick (Landsberg et al., 2005). Wnt/β-catenin signalling has been shown to be necessary for the dorsoventral patterning of the chick spinal cord (Alvarez-Medina et al., 2008). However, a Wnt/β-catenin-responsive reporter mouse and the expression of *axin2*, a Wnt/ β-catenin signalling target gene, show that the E12.5 and E14.5 choroid plexus epithelium is not responsive to Wnt/β-catenin signalling (Selvadurai and Mason, 2011), although these ages are after the initial differentiation of choroid plexus epithelium so these results do not preclude an earlier role for Wnt/β-catenin signalling in induction of choroid plexus epithelium differentiation.

Lastly, retinoic acid is another good candidate molecule as *cyp26C1*, expressed in the roof plate epithelium and choroid plexus epithelium, encodes a retinoic acid catabolising enzyme whose expression in the neuroepithelium is dependent on retinoic acid signalling (Reijntjes et al., 2004). Additionally the cytochrome p450 retinoic acid-synthesising enzyme, *cyp1b1*, shows localised expression at the roof plate boundary at E5 (Wilson et al., 2007), although it and another retinoic acid synthesising enzyme, *raldh2*, are also expressed in the mesenchyme overlying the roof plate so retinoic acid signals may not specifically derive from the roof plate boundary. Retinoic acid is derived from vitamin A and vitamin A-deficiency studies in mice show that a lack of retinoic acid results in hydrocephalus and poorly developed choroid plexuses, further supporting a role for retinoic acid in choroid plexus development (see discussion in Ruberte et al. (1993)).

5.3.3 Choroidal blood vessel development

As mentioned above, the prospective telencephalic choroid plexus epithelium can induce the differentiation of organ-typical capillaries from the body-wall mesenchyme of chick embryos (Wilting and Christ, 1989). The nature of this signal has not yet been identified, however in mice it has been shown that *shh* expressed in the choroid plexus epithelium is required for vascular outgrowth in the hindbrain choroid plexus (Nielsen and Dymecki, 2010). However *shh* was not required for the correct specification of organ-typical fenestrated capillaries. Therefore the mechanism of specification of hindbrain choroid plexus blood vessel development remains elusive.

A microarray study to compare genes expressed at the roof plate boundary/ rhombic lip domain in comparison with more ventral neuroepithelium in E4 and E6 chick hindbrains

indicates that a number of pro- and anti-angiogenic factors are expressed at the roof plate boundary/ rhombic lip at these time points (Wilson, Chambers and Wingate, unpublished). It will be interesting to determine whether pro- and anti-angiogenic factors from the roof plate boundary are involved in the induction or patterning of choroid plexus blood vessel development.

5.3.4 Role of the roof plate boundary-organiser and the integrated coordination of choroid plexus and neural development

Aside from its role in the physical protection of the developing brain, CSF produced by the choroid plexuses has a number of distinct roles in the coordination of neural development (Redzic et al., 2005). The embryonic and postnatal mammalian fourth ventricle choroid plexus expresses high levels of the retinoic acid synthesising enzyme Raldh2, and retinoic acid secreted by the fourth ventricle choroid plexus has been shown to induce neurite outgrowth of cerebellar explant cultures (Yamamoto et al., 1996). This effect was age-dependent and correlated with choroid plexus Raldh2 activity at different ages. Further, excess retinoic acid has been shown to have potent teratogenic effects on the development of the cerebellum, supporting a role for choroid plexus-derived retinoic acid in the coordination of cerebellum development (McCaffery et al., 2003). More recently it has been shown that, Shh present in the CSF, most likely secreted by the hindbrain choroid plexus epithelium, regulates proliferation of cerebellar radial glial cells and production of GABAergic neuronal progenitors (Huang et al., 2010). Therefore CSF-derived retinoic acid and Shh have distinct roles in the development of the cerebellum, with retinoic acid secretion highlighting the role of a dynamically regulated signal present in the CSF.

Recently it has been shown that Igf2 present in the CSF, the source of which is most likely to be telencephalic choroid plexus, stimulates the proliferation of cerebral cortical progenitor cells in mice (Lehtinen et al., 2011). The stimulatory effect of CSF on cerebral cortical progenitor cell proliferation and survival was age-dependent and closely mimicked the temporal profile of CSF Igf2 concentration. Further, genetic loss of *Igf2* or its receptor *Igf1r* significantly reduced CSF-stimulated cortical progenitor cell proliferation with genetic loss of *Igf2* resulting in mice with smaller brains. These results demonstrated the importance of CSF-borne Igf2 for the stimulation of cortical progenitor cell proliferation, but did not rule out a role for other CSF-borne growth factors. Indeed the authors of this study identified that the CSF contained Wnt, Bmp and retinoic acid signalling capacity, which varied depending on the age of CSF sampled. Furthermore, a number of signalling molecules of the TGF-β superfamily, which includes proteins of the Bmp family, the FGF family and retinoic acid synthesising enzymes are expressed by the choroid plexus during development (Redzic et al.,

2005; Lehtinen et al., 2011). Future work will determine if these signalling molecules have any function in coordinating neuroepithelial cell proliferation, differentiation or survival either via a CSF route or via a paracrine route from the choroid plexus to the adjacent dorsal neuroepithelium.

In the forebrain, choroid plexus-expressed Slit2 is thought to contribute to the orientation of migration of cerebral cortical neurons and olfactory interneuron precursors via chemorepulsion (Hu, 1999; Nguyen-Ba-Charvet et al., 2004). This raises the possibility that the fourth ventricle choroid plexus might also be involved in axon guidance during neuronal network formation, although this has not yet been shown.

The above demonstrates that choroid plexus-derived factors have multiple roles in the dynamic coordination of neuroepithelial cell proliferation, survival and differentiation, and may also have a role in directing neuronal path-finding. Therefore it is imperative that the timing of development of neuroepithelium and the choroid plexus is well-coordinated. One method to achieve this coordination of development is the use of a single organiser or signal source to direct the development of both tissues simultaneously. The coordinated development of two tissues by a single organiser or signal is a feature of other developmental processes, such as the stimulation of growth of the choroid plexus epithelium and vasculature by choroid plexus epithelium-derived *shh* (Nielsen and Dymecki, 2010), the patterning of the adjacent thalamus and pre-thalamus by *shh* from the ZLI (Kiecker and Lumsden, 2004) or the patterning of the adjacent midbrain and rhombomere 1 by the MHB (Wassef and Joyner, 1997). The hindbrain roof plate boundary-organiser, which is required for development of both the dorsal neuroepithelium and the choroid plexus epithelium, is therefore another example of an organiser that directs the development of two separate, but functionally linked tissues. It will be interesting to see if shared boundary-organisers that simultaneously coordinate the development of the neuroepithelium and the choroid plexus at the lateral and third ventricles also exist.

5.4 Conclusions

This thesis presents the argument that organiser properties of the chicken hindbrain roof plate are localised to its boundaries. The chick roof pate boundary is characterised by *gdf7* expression, but a comparable boundary is also likely to exist in mouse, being marked by high mRNA expression of *gdf7*, *wnt1* and *lmx1a*. The roof plate organiser not only signals to the hindbrain neuroepithelium, but is also involved in patterning the development of the choroid plexus epithelium, which is derived from the roof plate epithelium. Thus I have established new insights into how the development of the choroid plexus is coordinated, a tissue whose development, until recently, has received little attention. A shared organiser that directs the development of both neuroepithelium and choroid plexus epithelium is a simple mechanism that ensures coordinated development of the two tissues.

The roof plate boundary is maintained by tissue interactions between the roof plate epithelium and the hindbrain neuroepithelium, which are molecularly mediated by Notch signalling. Downstream of Notch activation at the roof plate boundary, the *hes* transcription factor, *chairy2* must be expressed at the correct level to mediate maintenance of the *gdf7*-positive organiser. The remarkable conservation of the localisation of organisers at boundaries and the use of tissue interactions between molecularly distinct tissue compartments, activated Notch signalling and Hes transcription factors for the maintenance of those boundary-localised organisers suggests a generalizable model for other organisers in the developing CNS, and indeed in other tissues such as the developing skeletal elements.

Chapter 6 Materials and Methods

6.1 Common Solutions

ddH_2O	double-distilled H_2O. Autoclave.
PBS	phosphate buffered saline (Oxoid). Autoclave.
PFA	4% paraformaldehyde (Sigma) in PBS.
PBTw	PBS with 0.1% Tween-20 (Sigma).
Tris-HCL	Trizma base, minimum (Sigma) in ddH_2O. pH to desired pH with 2M HCl. Autoclave.
20x SSC (pH 4.5)	3M NaCl (BDH), 0.3M sodium citrate (Fisher Scientific). pH using 5M citric acid. Autoclave.
5x MAB pH7.5	500mM maleic acid (Sigma), 750mM NaCl (BDH). pH using NaOH pellets (BDH). Autoclave.
MABT	1xMAB with 0.1% Tween-20 (Sigma).
10% BBR	Boehringer Blocking Reagent (Boehringer) dissolved in 1x MAB.
Detergent Mix	1% IGEPAL CA-630 (Sigma), 1% SDS (Sigma), 0.5% deoxycholate (Fluka), 50mM Tris-HCL (pH8), 1mM EDTA (Ambion), 150mM NaCl (BDH).
whole-mount hybridisation buffer	50% formamide (Sigma), 5x SSC (pH4.5), 2% SDS (Sigma), 2% BBR.
Solution X	50% formamide (Sigma), 2x SSC (pH4.5), 1% SDS (Sigma).
heat-inactivated sheep serum	Sheep Serum (Sigma) heated to 56°C for 30 min.
blocking solution	2% BBR, 20% heat-inactivated sheep serum in MABT.
whole-mount pH 8 NTMT	100mM NaCl (BDH), 100mM Tris-HCL (pH8), 50mM $MgCl_2$ (BDH), 1% Tween-20 (Sigma). Made up on the

	day it was to be used.
whole-mount pH 9.5 NTMT	100mM NaCl (BDH), 100mM Tris-HCL (pH9.5), 50mM $MgCl_2$ (BDH), 1% Tween-20 (Sigma). Made up on the day it was to be used.
10x Salts	114g NaCl (BDH), 14.04g Trizma ® HCL (Sigma), 1.34g Trizma ® base minimum (Sigma), 7.1g $NaH_2PO_4.2H_2O$ (BDH), 0.5M EDTA (Sigma) in 1L ddH_2O.
cryostat hybridisation buffer	1x Salts, 50% formamide (Sigma), 10% dextran sulphate (Fluka), 250µg/ml Yeast tRNA (Ambion), 1x Denhardt's (Fluka).
cryostat washing solution	1x SSC pH7 (Sigma), 50% formamide (Sigma) 0.1% Tween-20 (Sigma).
cryostat pH 8 NTMT	100mM NaCl (BDH), 100mM Tris-HCL (pH8), 50mM $MgCl_2$ (BDH), 0.1% Tween-20 (Sigma). Made up on the day it was to be used.
cryostat pH 9.5 NTMT	100mM NaCl (BDH), 100mM Tris-HCL (pH9.5), 50mM $MgCl_2$ (BDH), 0.1% Tween-20 (Sigma). Made up on the day it was to be used.
Staining Solution	cryostat pH 9.5 NTMT with 5% poly(vinyl alcohol) (Sigma) dissolved.
Tyrodes	137.0mM NaCl (BDH), 2.7mM KCl (Sigma), 2.4mM $CaCl_2$ (Sigma), 2.1mM $MgCl_2.6H_2O$ (BDH), 0.4mM $NaH_2PO_4.2H_2O$ (BDH), 5.6mM glucose (Sigma). Autoclave then add 100U/ml penicillin, 100µg/ml streptomycin, 0.3 µg/ml Fungizone (Gibco).
Slice media	Basal Medium Eagle (Gibco) supplemented with 0.5% D-(+)-glucose (Sigma), 1% I-1884 supplement (Sigma), 2mM L-Glutamine (Sigma), 100U/ml penicillin, 100µg/ml streptomycin, 0.25 µg/ml Fungizone® (Gibco).
10x MEMFA salts	1M MOPS (Sigma), 20mM EGTA (Sigma), 10mM $MgSO_4$ (Sigma) solution. pH to 7.4 using NaOH pellets

	(BDH). Autoclave.
MEMFA Fix	1x MEMFA salts, 3.7% formaldehyde (Sigma).

6.2 Animals

Fertilised GFP transgenic eggs (gift of Helen Sang, Roslin Institute) and wild type eggs (Henry Stewart, UK) were incubated at 38°C for 3 to 6 days before windowing with sharp surgical scissors. Staging of chick embryos was made according to Hamburger and Hamilton (1951) (labelled as st) or according to the embryonic day of development (labelled as E). The relationship between embryonic day of development and Hamburger and Hamilton stages are detailed in Appendix A. Wild-type embryos were dissected appropriately in PBS using ridged forceps (Fine Science Tools) and fixed and stored in PFA.

6.3 Molecular Biology

6.3.1 Cloning of *chairy2ΔWRPW* and full length *chairy2* from chick cDNA

Total RNA was extracted from E3 chick embryos by TRIzol RNA isolation. This involved isolating the hindbrain, midbrain and forebrain from a st.17 chick embryo in ice-cold PBS then homogenizing it in 1ml TRIzol reagent (Invitrogen) in a 1.5 ml Eppendorf tube. The tube was then centrifuged for 1 min at 12000g to remove cell debris. The supernatant was then transferred to a new 1.5 ml Eppendorf tube. To extract RNA, 0.2ml chloroform (Sigma) was added to 1ml TRIzol Reagent and sample tubes were vortexed for 15 seconds, then incubated for 2 minutes at room temperature. Samples were then centrifuged at 12000g for 15 minutes at 4°C. The upper colourless aqueous phase was isolated and transferred into a new Eppendorf tube. RNA was precipitated by mixing the aqueous solution with 500µl of isopropanol well then incubating the tube at room temperature for 10 minutes, then centrifuging the rube at 12000g for 10 minutes at 4°C. The supernatant was then removed from the RNA pellet and 1ml of 75% ethanol was added to the RNA pellet. The sample was then vortexed and then centrifuged at 7500g for 5 minutes at 4°C. This washing procedure with ethanol was repeated and all ethanol was removed from the RNA pellet. The RNA pellet was air-dried for 10 minutes. The RNA pellet was re-suspended in 15µl of RNAase-free ddH_2O (Ambion) and 1.5µl of sample was diluted with 6.5µl ddH_2O and 2µl 5x DNA loading buffer (Bioline) and run out on a 1% agarose (Sigma) in TBE (Severn Biotech) gel stained with SYBR Safe DNA gel stain (Invitrogen) alongside 5µl Hyperladder 1 (Bioline) to check for the presence of ribosomal and messenger RNA. The concentration of RNA was measured using a NanoVue Plus Spectrophotometer (GE Healthcare).

First-strand cDNA was synthesised using the SuperScript First-Strand Synthesis System for RT-PCR (Invitrogen) according to the manufacturer's instructions. Briefly, an RNA/ primer mixture was created by mixing 1µg total RNA with 1µl of 10mM dNTP mix and 1µl of 0.5µg/µl Oligo(dT)$_{12-18}$ in 10µl ddH_2O. This mix was heated to 65°C for 5mins then cooled for 1 min on ice. The reaction mixture was created by mixing 2µl of 10x reverse transcription buffer with 4µl of 25mM $MgCl_2$, 2µl of 0.1M DTT and 1µl of RNaseOUT Recombinant RNase inhibitor. This mixture was added to the RNA/ primer mixture and mixed by centrifugation for 1 min at 12000g. The mixture was then incubated at 42°C for 2mins before 1µl of SuperScript II reverse transcriptase was added to the reaction. The reaction was then incubated for 50mins at 42°C. The reaction was terminated by incubating at 70°C for 15mins and then chilled on ice. 1µl of RNaseH was added to the reaction for 20mins at 37°C to remove RNA.

chairy2ΔWRPW and full length *chairy2* were then amplified by polymerase chain reaction (PCR). 2µl of the cDNA reaction was mixed with 5µl of 10X AccuPrime *Pfx* Reaction Mix (Invitrogen), 1µl each of 10µM forward and reverse primers, 40.6µl of ddH_2O and 0.4µl of AccuPrime *Pfx* DNA Polymerase (Invitrogen). The forward primer used was 5'ATTGCGGCCGCATGCCTGCCGACCTGATGGAG 3' and the reverse primer used was 5' TGAATTCTCACCAGGGCCTCCAGACTG 3' for full length *chairy2* and 5' TGAATTCTCAGACTGAGTCAGCGGTG 3' for *chairy2ΔWRPW* (primers were ordered from Sigma). PCR amplification was achieved by subjecting the reaction to the following conditions: The template was denatured by heating to 95°C for 2mins then 25–35 cycles of PCR amplification followed by heating the reaction to 95°C for 15secs, annealing was allowed by heating at 60°C for 30secs, then extension of DNA was allowed by heating at 68°C for 1min. The reaction was then chilled to 4°C.The PCR reaction was then checked by running 5µl of PCR product mixed with 2µl 5x DNA loading buffer (Bioline) and 4µl ddH_2O, out on a 1% agarose (Sigma) in TBE (Severn Biotech) gel stained with SYBR Safe DNA gel stain (Invitrogen) alongside 5µl Hyperladder 1 (Bioline). The PCR product was purified using an illustra GFX PCR DNA and Gel Band purification kit (GE Healthcare) as per the manufacturer's instructions.

6.3.2 Restriction enzyme digestion of PCR products and receptive pBluescript II KS+ vector

The PCR products were transferred into pBluescript II KS+ (Agilent) by first digesting the PCR products and the plasmid with the restriction enzymes Not1 and EcoR1. For the PCR product this was carried out by mixing 49µl of the PCR product with 6µl of Buffer H (Roche) and 2.5µl each of the enzymes Not1 and EcoR1 (Roche). For the plasmid this was

carried out by mixing 5µg of plasmid with 6µl of Buffer H (Roche) and 2.5µl each of the enzymes Not1 and EcoR1 (Roche) in a total volume of 60µl of ddH_2O. Digestion reaction mixtures were incubated for two hours at 37°C. Reaction products were mixed with 12µl of 5x DNA loading buffer (Bioline) and run out on a 1% agarose (Sigma) in TBE (Severn Biotech) gel stained with ethidium bromide, alongside 5µl Hyperladder 1 (Bioline) overnight at 25V. The correct bands were isolated and purified using an illustra GFX PCR DNA and Gel Band purification kit (GE Healthcare).

6.3.3 Ligation reaction and mini-preparation of DNA constructs

2µl of purified, digested inserts and 2µl of the purified, digested plasmid were mixed with 2µl of 5x DNA loading buffer (Bioline) and 6µl of ddH_2O then run out on a 1% agarose (Sigma) in TBE (Severn Biotech) gel stained with ethidium bromide, alongside 5µl Hyperladder 1 (Bioline) to gauge the relative concentration and sizes of the inserts and plasmid. The appropriate volumetric ratio to mix the purified, digested insert solution with the purified, digested plasmid so that the relative nucleotide concentration was equal was subsequently determined. Thus the appropriate volumes of purified, digested inserts and plasmids were mixed with 1.5µl ligation buffer (Roche) and 1.3µl T4 DNA ligase (Roche) in a total volume of 15µl ddH_2O and the ligation reaction was incubated overnight at 16°C. As a control the same volume as the reaction above of purified, digested plasmid solution was incubated with 1.5µl ligation buffer (Roche) and 1.3µl T4 DNA ligase (Roche) in a total volume of 15µl ddH_2O overnight at 16°C. One shot Top10 chemically competent *E. Coli* (Invitrogen) were then transformed with 3µl of each ligation reaction according to the manufacturer's instructions, and the resulting transformed cells were plated out on LB agar (Sigma) plates containing 100µg/ml ampicillin (Sigma). Transformed cells were grown overnight at 37°C. 10 colonies were then picked and grown overnight at 37°C, shaking at 213rpm in 3ml LB (Sigma) containing 100µg/ml ampicillin (Sigma). Plasmid DNA was purified from overnight cultures using a QIAprep Spin MiniPrep Kit (Qiagen) according to the manufacturer's instructions. A diagnostic restriction digest was then carried out by mixing 5µl of each miniprep with 2µl Buffer H (Roche) and 0.8µl of both EcoR1 (Roche) and Not1 (Roche) in a total volume of 20µl ddH_2O, and incubating for two hours at 37°C. 4µl of 5x DNA loading buffer (Bioline) was then added to each diagnostic reaction and the solution was run out on a 1% agarose (Sigma) in TBE (Severn Biotech) gel stained with SYBR Safe DNA gel stain (1:10000; Invitrogen), alongside 10µl purified, digested plasmid solution mixed with 4µl of 5x DNA loading buffer (Bioline) and 8µl ddH_2O, and 5µl Hyperladder 1 (Bioline).

6.3.4 Sequencing of *chairy2* and *chairy2ΔWRPW*

From this diagnostic restriction reaction, three miniprep clones seen to contain the correct size insert were sent for sequencing (Eurofins). The correct sequences for *chairy2* and *chairy2ΔWRPW* were verified for all clones and are shown in Appendix D and E respectively.

6.3.5 Construction of the *chairy2ΔWRPWv2-IRESeGFPm5* and *chairy2-IRESeGFPm5* constructs

5µg of pBluescript II KS+*chairy2ΔWRPW*, pBluescript II KS+*chairy2* and the pCAβ-*IRESeGFPm5* vector (Andreae et al., 2009) (see Appendix C for explanation of abbreviations) were digested with EcoR1 and Not1 by mixing with 6µl Buffer H (Roche) and 2µl each of EcoR1 and Not1 (Roche) in a total volume of 60µl ddH_2O, and incubating at 37°C for two hours. 12µl of 5x DNA loading buffer (Bioline) was added to each reaction and the reaction was run out on a 1% agarose (Sigma) in TBE (Severn Biotech) gel stained with ethidium bromide overnight at 25V. The appropriate DNA bands for *chairy2ΔWRPW*, *chairy2* and linearized pCAβ-*IRESeGFPm5* vector were isolated and purified using an illustra GFX PCR DNA and Gel Band purification kit (GE Healthcare). A diagnostic gel to determine the relative size and concentration of inserts and plasmid was then run as described above in 'Ligation reaction and mini-preparation of DNA constructs'. Ligation reactions and subsequent mini-preparation of constructs was then carried out as described above in 'Ligation reaction and mini-preparation of DNA constructs'.

6.3.6 Amplification of DNA constructs

Mini-prepared DNA solutions were used to transform Subcloning Efficiency 5-alpha competent *E. coli* (NEB) according to the manufacturer's instructions. The resulting transformed cells were plated out on appropriately selective LB agar (Sigma) plates. Transformed cells were grown overnight at 37°C. Individual colonies were then picked and used to inoculate 3ml of appropriately selective LB (Sigma). This starter culture was grown for 8 hours at 37°C, shaking at 213rpm and was then diluted in the appropriate volume of selective LB (Sigma) at a 1:500 ratio. This culture was grown overnight at 37°C, shaking at 213rpm, then DNA was purified using either a QIAfilter Plasmid Midi Kit (Qiagen) or a QIAfilter Plasmid Maxi Kit (Qiagen), according to the manufacturer's instructions.

6.3.7 Generation of antisense riboprobes for *in situ* hybridisation

DNA *in situ* plasmids (listed in Appendix B) were linearized with the appropriate restriction endonuclease (Roche) by incubating 10µg of DNA with 10U of enzyme and the appropriate buffer in a 30µl volume for 2 hours. Linearized plasmid was then purified using an illustra GFX PCR DNA and Gel Band purification kit (GE Healthcare). 1µg of linearized plasmid

was then incubated with 30U of the appropriate RNA polymerase (Roche) in a 20µl *in vitro* transcription reaction (1x transcription buffer (Roche), 20U Protector RNase inhibitor (Roche)) with either 1x DIG RNA labelling mix or 1x fluorescein RNA labelling mix (Roche), for 2 hours at 37°C. DNA was then removed from the reaction by incubation for 45 min at 37°C with 10U DNAase 1 (Roche). This reaction was quenched by the addition of 42mM EDTA, pH8 (Ambion). Success of the reaction was checked by running 2µl of the reaction diluted with 2 µl ddH_2O and 1µl 5x DNA loading buffer (Bioline) out on a 1% agarose (Sigma) in TBE (Severn Biotech) gel stained with SYBR Safe DNA gel stain (Invitrogen) alongside 5µl Hyperladder 1 (Bioline). RNA probe solutions were then purified using illustra Microspin G50 Columns (GE Healthcare). RNA concentration was quantified using a NanoVue Plus Spectrophotometer (GE Healthcare).

6.4 Histological techniques

6.4.1 Cryostat sectioning

Wild type embryos stored in 4% PFA were washed in PBS three times for 15 minutes. Embryos were then perfused with 30% sucrose (Sigma) in PBS overnight at 4ºC. Embryos were then perfused for 1 hour at 4°C in OCT compound. Embryos were then transferred into approximately 1.5ml of fresh OCT compound in a mould made from foil and oriented as desired. Embryos were frozen by placing on a 10cm petri dish floating on liquid nitrogen. 20µm serial transverse sections were cut using a cryostat (Zeiss Microm HM 560) and collected on SuperFrost® Plus slides. Sections were allowed to air-dry for 2 hours and were then transferred into a –80ºC freezer for storage

6.4.2 Vibrotome sectioning

Embryos that had been in through the *in situ* hybridisation process were embedded in 20% gelatine (Fluka) in PBS by first washing the embryos in PBS three times for 10mins at room temperature, then placing embryos into pre-warmed 20% gelatine in PBS for 1.5hrs at 65°C or until they sink. Embryos were then transferred in 20% gelatine in PBS into moulds and embryos were oriented as desired. Blocks were set by cooling on an ice block and then storing in the fridge for 2 hours. Blocks were then cut to the appropriate size using a razor blade and were fixed in PFA for 2 days.

To section the embryos, blocks were washed three times for 15mins in PBS at room temperature then glued to the chuck of a vibrotome (Leica VT1000S) using superglue. The block and chuck were bathed in PBS and 40µm sections were cut and mounted on Polysine slides. Excess PBS was removed from sections and sections were mounted under a coverslip in 90% glycerol (MP) in PBS. Slides were sealed using nail varnish (Boots).

6.4.3 RNA *in situ* hybridisation

6.4.3.1 Whole mount *in situ* hybridisation

Wild type embryos, cultured explants or embryos that had been electroporated were subjected to whole-mount double *in situ* hybridisation. Embryos stored in PFA were washed and dissected appropriately in PBS. Embryos were then washed overnight in PBTw at 4ºC, then were gradually dehydrated by washing in 25%, 50%, 75% methanol in PBTw and finally in 100% methanol for 5 min each. Embryos were then re-hydrated gradually by washing in 75%, 50% then 25% methanol in PBTw and finally in PBTw for 5 min each. Embryos were then washed twice for 20 min in Detergent mix then post-fixed for 20 min in PFA with 25% glutaraldehyde (Sigma). Embryos are then washed twice in PBTw prior to pre-hybridisation in whole-mount hybridisation buffer at 70ºC for 1 hour. Hybridisation of riboprobes took place overnight at 70ºC by incubation of embryos in whole-mount hybridisation buffer with 1µg/ml DIG- or fluorescien-lablled riboprobe. After hybridisation, embryos were washed in pre-warmed Solution X at 70ºC twice for 5 min, then twice for 30 min. Embryos were then washed for 10 min in 50% Solution X in MABT, prior to being washed four times in MABT at room temperature for 20 min per wash. Embryos were then blocked for 1 – 2 hours in blocking solution prior to being incubated overnight at 4ºC with an alkaline phosphatase- conjugated anti-flourescein antibody (for double *in situs*) or an alkaline phosphatase- conjugated anti-DIG antibody (for single *in situs*) (1:2000, Roche) in blocking solution. Embryos were then rinsed 3 times in MABT then washed four times for 10 min, then once for 30 min in MABT, then overnight at 4ºC in MABT. Then a red signal was developed to detect antibody bound to fluorescein-labelled probes, and a blue signal was developed to detect antibody bound to DIG-labelled probes.

The red signal was developed by washing embryos in whole-mount pH 8 NTMT twice for 10 min prior to the colour reaction. For the colour reaction one Fast-Red (Sigma) tablet was dissolved per 12ml whole-mount pH8 NTMT and embryos were then incubated with the Fast-Red substrate at 4ºC in the dark until an appropriate level of red signal had developed. Embryos were washed overnight at 4ºC in MABT to allow the colour reaction to be carried out again the next day. To stop the colour reaction, embryos were washed three times for 5 min in PBS (Phosphate buffered saline), then were treated with 5mM EDTA (Ambion) in PBS for 1 hour at 70ºC, then rinsed twice in PBS prior to fixation overnight at 4ºC in PFA.

To develop the blue signal embryos were washed twice for 10min in whole-mount pH 9.5 NTMT. The colour reaction was carried out by incubating embryos with NBT/BCIP mix (Roche) (5µl/ml in whole-mount pH 9.5 NTMT) at room temperature in the dark. After the appropriate level of blue signal was achieved the colour reaction was stopped by washing

embryos for 10 min in whole-mount pH9.5 NTMT, then washing twice for 10 min in PBTw, then twice for 5 min in PBS, prior to storage of embryos in PFA at 4ºC.

For double *in situs*, after the red signal was developed and stopped, embryos were washed four times in MABT at room temperature for 20 min per wash. Embryos were then blocked for 1 – 2 hours in Block prior to being incubated overnight at 4ºC with alkaline phosphatase-conjugated anti-DIG antibody (1:2000; Roche) in Block. Embryos were then rinsed 3 times in MABT then washed four times for 10 min, then once for 30 min in MABT, then overnight at 4ºC in MABT. The blue signal was then developed and the reaction stopped as described above.

6.4.3.2 *In situ* hybridisation on cryostat sections.

Cryostat sections were defrosted for 30 min then washed for 10 min in PBS to dissolve OCT. Riboprobes in cryostat hybridisation buffer were prepared by diluting 1µg/ml of riboprobe in cryostat hybridisation buffer and heating at 70°C for 10 min. Sections were then incubated overnight in the riboprobe mix under a coverslip at 70°C in a sealed box in the presence of Whatman filter paper wetted with a solution of 1x Salts/ 50% Formamide (Sigma). Slides were then washed in pre-warmed cryostat washing solution at 70°C firstly for 15 minutes to allow coverslips to fall off, then twice for 30 minutes. Slides were then washed three times for 30 min in MABT then blocked by incubating in blocking solution for 1hr in a humidified chamber. Slides were then incubated overnight at room temperature in a humidified chamber with an alkaline phosphatase- conjugated anti-flourescein antibody (for double *in situs*) or an alkaline phosphatase- conjugated anti-DIG antibody (for single *in situs*) (1:2000; Roche) in blocking solution. The next day slides were washed with MABT four times at room temperature for 20 min then overnight at 4°C in MABT. Then a red signal was developed to detect antibody bound to fluorescein-labelled probes, and a blue signal was developed to detect antibody bound to DIG-labelled probes.

The red signal was developed by washing slides in cryostat pH 8 NTMT twice for 10 min prior to the colour reaction. For the colour reaction one Fast-Red (Sigma) tablet was dissolved per 12ml cryostat pH8 NTMT and slides were then incubated with the Fast-Red substrate at 4ºC in the dark until an appropriate level of red signal had developed. Slides were washed overnight at 4ºC in MABT to allow the colour reaction to be carried out again the next day. To stop the colour reaction, Slides were washed three times for 5 min in PBS (Phosphate buffered saline), then were treated with 5mM EDTA (Ambion) in PBS for 15 min at 70ºC, and then washed in PBS overnight at 4°C.

To develop the blue signal slides were washed twice for 10min in cryostat pH 9.5 NTMT. The colour reaction was carried out by incubating sections with NBT/BCIP mix (Roche)

(20µl/ml in Staining Solution) at room temperature in the dark. After the appropriate level of blue signal was achieved the colour reaction was stopped by washing slides twice for 10 min in PBS with 0.25% Triton X-100 (Alfa Aesar) and 2mM EDTA (Ambion), then once for 5 min in PBS, then post-fixed with PFA. Slides were then rinsed twice for 5 min in PBS and mounted in 90% glycerol (MP) in PBS. Coverslips were sealed with nail polish (Boots).

For double *in situs*, after the red signal was developed and stopped, slides were washed three times in MABT at room temperature for 30 min per wash. Sections were then blocked by incubating in blocking solution for 1hr in a humidified chamber. Slides were then incubated overnight at room temperature in a humidified chamber with an alkaline phosphatase-conjugated anti-DIG antibody (1:2000; Roche) in blocking solution. The next day slides were washed with MABT four times at room temperature for 20 min then overnight at 4°C in MABT. The blue signal was then developed and the reaction stopped as described above.

6.4.4 Immunohistochemical Staining

6.4.4.1 Whole-mount

Cultured explants and electroporated embryos were washed in PBS for 60 min to remove PFA. Embryos were then washed twice for 30 min in PBS with 1% Triton X-100 (PBSTrit), then blocked by washing three times for 60 min in 5% neonatal calf serum (NCS; Sigma) in PBSTrit. Embryos were then exposed to the primary antibody, rabbit anti-GFP, IgG (1:150; Invitrogen) in 10% NCS/ PBSTrit for 2 - 3 nights at 4ºC. The primary antibody was then washed off with four times 60 min washes in 1% goat serum (GS; Sigma) in PBSTrit and the embryos were exposed overnight at 4ºC to the secondary antibody, Alexa Fluor 488 – conjugated goat anti – rabbit IgG (1:1000; Invitrogen; highly cross-adsorbed) in 1% GS/ PBSTrit. Embryos were then washed four times for 30 min in 1% GS/ PBSTrit to remove residual secondary antibody, then twice for 5 min in PBS, then were fixed and stored in 4% PFA.

6.4.4.2 Cryostat sections

Cryostat sections that had been through the *in situ* hybridisation procedure but not mounted were washed three times for five minutes in PBS and then blocked by incubation with 5% GS in PBSTw and then incubated overnight at 4°C with the primary antibody, rabbit anti-GFP, IgG (1:150; Invitrogen) in 5%GS in PBSTw. Embryos were then washed three times for 10 minutes in PBS then incubated for one hour at room temperature with Alexa Fluor 488 – conjugated goat anti – rabbit IgG (1:1000; Invitrogen; highly cross-adsorbed) in 5% GS in PBSTw. Embryos are then washed four times for 10 minutes in PBS and mounted in 90% glycerol (MP) in PBS under a coverslip. Slides are sealed with nail polish (Boots).

6.5 Explant co-cultures

E4, E5 or E6 GFP – transgenic chick embryos and stage matched wild type chick embryos were dissected in Tyrodes solution to isolate the hindbrains or spinal cords from the anterior limb-bud level. Hindbrains were flat-mounted as illustrated in Figure 3-2 and the roof plate epithelium including the *gdf7*-domain (the most dorsal region of neuroepithelium that is removed when roof plate epithelium is dissected away) is removed. Most of the *gdf7*-domain is accurately removed by this method as evidenced by *in situ* hybridisation performed on hindbrains after 0hrs incubation (Figure 3-10). To assess the requirement for the roof plate for the maintenance of *cath1* in the rhombic lip, roof plate epithelium including the *gdf7* domain was only removed from one side of the flat-mounted hindbrain. For co-cultures, rhombic lips (estimated as the dorsal third of the neural tube to be sure of complete removal) from both sides of the hindbrains were either removed or left intact as indicated. For co-cultures involving spinal cord, spinal cords were flat-mounted and the dorsal 1/3rd of the neural tube was removed using a flame-sharpened tungsten wire (0.1mm). Pieces of roof plate epithelium (isolated as illustrated in Figure 3-2) were cultured adjacent to the flat-mounted hindbrains either along the dorsal edge of the hindbrain or along the dorsoventral axis of the hindbrain as indicated. Pieces of roof plate epithelium were cultured along the dorsal cut edge of the flat-mounted spinal cords. Alternatively, pieces of roof plate epithelium were cultured adjacent to other pieces of roof plate epithelium. Explants were cultured at an air-liquid interface with the pial surface of the hindbrain facing upwards, on 0.4μm culture plate inserts (Millicell – CM, Millipore) that had been placed in 3mls of sterile slice media that had been pre-warmed to 37ºC, with 6% CO_2, in a 60mm tissue culture dish (Nunc). Explants were cultured for 48 hours at 37°C with CO_2 maintained at 6% in a Sanyo CO_2 incubator, then fixed by replacing the 3ml slice media with 3ml 4% PFA and leaving the plates for 30 minutes at room temperature. 4% PFA was then applied directly to the explant tissue and left for a further 30 minutes at room temperature. The area of Millipore Membrane that contained the explanted hindbrains was cut out using a scalpel and the whole membrane was then stored in 4% PFA prior to processing by whole mount *in situ* hybridisation.

6.6 Microsurgical transplantation

Wild-type host eggs that had been incubated at 38°C to E3 were windowed and yolks underlying embryos were injected with Fount India ink (Pelikan). E4 GFP-transgenic embryos were dissected in Tyrodes to isolate and flat-mount hindbrains. Flame-sharpened tungsten wire (0.1mm) was also used to dissect out small pieces of roof plate epithelium from flat-mounted hindbrains. Pieces of rhombic lip were isolated by removing the roof plate

epithelium and *gdf7*-domain as illustrated in Figure 3-1-1, and then dissecting off small squares of rhombic lip (the dorsal-most neuroepithelium) using a flame-sharpened tungsten wire. The pieces of roof plate epithelium or rhombic lip tissue were grafted into the wild-type E3 embryo by first removing the vitelline membranes of the host embryo and cutting a receptive hole in either the roof plate epithelium, dorsal rhombomere 1 or the midbrain using flame-sharpened tungsten wire. The piece of donor tissue was then transferred into the receptive hole using a Gilson pipette coated in GS (Sigma) and flame-sharpened tungsten wire for fine manipulations. The host eggs were then incubated at 38°C for 24 hours.

6.7 *In ovo* electroporation

Eggs that had been incubated at 38°C were windowed and yolks underlying embryonic day 3 (E3, st16 – st17) embryos were injected with Fount India ink (Pelikan) diluted 1 in 5 in Tyrodes solution to generate visual contrast. Ink was not used for E4 (st21 – st24) embryos. The vitelline membranes were removed using ridged forceps (Fine Science Tools) and DNA constructs were injected into the fourth ventricle. DNA constructs (listed in Appendix C) were diluted to 1-2 µg/µl and mixed with trace amounts of fast green (Sigma) prior to injection. Where constructs were co-electroporated they were mixed together so that they were mixed at a 1:1 concentration ratio and the final concentration of each construct was 1.0 µg/µl, prior to injection. The negative electrode was placed to the left of the neural tube and the positive electrode placed to the right at the hindbrain level to target the site of electroporation. Three 50 ms/10 V square waveform electrical pulses were passed between electrodes so that DNA entered the right side of the neural tube or roof plate epithelium. Eggs were then sealed and incubated at 38°C until E5 when embryos were harvested and either fixed in PFA at 4°C, MEMFA Fix at 4°C for embryos co-electroporated with CAβ-*GFP* and RCAS-*RFP*, or processed for LysoTracker staining.

6.8 LysoTracker staining

Electroporated embryos collected in PBS were organised into 12-well plates with 250µl of PBS in each well. 250µl of LysoTracker Red DND99 stain (Invitrogen; 10µM in PBS) was added to each well so that the final concentration of Lyso Tracker Red was 5µM. The 12-well plate was covered in foil and incubated at 37ºC for 30 minutes. Embryos were then rinsed five times for 5 min with PBS then embryos were fixed in MEMFA Fix.

6.9 Imaging and image processing

'Flat-mounted hindbrains' indicate that hindbrains dissected in PBS were dissected along the dorsal midline and mounted pial side up on Polysine slides. 'Flat-mounted roof plates'

indicate that dissected hindbrains were dissected along the ventral midline and mounted on Polysine slides with either the pial or the ventricular surface upwards. Silicon grease was then used to support a coverslip and flat-mounted brains were mounted in 90% glycerol (MP) in PBS. Cultured explants that had been through the in situ hybridisation procedure were washed in PBS and removed from Millipore Membranes, then mounted on Polysine slides in 90% glycerol (MP) in PBS under a coverslip.

Low magnification images of whole-mount embryos in PBS, flat-mounted embryos or cultured explants were captured using a Leica stereo photomicroscope fitted with a Leica digital microscope. High magnification images of flat-mounted embryos and cultured explants were captured using a Zeiss Axioplan2 compound microscope fitted with a SPOT Insight Firewire 4 digital camera. Vibrotome and cryostat sections were imaged using a Zeiss Axiophot stereovision compound microscope fitted with a Zeiss AxioCam digital camera. Confocal micrographs were collected using an Olympus Fluoview AX70 and images shown are projections of z-stacks or an individual optical section as indicated. Optical sections in z-stacks were taken at 5µm intervals. All images were processed using Photoshop 6.0 (Adobe).

6.10 Cell counting and statistical analysis

The number of cells co-expressing GFP and RFP were counted out of the total number of electroporated cells in a confocal optical section using the Cell Counter plug-in for ImageJ (NIH). The percentage of cells co-expressing GFP and RFP, only expressing RFP or only expressing GFP was worked out. This was carried out for four optical sections derived from two electroporated embryos and means and standard errors of the means were calculated using Excel 2010 (Microsoft).

The number of dead cells per mm^2 was calculated by counting the total number of dead cells in an area of 70 – 100 μm^2 within the electroporated domain or in a similar region of the un-electroporated side of the flat-mounted hindbrain, in projections of z-stacks of optical sections, using ImageJ (NIH) software. Hence the number of dead cells per mm^2 was calculated for both the electroporated domain and a similar region of the un-electroporated side of the flat-mounted hindbrain. The Wilcoxon paired comparison test was used to determine the significance of differences in the extent of cell death between the electroporated and un-electroporated side of hindbrains electroporated with CAβ-*GFP* or *chairy2ΔWRPWv1-IRESeGFPm5* (n=3 for both). After the amount of cell death on the un-electroporated side is subtracted from the amount on the electroporated side, the Man-Whitney test was used to test the significance of differences between electroporation with

CAβ-*GFP* and electroporation with *chairy2ΔWRPWv1-IRESeGFPm5* (n=3 for both). For all statistical tests a 5% significance level was chosen to denote significance.

Appendix A

Relationship between embryonic day (E) and Hamburger and Hamilton (1951) stages (st).

Embryonic Day	Hamburger and Hamilton Stages
E2	st10 – st13
E2.5	st14 – st15
E3	st16 – st19
E4	st20 – st24
E5	st25 – st27
E6	st28 – st29
E7	st30

Appendix B

Plasmids for the generation of RNA *in situ* hybridisation riboprobes:

	For antisense riboprobe:		
Gene	**Cut:**	**Transcribe with:**	**Obtained from/ Reference**
bmp4	BamH1	T3	(Graham et al., 1994)
bmp7	Xho1	T3	(Begbie et al., 1999)
cash1	EcoR1	T7	Alessio Delogu, KCL
cath1	Not1	T3	(Wilson and Wingate, 2006)
cyp26C1	Sal1	T7	(Reijntjes et al., 2004)
delta1	EcoR1	T3	(Myat et al., 1996)
gdf7	Not1	SP6	Anthony Graham, KCL
chairy1	Hind3	T7	Jon Gilthorpe, Umea University
chairy2	Hind3	T7	Jon Gilthorpe, Umea University
lfng	Cla1	T3	(Laufer et al., 1997)
notch1	Hind3	T7	(Myat et al., 1996)
notch2	Hind3	T7	(le Roux et al., 2003)
otx2	Not1	T7	(Millet et al., 1996)
serrate1	Hind3	T7	(Myat et al., 1996)
ttr	Nco1	T7	(Duan et al., 1991)
wnt1	EcoR1	T7	(Hollyday et al., 1995)

Appendix C

List of DNA constructs used in electroporation studies.

Electroporation construct	**Reference**
RCAS-*RFP*	Wingate lab (unpublished). Made by replacing eGFP with RFP from the RCASBP(B)-*eGFP* construct (Gilthorpe et al., 2002)
CAβ-*GFP*	pCAβ-*eGFPm5* (Yaneza et al., 2002)
RCAS-*delta1*	(Henrique et al., 1997).
chairy2ΔWRPWv1-IRESeGFPm5	gift from J. Gilthorpe, Umea University
chairy2ΔWRPWv2-IRESeGFPm5	this study
chairy2-IRESeGFPm5	this study

Explanation of abbreviations used to describe constructs:

Abbreviation	**Explanation**
RCAS	Replication-Competent with an ALV long terminal repeat (LTR) with a Splice acceptor.
RCASBP(B)	As above but BP stands for Bryan Polymerase and (B) indicates the type of *env* gene in the vector.
pCAβ	Refers to a vector containing the cytomegalovirus enhancer and chicken β-Actin promoter.
IRES	Internal Ribosome Entry Site

Appendix D

Full length cHairy2

```
1     ATG CCT GCC GAC CTG ATG GAG AAG AGC AGC GCC TCG CCG GTG GCC   45
1      M   P   A   D   L   M   E   K   S   S   A   S   P   V   A    15

46    GCC ACC CCC GCC AGC ATC AAC GCG ACG CCC GAT AAG CCC AAA ACG   90
16     A   T   P   A   S   I   N   A   T   P   D   K   P   K   T    30

91    GCG GCG GAG CAC CGG AAG TCC TCC AAA CCC ATC ATG GAG AAG CGG   135
31     A   A   E   H   R   K   S   S   K   P   I   M   E   K   R    45

136   CGG CGG GCG CGC ATC AAC GAG AGC CTG GGG CAG CTG AAG ACG CTG   180
46     R   R   A   R   I   N   E   S   L   G   Q   L   K   T   L    60

181   ATC CTG GAC GCG CTG AAG AAG GAT AGT TCG CGG CAC TCC AAG CTG   225
61     I   L   D   A   L   K   K   D   S   S   R   H   S   K   L    75

226   GAG AAG GCC GAC ATC CTG GAG ATG ACC GTC AAG CAC CTG CGG AGC   270
76     E   K   A   D   I   L   E   M   T   V   K   H   L   R   S    90

271   CTG CAG CGG GCG CAG ATG ACC GCT GCG CTG AGC ACA GAC CCT ACG   315
91     L   Q   R   A   Q   M   T   A   A   L   S   T   D   P   T   105

316   GTG CTG GGC AAG TAC CGC GCC GGC TTC AGC GAG TGC ATG AAC GAA   360
106    V   L   G   K   Y   R   A   G   F   S   E   C   M   N   E   120

361   GTG ACG CGG TTC CTC TCC ACC TGC GAA GGC GTC AAC GCT GAG GTG   405
```

```
121   V   T   R   F   L   S   T   C   E   G   V   N   A   E   V   135

406   CGC ACC CGG CTC CTG GGC CAC CTG GCC AGC TGC ATG ACC CAG ATC   450

136   R   T   R   L   L   G   H   L   A   S   C   M   T   Q   I   150

451   AAC GCC ATC AAC TAC CCC GTG CCG CCC CCG CCG CTG CCA CCC CCA   495

151   N   A   I   N   Y   P   V   P   P   P   P   L   P   P   P   165

496   CCC GCA GCC TTC GGG CCG CCC CTG GTG CCG CCG GGC GGA GGC GCG   540

166   P   A   A   F   G   P   P   L   V   P   P   G   G   G   A   180

541   GGG CCG CTC CCA GCC GTA CCC TGC AAG CCA GGT GCC GAT GCG GCC   585

181   G   P   L   P   A   V   P   C   K   P   G   A   D   A   A   195

586   AAG GTG TAC GGT GGT TTC CAG CTG CTG CCT GCC TCT GAT GGG CAG   630

196   K   V   Y   G   G   F   Q   L   L   P   A   S   D   G   Q   210

631   TTC GCC TTC CTC ATC CCC AGC GCT GCC TTT GCT CCC GGC GGG GCT   675

211   F   A   F   L   I   P   S   A   A   F   A   P   G   G   A   225

676   GTG CTG CCC CTC TAT GGC GGT CCC CCC ACA GCT GCC ACC ACC GCC   720

226   V   L   P   L   Y   G   G   P   P   T   A   A   T   T   A   240

721   TCG CCT CCC GGC CCC TCA CCC GGC ACC GCT GAC TCA GTC TGG AGG   765

241   S   P   P   G   P   S   P   G   T   A   D   S   V   W   R   255

766   CCC TGG TGA   774

256   P   W   *
```

Appendix E

cHairy2ΔWRPW

```
1     ATG CCT GCC GAC CTG ATG GAG AAG AGC AGC GCC TCG CCG GTG GCC   45
1      M   P   A   D   L   M   E   K   S   S   A   S   P   V   A    15

46    GCC ACC CCC GCC AGC ATC AAC GCG ACG CCC GAT AAG CCC AAA ACG   90
16     A   T   P   A   S   I   N   A   T   P   D   K   P   K   T    30

91    GCG GCG GAG CAC CGG AAG TCC TCC AAA CCC ATC ATG GAG AAG CGG   135
31     A   A   E   H   R   K   S   S   K   P   I   M   E   K   R    45

136   CGG CGG GCG CGC ATC AAC GAG AGC CTG GGG CAG CTG AAG ACG CTG   180
46     R   R   A   R   I   N   E   S   L   G   Q   L   K   T   L    60

181   ATC CTG GAC GCG CTG AAG AAG GAT AGT TCG CGG CAC TCC AAG CTG   225
61     I   L   D   A   L   K   K   D   S   S   R   H   S   K   L    75

226   GAG AAG GCC GAC ATC CTG GAG ATG ACC GTC AAG CAC CTG CGG AGC   270
76     E   K   A   D   I   L   E   M   T   V   K   H   L   R   S    90

271   CTG CAG CGG GCG CAG ATG ACC GCT GCG CTG AGC ACA GAC CCT ACG   315
91     L   Q   R   A   Q   M   T   A   A   L   S   T   D   P   T   105

316   GTG CTG GGC AAG TAC CGC GCC GGC TTC AGC GAG TGC ATG AAC GAA   360
106    V   L   G   K   Y   R   A   G   F   S   E   C   M   N   E   120

361   GTG ACG CGG TTC CTC TCC ACC TGC GAA GGC GTC AAC GCT GAG GTG   405
```

```
121    V   T   R   F   L   S   T   C   E   G   V   N   A   E   V    135

406   CGC ACC CGG CTC CTG GGC CAC CTG GCC AGC TGC ATG ACC CAG ATC   450

136    R   T   R   L   L   G   H   L   A   S   C   M   T   Q   I    150

451   AAC GCC ATC AAC TAC CCC GTG CCG CCC CCG CCG CTG CCA CCC CCA   495

151    N   A   I   N   Y   P   V   P   P   P   P   L   P   P   P    165

496   CCC GCA GCC TTC GGG CCG CCC CTG GTG CCG CCG GGC GGA GGC GCG   540

166    P   A   A   F   G   P   P   L   V   P   P   G   G   G   A    180

541   GGG CCG CTC CCA GCC GTA CCC TGC AAG CCA GGT GCC GAT GCG GCC   585

181    G   P   L   P   A   V   P   C   K   P   G   A   D   A   A    195

586   AAG GTG TAC GGT GGT TTC CAG CTG CTG CCT GCC TCT GAT GGG CAG   630

196    K   V   Y   G   G   F   Q   L   L   P   A   S   D   G   Q    210

631   TTC GCC TTC CTC ATC CCC AGC GCT GCC TTT GCT CCC GGC GGG GCT   675

211    F   A   F   L   I   P   S   A   A   F   A   P   G   G   A    225

676   GTG CTG CCC CTC TAT GGC GGT CCC CCC ACA GCT GCC ACC ACC GCC   720

226    V   L   P   L   Y   G   G   P   P   T   A   A   T   T   A    240

721   TCG CCT CCC GGC CCC TCA CCC GGC ACC GCT GAC TCA GTC TGA   762

241    S   P   P   G   P   S   P   G   T   A   D   S   V   *
```

Bibliography

Alder, J., Lee, K. J., Jessell, T. M. and Hatten, M. E. (1999) 'Generation of cerebellar granule neurons in vivo by transplantation of BMP-treated neural progenitor cells', *Nature neuroscience* 2(6): 535-40.

Alvarez-Medina, R., Cayuso, J., Okubo, T., Takada, S. and Marti, E. (2008) 'Wnt canonical pathway restricts graded Shh/Gli patterning activity through the regulation of Gli3 expression', *Development* 135(2): 237-47.

Amoyel, M., Cheng, Y. C., Jiang, Y. J. and Wilkinson, D. G. (2005) 'Wnt1 regulates neurogenesis and mediates lateral inhibition of boundary cell specification in the zebrafish hindbrain', *Development* 132(4): 775-85.

Andreae, L. C., Lumsden, A. and Gilthorpe, J. D. (2009) 'Chick Lrrn2, a novel downstream effector of Hoxb1 and Shh, functions in the selective targeting of rhombomere 4 motor neurons', *Neural Dev* 4: 27.

Assimacopoulos, S., Grove, E. A. and Ragsdale, C. W. (2003) 'Identification of a Pax6-dependent epidermal growth factor family signaling source at the lateral edge of the embryonic cerebral cortex', *The Journal of neuroscience : the official journal of the Society for Neuroscience* 23(16): 6399-403.

Augustine, K., Liu, E. T. and Sadler, T. W. (1993) 'Antisense attenuation of Wnt-1 and Wnt-3a expression in whole embryo culture reveals roles for these genes in craniofacial, spinal cord, and cardiac morphogenesis', *Developmental genetics* 14(6): 500-20.

Awatramani, R., Soriano, P., Rodriguez, C., Mai, J. J. and Dymecki, S. M. (2003) 'Cryptic boundaries in roof plate and choroid plexus identified by intersectional gene activation', *Nature genetics* 35(1): 70-5.

Bach, A., Lallemand, Y., Nicola, M. A., Ramos, C., Mathis, L., Maufras, M. and Robert, B. (2003) 'Msx1 is required for dorsal diencephalon patterning', *Development* 130(17): 4025-36.

Baek, J. H., Hatakeyama, J., Sakamoto, S., Ohtsuka, T. and Kageyama, R. (2006) 'Persistent and high levels of Hes1 expression regulate boundary formation in the developing central nervous system', *Development* 133(13): 2467-76.

Barth, K. A., Kishimoto, Y., Rohr, K. B., Seydler, C., Schulte-Merker, S. and Wilson, S. W. (1999) 'Bmp activity establishes a gradient of positional information throughout the entire neural plate', *Development* 126(22): 4977-87.

Begbie, J., Brunet, J. F., Rubenstein, J. L. and Graham, A. (1999) 'Induction of the epibranchial placodes', *Development* 126(5): 895-902.

Bel-Vialar, S., Itasaki, N. and Krumlauf, R. (2002) 'Initiating Hox gene expression: in the early chick neural tube differential sensitivity to FGF and RA signaling subdivides the HoxB genes in two distinct groups', *Development* 129(22): 5103-15.

Bell, E., Wingate, R. J. and Lumsden, A. (1999) 'Homeotic transformation of rhombomere identity after localized Hoxb1 misexpression', *Science* 284(5423): 2168-71.

Ben-Arie, N., Hassan, B. A., Bermingham, N. A., Malicki, D. M., Armstrong, D., Matzuk, M., Bellen, H. J. and Zoghbi, H. Y. (2000) 'Functional conservation of atonal and Math1 in the CNS and PNS', *Development* 127(5): 1039-48.

Bill, B. R., Balciunas, D., McCarra, J. A., Young, E. D., Xiong, T., Spahn, A. M., Garcia-Lecea, M., Korzh, V., Ekker, S. C. and Schimmenti, L. A. (2008) 'Development and Notch signaling requirements of the zebrafish choroid plexus', *PloS one* 3(9): e3114.

Bingham, S., Chaudhari, S., Vanderlaan, G., Itoh, M., Chitnis, A. and Chandrasekhar, A. (2003) 'Neurogenic phenotype of mind bomb mutants leads to severe patterning defects in the zebrafish hindbrain', *Developmental dynamics : an official publication of the American Association of Anatomists* 228(3): 451-63.

Bishop, S. A., Klein, T., Arias, A. M. and Couso, J. P. (1999) 'Composite signalling from Serrate and Delta establishes leg segments in Drosophila through Notch', *Development* 126(13): 2993-3003.

Bonner, J., Gribble, S. L., Veien, E. S., Nikolaus, O. B., Weidinger, G. and Dorsky, R. I. (2008) 'Proliferation and patterning are mediated independently in the dorsal spinal cord downstream of canonical Wnt signaling', *Developmental biology* 313(1): 398-407.

Bray, S. J. (2006) 'Notch signalling: a simple pathway becomes complex', *Nature reviews. Molecular cell biology* 7(9): 678-89.

Briscoe, J. and Ericson, J. (2001) 'Specification of neuronal fates in the ventral neural tube', *Current opinion in neurobiology* 11(1): 43-9.

Briscoe, J., Pierani, A., Jessell, T. M. and Ericson, J. (2000) 'A homeodomain protein code specifies progenitor cell identity and neuronal fate in the ventral neural tube', *Cell* 101(4): 435-45.

Briscoe, J., Sussel, L., Serup, P., Hartigan-O'Connor, D., Jessell, T. M., Rubenstein, J. L. and Ericson, J. (1999) 'Homeobox gene Nkx2.2 and specification of neuronal identity by graded Sonic hedgehog signalling', *Nature* 398(6728): 622-7.
Bronner-Fraser, M. and Fraser, S. E. (1988) 'Cell lineage analysis reveals multipotency of some avian neural crest cells', *Nature* 335(6186): 161-4.
Bruckner, K., Perez, L., Clausen, H. and Cohen, S. (2000) 'Glycosyltransferase activity of Fringe modulates Notch-Delta interactions', *Nature* 406(6794): 411-5.
Carpenter, E. M., Goddard, J. M., Davis, A. P., Nguyen, T. P. and Capecchi, M. R. (1997) 'Targeted disruption of Hoxd-10 affects mouse hindlimb development', *Development* 124(22): 4505-14.
Catala, M., Teillet, M. A., De Robertis, E. M. and Le Douarin, M. L. (1996) 'A spinal cord fate map in the avian embryo: while regressing, Hensen's node lays down the notochord and floor plate thus joining the spinal cord lateral walls', *Development* 122(9): 2599-610.
Cavallaro, T., Martone, R. L., Stylianopoulou, F. and Herbert, J. (1993) 'Differential expression of the insulin-like growth factor II and transthyretin genes in the developing rat choroid plexus', *J Neuropathol Exp Neurol* 52(2): 153-62.
Chamberlain, C. E., Jeong, J., Guo, C., Allen, B. L. and McMahon, A. P. (2008) 'Notochord-derived Shh concentrates in close association with the apically positioned basal body in neural target cells and forms a dynamic gradient during neural patterning', *Development* 135(6): 1097-106.
Chaplin, N., Tendeng, C. and Wingate, R. J. (2010) 'Absence of an external germinal layer in zebrafish and shark reveals a distinct, anamniote ground plan of cerebellum development', *The Journal of neuroscience : the official journal of the Society for Neuroscience* 30(8): 3048-57.
Cheng, Y. C., Amoyel, M., Qiu, X., Jiang, Y. J., Xu, Q. and Wilkinson, D. G. (2004) 'Notch activation regulates the segregation and differentiation of rhombomere boundary cells in the zebrafish hindbrain', *Developmental cell* 6(4): 539-50.
Chenn, A. and Walsh, C. A. (2002) 'Regulation of cerebral cortical size by control of cell cycle exit in neural precursors', *Science* 297(5580): 365-9.
Chesnutt, C., Burrus, L. W., Brown, A. M. and Niswander, L. (2004) 'Coordinate regulation of neural tube patterning and proliferation by TGFbeta and WNT activity', *Developmental biology* 274(2): 334-47.
Chiang, C., Litingtung, Y., Lee, E., Young, K. E., Corden, J. L., Westphal, H. and Beachy, P. A. (1996) 'Cyclopia and defective axial patterning in mice lacking Sonic hedgehog gene function', *Nature* 383(6599): 407-13.
Chizhikov, V. V., Lindgren, A. G., Currle, D. S., Rose, M. F., Monuki, E. S. and Millen, K. J. (2006) 'The roof plate regulates cerebellar cell-type specification and proliferation', *Development* 133(15): 2793-804.
Chizhikov, V. V., Lindgren, A. G., Mishima, Y., Roberts, R. W., Aldinger, K. A., Miesegaes, G. R., Currle, D. S., Monuki, E. S. and Millen, K. J. (2010) 'Lmx1a regulates fates and location of cells originating from the cerebellar rhombic lip and telencephalic cortical hem', *Proceedings of the National Academy of Sciences of the United States of America* 107(23): 10725-30.
Chizhikov, V. V. and Millen, K. J. (2004a) 'Control of roof plate development and signaling by Lmx1b in the caudal vertebrate CNS', *The Journal of neuroscience : the official journal of the Society for Neuroscience* 24(25): 5694-703.
Chizhikov, V. V. and Millen, K. J. (2004b) 'Control of roof plate formation by Lmx1a in the developing spinal cord', *Development* 131(11): 2693-705.
Chizhikov, V. V. and Millen, K. J. (2004c) 'Mechanisms of roof plate formation in the vertebrate CNS', *Nature reviews. Neuroscience* 5(10): 808-12.
Chizhikov, V. V. and Millen, K. J. (2005) 'Roof plate-dependent patterning of the vertebrate dorsal central nervous system', *Developmental biology* 277(2): 287-95.
Cooke, J., Moens, C., Roth, L., Durbin, L., Shiomi, K., Brennan, C., Kimmel, C., Wilson, S. and Holder, N. (2001) 'Eph signalling functions downstream of Val to regulate cell sorting and boundary formation in the caudal hindbrain', *Development* 128(4): 571-80.
Cooke, J. E., Kemp, H. A. and Moens, C. B. (2005) 'EphA4 is required for cell adhesion and rhombomere-boundary formation in the zebrafish', *Current biology : CB* 15(6): 536-42.
Cooke, J. E. and Moens, C. B. (2002) 'Boundary formation in the hindbrain: Eph only it were simple', *Trends in neurosciences* 25(5): 260-7.
Crossley, P. H., Martinez, S. and Martin, G. R. (1996) 'Midbrain development induced by FGF8 in the chick embryo', *Nature* 380(6569): 66-8.
Currle, D. S., Cheng, X., Hsu, C. M. and Monuki, E. S. (2005) 'Direct and indirect roles of CNS dorsal midline cells in choroid plexus epithelia formation', *Development* 132(15): 3549-59.

Curtin, J. A., Quint, E., Tsipouri, V., Arkell, R. M., Cattanach, B., Copp, A. J., Henderson, D. J., Spurr, N., Stanier, P., Fisher, E. M. et al. (2003) 'Mutation of Celsr1 disrupts planar polarity of inner ear hair cells and causes severe neural tube defects in the mouse', *Current biology : CB* 13(13): 1129-33.
Dale, J. K., Maroto, M., Dequeant, M. L., Malapert, P., McGrew, M. and Pourquie, O. (2003) 'Periodic notch inhibition by lunatic fringe underlies the chick segmentation clock', *Nature* 421(6920): 275-8.
Dasen, J. S., Liu, J. P. and Jessell, T. M. (2003) 'Motor neuron columnar fate imposed by sequential phases of Hox-c activity', *Nature* 425(6961): 926-33.
Dawson, S. R., Turner, D. L., Weintraub, H. and Parkhurst, S. M. (1995) 'Specificity for the hairy/enhancer of split basic helix-loop-helix (bHLH) proteins maps outside the bHLH domain and suggests two separable modes of transcriptional repression', *Molecular and cellular biology* 15(12): 6923-31.
de Celis, J. F. and Bray, S. (1997) 'Feed-back mechanisms affecting Notch activation at the dorsoventral boundary in the Drosophila wing', *Development* 124(17): 3241-51.
de Celis, J. F., Tyler, D. M., de Celis, J. and Bray, S. J. (1998) 'Notch signalling mediates segmentation of the Drosophila leg', *Development* 125(23): 4617-26.
del Álamo D, Rouault H, Schweisguth F. (2011) ‘Mechanism and significance of cis-inhibition in Notch signalling’, *Current Biology* 21(1):R40-7.
De Robertis, E. M. and Kuroda, H. (2004) 'Dorsal-ventral patterning and neural induction in Xenopus embryos', *Annual review of cell and developmental biology* 20: 285-308.
Deardorff, M. A., Tan, C., Saint-Jeannet, J. P. and Klein, P. S. (2001) 'A role for frizzled 3 in neural crest development', *Development* 128(19): 3655-63.
Dessaud, E., McMahon, A. P. and Briscoe, J. (2008) 'Pattern formation in the vertebrate neural tube: a sonic hedgehog morphogen-regulated transcriptional network', *Development* 135(15): 2489-503.
Dessaud, E., Yang, L. L., Hill, K., Cox, B., Ulloa, F., Ribeiro, A., Mynett, A., Novitch, B. G. and Briscoe, J. (2007) 'Interpretation of the sonic hedgehog morphogen gradient by a temporal adaptation mechanism', *Nature* 450(7170): 717-20.
Diaz-Benjumea, F. J. and Cohen, S. M. (1995) 'Serrate signals through Notch to establish a Wingless-dependent organizer at the dorsal/ventral compartment boundary of the Drosophila wing', *Development* 121(12): 4215-25.
Dickinson, M. E., Krumlauf, R. and McMahon, A. P. (1994) 'Evidence for a mitogenic effect of Wnt-1 in the developing mammalian central nervous system', *Development* 120(6): 1453-71.
Dickinson, M. E., Selleck, M. A., McMahon, A. P. and Bronner-Fraser, M. (1995) 'Dorsalization of the neural tube by the non-neural ectoderm', *Development* 121(7): 2099-106.
Doherty, D., Feger, G., Younger-Shepherd, S., Jan, L. Y. and Jan, Y. N. (1996) 'Delta is a ventral to dorsal signal complementary to Serrate, another Notch ligand, in Drosophila wing formation', *Genes & development* 10(4): 421-34.
Dohrmann, G. J. (1970) 'The choroid plexus: a historical review', *Brain research* 18(2): 197-218.
Doudney, K. and Stanier, P. (2005) 'Epithelial cell polarity genes are required for neural tube closure', *American journal of medical genetics. Part C, Seminars in medical genetics* 135C(1): 42-7.
Duan, W., Achen, M. G., Richardson, S. J., Lawrence, M. C., Wettenhall, R. E., Jaworowski, A. and Schreiber, G. (1991) 'Isolation, characterization, cDNA cloning and gene expression of an avian transthyretin. Implications for the evolution of structure and function of transthyretin in vertebrates', *European journal of biochemistry / FEBS* 200(3): 679-87.
Duester, G. (2000) 'Families of retinoid dehydrogenases regulating vitamin A function: production of visual pigment and retinoic acid', *European journal of biochemistry / FEBS* 267(14): 4315-24.
Durston, A. J., Timmermans, J. P., Hage, W. J., Hendriks, H. F., de Vries, N. J., Heideveld, M. and Nieuwkoop, P. D. (1989) 'Retinoic acid causes an anteroposterior transformation in the developing central nervous system', *Nature* 340(6229): 140-4.
Dziegielewska, K. M., Ek, J., Habgood, M. D. and Saunders, N. R. (2001) 'Development of the choroid plexus', *Microsc Res Tech* 52(1): 5-20.
Echelard, Y., Epstein, D. J., St-Jacques, B., Shen, L., Mohler, J., McMahon, J. A. and McMahon, A. P. (1993) 'Sonic hedgehog, a member of a family of putative signaling molecules, is implicated in the regulation of CNS polarity', *Cell* 75(7): 1417-30.
Echelard, Y., Vassileva, G. and McMahon, A. P. (1994) 'Cis-acting regulatory sequences governing Wnt-1 expression in the developing mouse CNS', *Development* 120(8): 2213-24.
Elsen, G. E., Choi, L. Y., Millen, K. J., Grinblat, Y. and Prince, V. E. (2008) 'Zic1 and Zic4 regulate zebrafish roof plate specification and hindbrain ventricle morphogenesis', *Developmental biology* 314(2): 376-92.

Ericson, J., Briscoe, J., Rashbass, P., van Heyningen, V. and Jessell, T. M. (1997) 'Graded sonic hedgehog signaling and the specification of cell fate in the ventral neural tube', *Cold Spring Harbor symposia on quantitative biology* 62: 451-66.
Ericson, J., Morton, S., Kawakami, A., Roelink, H. and Jessell, T. M. (1996) 'Two critical periods of Sonic Hedgehog signaling required for the specification of motor neuron identity', *Cell* 87(4): 661-73.
Ericson, J., Thor, S., Edlund, T., Jessell, T. M. and Yamada, T. (1992) 'Early stages of motor neuron differentiation revealed by expression of homeobox gene Islet-1', *Science* 256(5063): 1555-60.
Fehon, R. G., Johansen, K., Rebay, I. and Artavanis-Tsakonas, S. (1991) 'Complex cellular and subcellular regulation of notch expression during embryonic and imaginal development of Drosophila: implications for notch function', *The Journal of cell biology* 113(3): 657-69.
Fishell, G., Mason, C. A. and Hatten, M. E. (1993) 'Dispersion of neural progenitors within the germinal zones of the forebrain', *Nature* 362(6421): 636-8.
Fisher, A. L., Ohsako, S. and Caudy, M. (1996) 'The WRPW motif of the hairy-related basic helix-loop-helix repressor proteins acts as a 4-amino-acid transcription repression and protein-protein interaction domain', *Molecular and cellular biology* 16(6): 2670-7.
Fleming, R. J., Gu, Y. and Hukriede, N. A. (1997) 'Serrate-mediated activation of Notch is specifically blocked by the product of the gene fringe in the dorsal compartment of the Drosophila wing imaginal disc', *Development* 124(15): 2973-81.
Francis-West, P. H., Abdelfattah, A., Chen, P., Allen, C., Parish, J., Ladher, R., Allen, S., MacPherson, S., Luyten, F. P. and Archer, C. W. (1999) 'Mechanisms of GDF-5 action during skeletal development', *Development* 126(6): 1305-15.
Fraser, S., Keynes, R. and Lumsden, A. (1990) 'Segmentation in the chick embryo hindbrain is defined by cell lineage restrictions', *Nature* 344(6265): 431-5.
Frowein, J., Campbell, K. and Gotz, M. (2002) 'Expression of Ngn1, Ngn2, Cash1, Gsh2 and Sfrp1 in the developing chick telencephalon', *Mechanisms of development* 110(1-2): 249-52.
Fukuchi-Shimogori, T. and Grove, E. A. (2001) 'Neocortex patterning by the secreted signaling molecule FGF8', *Science* 294(5544): 1071-4.
Furuta, Y., Piston, D. W. and Hogan, B. L. (1997) 'Bone morphogenetic proteins (BMPs) as regulators of dorsal forebrain development', *Development* 124(11): 2203-12.
Galceran, J., Miyashita-Lin, E. M., Devaney, E., Rubenstein, J. L. and Grosschedl, R. (2000) 'Hippocampus development and generation of dentate gyrus granule cells is regulated by LEF1', *Development* 127(3): 469-82.
Garcia-Bellido, A., Ripoll, P. and Morata, G. (1973) 'Developmental compartmentalisation of the wing disk of Drosophila', *Nature: New biology* 245(147): 251-3.
Garcia-Bellido, A., Ripoll, P. and Morata, G. (1976) 'Developmental compartmentalization in the dorsal mesothoracic disc of Drosophila', *Developmental biology* 48(1): 132-47.
Garcia-Castro, M. I., Marcelle, C. and Bronner-Fraser, M. (2002) 'Ectodermal Wnt function as a neural crest inducer', *Science* 297(5582): 848-51.
Garcia-Lecea, M., Kondrychyn, I., Fong, S. H., Ye, Z. R. and Korzh, V. (2008) 'In vivo analysis of choroid plexus morphogenesis in zebrafish', *PloS one* 3(9): e3090.
Garel, S., Huffman, K. J. and Rubenstein, J. L. (2003) 'Molecular regionalization of the neocortex is disrupted in Fgf8 hypomorphic mutants', *Development* 130(9): 1903-14.
Geling, A., Itoh, M., Tallafuss, A., Chapouton, P., Tannhauser, B., Kuwada, J. Y., Chitnis, A. B. and Bally-Cuif, L. (2003) 'bHLH transcription factor Her5 links patterning to regional inhibition of neurogenesis at the midbrain-hindbrain boundary', *Development* 130(8): 1591-604.
Geling, A., Plessy, C., Rastegar, S., Strahle, U. and Bally-Cuif, L. (2004) 'Her5 acts as a prepattern factor that blocks neurogenin1 and coe2 expression upstream of Notch to inhibit neurogenesis at the midbrain-hindbrain boundary', *Development* 131(9): 1993-2006.
Gerety, S. S. and Wilkinson, D. G. (2011) 'Morpholino artifacts provide pitfalls and reveal a novel role for pro-apoptotic genes in hindbrain boundary development', *Developmental biology* 350(2): 279-89.
Gibson, P., Tong, Y., Robinson, G., Thompson, M. C., Currle, D. S., Eden, C., Kranenburg, T. A., Hogg, T., Poppleton, H., Martin, J. et al. (2010) 'Subtypes of medulloblastoma have distinct developmental origins', *Nature* 468(7327): 1095-9.
Giebel, B. and Campos-Ortega, J. A. (1997) 'Functional dissection of the Drosophila enhancer of split protein, a suppressor of neurogenesis', *Proceedings of the National Academy of Sciences of the United States of America* 94(12): 6250-4.
Gilthorpe, J. D., Papantoniou, E. K., Chedotal, A., Lumsden, A. and Wingate, R. J. (2002) 'The migration of cerebellar rhombic lip derivatives', *Development* 129(20): 4719-28.

Gospodarowicz, D. (1974) 'Localisation of a fibroblast growth factor and its effect alone and with hydrocortisone on 3T3 cell growth', *Nature* 249(453): 123-7.
Goulding, M. D., Lumsden, A. and Gruss, P. (1993) 'Signals from the notochord and floor plate regulate the region-specific expression of two Pax genes in the developing spinal cord', *Development* 117(3): 1001-16.
Gowan, K., Helms, A. W., Hunsaker, T. L., Collisson, T., Ebert, P. J., Odom, R. and Johnson, J. E. (2001) 'Crossinhibitory activities of Ngn1 and Math1 allow specification of distinct dorsal interneurons', *Neuron* 31(2): 219-32.
Graham, A., Francis-West, P., Brickell, P. and Lumsden, A. (1994) 'The signalling molecule BMP4 mediates apoptosis in the rhombencephalic neural crest', *Nature* 372(6507): 684-6.
Grbavec, D., Lo, R., Liu, Y. and Stifani, S. (1998) 'Transducin-like Enhancer of split 2, a mammalian homologue of Drosophila Groucho, acts as a transcriptional repressor, interacts with Hairy/Enhancer of split proteins, and is expressed during neuronal development', *European journal of biochemistry / FEBS* 258(2): 339-49.
Grove, E. A., Tole, S., Limon, J., Yip, L. and Ragsdale, C. W. (1998) 'The hem of the embryonic cerebral cortex is defined by the expression of multiple Wnt genes and is compromised in Gli3-deficient mice', *Development* 125(12): 2315-25.
Guinazu, M. F., Chambers, D., Lumsden, A. and Kiecker, C. (2007) 'Tissue interactions in the developing chick diencephalon', *Neural Dev* 2: 25.
Guo, S., Brush, J., Teraoka, H., Goddard, A., Wilson, S. W., Mullins, M. C. and Rosenthal, A. (1999) 'Development of noradrenergic neurons in the zebrafish hindbrain requires BMP, FGF8, and the homeodomain protein soulless/Phox2a', *Neuron* 24(3): 555-66.
Gurdon, J. B. (1992) 'The generation of diversity and pattern in animal development', *Cell* 68(2): 185-99.
Guthrie, S., Butcher, M. and Lumsden, A. (1991) 'Patterns of cell division and interkinetic nuclear migration in the chick embryo hindbrain', *Journal of neurobiology* 22(7): 742-54.
Guthrie, S. and Lumsden, A. (1991) 'Formation and regeneration of rhombomere boundaries in the developing chick hindbrain', *Development* 112(1): 221-9.
Guthrie, S., Prince, V. and Lumsden, A. (1993) 'Selective dispersal of avian rhombomere cells in orthotopic and heterotopic grafts', *Development* 118(2): 527-38.
Hamburger, V. and Hamilton, H. L. (1951) 'A series of normal stages in the development of the chick embryo', *Journal of Morphology* 88(1): 49 - 92.
Hatakeyama, J., Bessho, Y., Katoh, K., Ookawara, S., Fujioka, M., Guillemot, F. and Kageyama, R. (2004) 'Hes genes regulate size, shape and histogenesis of the nervous system by control of the timing of neural stem cell differentiation', *Development* 131(22): 5539-50.
Hebert, J. M., Mishina, Y. and McConnell, S. K. (2002) 'BMP signaling is required locally to pattern the dorsal telencephalic midline', *Neuron* 35(6): 1029-41.
Helms, A. W. and Johnson, J. E. (1998) 'Progenitors of dorsal commissural interneurons are defined by MATH1 expression', *Development* 125(5): 919-28.
Henrique, D., Hirsinger, E., Adam, J., Le Roux, I., Pourquie, O., Ish-Horowicz, D. and Lewis, J. (1997) 'Maintenance of neuroepithelial progenitor cells by Delta-Notch signalling in the embryonic chick retina', *Current biology : CB* 7(9): 661-70.
Heyman, I., Faissner, A. and Lumsden, A. (1995) 'Cell and matrix specialisations of rhombomere boundaries', *Developmental dynamics : an official publication of the American Association of Anatomists* 204(3): 301-15.
Heyman, I., Kent, A. and Lumsden, A. (1993) 'Cellular morphology and extracellular space at rhombomere boundaries in the chick embryo hindbrain', *Developmental dynamics : an official publication of the American Association of Anatomists* 198(4): 241-53.
Hicks, C., Johnston, S. H., diSibio, G., Collazo, A., Vogt, T. F. and Weinmaster, G. (2000) 'Fringe differentially modulates Jagged1 and Delta1 signalling through Notch1 and Notch2', *Nature cell biology* 2(8): 515-20.
Hirabayashi, Y., Itoh, Y., Tabata, H., Nakajima, K., Akiyama, T., Masuyama, N. and Gotoh, Y. (2004) 'The Wnt/beta-catenin pathway directs neuronal differentiation of cortical neural precursor cells', *Development* 131(12): 2791-801.
Hirata, H., Tomita, K., Bessho, Y. and Kageyama, R. (2001) 'Hes1 and Hes3 regulate maintenance of the isthmic organizer and development of the mid/hindbrain', *The EMBO journal* 20(16): 4454-66.
Hirata, H., Yoshiura, S., Ohtsuka, T., Bessho, Y., Harada, T., Yoshikawa, K. and Kageyama, R. (2002) 'Oscillatory expression of the bHLH factor Hes1 regulated by a negative feedback loop', *Science* 298(5594): 840-3.

Hollyday, M., McMahon, J. A. and McMahon, A. P. (1995) 'Wnt expression patterns in chick embryo nervous system', *Mechanisms of development* 52(1): 9-25.
Honig, L. S. (1981) 'Positional signal transmission in the developing chick limb', *Nature* 291(5810): 72-3.
Hu, H. (1999) 'Chemorepulsion of neuronal migration by Slit2 in the developing mammalian forebrain', *Neuron* 23(4): 703-11.
Huang, X., Ketova, T., Fleming, J. T., Wang, H., Dey, S. K., Litingtung, Y. and Chiang, C. (2009) 'Sonic hedgehog signaling regulates a novel epithelial progenitor domain of the hindbrain choroid plexus', *Development* 136(15): 2535-43.
Huang, X., Liu, J., Ketova, T., Fleming, J. T., Grover, V. K., Cooper, M. K., Litingtung, Y. and Chiang, C. (2010) 'Transventricular delivery of Sonic hedgehog is essential to cerebellar ventricular zone development', *Proceedings of the National Academy of Sciences of the United States of America* 107(18): 8422-7.
Hunter, N. L. and Dymecki, S. M. (2007) 'Molecularly and temporally separable lineages form the hindbrain roof plate and contribute differentially to the choroid plexus', *Development* 134(19): 3449-60.
Ikeya, M., Lee, S. M., Johnson, J. E., McMahon, A. P. and Takada, S. (1997) 'Wnt signalling required for expansion of neural crest and CNS progenitors', *Nature* 389(6654): 966-70.
Imayoshi, I., Shimogori, T., Ohtsuka, T. and Kageyama, R. (2008) 'Hes genes and neurogenin regulate non-neural versus neural fate specification in the dorsal telencephalic midline', *Development* 135(15): 2531-41.
In der Rieden, P. M., Vilaspasa, F. L. and Durston, A. J. (2010) 'Xwnt8 directly initiates expression of labial Hox genes', *Developmental dynamics : an official publication of the American Association of Anatomists* 239(1): 126-39.
Irvine, K. D. and Rauskolb, C. (2001) 'Boundaries in development: formation and function', *Annual review of cell and developmental biology* 17: 189-214.
Irvine, K. D. and Wieschaus, E. (1994) 'fringe, a Boundary-specific signaling molecule, mediates interactions between dorsal and ventral cells during Drosophila wing development', *Cell* 79(4): 595-606.
Irving, C. and Mason, I. (1999) 'Regeneration of isthmic tissue is the result of a specific and direct interaction between rhombomere 1 and midbrain', *Development* 126(18): 3981-9.
Irving, C. and Mason, I. (2000) 'Signalling by FGF8 from the isthmus patterns anterior hindbrain and establishes the anterior limit of Hox gene expression', *Development* 127(1): 177-86.
Itoh M., Kim C.H., Palardy G., Oda T., Jiang Y.J., Maust D., Yeo S.Y., Lorick K., Wright G.J., Ariza-McNaughton L., Weissman A.M., Lewis J., Chandrasekharappa S.C. and Chitnis A.B. (2003) 'Mind bomb is a ubiquitin ligase that is essential for efficient activation of Notch signaling by Delta', *Developmental Cell* 4(1):67-82.
Jacobsen, M., Clausen, P. P., Jacobsen, G. K., Saunders, N. R. and Mollgard, K. (1982) 'Intracellular plasma proteins in human fetal choroid plexus during development. I. Developmental stages in relation to the number of epithelial cells which contain albumin in telencephalic, diencephalic and myelencephalic choroid plexus', *Brain research* 255(2): 239-50.
Jimenez-Guri, E., Udina, F., Colas, J. F., Sharpe, J., Padron-Barthe, L., Torres, M. and Pujades, C. (2010) 'Clonal analysis in mice underlines the importance of rhombomeric boundaries in cell movement restriction during hindbrain segmentation', *PloS one* 5(4): e10112.
Johansson, P. A., Dziegielewska, K. M., Liddelow, S. A. and Saunders, N. R. (2008) 'The blood-CSF barrier explained: when development is not immaturity', *BioEssays : news and reviews in molecular, cellular and developmental biology* 30(3): 237-48.
Jouve, C., Palmeirim, I., Henrique, D., Beckers, J., Gossler, A., Ish-Horowicz, D. and Pourquie, O. (2000) 'Notch signalling is required for cyclic expression of the hairy-like gene HES1 in the presomitic mesoderm', *Development* 127(7): 1421-9.
Jungbluth, S., Larsen, C., Wizenmann, A. and Lumsden, A. (2001) 'Cell mixing between the embryonic midbrain and hindbrain', *Current biology : CB* 11(3): 204-7.
Kageyama, R., Ohtsuka, T. and Kobayashi, T. (2007) 'The Hes gene family: repressors and oscillators that orchestrate embryogenesis', *Development* 134(7): 1243-51.
Kageyama, R., Ohtsuka, T. and Kobayashi, T. (2008) 'Roles of Hes genes in neural development', *Development, growth & differentiation* 50 Suppl 1: S97-103.
Kahane, N. and Kalcheim, C. (1998) 'Identification of early postmitotic cells in distinct embryonic sites and their possible roles in morphogenesis', *Cell and tissue research* 294(2): 297-307.
Kato T.M., Kawaguchi A., Kosodo Y., Niwa H. and Matsuzaki F. (2010) 'Lunatic fringe potentiates Notch signalling in the developing brain', Mol Cell Neurosci. 45(1):12-25.

Kiecker, C. and Lumsden, A. (2004) 'Hedgehog signaling from the ZLI regulates diencephalic regional identity', *Nature neuroscience* 7(11): 1242-9.
Kiecker, C. and Lumsden, A. (2005) 'Compartments and their boundaries in vertebrate brain development', *Nature reviews. Neuroscience* 6(7): 553-64.
Kiecker, C. and Niehrs, C. (2001a) 'A morphogen gradient of Wnt/beta-catenin signalling regulates anteroposterior neural patterning in Xenopus', *Development* 128(21): 4189-201.
Kiecker, C. and Niehrs, C. (2001b) 'The role of prechordal mesendoderm in neural patterning', *Current opinion in neurobiology* 11(1): 27-33.
Kim, J., Irvine, K. D. and Carroll, S. B. (1995) 'Cell recognition, signal induction, and symmetrical gene activation at the dorsal-ventral boundary of the developing Drosophila wing', *Cell* 82(5): 795-802.
Knudsen, P. A. (1964) 'Mode of Growth of the Choroid Plexus in Mouse Embryos', *Acta Anat (Basel)* 57: 172-82.
Krauss, S., Concordet, J. P. and Ingham, P. W. (1993) 'A functionally conserved homolog of the Drosophila segment polarity gene hh is expressed in tissues with polarizing activity in zebrafish embryos', *Cell* 75(7): 1431-44.
Kriebitz, N. N., Kiecker, C., McCormick, L., Lumsden, A., Graham, A. and Bell, E. (2009) 'PRDC regulates placode neurogenesis in chick by modulating BMP signalling', *Developmental biology* 336(2): 280-92.
Krizhanovsky, V. and Ben-Arie, N. (2006) 'A novel role for the choroid plexus in BMP-mediated inhibition of differentiation of cerebellar neural progenitors', *Mechanisms of development* 123(1): 67-75.
LaBonne, C. and Bronner-Fraser, M. (1998a) 'Induction and patterning of the neural crest, a stem cell-like precursor population', *Journal of neurobiology* 36(2): 175-89.
LaBonne, C. and Bronner-Fraser, M. (1998b) 'Neural crest induction in Xenopus: evidence for a two-signal model', *Development* 125(13): 2403-14.
Lai E.C., Deblandre G.A., Kintner C. and Rubin G.M. (2001) 'Drosophila neuralized is a ubiquitin ligase that promotes the internalization and degradation of delta', *Developmental Cell*. 1(6):783-94.
Landsberg, R. L., Awatramani, R. B., Hunter, N. L., Farago, A. F., DiPietrantonio, H. J., Rodriguez, C. I. and Dymecki, S. M. (2005) 'Hindbrain rhombic lip is comprised of discrete progenitor cell populations allocated by Pax6', *Neuron* 48(6): 933-47.
Langenberg, T. and Brand, M. (2005) 'Lineage restriction maintains a stable organizer cell population at the zebrafish midbrain-hindbrain boundary', *Development* 132(14): 3209-16.
Larsen, C. W., Zeltser, L. M. and Lumsden, A. (2001) 'Boundary formation and compartition in the avian diencephalon', *The Journal of neuroscience : the official journal of the Society for Neuroscience* 21(13): 4699-711.
Laufer, E., Dahn, R., Orozco, O. E., Yeo, C. Y., Pisenti, J., Henrique, D., Abbott, U. K., Fallon, J. F. and Tabin, C. (1997) 'Expression of Radical fringe in limb-bud ectoderm regulates apical ectodermal ridge formation', *Nature* 386(6623): 366-73.
Le Douarin, N. M. and Halpern, M. E. (2000) 'Discussion point. Origin and specification of the neural tube floor plate: insights from the chick and zebrafish', *Current opinion in neurobiology* 10(1): 23-30.
le Roux, I., Lewis, J. and Ish-Horowicz, D. (2003) 'Notch activity is required to maintain floorplate identity and to control neurogenesis in the chick hindbrain and spinal cord', *The International journal of developmental biology* 47(4): 263-72.
Lee, K. J., Dietrich, P. and Jessell, T. M. (2000a) 'Genetic ablation reveals that the roof plate is essential for dorsal interneuron specification', *Nature* 403(6771): 734-40.
Lee, K. J. and Jessell, T. M. (1999) 'The specification of dorsal cell fates in the vertebrate central nervous system', *Annu Rev Neurosci* 22: 261-94.
Lee, K. J., Mendelsohn, M. and Jessell, T. M. (1998) 'Neuronal patterning by BMPs: a requirement for GDF7 in the generation of a discrete class of commissural interneurons in the mouse spinal cord', *Genes & development* 12(21): 3394-407.
Lee, S. M., Danielian, P. S., Fritzsch, B. and McMahon, A. P. (1997) 'Evidence that FGF8 signalling from the midbrain-hindbrain junction regulates growth and polarity in the developing midbrain', *Development* 124(5): 959-69.
Lee, S. M., Tole, S., Grove, E. and McMahon, A. P. (2000b) 'A local Wnt-3a signal is required for development of the mammalian hippocampus', *Development* 127(3): 457-67.
Lehtinen, M. K., Zappaterra, M. W., Chen, X., Yang, Y. J., Hill, A. D., Lun, M., Maynard, T., Gonzalez, D., Kim, S., Ye, P. et al. (2011) 'The cerebrospinal fluid provides a proliferative niche for neural progenitor cells', *Neuron* 69(5): 893-905.

Lewis J. (1998) ‘Notch signaling and the control of cell fate choices in vertebrates’, *Seminars in Cell and Developmental Biology* 9(6):583-9.
Liem, K. F., Jr., Tremml, G. and Jessell, T. M. (1997) 'A role for the roof plate and its resident TGFbeta-related proteins in neuronal patterning in the dorsal spinal cord', *Cell* 91(1): 127-38.
Liem, K. F., Jr., Tremml, G., Roelink, H. and Jessell, T. M. (1995) 'Dorsal differentiation of neural plate cells induced by BMP-mediated signals from epidermal ectoderm', *Cell* 82(6): 969-79.
Liu, J. P., Laufer, E. and Jessell, T. M. (2001) 'Assigning the positional identity of spinal motor neurons: rostrocaudal patterning of Hox-c expression by FGFs, Gdf11, and retinoids', *Neuron* 32(6): 997-1012.
Liu, Y., Helms, A. W. and Johnson, J. E. (2004) 'Distinct activities of Msx1 and Msx3 in dorsal neural tube development', *Development* 131(5): 1017-28.
Liu, Z. R., Shi, M., Hu, Z. L., Zheng, M. H., Du, F., Zhao, G. and Ding, Y. Q. (2010) 'A refined map of early gene expression in the dorsal rhombomere 1 of mouse embryos', *Brain Res Bull*.
Louvi, A., Yoshida, M. and Grove, E. A. (2007) 'The derivatives of the Wnt3a lineage in the central nervous system', *The Journal of comparative neurology* 504(5): 550-69.
Lowery, L. A., De Rienzo, G., Gutzman, J. H. and Sive, H. (2009) 'Characterization and classification of zebrafish brain morphology mutants', *Anatomical record* 292(1): 94-106.
Lowery, L. A. and Sive, H. (2004) 'Strategies of vertebrate neurulation and a re-evaluation of teleost neural tube formation', *Mechanisms of development* 121(10): 1189-97.
Lowery, L. A. and Sive, H. (2005) 'Initial formation of zebrafish brain ventricles occurs independently of circulation and requires the nagie oko and snakehead/atp1a1a.1 gene products', *Development* 132(9): 2057-67.
Lumsden, A. and Keynes, R. (1989) 'Segmental patterns of neuronal development in the chick hindbrain', *Nature* 337(6206): 424-8.
Machold, R. and Fishell, G. (2005) 'Math1 is expressed in temporally discrete pools of cerebellar rhombic-lip neural progenitors', *Neuron* 48(1): 17-24.
Machon, O., Backman, M., Machonova, O., Kozmik, Z., Vacik, T., Andersen, L. and Krauss, S. (2007) 'A dynamic gradient of Wnt signaling controls initiation of neurogenesis in the mammalian cortex and cellular specification in the hippocampus', *Developmental biology* 311(1): 223-37.
Machon, O., van den Bout, C. J., Backman, M., Kemler, R. and Krauss, S. (2003) 'Role of beta-catenin in the developing cortical and hippocampal neuroepithelium', *Neuroscience* 122(1): 129-43.
Maden, M. (2002) 'Retinoid signalling in the development of the central nervous system', *Nature reviews. Neuroscience* 3(11): 843-53.
Marklund U., Hansson E.M., Sundström E., de Angelis M.H., Przemeck G.K., Lendahl U., Muhr J. and Ericson J. (2010) ‘Domain-specific control of neurogenesis achieved through patterned regulation of Notch ligand expression’, *Development* 137(3):437-45.
Marti, E., Bumcrot, D. A., Takada, R. and McMahon, A. P. (1995a) 'Requirement of 19K form of Sonic hedgehog for induction of distinct ventral cell types in CNS explants', *Nature* 375(6529): 322-5.
Marti, E., Takada, R., Bumcrot, D. A., Sasaki, H. and McMahon, A. P. (1995b) 'Distribution of Sonic hedgehog peptides in the developing chick and mouse embryo', *Development* 121(8): 2537-47.
Martinez, S., Crossley, P. H., Cobos, I., Rubenstein, J. L. and Martin, G. R. (1999) 'FGF8 induces formation of an ectopic isthmic organizer and isthmocerebellar development via a repressive effect on Otx2 expression', *Development* 126(6): 1189-200.
Mason, I. (2007) 'Initiation to end point: the multiple roles of fibroblast growth factors in neural development', *Nature reviews. Neuroscience* 8(8): 583-96.
McCaffery, P. J., Adams, J., Maden, M. and Rosa-Molinar, E. (2003) 'Too much of a good thing: retinoic acid as an endogenous regulator of neural differentiation and exogenous teratogen', *The European journal of neuroscience* 18(3): 457-72.
Megason, S. G. and McMahon, A. P. (2002) 'A mitogen gradient of dorsal midline Wnts organizes growth in the CNS', *Development* 129(9): 2087-98.
Mellitzer, G., Xu, Q. and Wilkinson, D. G. (1999) 'Eph receptors and ephrins restrict cell intermingling and communication', *Nature* 400(6739): 77-81.
Merino, R., Macias, D., Ganan, Y., Economides, A. N., Wang, X., Wu, Q., Stahl, N., Sampath, K. T., Varona, P. and Hurle, J. M. (1999) 'Expression and function of Gdf-5 during digit skeletogenesis in the embryonic chick leg bud', *Developmental biology* 206(1): 33-45.
Meyers, E. N., Lewandoski, M. and Martin, G. R. (1998) 'An Fgf8 mutant allelic series generated by Cre- and Flp-mediated recombination', *Nature genetics* 18(2): 136-41.
Micchelli, C.A., Rulifson E.J., Blair S.S. (1997) ‘The function and regulation of cut expression on the wing margin of Drosophila: Notch, Wingless and a dominant negative role for Delta and Serrate’, *Development* 124(8):1485-95.

Micchelli, C. A. and Blair, S. S. (1999) 'Dorsoventral lineage restriction in wing imaginal discs requires Notch', *Nature* 401(6752): 473-6.
Millet, S., Bloch-Gallego, E., Simeone, A. and Alvarado-Mallart, R. M. (1996) 'The caudal limit of Otx2 gene expression as a marker of the midbrain/hindbrain boundary: a study using in situ hybridisation and chick/quail homotopic grafts', *Development* 122(12): 3785-97.
Millonig, J. H., Millen, K. J. and Hatten, M. E. (2000) 'The mouse Dreher gene Lmx1a controls formation of the roof plate in the vertebrate CNS', *Nature* 403(6771)*:*764 -769.
Mishima, Y., Lindgren, A. G., Chizhikov, V. V., Johnson, R. L. and Millen, K. J. (2009) 'Overlapping function of Lmx1a and Lmx1b in anterior hindbrain roof plate formation and cerebellar growth', *The Journal of neuroscience : the official journal of the Society for Neuroscience* 29(36): 11377-84.
Moloney, D. J., Panin, V. M., Johnston, S. H., Chen, J., Shao, L., Wilson, R., Wang, Y., Stanley, P., Irvine, K. D., Haltiwanger, R. S. et al. (2000) 'Fringe is a glycosyltransferase that modifies Notch', *Nature* 406(6794): 369-75.
Monuki, E. S., Porter, F. D. and Walsh, C. A. (2001) 'Patterning of the dorsal telencephalon and cerebral cortex by a roof plate-Lhx2 pathway', *Neuron* 32(4): 591-604.
Moran, J. L., Johnston, S. H., Rauskolb, C., Bhalerao, J., Bowcock, A. M. and Vogt, T. F. (1999) 'Genomic structure, mapping, and expression analysis of the mammalian Lunatic, Manic, and Radical fringe genes', *Mamm Genome* 10(6): 535-41.
Morata, G. and Lawrence, P. A. (1975) 'Control of compartment development by the engrailed gene in Drosophila', *Nature* 255(5510): 614-7.
Moury, J. D. and Jacobson, A. G. (1989) 'Neural fold formation at newly created boundaries between neural plate and epidermis in the axolotl', *Developmental biology* 133(1): 44-57.
Moury, J. D. and Jacobson, A. G. (1990) 'The origins of neural crest cells in the axolotl', *Developmental biology* 141(2): 243-53.
Murdoch, J. N., Doudney, K., Paternotte, C., Copp, A. J. and Stanier, P. (2001) 'Severe neural tube defects in the loop-tail mouse result from mutation of Lpp1, a novel gene involved in floor plate specification', *Human molecular genetics* 10(22): 2593-601.
Muroyama, Y., Fujihara, M., Ikeya, M., Kondoh, H. and Takada, S. (2002) 'Wnt signaling plays an essential role in neuronal specification of the dorsal spinal cord', *Genes & development* 16(5): 548-53.
Muzio, L., Soria, J. M., Pannese, M., Piccolo, S. and Mallamaci, A. (2005) 'A mutually stimulating loop involving emx2 and canonical wnt signalling specifically promotes expansion of occipital cortex and hippocampus', *Cerebral cortex* 15(12): 2021-8.
Myat, A., Henrique, D., Ish-Horowicz, D. and Lewis, J. (1996) 'A chick homologue of Serrate and its relationship with Notch and Delta homologues during central neurogenesis', *Developmental biology* 174(2): 233-47.
Nguyen-Ba-Charvet, K. T., Picard-Riera, N., Tessier-Lavigne, M., Baron-Van Evercooren, A., Sotelo, C. and Chedotal, A. (2004) 'Multiple roles for slits in the control of cell migration in the rostral migratory stream', *The Journal of neuroscience : the official journal of the Society for Neuroscience* 24(6): 1497-506.
Nguyen, V. H., Trout, J., Connors, S. A., Andermann, P., Weinberg, E. and Mullins, M. C. (2000) 'Dorsal and intermediate neuronal cell types of the spinal cord are established by a BMP signaling pathway', *Development* 127(6): 1209-20.
Nielsen, C. M. and Dymecki, S. M. (2010) 'Sonic hedgehog is required for vascular outgrowth in the hindbrain choroid plexus', *Developmental biology*.
Nikolaou N., Watanabe-Asaka T., Gerety S., Distel M., Köster R.W. and Wilkinson D.G. (2009) 'Lunatic fringe promotes the lateral inhibition of neurogenesis. *Development* 136(15):2523-33.
Ninkovic, J., Tallafuss, A., Leucht, C., Topczewski, J., Tannhauser, B., Solnica-Krezel, L. and Bally-Cuif, L. (2005) 'Inhibition of neurogenesis at the zebrafish midbrain-hindbrain boundary by the combined and dose-dependent activity of a new hairy/E(spl) gene pair', *Development* 132(1): 75-88.
Nordstrom, U., Maier, E., Jessell, T. M. and Edlund, T. (2006) 'An early role for WNT signaling in specifying neural patterns of Cdx and Hox gene expression and motor neuron subtype identity', *PLoS biology* 4(8): e252.
Nusse, R., van Ooyen, A., Cox, D., Fung, Y. K. and Varmus, H. (1984) 'Mode of proviral activation of a putative mammary oncogene (int-1) on mouse chromosome 15', *Nature* 307(5947): 131-6.
Ohtsuka, T., Ishibashi, M., Gradwohl, G., Nakanishi, S., Guillemot, F. and Kageyama, R. (1999) 'Hes1 and Hes5 as notch effectors in mammalian neuronal differentiation', *The EMBO journal* 18(8): 2196-207.
Pacifici, M., Koyama, E., Iwamoto, M. and Gentili, C. (2000) 'Development of articular cartilage: what do we know about it and how may it occur?', *Connective tissue research* 41(3): 175-84.

Panchision, D. M., Pickel, J. M., Studer, L., Lee, S. H., Turner, P. A., Hazel, T. G. and McKay, R. D. (2001) 'Sequential actions of BMP receptors control neural precursor cell production and fate', *Genes & development* 15(16): 2094-110.
Panin, V. M., Papayannopoulos, V., Wilson, R. and Irvine, K. D. (1997) 'Fringe modulates Notch-ligand interactions', *Nature* 387(6636): 908-12.
Parody, T. R. and Muskavitch, M. A. (1993) 'The pleiotropic function of Delta during postembryonic development of Drosophila melanogaster', *Genetics* 135(2): 527-39.
Paroush, Z., Finley, R. L., Jr., Kidd, T., Wainwright, S. M., Ingham, P. W., Brent, R. and Ish-Horowicz, D. (1994) 'Groucho is required for Drosophila neurogenesis, segmentation, and sex determination and interacts directly with hairy-related bHLH proteins', *Cell* 79(5): 805-15.
Pascual, M., Abasolo, I., Mingorance-Le Meur, A., Martinez, A., Del Rio, J. A., Wright, C. V., Real, F. X. and Soriano, E. (2007) 'Cerebellar GABAergic progenitors adopt an external granule cell-like phenotype in the absence of Ptf1a transcription factor expression', *Proceedings of the National Academy of Sciences of the United States of America* 104(12): 5193-8.
Patten, I. and Placzek, M. (2000) 'The role of Sonic hedgehog in neural tube patterning', *Cellular and molecular life sciences : CMLS* 57(12): 1695-708.
Peng C.Y., Yajima H., Burns C.E., Zon L.I., Sisodia S.S., Pfaff S.L. and Sharma K. (2007) 'Notch and MAML signaling drives Scl-dependent interneuron diversity in the spinal cord', *Neuron* 53(6):813-27.
Placzek, M. (1995) 'The role of the notochord and floor plate in inductive interactions', *Current opinion in genetics & development* 5(4): 499-506.
Placzek, M., Jessell, T. M. and Dodd, J. (1993) 'Induction of floor plate differentiation by contact-dependent, homeogenetic signals', *Development* 117(1): 205-18.
Placzek, M., Tessier-Lavigne, M., Yamada, T., Jessell, T. and Dodd, J. (1990) 'Mesodermal control of neural cell identity: floor plate induction by the notochord', *Science* 250(4983): 985-8.
Placzek, M., Yamada, T., Tessier-Lavigne, M., Jessell, T. and Dodd, J. (1991) 'Control of dorsoventral pattern in vertebrate neural development: induction and polarizing properties of the floor plate', *Development* Suppl 2: 105-22.
Qin, L., Wine-Lee, L., Ahn, K. J. and Crenshaw, E. B., 3rd (2006) 'Genetic analyses demonstrate that bone morphogenetic protein signaling is required for embryonic cerebellar development', *The Journal of neuroscience : the official journal of the Society for Neuroscience* 26(7): 1896-905.
Rauskolb, C., Correia, T. and Irvine, K. D. (1999) 'Fringe-dependent separation of dorsal and ventral cells in the Drosophila wing', *Nature* 401(6752): 476-80.
Ray, R. S. and Dymecki, S. M. (2009) 'Rautenlippe Redux -- toward a unified view of the precerebellar rhombic lip', *Current opinion in cell biology* 21(6): 741-7.
Redzic, Z. B., Preston, J. E., Duncan, J. A., Chodobski, A. and Szmydynger-Chodobska, J. (2005) 'The choroid plexus-cerebrospinal fluid system: from development to aging', *Curr Top Dev Biol* 71: 1-52.
Reijntjes, S., Gale, E. and Maden, M. (2004) 'Generating gradients of retinoic acid in the chick embryo: Cyp26C1 expression and a comparative analysis of the Cyp26 enzymes', *Developmental dynamics : an official publication of the American Association of Anatomists* 230(3): 509-17.
Riley, B. B., Chiang, M. Y., Storch, E. M., Heck, R., Buckles, G. R. and Lekven, A. C. (2004) 'Rhombomere boundaries are Wnt signaling centers that regulate metameric patterning in the zebrafish hindbrain', *Developmental dynamics : an official publication of the American Association of Anatomists* 231(2): 278-91.
Rodriguez-Esteban, C., Schwabe, J. W., De La Pena, J., Foys, B., Eshelman, B. and Izpisua Belmonte, J. C. (1997) 'Radical fringe positions the apical ectodermal ridge at the dorsoventral boundary of the vertebrate limb', *Nature* 386(6623): 360-6.
Roelink, H., Augsburger, A., Heemskerk, J., Korzh, V., Norlin, S., Ruiz i Altaba, A., Tanabe, Y., Placzek, M., Edlund, T., Jessell, T. M. et al. (1994) 'Floor plate and motor neuron induction by vhh-1, a vertebrate homolog of hedgehog expressed by the notochord', *Cell* 76(4): 761-75.
Roelink, H., Porter, J. A., Chiang, C., Tanabe, Y., Chang, D. T., Beachy, P. A. and Jessell, T. M. (1995) 'Floor plate and motor neuron induction by different concentrations of the amino-terminal cleavage product of sonic hedgehog autoproteolysis', *Cell* 81(3): 445-55.
Rose, M. F., Ahmad, K. A., Thaller, C. and Zoghbi, H. Y. (2009a) 'Excitatory neurons of the proprioceptive, interoceptive, and arousal hindbrain networks share a developmental requirement for Math1', *Proceedings of the National Academy of Sciences of the United States of America* 106(52): 22462-7.

Rose, M. F., Ren, J., Ahmad, K. A., Chao, H. T., Klisch, T. J., Flora, A., Greer, J. J. and Zoghbi, H. Y. (2009b) 'Math1 is essential for the development of hindbrain neurons critical for perinatal breathing', *Neuron* 64(3): 341-54.
Ruberte, E., Friederich, V., Chambon, P. and Morriss-Kay, G. (1993) 'Retinoic acid receptors and cellular retinoid binding proteins. III. Their differential transcript distribution during mouse nervous system development', *Development* 118(1): 267-82.
Rulifson, E. J. and Blair, S. S. (1995) 'Notch regulates wingless expression and is not required for reception of the paracrine wingless signal during wing margin neurogenesis in Drosophila', *Development* 121(9): 2813-24.
Saint-Jeannet, J. P., He, X., Varmus, H. E. and Dawid, I. B. (1997) 'Regulation of dorsal fate in the neuraxis by Wnt-1 and Wnt-3a', *Proceedings of the National Academy of Sciences of the United States of America* 94(25): 13713-8.
Sakamoto K., Ohara O., Takagi M., Takeda S. and Katsube K. (2002) 'Intracellular Cell-Autonomous Association of Notch and Its Ligands: A Novel Mechanism of Notch Signal Modification', *Developmental Biology* 241(2):313-26.
Sanalkumar, R., Indulekha, C. L., Divya, T. S., Divya, M. S., Anto, R. J., Vinod, B., Vidyanand, S., Jagatha, B., Venugopal, S. and James, J. (2010) 'ATF2 maintains a subset of neural progenitors through CBF1/Notch independent Hes-1 expression and synergistically activates the expression of Hes-1 in Notch-dependent neural progenitors', *Journal of neurochemistry* 113(4): 807-18.
Saunders, J. W., Jr. (1948) 'The proximo-distal sequence of origin of the parts of the chick wing and the role of the ectoderm', *The Journal of experimental zoology* 108(3): 363-403.
Scholpp, S., Wolf, O., Brand, M. and Lumsden, A. (2006) 'Hedgehog signalling from the zona limitans intrathalamica orchestrates patterning of the zebrafish diencephalon', *Development* 133(5): 855-64.
Selleck, M. A. and Bronner-Fraser, M. (1995) 'Origins of the avian neural crest: the role of neural plate-epidermal interactions', *Development* 121(2): 525-38.
Selvadurai, H. J. and Mason, J. O. (2011) 'Wnt/beta-catenin Signalling Is Active in a Highly Dynamic Pattern during Development of the Mouse Cerebellum', *PloS one* 6(8): e23012.
Settle, S. H., Jr., Rountree, R. B., Sinha, A., Thacker, A., Higgins, K. and Kingsley, D. M. (2003) 'Multiple joint and skeletal patterning defects caused by single and double mutations in the mouse Gdf6 and Gdf5 genes', *Developmental biology* 254(1): 116-30.
Sharma, R. P. and Chopra, V. L. (1976) 'Effect of the Wingless (wg1) mutation on wing and haltere development in Drosophila melanogaster', *Developmental biology* 48(2): 461-5.
Shimamura, K. and Rubenstein, J. L. (1997) 'Inductive interactions direct early regionalization of the mouse forebrain', *Development* 124(14): 2709-18.
Shimojo, H., Ohtsuka, T. and Kageyama, R. (2008) 'Oscillations in notch signaling regulate maintenance of neural progenitors', *Neuron* 58(1): 52-64.
Shinozaki, K., Yoshida, M., Nakamura, M., Aizawa, S. and Suda, Y. (2004) 'Emx1 and Emx2 cooperate in initial phase of archipallium development', *Mechanisms of development* 121(5): 475-89.
Sidow, A., Bulotsky, M. S., Kerrebrock, A. W., Bronson, R. T., Daly, M. J., Reeve, M. P., Hawkins, T. L., Birren, B. W., Jaenisch, R. and Lander, E. S. (1997) 'Serrate2 is disrupted in the mouse limb-development mutant syndactylism', *Nature* 389(6652): 722-5.
Spemann, H. and Mangold, H. (1924) 'Uber Induktion von Embryonalanlagen durch Implantation artfremder Organisatoren', *Wilhelm Roux' Arch. Entwicklungsmech. Organ.* 100: 599 - 638.
Sprinzak D., Lakhanpal A., Lebon L., Santat L.A., Fontes M.E., Anderson G.A., Garcia-Ojalvo J., Elowitz M.B. (2010) 'Cis-interactions between Notch and Delta generate mutually exclusive signalling states', *Nature* 465(7294):86-90.
Stern, C. D. (2001) 'Initial patterning of the central nervous system: how many organizers?', *Nature reviews. Neuroscience* 2(2): 92-8.
Stern, C. D., Charite, J., Deschamps, J., Duboule, D., Durston, A. J., Kmita, M., Nicolas, J. F., Palmeirim, I., Smith, J. C. and Wolpert, L. (2006) 'Head-tail patterning of the vertebrate embryo: one, two or many unresolved problems?', *The International journal of developmental biology* 50(1): 3-15.
Steventon, B., Carmona-Fontaine, C. and Mayor, R. (2005) 'Genetic network during neural crest induction: from cell specification to cell survival', *Seminars in cell & developmental biology* 16(6): 647-54.
Storm, E. E. and Kingsley, D. M. (1996) 'Joint patterning defects caused by single and double mutations in members of the bone morphogenetic protein (BMP) family', *Development* 122(12): 3969-79.
Storm, E. E. and Kingsley, D. M. (1999) 'GDF5 coordinates bone and joint formation during digit development', *Developmental biology* 209(1): 11-27.

Strong, L. H. (1956) 'Early development of the ependyma and vascular pattern of the fourth ventricular choroid plexus in the rabbit', *Am J Anat* 99(2): 249-90.
Sturrock, R. R. (1979) 'A morphological study of the development of the mouse choroid plexus', *Journal of anatomy* 129(Pt 4): 777-93.
Subramanian, L. and Tole, S. (2009) 'Mechanisms underlying the specification, positional regulation, and function of the cortical hem', *Cerebral cortex* 19 Suppl 1: i90-5.
Takebayashi, K., Sasai, Y., Sakai, Y., Watanabe, T., Nakanishi, S. and Kageyama, R. (1994) 'Structure, chromosomal locus, and promoter analysis of the gene encoding the mouse helix-loop-helix factor HES-1. Negative autoregulation through the multiple N box elements', *The Journal of biological chemistry* 269(7): 5150-6.
Takiguchi-Hayashi, K., Sekiguchi, M., Ashigaki, S., Takamatsu, M., Hasegawa, H., Suzuki-Migishima, R., Yokoyama, M., Nakanishi, S. and Tanabe, Y. (2004) 'Generation of reelin-positive marginal zone cells from the caudomedial wall of telencephalic vesicles', *The Journal of neuroscience : the official journal of the Society for Neuroscience* 24(9): 2286-95.
Tamai, K., Semenov, M., Kato, Y., Spokony, R., Liu, C., Katsuyama, Y., Hess, F., Saint-Jeannet, J. P. and He, X. (2000) 'LDL-receptor-related proteins in Wnt signal transduction', *Nature* 407(6803): 530-5.
Tanabe, Y., Roelink, H. and Jessell, T. M. (1995) 'Induction of motor neurons by Sonic hedgehog is independent of floor plate differentiation', *Current biology : CB* 5(6): 651-8.
Teillet, M. A., Lapointe, F. and Le Douarin, N. M. (1998) 'The relationships between notochord and floor plate in vertebrate development revisited', *Proceedings of the National Academy of Sciences of the United States of America* 95(20): 11733-8.
Thoby-Brisson, M., Karlen, M., Wu, N., Charnay, P., Champagnat, J. and Fortin, G. (2009) 'Genetic identification of an embryonic parafacial oscillator coupling to the preBotzinger complex', *Nature neuroscience* 12(8): 1028-35.
Thomas, T. and Dziadek, M. (1993) 'Capacity to form choroid plexus-like cells in vitro is restricted to specific regions of the mouse neural ectoderm', *Development* 117(1): 253-62.
Thomas, T., Power, B., Hudson, P., Schreiber, G. and Dziadek, M. (1988) 'The expression of transthyretin mRNA in the developing rat brain', *Developmental biology* 128(2): 415-27.
Tickle, C. (1995) 'Vertebrate limb development', *Current opinion in genetics & development* 5(4): 478-84.
Tilleman, H., Hakim, V., Novikov, O., Liser, K., Nashelsky, L., Di Salvio, M., Krauthammer, M., Scheffner, O., Maor, I., Mayseless, O. et al. (2010) 'Bmp5/7 in concert with the mid-hindbrain organizer control development of noradrenergic locus coeruleus neurons', *Molecular and cellular neurosciences* 45(1): 1-11.
Timmer, J. R., Wang, C. and Niswander, L. (2002) 'BMP signaling patterns the dorsal and intermediate neural tube via regulation of homeobox and helix-loop-helix transcription factors', *Development* 129(10): 2459-72.
Tossell, K., Kiecker, C., Wizenmann, A., Lang, E. and Irving, C. (2011) 'Notch signalling stabilises boundary formation at the midbrain-hindbrain organiser', *Development*.
Toyoda, R., Assimacopoulos, S., Wilcoxon, J., Taylor, A., Feldman, P., Suzuki-Hirano, A., Shimogori, T. and Grove, E. A. (2010) 'FGF8 acts as a classic diffusible morphogen to pattern the neocortex', *Development* 137(20): 3439-48.
Trokovic, R., Jukkola, T., Saarimaki, J., Peltopuro, P., Naserke, T., Weisenhorn, D. M., Trokovic, N., Wurst, W. and Partanen, J. (2005) 'Fgfr1-dependent boundary cells between developing mid- and hindbrain', *Developmental biology* 278(2): 428-39.
Tsumaki, N., Tanaka, K., Arikawa-Hirasawa, E., Nakase, T., Kimura, T., Thomas, J. T., Ochi, T., Luyten, F. P. and Yamada, Y. (1999) 'Role of CDMP-1 in skeletal morphogenesis: promotion of mesenchymal cell recruitment and chondrocyte differentiation', *The Journal of cell biology* 144(1): 161-73.
van Ooyen, A. and Nusse, R. (1984) 'Structure and nucleotide sequence of the putative mammary oncogene int-1; proviral insertions leave the protein-encoding domain intact', *Cell* 39(1): 233-40.
Vieira, C., Garda, A. L., Shimamura, K. and Martinez, S. (2005) 'Thalamic development induced by Shh in the chick embryo', *Developmental biology* 284(2): 351-63.
Vogel-Hopker, A. and Rohrer, H. (2002) 'The specification of noradrenergic locus coeruleus (LC) neurones depends on bone morphogenetic proteins (BMPs)', *Development* 129(4): 983-91.
von Frowein, J., Wizenmann, A. and Gotz, M. (2006) 'The transcription factors Emx1 and Emx2 suppress choroid plexus development and promote neuroepithelial cell fate', *Developmental biology* 296(1): 239-52.

Vue, T. Y., Bluske, K., Alishahi, A., Yang, L. L., Koyano-Nakagawa, N., Novitch, B. and Nakagawa, Y. (2009) 'Sonic hedgehog signaling controls thalamic progenitor identity and nuclei specification in mice', *The Journal of neuroscience : the official journal of the Society for Neuroscience* 29(14): 4484-97.
Wall, D. S., Mears, A. J., McNeill, B., Mazerolle, C., Thurig, S., Wang, Y., Kageyama, R. and Wallace, V. A. (2009) 'Progenitor cell proliferation in the retina is dependent on Notch-independent Sonic hedgehog/Hes1 activity', *J Cell Biol* 184(1): 101-12.
Walshe, J. and Mason, I. (2003) 'Unique and combinatorial functions of Fgf3 and Fgf8 during zebrafish forebrain development', *Development* 130(18): 4337-49.
Wang, V. Y., Rose, M. F. and Zoghbi, H. Y. (2005) 'Math1 expression redefines the rhombic lip derivatives and reveals novel lineages within the brainstem and cerebellum', *Neuron* 48(1): 31-43.
Wassef, M. and Joyner, A. L. (1997) 'Early mesencephalon/metencephalon patterning and development of the cerebellum', *Perspectives on developmental neurobiology* 5(1): 3-16.
Williams, R., Nelson, L., Dowthwaite, G. P., Evans, D. J. and Archer, C. W. (2009) 'Notch receptor and Notch ligand expression in developing avian cartilage', *Journal of anatomy* 215(2): 159-69.
Wilson, L. and Maden, M. (2005) 'The mechanisms of dorsoventral patterning in the vertebrate neural tube', *Developmental biology* 282(1): 1-13.
Wilson, L. J., Myat, A., Sharma, A., Maden, M. and Wingate, R. J. (2007) 'Retinoic acid is a potential dorsalising signal in the late embryonic chick hindbrain', *BMC developmental biology* 7: 138.
Wilson, L. J. and Wingate, R. J. (2006) 'Temporal identity transition in the avian cerebellar rhombic lip', *Developmental biology* 297(2): 508-21.
Wilting, J. and Christ, B. (1989) 'An experimental and ultrastructural study on the development of the avian choroid plexus', *Cell and tissue research* 255(3): 487-94.
Wingate, R. J. and Hatten, M. E. (1999) 'The role of the rhombic lip in avian cerebellum development', *Development* 126(20): 4395-404.
Wizenmann, A. and Lumsden, A. (1997) 'Segregation of rhombomeres by differential chemoaffinity', *Molecular and cellular neurosciences* 9(5-6): 448-59.
Wolda, S. L., Moody, C. J. and Moon, R. T. (1993) 'Overlapping expression of Xwnt-3A and Xwnt-1 in neural tissue of Xenopus laevis embryos', *Developmental biology* 155(1): 46-57.
Wolpert, L. (1969) 'Positional information and the spatial pattern of cellular differentiation', *Journal of theoretical biology* 25(1): 1-47.
Wolpert, L. (1996) 'One hundred years of positional information', *Trends in genetics : TIG* 12(9): 359-64.
Wolpert, L., Beddington, R. S., Jessell, T., Lawrence, P., Meyerowitz, E. and Smith, J. (2002) *Principles of Development*: Oxford University Press.
Wozney, J. M., Rosen, V., Celeste, A. J., Mitsock, L. M., Whitters, M. J., Kriz, R. W., Hewick, R. M. and Wang, E. A. (1988) 'Novel regulators of bone formation: molecular clones and activities', *Science* 242(4885): 1528-34.
Wu, J., Saint-Jeannet, J. P. and Klein, P. S. (2003) 'Wnt-frizzled signaling in neural crest formation', *Trends in neurosciences* 26(1): 40-5.
Xu, Q., Alldus, G., Holder, N. and Wilkinson, D. G. (1995) 'Expression of truncated Sek-1 receptor tyrosine kinase disrupts the segmental restriction of gene expression in the Xenopus and zebrafish hindbrain', *Development* 121(12): 4005-16.
Xu, Q., Mellitzer, G., Robinson, V. and Wilkinson, D. G. (1999) 'In vivo cell sorting in complementary segmental domains mediated by Eph receptors and ephrins', *Nature* 399(6733): 267-71.
Xu, Q. and Wilkinson, D. G. (1997) 'Eph-related receptors and their ligands: mediators of contact dependent cell interactions', *Journal of molecular medicine* 75(8): 576-86.
Yamada, T., Pfaff, S. L., Edlund, T. and Jessell, T. M. (1993) 'Control of cell pattern in the neural tube: motor neuron induction by diffusible factors from notochord and floor plate', *Cell* 73(4): 673-86.
Yamada, T., Placzek, M., Tanaka, H., Dodd, J. and Jessell, T. M. (1991) 'Control of cell pattern in the developing nervous system: polarizing activity of the floor plate and notochord', *Cell* 64(3): 635-47.
Yamamoto, M., McCaffery, P. and Drager, U. C. (1996) 'Influence of the choroid plexus on cerebellar development: analysis of retinoic acid synthesis', *Brain research. Developmental brain research* 93(1-2): 182-90.
Yaneza, M., Gilthorpe, J. D., Lumsden, A. and Tucker, A. S. (2002) 'No evidence for ventrally migrating neural tube cells from the mid- and hindbrain', *Developmental dynamics : an official publication of the American Association of Anatomists* 223(1): 163-7.
Yoon, K. and Gaiano, N. (2005) 'Notch signaling in the mammalian central nervous system: insights from mouse mutants', *Nature neuroscience* 8(6): 709-15.

Yoshida, M., Assimacopoulos, S., Jones, K. R. and Grove, E. A. (2006) 'Massive loss of Cajal-Retzius cells does not disrupt neocortical layer order', *Development* 133(3): 537-45.
Zeltser, L. M., Larsen, C. W. and Lumsden, A. (2001) 'A new developmental compartment in the forebrain regulated by Lunatic fringe', *Nature neuroscience* 4(7): 683-4.
Zervas, M., Millet, S., Ahn, S. and Joyner, A. L. (2004) 'Cell behaviors and genetic lineages of the mesencephalon and rhombomere 1', *Neuron* 43(3): 345-57.